The Asymmetric Synthesis of Enol Phosphates and Their Application in Total Synthesis

Thesis submitted to the University of Strathclyde in fulfilment of the requirements for the degree of Doctor of Philosophy

By

Muralikrishnan Rajamanickam

2015

Department of Pure and Applied Chemistry
University of Strathclyde
Thomas Graham Building
295 Cathedral Street
Glasgow
G1 1XL

Declaration of Copyright

Signed:

Dated:

Acknowledgement

First and foremost I would like to thank my supervisor Prof. Billy Kerr for giving me the opportunity to work in his group. Throughout my PhD, under his supervision, I have gained countless talents, such as listening to epic stories, *pleasing* your boss (usually with a Saint Emilion), and also more importantly gained confidence and rigour for which I will be forever grateful.

I would also like to thank my industrial supervisor Dr. Vipul Patel for having me in his group and Chris Wellaway for guiding me in the *palace* (i.e. GSK Stevenage). I must also thank LPatz for all the help she provided, such as correcting my drafts, listening to my stories while I was bored, helping me with my placement and finally for all the gossip. A special thanks to Dave for correcting my thesis, even on a Sunday night, I really appreciate it.

My sincere thanks to all the past and present members of the Kerr group with whom I shared some good and bad times. *Yous* taught me Glaswegian and the specialties of Glasgow (i.e. Haggis supper, deep fried Mars bar and the Press Bar). Thanks to Tina, Calum, Malky, Monks, RBo, Goldie, Kirsten, Richard, Andy, Philippa, Renan, Leo and Peter. Also thanks to the part time members of the group, Kirsty, Jen, Jenny, Gayle, Mercedes, Big Beans, Graeme, Kai, for sharing the fun moments.

A special thanks to my brother, from another mother, Marc; I enjoyed all our discussions, dances, Sainsbury chillies, KFC buckets, pinto burritos, and I thank you for making me enjoy my Scottish experience.

I would like to express my gratitude for a very special person, who met me at the worst period of my thesis (the end) and still enjoyed my company through writing, job search and my exquisite noodle diet. Thank you for bearing with me Eilidh. <3

To finish, I would like to thank my best supporters, those who were always behind me through good and bad times. You have always done what you believed the best for me. Thank you Mum and Dad.

Abstract

The synthesis of a wide range of highly valuable enol phosphate products has been carried out. The use of carbon centred magnesium bases, previously developed in the group has allowed the formation of kinetic enol phosphate products under room temperature conditions. By applying specific quench conditions such as the reverse addition quench condition yields up to 95% were obtained while using di-*tert*-butylmagnesium base. Interestingly acetophenone derivatives required the use of di-mesitylmagnesium base to access the corresponding enol phosphate compounds.

Such enol phosphates can also be obtained under an enantioenriched fashion with the use of chiral magnesium bisamide bases. Previously studied *C2*- and *pseudo C2*-symmetric magnesium amide bases were synthesised and the process optimised to obtain up to 95% yield and 95:5 of selectivity on the benchmark substrate. A novel co-addition quench protocol was developed to access high reactivity and selectivity at mild temperature conditions (-20 °C).

The high stability of enol phosphate products allowed a detailed study of the chiral magnesium amide bases. Such study allowed the development of a practical methodology towards chiral alkyl-magnesium amide bases allowing similar results to chiral magnesium bisamide bases with half the amount of chiral amine. Further investigations of the reactive species in solution through DOSY NMR techniques were also carried out.

Finally the sum of knowledge gained through synthesis and application of enol phosphates allowed the total synthesis of a natural product (+)-Sporochnol. The key transformation of the synthesis consisted on the desymmetrisation of a prochiral ketone to generate an enantioenriched enol phosphate followed by a Kumada cross coupling reaction.

The novel Kumada coupling reaction was initially developed for the synthesis of (+)-Sporochnol. With the success encountered in such methodology we further developed the reaction, which, ultimately allowed the cross coupling of unactivated enol phosphate compounds with alkyl Grignard reagents at room temperature using commerically available and air stable PEPPSI catalysts.

Abbreviations

Bn	benzyl
Bz	benzoyl
DCE	dichloroethane
DCM	dichloromethane
dr	diastereomeric ratio
DOSY	diffusion ordered spectroscopy
DPPF	1,1'-bis(diphenylphosphino)ferrocene
e.e.	enantiomeric excess
eq.	equivalent
Et	ethyl
ESI	electrospray ionisation
Et_3Al	triethylaluminium
Et_3N	triethylamine
Et_2O	diethyl ether
EtOAc	ethyl acetate
EQ	external quench
e.r.	enantiomeric ratio
GC	gas chromatography
HCl	hydrochloric acid
HMPA	hexamethylphosphoramide
HPLC	high performance liquid chromatography
h	hour
HRMS	high resolution mass spectrum
Hz	hertz
IPA	*iso*-propanol
IQ	internal quench
IR	infrared
LDA	lithium di-*iso*-propyl amide
LiHMDS	lithium bis(trimethylsilyl)amide
Me	methyl

MeOH	methanol
Mes	mesityl
mg	milligram
min	minute
mL	milliliter
mmol	millimoles
NMR	nuclear magnetic resonance
	s singlet
	d doublet
	t triplet
	q quartet
	m multiplet
	br broad
n-BuLi	*n*-butyllithium
PE	petroleum ether
PEPPSI	pyridine-enhanced precatalyst preparation stabilization and initiation
Ph	phenyl
Pr	propyl
Py	pyridine
rt	room temperature
TBDPS	*tert*-butyldiphenylsilyl
t-Bu	*tert*-butyl
TES	triethylsilyl
Tf	trifluoromethanesulfonyl
THF	tetrahydrofuran
TLC	thin layer chromatography
TMS	trimethylsilyl
TTBPMgBr	2,4,6-tri-*t*-butylphenylmagnesium bromide
UV	ultraviolet
Z	benzyloxycarbonyl

Contents

Part I: Synthesis of Enol Phosphates

Chapter 1

Carbon centred magnesium bases

Contents

1. Introduction

1.1 An Introduction to Enol Phosphate Compounds

1.1.1 The Synthesis of Enol Phosphates

Phosphates are highly prevalent throughout nature, and, as such, their synthesis and properties have been the subject of investigation for over a century.[1] The first commonly used methodology for the efficient synthesis of enol phosphates was developed by Perkov.[2] In the early 20th century, following research carried out by Arbusov and Michelis,[3] Perkov reported on the rearrangement product observed when triethyl phosphite was reacted with α-haloketones. As shown below in **Scheme 1.1**, when compound **1** was reacted with triethyl phosphite, the enol phosphate **2** was obtained through a rearrangement process. The early development of a facile access to such compounds allowed them to be widely used for the synthesis of pesticides in agrochemical industries.[1]

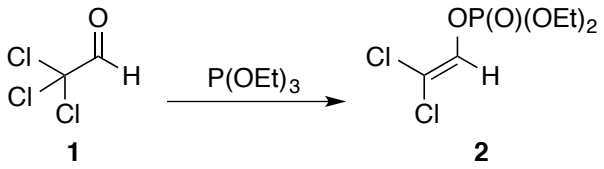

1 **2**

Scheme 1. 1

Although exhibiting good reactivity in the preparation of enol phosphates, the use of α-halo-ketones represents a major drawback for further development of this process. Drawbacks to the use of these substrates include their preparation and handling, and the lack of region- and stereocontrol in many of the reactions.

More recently, the development and commercialisation of strong metal amide bases, such as lithium bis(trimethylsilyl)amide (LiHMDS) and, lithium di-*iso*-propyl amide (LDA), allowed greater control in the formation of enol phosphates. The use of LiHMDS with an enolizable ketone such as **3**, resulted in the formation of a lithium enolate intermediate, which was trapped by diethylphosphoryl chloride to afford the enol phosphate **4** in 95% yield, exclusively as the (*Z*)-isomer (**Scheme 1.2**). This

approach has greatly facilitated the synthesis of enol phosphates by using widely available ketones, and results in the formation of the kinetic enol phosphate. Moreover, diphenylphosphoryl chloride has become more prevalent as the phosphate source, since the diphenyl enol phosphate products are reported to be more stable than their diethyl counterparts.[3]

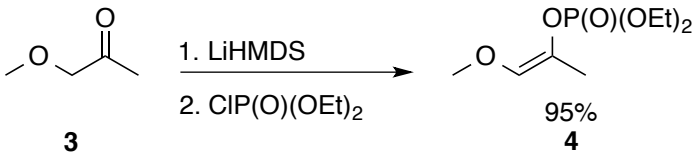

Scheme 1. 2

Access to the thermodynamic enol phosphate compounds has also been reported. The most accessible approach is by the isomerisation of the corresponding kinetic enol phosphate into the thermodynamic product by treatment with a substoichiometric quantity (5 mol%) of trifluoromethanesulfonic acid (TfOH).[5] This method is not only complementary to the above process, but it also allows for a wider diversification of products. As shown below in **Scheme 1.3**, the use of a substoichiometric amount of TfOH resulted isomerisation of the kinetic enol phosphate **5** to the thermodynamic enol phosphate **6** in excellent yield.

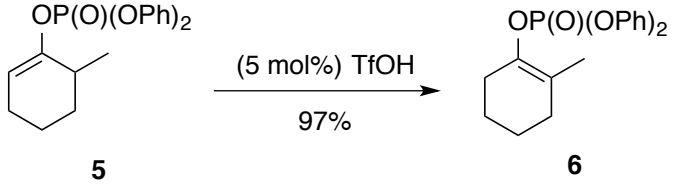

Scheme 1. 3

A slightly different approach has also been explored for the synthesis of kinetic and thermodynamic enol phosphates through addition of phosphates onto terminal alkynes using gold catalysis.[6] As shown in **Scheme 1.4** below, PPh_3AuCl, along with $AgPF_6$, catalyses the addition of diphenyl phosphate to terminal alkyne **7**, allowing the selective formation of the kinetic enol phosphate product **8** in 81% yield. On the

other hand, using $(C_6F_5)_3PAuCl$ with AgOTf allowed nearly exclusive formation of the thermodynamic product **9** in 85% yield.

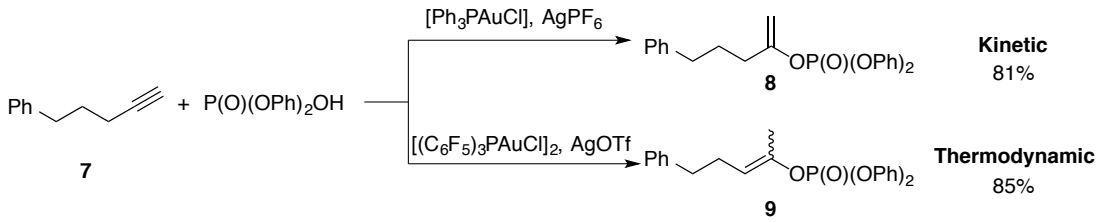

Scheme 1. 4

More recently Brown, has developed a strategy to access such enol phosphates from simple esters (**Scheme 1.5**).[7] Addition of a first equivalent of *n*-butyllithium (*n*-BuLi) to the ester **10** resulted in the formation of the lithium enolate, which was followed by elimination of the aryloxy group, generating a ketene intermediate. Upon addition of the second equivalent of *n*-BuLi to this ketene intermediate, followed by diethylphosphoryl chloride, gave access to the required enol phosphate **11** with a high stereo- and regiocontrol.

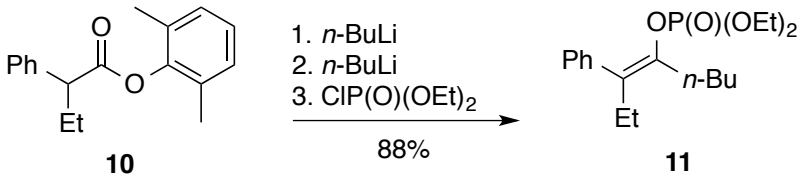

Scheme 1. 5

The scope of accessible products and the control over the reaction has been greatly improved by the use of lithium amide bases. Having said this, modern requirements of eco-friendly and energy efficient processes raise the problems generated by the use of lithium derived chemistry. Indeed, these reactions are generally carried out at -78 °C, representing a significant cost on the scaling up of industrial processes. Additionally, lithium-derived amide bases can present a range of aggregates in solution, which have the potential to affect the reproducibility of the given reaction process (further details will be disclosed in chapter 2).

1.1.2. Application of enol phosphates

Alongside the various methods developed for the synthesis of enol phosphates, a range of further transformations have been developed based on this functional group. More recently, the enol phosphate functional group has attracted further interest with the advent and development of palladium-catalysed cross-coupling reactions.

Earlier studies on the functionalization of enol phosphate compounds consisted of the reduction of such species to deliver olefins. This singular transformation was employed on a range of synthetic routes towards targeted natural products such as (α)-amorphene **13** (**Scheme 1.6**), where the action of lithium and liquid ammonia on the enol phosphate **12** produced the desired target compound.[8]

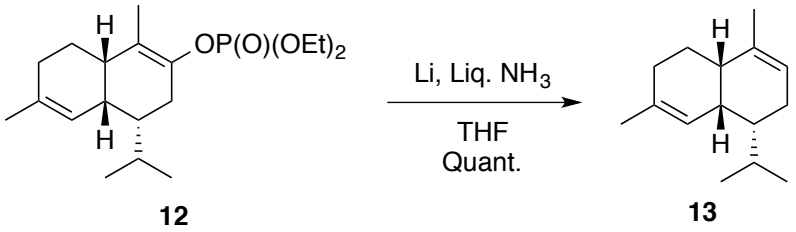

12 **13**

Scheme 1. 6

Further advances in the functionalization of enol phosphates were made while exploring the reactivity of transition metals such as palladium. Initial research carried out by Oshima showed that the use of triethylaluminium associated to Pd^0 catalysis, can selectively reduce enol phosphates.[9] Later, further work carried out by Thompson showed that a subtle change of the solvent (*i.e.* DCE to hexane) improved the selectivity over the conformation of the final olefin. As shown below in **Scheme 1.7**, by submitting enol phosphate **14** to a substoichiometric amount of tetrakis(triphenylphosphine)palladium(0) and Et_3Al in dichloroethane (DCE), a 33:67 ratio of *E*:*Z* isomers of **15** were obtained. In contrast, the use of hexane as solvent generated exclusively the *Z* isomer of **15**.[10]

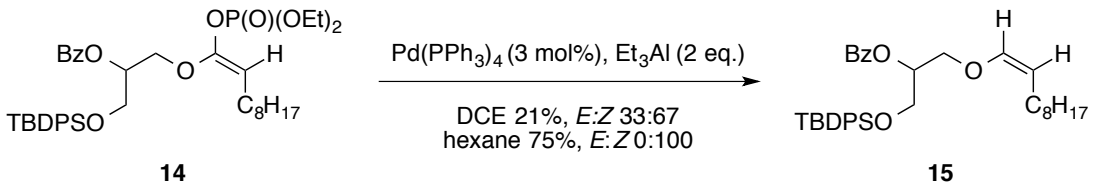

14 **15**

Scheme 1. 7

Access to more substituted alkenes via the transformation of enol phosphates was first achieved by Blaszcak, with the use of organocuprate reagents on both cyclic and acyclic enol phosphates.[11] As presented below in **Scheme 1.8**, the enol phosphate derived from 4-*tert*-butylcyclohexanone, **16**, was employed successfully in this methodology, to form the alkylated products **17** (59%) and **18** (11%) from the corresponding organocuprate reagent.

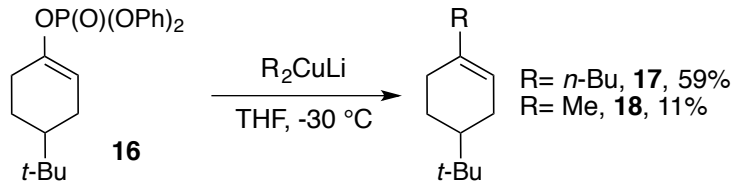

Scheme 1. 8

Further success was achieved in this area with the use of palladium as the transition metal catalyst. Several early studies made use of enol phosphates as cross coupling partner in the total synthesis of challenging natural products. One such example was reported by Fuwa, where he performed a Suzuki coupling reaction with an enol phosphate, from an *in situ* generated borane, for the synthesis of Gambierol.[12] As shown in the **Scheme 1.9** below, reaction of **19** with 9-BBN generated an alkylborane species *in situ*, which then underwent a palladium-catalysed cross-coupling reaction with the enol phosphate moiety **20** to give access to the intermediate **21**, which was further elaborated to the natural product, (-)-Gambierol.

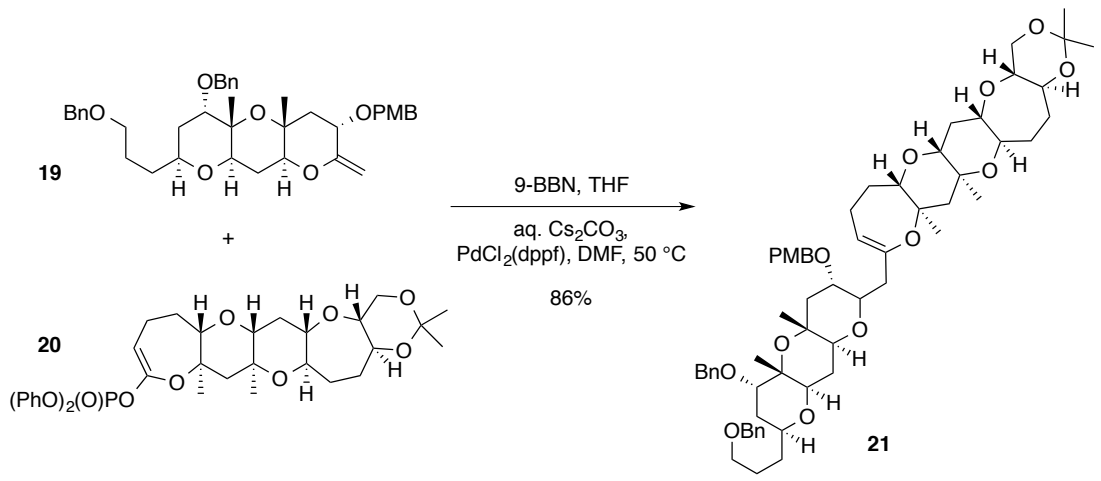

Scheme 1. 9

Over the past decade, a wide variety of cross coupling reactions have emerged, allowing a broader access to widely developed reactions such as the Stille, Suzuki, Negishi, Kumada and Heck transformations. Selected examples of these transformations are depicted in **Scheme 1.10** below. The first reaction, an example of a Stille coupling, starts with the cyclic chiral enol phosphate **(*S*)-22**, and is coupled to an organostannane to generate the desired chiral diene **(*S*)-23** in 84% yield.[13] This example demonstrates that the cross coupling of a chiral enol phosphate can be achieved without isomerisation. The second reaction demonstrates a Suzuki cross-coupling between a lactone-derived enol phosphate **24** and *o*-nitrophenylboronic acid, formatting the bicyclic compound **25** in a moderate 71% yield.[14] The third reaction; where an arylzinc reagent was used to cross-couple with an enol phosphate, shows an interesting selectivity pattern. In fact, employing the widely used dppf ligand in the reaction of enol phosphate **26**, allowed the normal Negishi transformation to take place and afford mainly compound **27**. In contrast, the use of a bulky, monodentate, electron-rich phosphine ((*R*)-(*S*)-PPF-P*t*-Bu_3) allowed the authors to gain access selectively to ß styrenes such as **28**, through a 1,2 shift in the vinyl metal intermediate.[15] In the following transformation, the Kumada coupling of an arylmagnesium bromide to the non-activated enol phosphate **16** was carried out using a simple $PdCl_2$ catalyst, to afford the desired olefin **29** in a high 82% yield.[16] Finally, the example of an intramolecular Heck reaction is presented, where the use

of a bulky tri(*o*-tolyl)phosphine ligand was necessary in the reaction of enol phosphate **30**, giving a moderate 57% yield of the tricyclic compound **31**.[20]

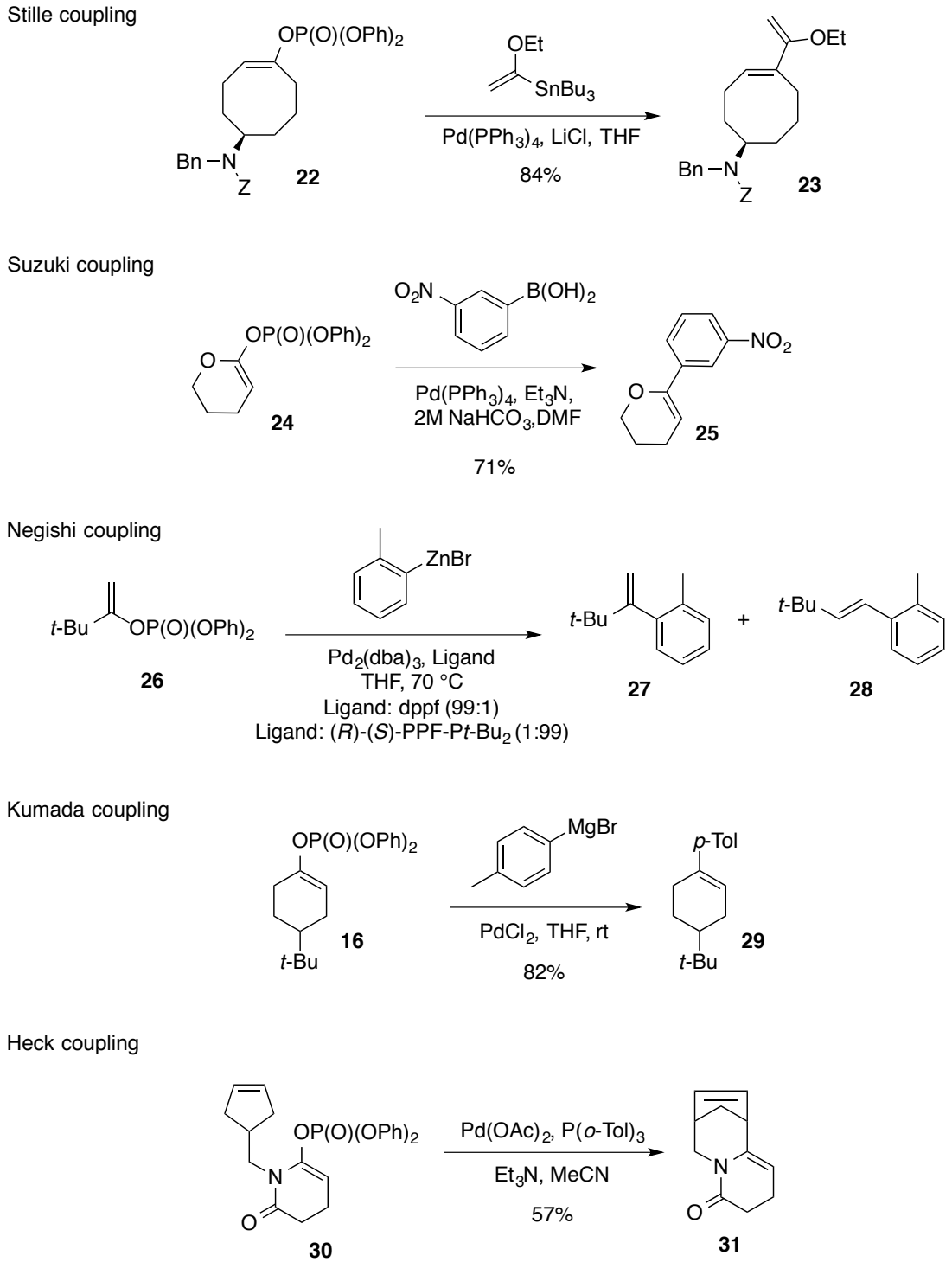

Scheme 1. 10

There is now a vast body of literature on such cross-coupling reactions of enol phosphates. In addition to these examples, other transition metal catalysts, such as those based on nickel and iron, have also begun to find use in the cross-coupling of enol phosphates.[4]

Despite their prominence in the literature, some aspects of their nature mean enol phosphates are underutilised compared to other insertable C-X bonds, such as triflates or halogens. It has long been the dogma that enol phosphates such as **16** were less activating, and therefore more challenging, substrates than activated enol phosphates, *i.e.* containing a heteroatom α– to the enol phosphate, such as **24**, which are more commonly used. Furthermore, the use of aryl coupling reagents was also predominant in the literate, leaving space for cross-coupling with alkyl partners to be further explored. Most examples of sp^2-sp^3 cross-coupling are exceptions in this area, due to the potential for a range of by-products to form alongside the desired cross-coupling. We proposed to explore various areas of the synthesis and applications of enol phosphates, through novel methodologies allowing a facile synthesis and application of enol phosphates.

1.2. Carbon Centred Magnesium Bases

The utility of enol phosphates is well established in modern synthetic organic chemistry. As mentioned earlier, with the variety of applications that have been developed over the last decade, it is clear that these versatile intermediates can play an important role within an industrial setting, in the key steps towards target molecules.[4] Having stated this, the common methods of preparation involves the use of strong bases at low temperature (usually -78 °C). These conditions create problems on a large scale, with low reaction temperatures requiring specialised equipment, in addition to the cost associated with such cooling of large scale reactions. Thus, these typical conditions represent a drawback in the use of enol phosphates.[18]

Within the field of strong bases for use in organic synthesis, the Kerr Laboratory has focused for several years on developing novel methodologies using stable, efficient and easy-to-use magnesium-based reagents. These magnesium reagents not only afforded high levels of reactivity in the deprotonation of ketones, but, more importantly, afforded high levels of reactivity under extremely mild conditions and relatively elevated temperatures. Among the different reagents developed within the group, carbon-centred bases have shown high levels of reactivity in the generation of kinetic enolates at temperatures as mild as 0 °C, whilst showing remarkable stability. The origin of these bases will now be described in detail.

1.2.1. Primary uses for a catalytic asymmetric process

The Kerr group initially developed magnesium amide bases for the environmentally friendly and efficient asymmetric deprotonation of ketones to generate enantioenriched silyl enol ethers (further details will be given in chapter 2).[19] Having observed high levels of reactivity and selectivity, they next envisaged the development of a catalytic asymmetric deprotonation reaction (**Scheme 1.11**).[20] The concept for this magnesium-based catalytic process required the use an alkylmagnesium amide base such as **(*R*)-34**, which was generated *in situ* by reaction of chiral amine **(*R*)-33** with commercially available dibutylmagnesium **32**. The use of this specific source of base was based on previous work within the group where it displayed good levels of reactivity and selectivity in stoichiometric asymmetric deprotonation reactions.[21] The deprotonation of **35** by amide **(*R*)-34** would generate the chiral amine **(*R*)-33**, which would be deprotonated by **32** to regenerate active base **(*R*)-34**, whilst magnesium enolate **(*S*)-36** would be quenched by the use of an electrophile such as chlorotrimethylsilane (TMSCl) to produce the desired product **(*S*)-37**.

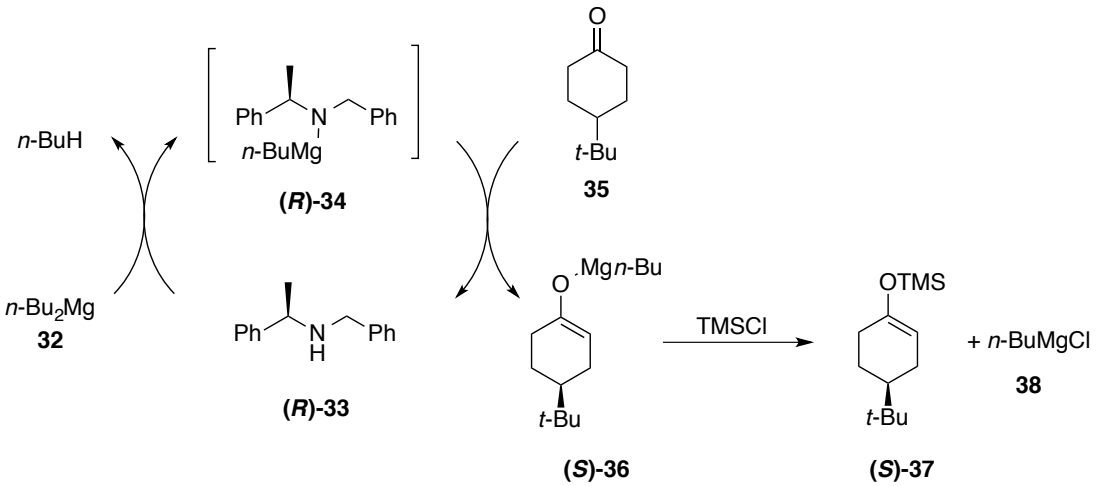

Scheme 1. 11

With this strategy towards development of a catalytic cycle, the first attempts towards the asymmetric deprotonation using magnesium base chemistry were carried out (**Scheme 1.12**).[20] Unfortunately, as shown below, these initial studies result in poor levels of selectivity (79:21) and yield (30%) for the synthesis of **(*S*)-37**, in comparison to standard stoichiometric conditions with the bisamide chemistry (i.e. 82% conversion, 91:9 er).[21]

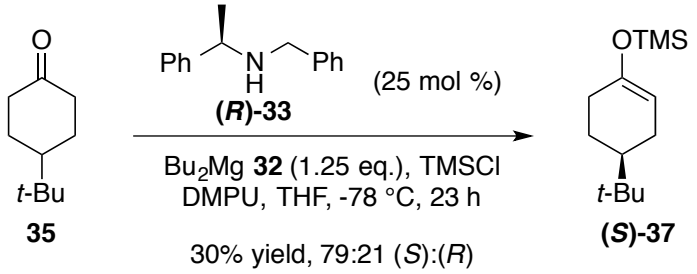

Scheme 1. 12

Although relatively poor selectivities were observed, the main concern was the lack of reactivity, which was proposed to result from slow formation of the active alkylmagnesium amide species, **(*R*)-34**. In fact, amine **(*R*)-33** was added to the solution containing stoichiometric base **32** at room temperature. At this temperature, the alkylmagnesium amide **(*R*)-34** could be generated, but as the reaction was held at -78 °C in order to generate good levels of selectivity, further amide formation, to

complete the cycle, could not be achieved at this temperature. In order to increase the reactivity, variables such as additives, amines and various magnesium species were studied, but no improvement was observed.[20] Resulting from this study of the catalytic asymmetric deprotonation, changing the starting dialkylmagnesium base **32** to a more reactive species was proposed. To this end, a simple synthetic method was employed to form new dialkyl- and diarylmagnesium species from commercially available Grignard reagents (**Scheme 1.13**).[1–3] The addition of 1,4-dioxane to a Grignard reagent, such as **39** or **40**, allows the disproportionation of the Schlenk equilibrium, resulting in the formation of the carbon-centred magnesium species dimesitylmagnesium Mes_2Mg (**41**) or di-*tert*-butylmagnesium *t*-Bu_2Mg (**42**).

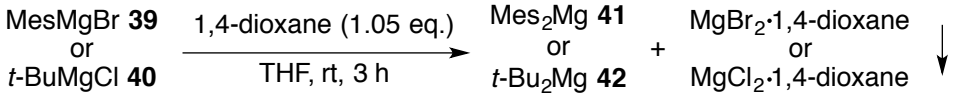

Scheme 1. 13

These new reagents were also applied to the catalytic reaction, but unfortunately, without further success. Nevertheless, a range of varied conditions were explored, among which was an increase in reaction temperature. Under a slightly elevated temperature of -40 °C, an extraordinarily high level of reactivity was observed, albeit with no selectivity (**Scheme 1.14**). In fact, these reaction conditions provided an 87% yield of the desired compound **(*S*)-37** but with only a 58:42 er.

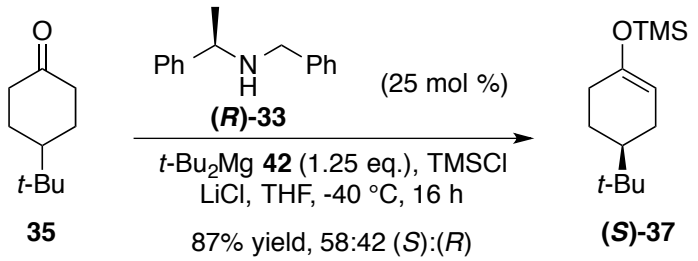

Scheme 1. 14

Following this observation, a series of experiments led to the conclusion that it was the dialkylmagnesium base **42**, and not the alkylmagnesium amide, which was responsible for the deprotonation of the ketone, notably without addition of the

organomagnesium reagent into the carbonyl unit, to deliver the silyl enol ether product **36**.[20] This realisation therefore led to the application of dialkylmagnesium reagents as a new base, which could function as an alternative to LDA.[22c] The presence of the bulky *t*-butyl group prevented nucleophilic attack into the ketone and due to its structure. The same reactivity has also been observed with the diarylmagnesium species Mes_2Mg.[22a] Further studies of these two species, to afford an energy efficient process towards kinetic deprotonation, was thus carried within the Kerr group.

1.2.2.Carbon centred deprotonations

In general, magnesium species are known to exhibit high thermally stability and generate fewer aggregation states than lithium species and, therefore, reactions employing magnesium bases have the potential to be carried at more accessible temperatures.[23] The ability of dialkyl- and diarylmagnesium species to perform as surrogates to LDA has been explored, and further optimisation with these reagents resulted in an efficient process for the formation of silyl enol ethers. Interestingly, as shown in **Table 1.1**, using stoichiometric quantities of electrophile, base and lithium chloride, the reaction afforded high reactivities at a convenient temperature of 0 °C, in the conversion of ketone **43** to silyl enol ether **44**. Under these conditions, *t*-Bu_2Mg **41** (**Entry 1**) and Mes_2Mg **42** (**Entry 2**) afforded 88% and 89% yields, respectively, of the desired silyl enol ether. Interestingly, with *t*-Bu_2Mg **41** the reaction was complete in only 1 h, whereas with Mes_2Mg **42**, the reaction required 16 h. It should be noted that, under similar conditions, using the corresponding lithium base, MesLi, only a poor 13% was observed. This difference in reactivity was explained by the presence of a competitive *C*-Silylation reaction.[20] Finally, the presence of LiCl salt was essential to enhance the reactivity of the base, as NMR spectroscopic analysis of the reaction in d_8-THF showed the presence of an ate complex $LiCl{\cdot}MgMes_2$ and the high reactivity observed for the desired transformation was attributed to this species.[22a]

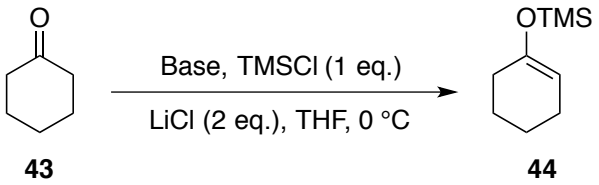

Scheme 1. 15

Entry	Base	Yield %
1	*t*-Bu_2Mg **42**	88
2	Mes_2Mg **41**	89

Table 1. 1

With the optimised conditions in hand, the substrate scope was explored and as depicted in **Figure 1.1** below, a series of cyclic ketone substrates were investigated.[22] In all cases, high yields of the silyl enol ether products (**45** – **53**) were afforded. The reactivity observed is remarkable but more importantly, the process displayed a high chemoselectivity for the kinetic enol ether product (**47**, **Figure 1.1**).

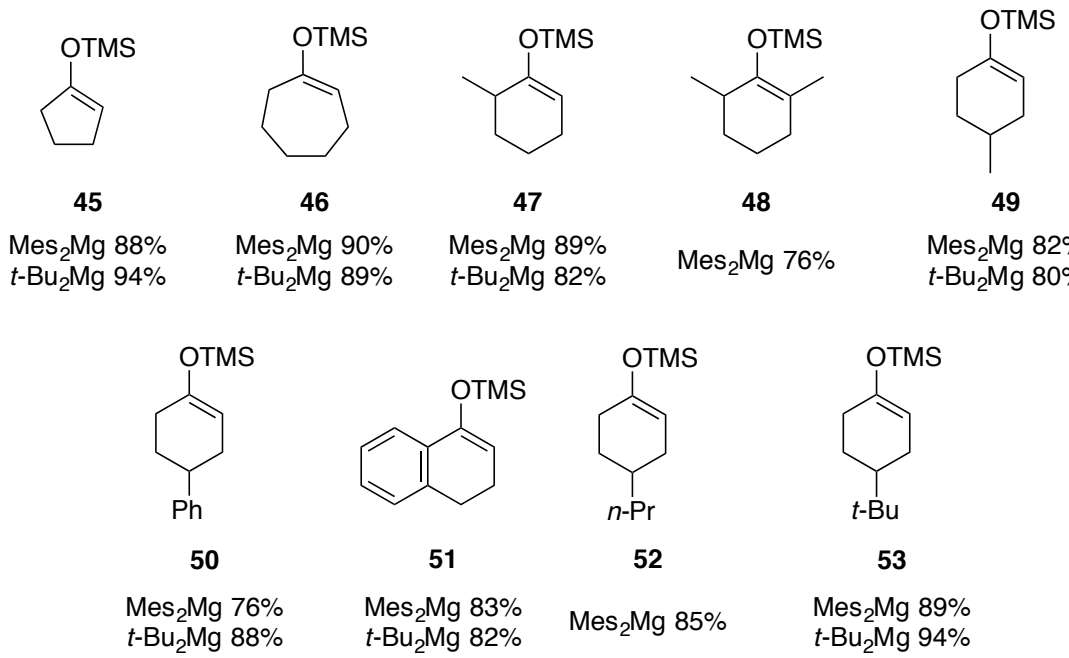

Figure 1. 1

Interestingly, the presence of a halide, as in compound **54** (**Scheme 1.16**),[22] did not lead to by-products derived from metal-halogen exchange, and afforded a high 98% conversion, providing a mild and efficient methodology for such halide-containing substrates. In contrast, the presence of such a halogen unit could prove problematic when a traditional lithium amide base is applied.

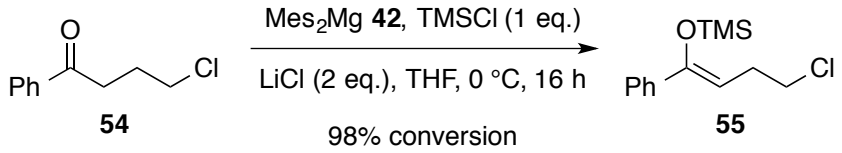

Scheme 1. 16

Having provided a process for silyl enol ether formation which afforded high levels of reactivity and chemoselectivity,[22] the Kerr group then focused their attention towards the development of an operationally simpler methodology. The carbon-centred bases were used as stock solutions, and were preformed from parent commercial Grignard reagents. To facilitate the adoption of such a reaction further, a one-pot process was developed, improving the reactivity of both bases to afforded high yields in only 1 h. As shown in **Scheme 1.17** below, the base was formed *in situ* by addition of 1,4-dioxane to the commercial Grignard reagent in the reaction mixture, and the reaction then performed under the previously developed conditions. As observed in **Table 1.2** the use of *t*-BuMgCl (**Entry 1**) afforded a 96% yield and MesMgBr (**Entry 2**) afforded 89% yield, respectively, of the silyl enol ether **44**.

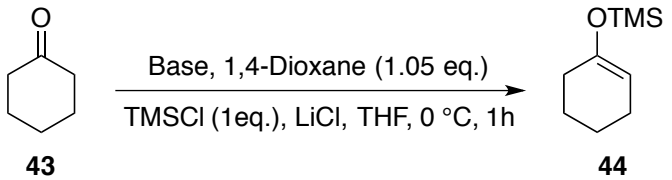

Scheme 1. 17

Entry	Base	Yield %
1	*t*-BuMgCl **40**	96
2	MesMgBr **39**	89

Table 1. 2

By developing these two main methodologies, the Kerr group has shown that a magnesium-derived base can not only perform a kinetic deprotonation of a ketone, but that the reaction can be carried out under mild temperature conditions, such as at 0 °C. To explore further the reactivity of such bases, the group then turned their attention towards other processes. As a first example of this, the Shapiro reaction was investigated.

1.2.3. The Shapiro Reaction

The Shapiro reaction was introduced in 1967,[24a] when the action of strong bases on tosyl hydrazones (**56**) was found to afford new, olefinic products (**Scheme 1.18**). The reaction was generally carried out using lithium amide bases, e.g. LDA, and upon application of two equivalents of the base, the alkenyllithium species **57** was formed. This intermediate can be quenched by the addition of an electrophile, to generate olefinic products such as **58**. Although much effort has been invested in the development of this reaction, the process remains extremely sensitive towards the stability of the lithium species present in solution, leading therefore to a series of cooling and warmings of the reaction mixture in order to afford good levels of reactivity.[24b]

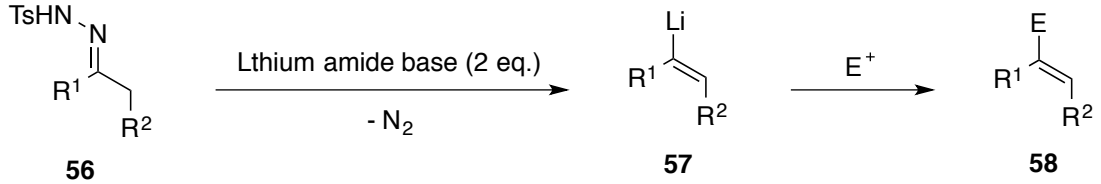

56 **57** **58**

Scheme 1. 18

In order to generate more stable intermediates, and thus a more facile process, the Kerr group employed their carbon-centred bases to the Shapiro reaction. Under the developed conditions, the reaction proceeded readily at a temperature of 40 °C, in a

facile process using Mes_2Mg as the carbon-centred base. Weinreb amides were used as electrophiles to quench the reaction, which generated various enones in a highly efficient manner (**Table 1.3**). As shown below, under the reaction conditions presented in **Scheme 1.19**, a range of enones **62** to **68** were generated in moderate to good yields (**Entries 1-7**).[25]

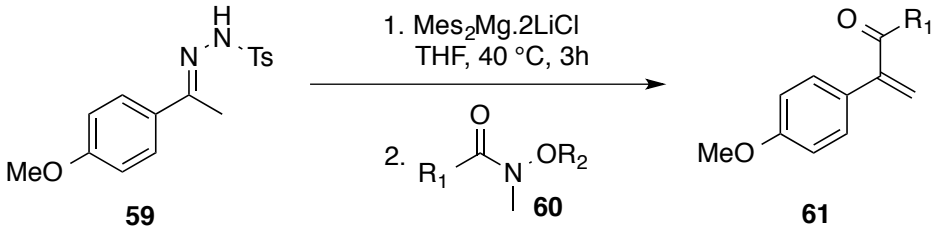

Scheme 1. 19

Entry	R^1,R^2	Quench conditions	Yield %
1	Ph, Me (**62**)	40 °C, 1 h	75
2	*t*-Bu, Me (**63**)	40 °C, 16 h	64
3	*i*-Pr, Me (**64**)	40 °C, 0.5 h	72
4	Et, Me (**65**)	40 °C, 1 h	77
5	Me, Me (**66**)	0 °C, 2 h	45
6	*t*-Bu, *t*-Bu (**67**)	40 °C, 1 h	53
7	CD_3, Me (**68**)	0 °C, 2 h	72

Table 1. 3

The recent advances made in this new area of carbon-centred magnesium bases are promising and exciting, as they afford increased reactivity, easy accessibility and higher temperature reactivity. Theses advantages allow these bases to be more energy efficient and therefore more environmentally friendly than their organolithium counterparts. Having explored the synthesis of silyl enol ethers, the Kerr group envisaged further exploring the applicability of these bases by studying new electrophiles. With this in mind, the generation of extremely valuable enol phosphates was envisaged, as such compounds are currently commonly synthesised

using lithium amide bases. Moreover, Miller, in 2002, has described the use of Grignard reagents for the formation of enol phosphates.[26] As described below, the use of various Grignard reagents on a range of ketones, allowed the formation of enol phosphates products from poor to excellent yields (**Scheme 1.20**, **Table 1.4**). The formation of **69** required the specific use of MesMgBr **39** (**Entry 3**), whilst the other Grignard reagents employed only afforded poor reactivity and small quantities of recovered starting material, demonstrating the potential for side reactions (**Entries 1 & 2**). On the other hand, the synthesis of **70** was extremely efficient, with all three bases used providing up to 98% isolated yield (**Entries 4-6**). Finally, when a less activated carbonyl was used for the formation of the desired enol phosphate **71**, an inefficient process resulted when MesMgBr was used (**Entry 7**, 32% yield and 17% starting material recovered). A more hindered and specific Grignard reagent 2,4,6-tri-*t*-butylphenylmagnesium bromide (TTBPMgBr) was required in this case, with increased quantity and prolonged reaction time. Under these conditions, the reaction afforded the desired product in 78% yield.

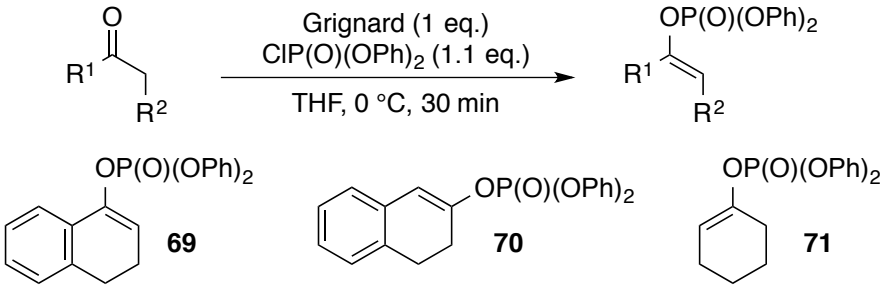

Scheme 1. 20

Entry	Enol phosphate	Grignard	Yield %	Recovered ketone %
1	**69**	*i*-PrMgCl	28	35
2	**69**	*t*-BuMgCl	14	18
3	**69**	MesMgBr	93	0
4	**70**	*i*-PrMgCl	97	0
5	**70**	*t*-BuMgCl	98	2
6	**70**	MesMgBr	97	0
7	**71**	MesMgBr	32	17
8[1]	**71**	TTBPMgBr	78	7

[1] TTBPMgBr (1.4 eq.), 24 h

Table 1. 4

Some useful information can be inferred from this study. Firstly, the use of Grignard reagents allowed the formation of enol phosphates under mild conditions, but more importantly, the reaction was highly substrate dependent. Moreover, the tetralone species, bearing a more acidic α-proton, were easily deprotonated, whereas cyclic ketones only afforded poor yields. Compared to the reactivity observed with the use of carbon-centred bases for the formation of silyl enol ethers, where cyclohexanones were converted to the desired enol silanes in high yields, it was clear that carbon-centred bases react very differently to their Grignard precursors, and their study in the formation of enol phosphates could lead to valuable results.

2. Proposed Work

The development of carbon-centred bases has shown that the mild reactivity displayed by these reagents can enable the deprotonation of carbonyl groups, and even promotes the Shapiro reaction. Furthermore, Grignard reagents have been shown to mediate the formation of enol phosphates.[26] It was therefore proposed to study the effects of carbon-centred bases in the formation of enol phosphates. Not only is there scope for performing the reaction under mild conditions, but a wider substrate scope may also be possible with these reagents, than those presented by the use of simple Grignard reagents as described by Miller.[26] We first envisaged developing novel conditions for the formation of enol phosphate from cyclic ketones, but moreover, we were interested in more reactive substrates, such as acetophenone and its derivatives. As shown below in **Scheme 1.21**, cyclic enol phosphates such as **61**-**74** and acetophenone derivative **75** to **78** were envisaged. With these substrates in hand, a wide range of examples will be available to study the reactivity of our bases.

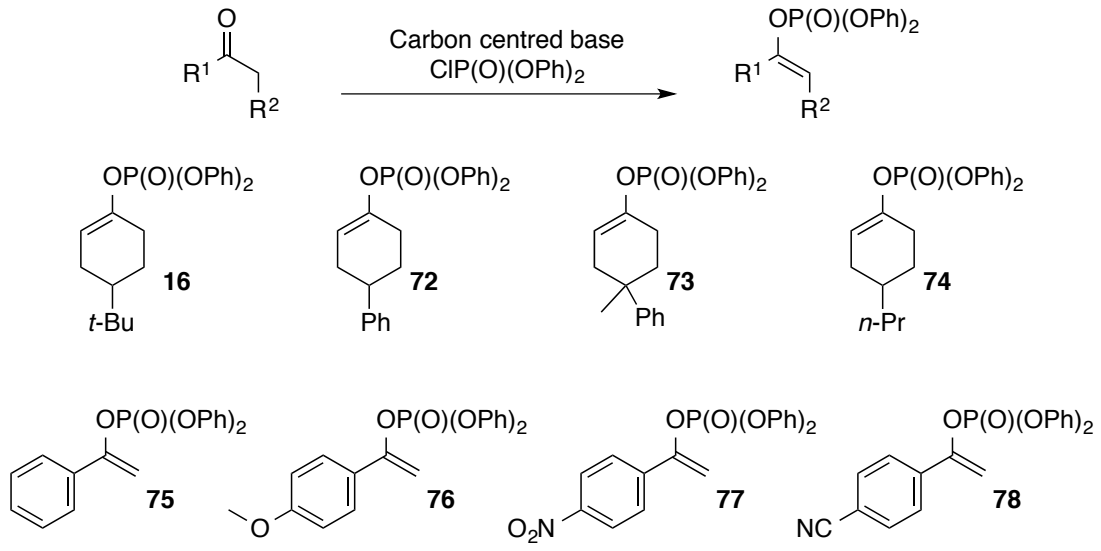

Scheme 1. 21

3. Results and Discussions

3.1. Primary Scope

Having previously established good levels of reactivity with cyclic ketones in the carbon-centred base-mediated formation of silyl enol ethers,[22] we initially focused our attention on varying the electrophile to generate cyclic enol phosphate products with these substrates.

3.1.1. Preparation of Carbon Centred Bases

To initiate these studies, we followed well-defined methodology for the preparation of the carbon centred bases, from the commercial Grignard reagents *t*-butylmagnesium chloride and mesitylmagnesium bromide. As shown below in **Scheme 1.22**, the addition of 1,4-dioxane to a freshly standardised solution of Grignard reagent in THF provided the carbon centred magnesium bases. The reaction was easily monitored, as a white precipitate, the $MgX_2 \cdot$1,4-dioxane complex, was gradually accumulated with stirring at room temperature. The resulting solution containing the carbon-centred base was then transferred into a separate flask, titrated and stored under an argon atmosphere.

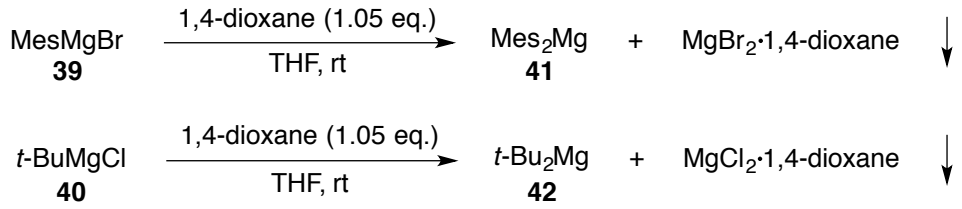

Scheme 1. 22

In order to prepare a cleaner, salt-free diorganomagnesium reagent, to avoid impurities present in the often variable quality commercial solution, preparation of the carbon-centred base was attempted directly from the alkyl/aryl halide (**Scheme 1.23**). Interestingly, the use of distilled mesityl bromide allowed clean formation of

the Grignard reagent in straightforward manner, which was then followed by the addition of 1,4-dioxane to provide the desired carbon-centred base **41**. Generally, this methodology worked extremely well, providing the same concentrations of base to those observed with the use of commercial solutions, and furthermore this method provided a clear yellow solution, which corresponded to previous observations on this chemistry from within our laboratories.[20,24] It should be noted that these conditions could also be applied to *t*-butylchloride, however the concentrations obtained for the Grignard reagent were lower, therefore making the concentration of **42** more dilute. It was thus decided to form this base using the commercial source of *t*-butylmagnesium chloride as higher concentrations of **42** were obtained this way.

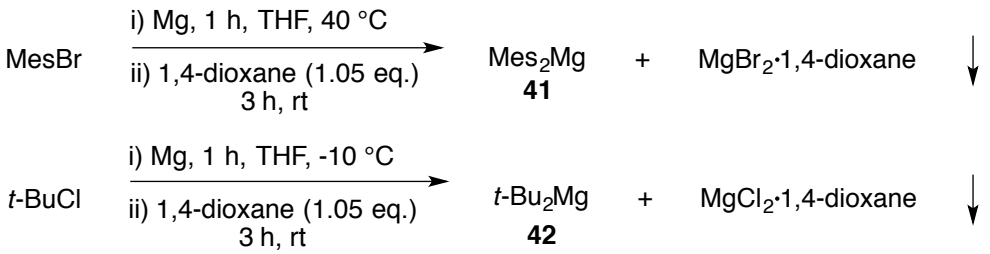

Scheme 1. 23

3.1.2. Benchmark Silyl Enol Ether Conditions

Having generated the desired bases, preliminary studies were carried out into the formation of enol phosphates, by first repeating the standard reaction conditions for the synthesis of silyl enol ethers,[22] as described in **Scheme 1.24**, in order to become familiar with the inert atmosphere techniques required for this chemistry. Having observed the same levels of conversion as described within the literature,[22] we then turned our attention towards the development of a novel methodology for the formation of enol phosphate products.

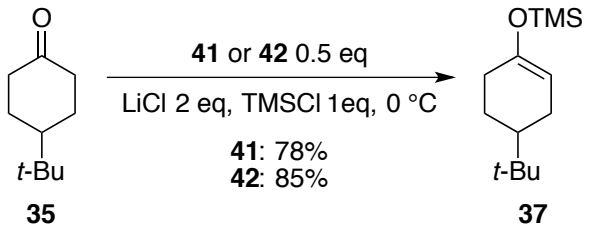

Scheme 1. 24

Preliminary attempts consisted of the direct replacement of the silyl electrophile with the phosphoryl chloride (**Scheme 1.25**), following the silyl enol ether formation conditions using the standard internal quench conditions (i.e. the ketone is slowly added to a mixture of base and electrophile in THF) developed by Corey.[27] Upon application of the carbon-centred base Mes_2Mg **41** at 0 °C, the reaction afforded only a poor 31% yield (**Entry 1**, **Table 1.5**), and even with a prolonged reaction time, similarly low levels of reactivity were observed (29% yield, **Entry 2**, **Table 1.5**). Previous work on the synthesis of silyl enol ethers had shown nearly quantitative levels of conversion for this substrate.[22a] However, employing a new electrophile, with a different reactivity, it was proposed to alter the aggregates present in solution *via* addition of a widely-used organic Lewis basic additive, namely DMPU. The use of such a Lewis base under similar conditions, however, failed to afford any improvement in the reactivity, as only a 33% yield was observed after 20 h (**Entry 4**, **Table 1.5**), which was similar to the levels of reactivity observed after only 1 h of reaction time. With the hypothesis of slower kinetics for this particular transformation, we elected to carry out the same reaction at room temperature instead of 0 °C. Interestingly, the reaction now afforded a good 59% yield after 1 h of reaction (**Entry 5**, **Table 1.5**), and a slight improvement to 66% isolated yield after 20 h reaction time (**Entry 6**, **Table 1.5**). To demonstrate the necessity of additives the reaction was carried out without at 0 °C in the absence of DMPU, affording a low 20% isolated yield (**Entry 7**, **Table 1.5**). Furthermore, a prolonged reaction time or addition of 1,4-dioxane to the reaction mixture both afforded lower levels of reactivity.

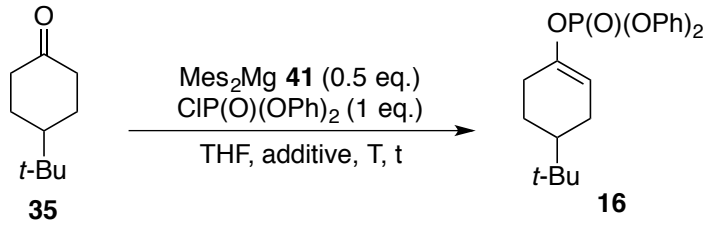

Scheme 1. 25

Entry	Time	Additive	Temperature	Yield %
1	8 h	LiCl (2eq.)	0 °C	31
2	16 h	LiCl (2eq.)	0 °C	29
3	1 h	DMPU (2eq.)	0 °C	30
4	20 h	DMPU (2eq.)	0 °C	33
5	1 h	DMPU (2eq.)	rt	59
6	20 h	DMPU (2eq.)	rt	66
7	1 h	-	0 °C	20

Table 1. 5

Having observed a small improvement in the reactivity, it was envisaged that a side reaction might be the cause of this low reactivity, and therefore more conventional external quench conditions were explored. Indeed, this common method consists of the addition of the electrophile after formation of the enolate in the reaction solution. Although it has shown great applicability when applied to lithium amide chemistry, [28] it only resulted in poor reactivity while applied to the above conditions. With a lack of reactivity with the current base, we turned our attention to the more active dialkylmangesium base *t*-Bu_2Mg **42**. Interestingly, when the reaction was carried out under standard conditions for the synthesis of silyl enol ethers, the reaction afforded a good 68% yield (**Entry 1**, **Table 1.6**). On the other hand, the use of DMPU, which allowed a higher reactivity when Mes_2Mg was employed, also improved the reactivity when *t*-Bu_2Mg was employed, reaching 75% yield (**Entry 2**, **Table 1.6**). Following these satisfying results when exploring higher temperature conditions (25 °C), no improvement of the reactivity was observed whether the reaction was carried out over 1 h (64% yield, **Entry 3**, **Table 1.6**) or even 8 h (**Entry 4**, **Table 1.6**).

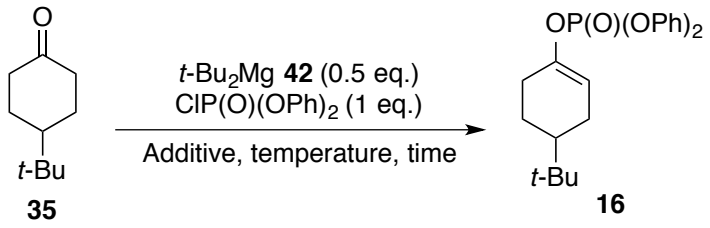

Scheme 1. 26

Run	Additive	Temperature	Time	Yield %
1	LiCl (2 eq.)	0 °C	1 h	68
2	DMPU(2 eq.)	0 °C	1 h	75
3	DMPU(2 eq.)	rt	1 h	64
4	DMPU(2 eq.)	rt	8 h	67

Table 1. 6

These primary results allowed us to study the reactivity of the electrophile, and, more importantly, showed the difference between the two carbon-centred bases. It appears that the more reactive *t*-Bu_2Mg generally provides higher levels of reactivity than those observed when Mes_2Mg was employed, but nevertheless the use of *t*-Bu_2Mg did not result in full conversion, with some recovery of starting material after the reaction was quenched. It was therefore hypothesised that the presence of the more reactive phosphoryl electrophile resulted in formation of addition products, such as **79 (Scheme 1.27**). Unfortunately, however, the isolation of this proposed by-product was never achieved.

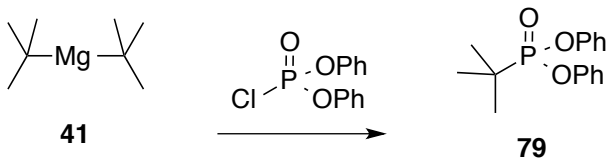

Scheme 1. 27

In order to control the range of various parameters in the reaction mixture such as the presence and appearance of novel aggregates in solution and the kinetic variation of

substrate and product concentration, a range of quench techniques were explored along with the classical parameters such as additive, time, and temperature.

3.2. Quench methods

Among the range of different parameters having influence on the reactivity of lithium bases is the quench conditions employed. The most classical methods employed are the internal quench (IQ) and the external quench (EQ).[29] To further improve our understanding of the effect of the various quench methodologies employed, the processes depicted in **Figure 1.2** were studied. The internal quench (IQ) consists of the slow addition of the ketone to a mixture containing the base and the electrophile. This method is generally employed to trap an unstable intermediate, such as a lithium enolate, which can undergo a C-alkylation. On the other hand, the external quench (EQ) consists of the addition of the electrophile after the formation of the enolate. This technique is often employed when the electrophile is highly reactive towards the base (*i.e.* addition of the base into the electrophile) or when the by-products of the reactions (*e.g.* LiCl) can modify the aggregation state of the base in the reaction mixture.[30]

Within the present studies, employing the phosphoryl chloride electrophile, we also included two relatively less common quench methodologies; the co-addition and the reverse addition. The co-addition method consists of the addition of the electrophile and the substrate as a single solution. This method therefore has the advantage of controlling the concentration of the substrate and electrophile in the reaction mixture at all times. This method was revealed to be extremely useful at higher temperatures, when the reactivity of the base was enhanced. On the other hand, the reverse addition inverts the classical internal quench; and the base is added to a solution containing a mixture of substrate and electrophile.

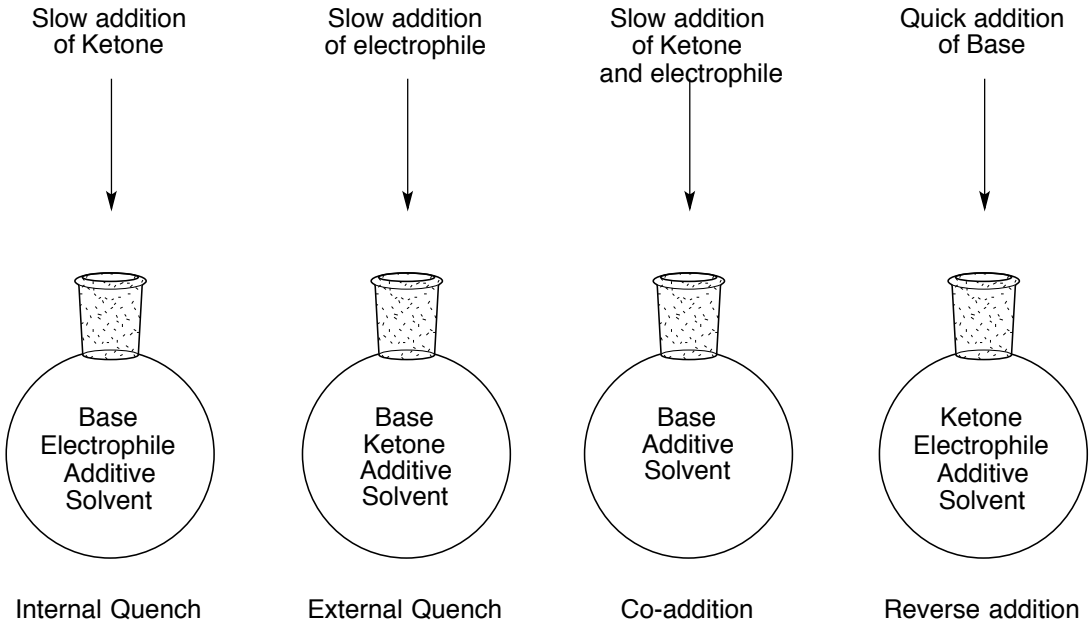

Figure 1. 2

3.3. Using Dimesitylmagnesium as Base

3.3.1. Exploring novel Quench Methods

With the range of quench conditions described above, we first explored these various options using Mes_2Mg as the base (**Scheme 1.28**). Indeed, our previous results have shown that this base afforded high yields when the reaction was carried out at room temperature. Upon application of the classical external quench conditions, the reaction afforded a lowered 31% yield of the desired product (**Entry 1**, **Table 1.7**). On the other hand, as shown in **Entry 2**, the use of the co-addition methodology resulted in a slight improvement (48% yield) to that those observed with the classical IQ conditions. Reverse quench conditions resulted in a decreased 35% isolated yield (**Entry 3**, **Table 1.7**).

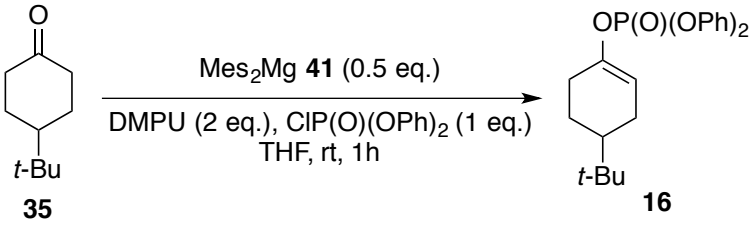

Scheme 1. 28

Entry	Quench	Yield %
1	EQ	31
2	Co-addition (1 h addition)	48
3	Reverse addition	35

Table 1. 7

This experiment allowed us to define the internal quench condition as the best quench conditions for the synthesis of enol phosphates using Mes_2Mg.

3.3.2. Additive Study

Having previously established the importance of the DMPU additive in the reaction mixture, we studied various DMPU loadings in the reaction. As shown in **Scheme 1.29** below, under IQ conditions at room temperature, decreasing the additive loading to 1 eq. afforded a lowered yield of 36% (**Entry 1**, **Table 1.8**), whereas upon increasing the additive amount to 4 eq. (**Entry 2**, **Table 1.8**), a higher 57% yield was obtained. On the other hand, further increase of the additive charge, to 6, 8 or 10 equivalents, generally decreased the overall yield, reaching a minimum of 41% (**Entries 3-5**, **Table 1.8**).

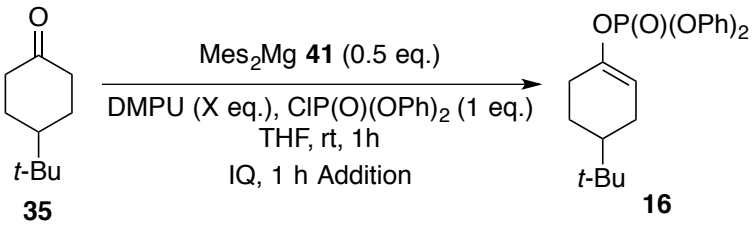

Scheme 1. 29

Entry	DMPU (X eq.)	Yield %
1	1	36
2	4	57
3	6	45
4	8	41
5	10	42

Table 1. 8

With the additive studied, one other parameter was worth exploring: the electrophile loading. Previously, the work carried out on the synthesis of silyl enol ethers had shown the optimal reactivity with a stoichiometric amount of the electrophile.

3.3.3. Electrophile Loading

Having obtained low levels of conversion to enol phosphates under these conditions, the electrophile stoichiometry was thus explored (**Scheme 1.30**). As shown in **Entry 1**, **Table 1.9** below, having 1.5 equivalents of the electrophile significantly increased the overall yield to afford 74% of the enol phosphate product. On the other hand, further increase to 2 or even 4 equivalents of electrophile afforded a lower 69% yield (**Entries 2 - 3**, **Table 1.9**).

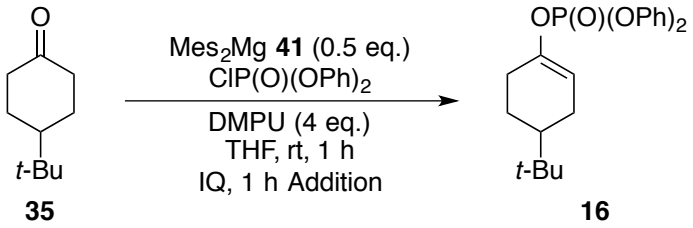

Scheme 1. 30

Entry	Electrophile (eq.)	Yield %
1	1.5	74
2	2	69
3	4	69

Table 1. 9

3.3.4. Base Mes_2Mg Loading

At the same time, striving to reduce the amount of waste generated through excesses of the electrophile, we envisaged an alternative increase in the quantity of base employed. As shown in **Scheme 1.31** below, with an increase to 0.75 eq., corresponding to 1.5 equivalents of active species present in solution, an excellent 91% isolated yield was obtained.

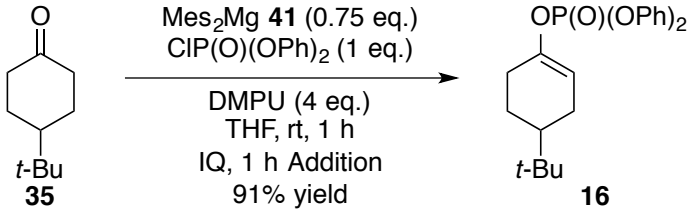

Scheme 1. 31

Increasing the temperature to 40 °C was also considered, but only low levels of reactivity were observed. Pleased by the levels of isolated yields observed with the kinetic deprotonation reaction using Mes_2Mg base for the formation of enol phosphate compounds, we then turned our attention to optimising the other base system, *t*-Bu_2Mg.

3.4. Using Di-*t*-butylmagnesium as Base

3.4.1. Exploring novel Quench Methods

We have previously shown that *t*-Bu_2Mg afforded higher levels of reactivity than that observed when Mes_2Mg was used. We therefore began by exploring the reactivity of this base under the two less common quench conditions; co-addition and reverse addition (**Scheme 1.32**). As observed below in **Entry 1**, **Table 1.10** when the reaction was carried out using the co-addition quench conditions, the reaction afforded an excellent 84% isolated yield of enol phosphate. In contrast, the use of the reverse addition conditions afforded only an 80% yield (**Entry 2**, **Table 1.10**).

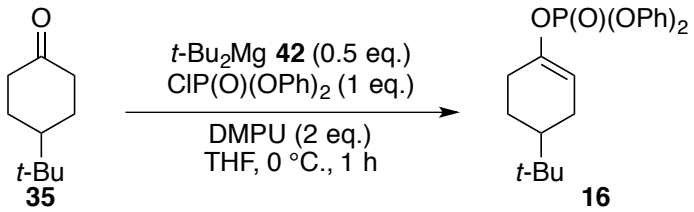

Scheme 1. 32

Entry	Conditions	Yield %
1	Co-addition	84
2	Reverse addition	80

Table 1. 10

Pleased by the high yields observed using the co-addition methodology, we explored the additive content under these quench conditions, but unfortunately no improvement was observed. Furthermore, we have shown with Mes_2Mg that when the reaction was carried out at temperatures above 0 °C, the reaction improved considerably; and this observation was also true for *t*-Bu_2Mg, where room temperature conditions showed higher yields. Interestingly, having re-explored the quench conditions at room temperature, the reverse addition conditions afforded high levels of reactivity. Thus we attempted to improve the reactivity further by exploring the additive loading.

3.4.2. Additive Study

The additive loading was explored under reverse addition conditions at room temperature as shown in **Scheme 1.33** below. Under such conditions, the absence of additive provide a high 84% yield (**Entry 1**, **Table 1.11**), with an steady increase in reactivity observed in the presence of the additive; starting from an 86% yield with 0.5 equivalents of DMPU and reaching a high 95% with 4 equivalents (**Entries 2-7**, **Table 1.11**). Interestingly, further increase of the additive loading decreased the reactivity slightly, to afford a 93% yield (**Entry 8**, **Table 1.11**), establishing the cut-off point of the additive loading at 4 equivalents.

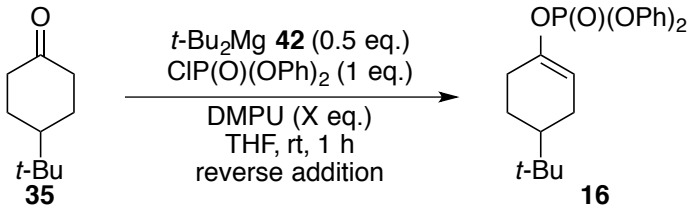

Scheme 1. 33

Entry	DMPU (eq.)	Yield %
1	0	84
2	0.5	86
3	1	88
4	1.5	90
5	2	91
6	3	94
7	4	95
8	5	93

Table 1. 11

So far, the highest levels of reactivity have been achieved using *t*-Bu_2Mg as base, under reverse addition conditions at room temperature with 4 equivalents of DMPU, delivering a 95% isolated yield of the enol phosphate. With this optimal result in hand, we further explored various parameters such as reaction time and dilution, to validate the robustness of the reaction. These studies showed that the reaction was

close to completion after 30 min, and that the concentration of the reaction had little effect on the reactivity. Considering all the kinetic parameters, and solubility parameters of various substrates, we decided to define our optimised conditions for this base as: 1 h reaction time, using the reverse addition protocol with 4 equivalents of DMPU.

The impact of DMPU was investigated by monitoring the ^{31}P NMR spectrum of the reaction mixture. We postulated that DMPU might not only help the disaggregation of the carbon-centred bases, but may also activate the electrophile, and this influence might be revealed in the ^{31}P NMR spectrum. Having explored various conditions, the appearance of two minor signals in the 31P NMR spectrum were observed, but in both cases they showed a constant increase in intensity, suggesting a by-product rather than a reaction intermediate. We conclude that DMPU promotes the disaggregation of the carbon-centred bases through coordination to the magnesium centre, thus increasing the reactivity of these reagents.

3.5. Optimised Conditions for Enol Phosphate Synthesis

So far we have focussed on optimisation of the kinetic deprotonation reaction using carbon centred bases Mes_2Mg and *t*-Bu_2Mg, for the formation of enol phosphates (**Scheme 1.34**). Both bases afforded the highest reactivity levels when carried out at room temperature using stoichiometric amounts of electrophile and 4 equivalents of DMPU, over 1 hour. In the case of Mes_2Mg, a slight excess of the base was required to afford 91% isolated yield of **16**, while a stoichiometric amount of *t*-Bu_2Mg was required to afford a 95% isolated yield of the desired product.

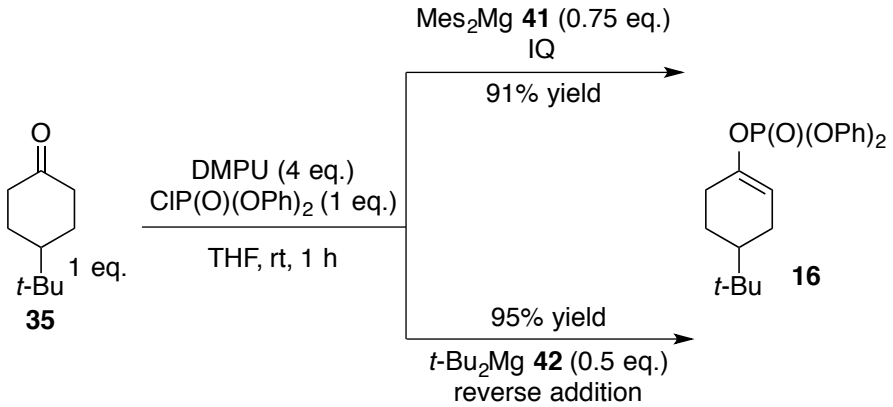

Scheme 1. 34

3.6. Substrate scope

With the optimised conditions in hand, we turned our attention towards the substrate scope. Although both bases performed to good levels, the high reactivity and low waste generated by *t*-Bu_2Mg led to our focus on this base for the exploration of the substrate scope.

*3.6.1. Substrate scope using base **42** t-Bu_2Mg*

With the conditions shown in **Scheme 1.35** below, a range of substrates were explored for the enol phosphate formation. A range of 4-substituted ketones led to the corresponding enol phosphate in good yields. For example, the 4-methyl derivative afforded **80** in 94% yield, while the product from the 4-phenyl substrate, **72**, was formed in a high yield of 90%. Quaternary centres in the substrate were tolerated, with 4-methyl-4-phenylcyclohexanone affording the corresponding enol phosphate **73** in an excellent 90% yield. In contrast, the *n*-Pr-containing enol phosphate **74** was only formed in 72% isolated yield. When the substituent contained a heteroatom such as OTBS, the enol phosphate **81** was formed in 80% yield, whereas the 4-dimethylamino-susbtituted enol phosphate **82** was generated in a moderate 75% isolated yield. With the monoprotected ethylene acetal of cyclohexane-1,4-dione, the enol phosphate **83** was generated in 67% yield. In the case of the more hindered ketone, menthone, a moderate 59% yield of enol phosphate **84** was obtained. Departing from substituted cyclohexanones, when acetophenone was used as the ketone, the corresponding enol phosphate **75** was only formed in trace amounts. More importantly, it was noted that no starting material was recovered, with full conversion to a mixture of unidentified materials. We postulated that, in the presence of a reactive enolate, such as in this case, aldol type reactions with the free ketone might be occurring.

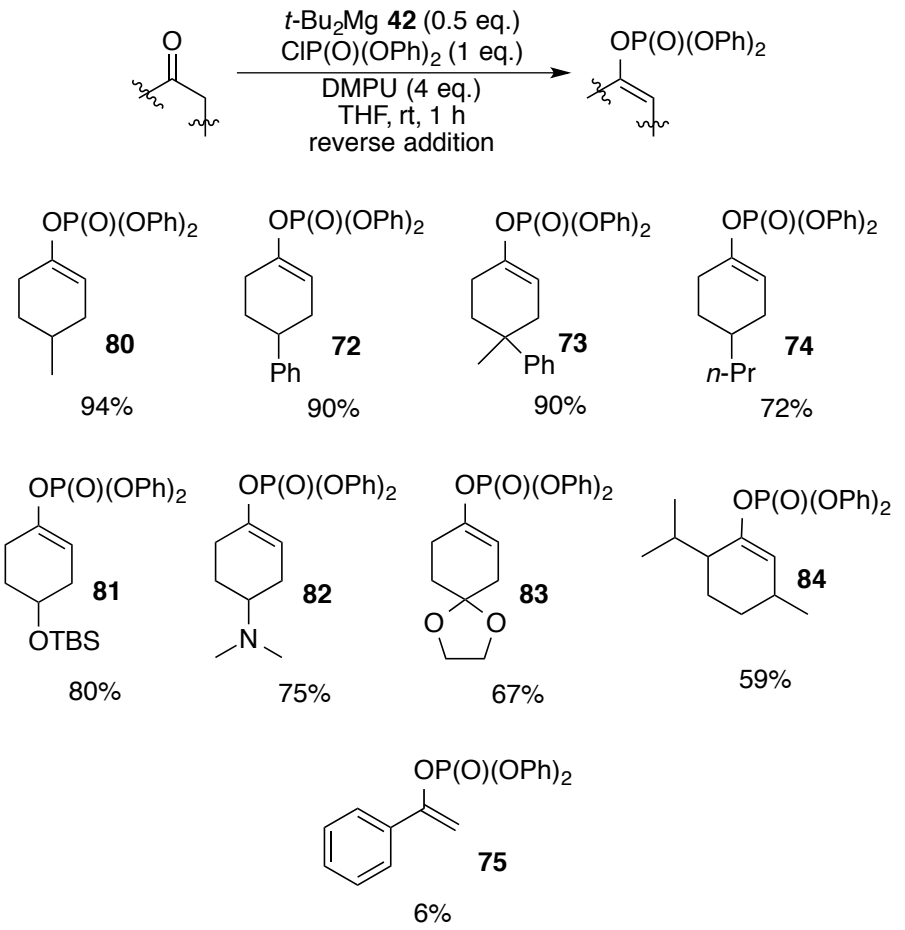

Scheme 1. 35

*3.6.2. Substrate scope using base **41** Mes_2Mg*

With this poor result in hand, we explored a range of conditions (*e.g.* temperature, addition, additive) in an attempt to generate sufficient levels of the desired enol phosphate **75**, but with little success. Interestingly, when the optimised conditions for Mes_2Mg were applied, however, we were pleased to obtain high levels of reactivity. Not only was the reaction clean, but we were able to isolate moderate to good levels of enol phosphate products. When the optimised conditions shown in **Scheme 1.36** were employed, the desired enol phosphate **75** was obtained in a good 77% isolated yield. With the acetophenone derivative bearing a halogen unit at the 4-position, a good 75% isolated yield of the desired compound **85** was obtained without any metal-halogen exchange observed. The presence of an electron-donating unit such as a *p*-methoxy unit had no detrimental effect, allowing a high 77% yield of **76**. Even in the presence of a sensitive cyano unit at the 4-position, a 68% yield of the enol

phosphate product **78** was obtained, without any addition product detected. The presence of a bulky mesityl unit only afforded a moderate 62% isolated yield of **86**, whereas the presence of the nitro unit led to only trace amounts (4% yield) of the desired enol phosphate **77**. Interestingly, no side reactions were observed in this case, with full recovery of the starting material after an aqueous quench, indicating that the presence of the nitro unit interacts with the carbon centred base in an unknown, but probably deactivating, fashion.

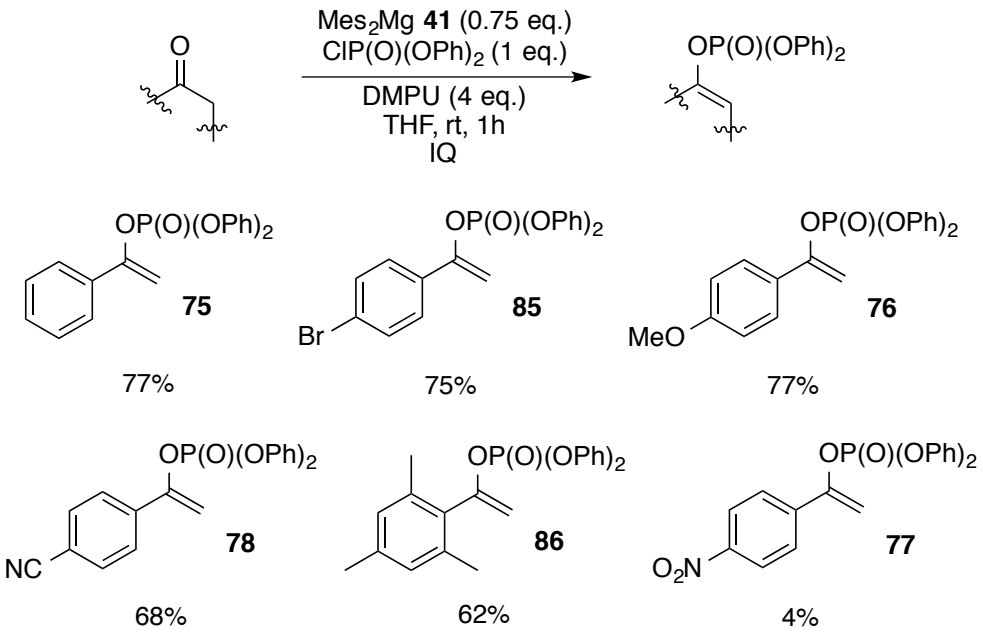

Scheme 1. 36

3.6.3. Demonstration of a Kinetic Deprotonation Process

Having successfully demonstrated the scope of enol phosphates accessible by our carbon-centred magnesium bases, we next studied 2-methyl cyclohexanone as a substrate, in order to investigate kinetic vs thermodynamic enol phosphate formation. As shown below in **Scheme 1.37**, both bases afforded solely the kinetic enol phosphate **5**, in 67% and 51% yields, using Mes_2Mg and *t*-Bu_2Mg, respectively.

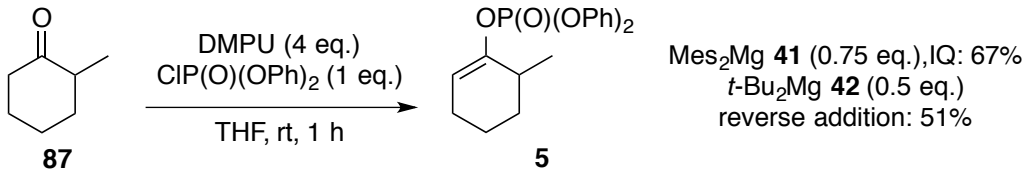

Scheme 1. 37

Thus far, we have developed a novel methodology for the synthesis of kinetic enol phosphate products, using carbon-centred bases. The deprotonation reaction, although requiring 4 equivalents of DMPU, was easily carried out at room temperature with either a slight excess of base for Mes_2Mg, or a stoichiometric amount of base for *t*-Bu_2Mg, and, more importantly, a stoichiometric amount of electrophile. We have shown that the exploration of the quench conditions was critical in obtaining high levels of reactivity, with up to 95% isolated of the desired enol phosphate being obtained following quench protocol optimisation. Further, this reaction displays a high reliability and scalability, with a reaction carried out on 10 g scale providing similar results. Having explored the reaction scope on a range of substrates, establishing the limitations of this methodology, we were interested in exploring further uses of these base systems.

3.7. Future work

We first breifly explored various electrophiles, such as chlorotriethylsilane (TESCl), as the corresponding enol silane could be easily used as a more stable substitute to a TMSCl, and as shown below (**Scheme 1.38**), under classical conditions only Mes_2Mg afforded the desired product **88**, in only a moderate 53% isolated yield. Interestingly, when the optimised conditions developed for the formation of enol phosphates were used, moderate to good levels of isolated yields were obtained; from a 64% yield using *t*-Bu_2Mg, to an 85% yield with the use of Mes_2Mg.

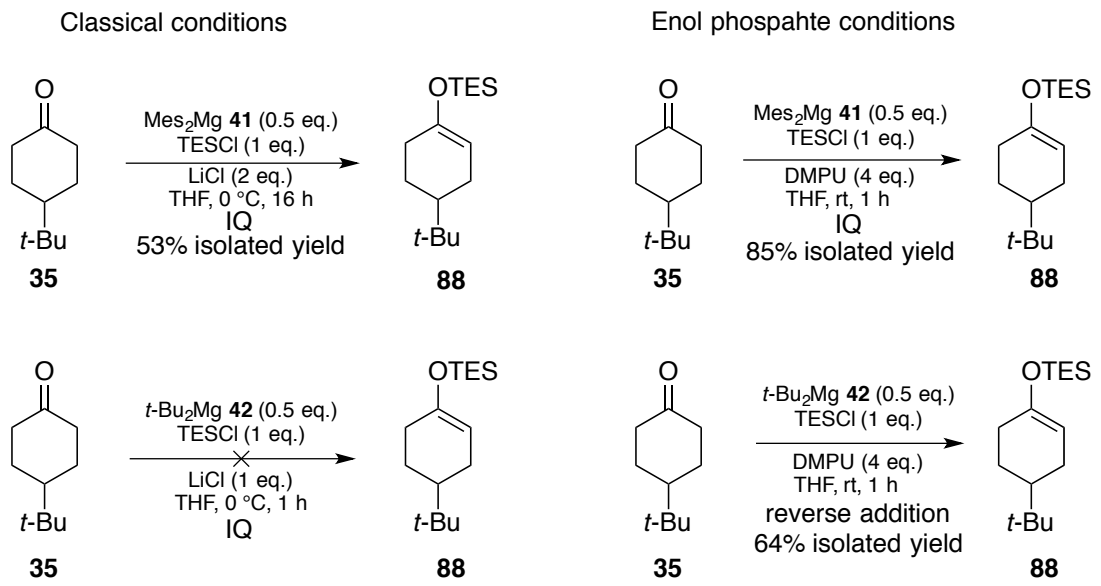

Scheme 1. 38

With the base providing access to a range of novel enol esters, we envisaged that the conditions developed herein could be used to explore a range of novel electrophile reagents.

Whilst studying the scope of our bases, we also explored the use of alternative substrates, such as enones. Interestingly, under the previously optimised conditions, an unexpected 1,4 addition was observed (**Scheme 1.39**). To explore the scope of this process, we targeted the simple methyl vinyl ketone **89** as substrate, and as shown below the reaction generated enol phosphate addition product **90** in up to 82% yield, with a selectivity of 1:1.1 towards the (*Z*)-enol phosphate.

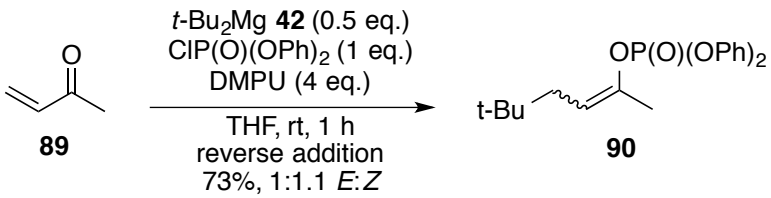

Scheme 1. 39

Although a brief study was carried out, varying the addition method, and changing the electrophile, no further improvement was made. We next studied the scope of this reaction with the use of various Grignard reagents, again with little success. Further, more detailed exploration of this unique process is, we believe warranted in future, and could lead to a useful and exploitable novel transformation.

While addressing the requirements in Chapter 5 for a range of enol phosphates, we came across another unexpected result. We were interested in generating the enol phosphate **92** from a mixture of diastereomers generated from ketone **91** (**Scheme 1.40**). It was observed that when the reaction was carried out in LDA at -78 °C (Conditions A), the desired enol phosphate **92** was obtained with retention of the starting material's 1:1 dr, as expected. In contrast, under the optimised conditions using our carbon-centred base **42**, the product **92** was obtained with a dr of 1:3.3, and in a high yield of 88%. Based on this, it seems plausible to propose some type of dynamic kinetic resolution, where the ketone appears to be deprotonated at the thermodynamic position, but only trapped at the kinetic site. Although we currently have no mechanistic evidence for this process, this unprecedented observation should be further explored in the future.

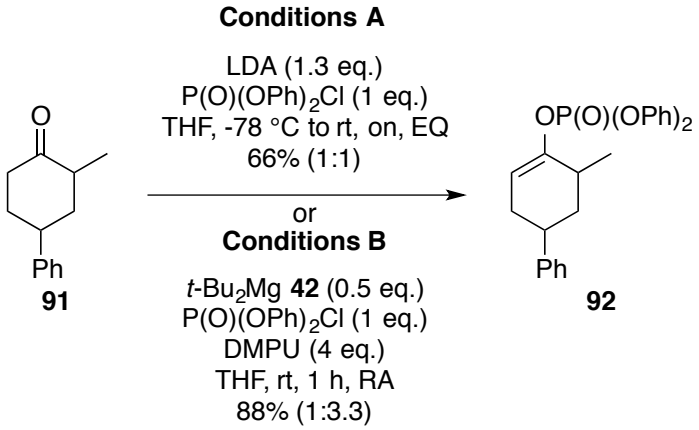

Scheme 1. 40

4. Summary

Herein we have developed a novel methodology for the synthesis of kinetic enol phosphates using carbon-centred magnesium bases. We have shown that both bases **41** and **42** display unique abilities in the formation of the desired enol phosphate products. Although both bases performed very efficiently at room temperature, for high levels of reactivity and chemoselectivity they required the presence of DMPU, and, more importantly, performed at optimal levels under different quench methodologies. Specifically, Mes_2Mg required classical internal quench conditions, whereas *t*-Bu_2Mg afforded the best results when employing reverse addition conditions. The most important observation was the scope of substrates these bases allowed, as a range of cyclic ketone substrates were readily converted to enol phosphates with the use of base **42**, whereas only Mes_2Mg **41** allowed successful transformation for more reactive and sensitive substrates such as acetophenone derivatives. Further, we have also uncovered interesting and novel process mediated by these carbon-centred bases, including an unexpected 1-4 addition reaction, and a dynamic kinetic resolution. Thus, the potential of these carbon-centred magnesium base species and the utility of their unique properties has been further established.

5. Experimental

5.1. General

All reagents were obtained from commercial suppliers (Aldrich, Lancaster, Alfa-aesar or Acros) and used without further purification, unless otherwise stated. Purification was carried out according to standard laboratory methods.[31]

- Dichloromethane, diethyl ether, hexane and toluene were obtained from an Innovative Technology, Pure Solv, SPS-400-5 solvent purification system.
- Tetrahydrofuran and 1,4-dioxane were dried by heating to reflux over sodium wire, using benzophenone ketyl as an indicator, then distilled under nitrogen.
- TMSCl, and TESCl were distilled from CaH_2 under argon and were stored over 4Å molecular sieves under an argon atmosphere.
- Acetophenone was purified by distillation over CaH_2 at 88 °C, 18 mbar.
- DMPU and diphenylphosphoryl chloride were distilled from CaH_2 under high vacuum and were stored over 4 Å molecular sieves under an argon atmosphere.
- Methyl vinyl ketone was distilled under argon by applying a slight vacuum and the distillate was collected in a cooled flask (-78 °C) filled and stored over 4 Å molecular sieves under an argon atmosphere.
- Organometallic reagents were standardised by titration using salicylaldehyde phenylhydrazone.[32]
- 4-*tert*-Butylcyclohexanone, 4-phenylcyclohexanone 4-methyl-4-phenylcyclohexanone,[33] 4'-bromoacetophenone, 4'-methoxyacetophenone, 4-acetylbenzonitrile, mesitylethanone, 1,4-dioxaspiro[4.5]decan-8-one and 4'-nitroacetophenone were purified by recrystallization from hexane and were dried under vacuum (0.005 mbar) for 16 h.
- 4-*n*-propylcyclohexanone, (±)-menthone, 4-methylcyclohexanone4-methylcyclohexanone, 4-((*tert*-butyldimethylsilyl)oxy)cyclohexanone,[34] 4-(dimethylamino)cyclohexanone,[35] acetophenone, and 2-methylcyclohexanone

were dried by distillation over $CaCl_2$ and were stored under argon over 4 Å molecular sieves.

Thin layer chromatography was carried out using CamLab silica plates, coated with fluorescent indicator UV_{254}, and analysed using a Mineralight UVGL-25 lamp.

Flash column chromatography was carried out using Prolabo silica gel (230-400 mesh).

IR spectra were recorded carried out on a SHIMADZU IRAFFINITY-1 spectrophotometer.

^{1}H, ^{13}C and ^{31}P NMR spectra were recorded on a Bruker DPX 400 spectrometer at 400 MHz, 100 MHz, and 162 MHz, respectively. Chemical shifts are reported in ppm. Coupling constants are reported in Hz and refer to $^{3}J_{H\text{-}H}$ interactions unless otherwise specified.

5.2. General Procedures

General Procedure A: Deprotonations of Ketones Using Carbon-Centred-Bases - IQ conditions

A solution of base (0.5 M solution in THF, 0.5 eq., 0.5 mmol, 1 mL, unless otherwise stated) was added to a Schlenk flask which had been flame-dried under vacuum (0.005 mbar), purged with argon three times and allowed to cool to room temperature (if LiCl or any other salt was used as additive it was be flame-dried along with the Schlenk tube, taking care not to melt the salts). THF (10 mL) was added and the mixture was stirred to the stated temperature. The additive (any additive in a solution state at room temperature) and the electrophile were added and stirred at the stated temperature for 5 min, then the ketone was added as a solution in THF (2 mL) over 1 h using a syringe pump and stirred at the stated temperature. After the stated time the reaction mixture was quenched with a saturated solution of $NaHCO_3$ (10 mL) and allowed to warm to room temperature. The mixture was

extracted with Et_2O (50, 25, 25 mL) and the organic layers dried over $MgSO_4$. Removal of the solvent *in vacuo* gave an oil which was purified by column chromatography on silica gel using 0-30 % Et_2O in petroleum ether (40-60 °C) to give the desired product.

General Procedure B: Deprotonations of Ketones Using Carbon-Centred Bases – EQ Conditions

A solution of base (0.5 M solution in THF, 0.5 eq., 0.5 mmol, 1 mL) was added to a Schlenk flask, which was flame-dried under vacuum (0.005 mbar), purged with argon three times and allowed to cool to room temperature (if LiCl or any other salt was used as additive it was be flame-dried along with the Schlenk tube, taking care not to melt the salts). THF (9 mL) was added and the reaction mixture was stirred at the stated temperature. The additives (any additive in a solution state at room temperature) were added and the reaction mixture stirred at the stated temperature for 5 min, then the ketone was added as a solution in THF (1 mL) dropwise (unless otherwise stated). The electrophile was added as solution in THF (2 mL) over 1 h using a syringe pump and stirred at the stated temperature (unless otherwise stated). After the stated time, the mixture was quenched with a saturated solution of $NaHCO_3$ (10 mL) and allowed to warm to room temperature. The mixture was extracted with Et_2O (50, 25, 25 mL) and the organic layers dried over $MgSO_4$. Removal of the solvent *in vacuo* gave an oil which was purified by column chromatography on silica gel using 0-30 % Et_2O in petroleum ether (40-60 °C) to give the desired product.

General Procedure C: Deprotonations of Ketones Using Carbon-Centred Bases - Co-Addition Conditions

A solution of base (0.5 M solution in THF, 0.5 eq., 0.5 mmol, 1 mL) was added to a Schlenk flask which was flame-dried under vacuum (0.005 mbar), purged with argon three times and allowed to cool to room temperature (if LiCl or any other salt was used as additive it was be flame-dried along with the Schlenk tube, taking care not to melt the salts). THF (9 mL) was added and the mixture was stirred to the stated temperature. The additives (any additive in a solution state at room temperature) were added and the reaction mixture stirred at the stated temperature for 5 min. The

ketone and the electrophile were added as solution in THF (2 mL) over 1 h using a syringe pump and stirred at the stated temperature (unless otherwise stated). After the stated time the mixture was quenched with a saturated solution of $NaHCO_3$ (10 mL) and allowed to warm to room temperature. The mixture was extracted with Et_2O (50, 25, 25 mL) and the organic layers dried over $MgSO_4$. Removal of the solvent *in vacuo* gave an oil which was purified by column chromatography on silica gel using 0-30 % Et_2O in petroleum ether (40-60 °C) to give the desired product.

General Procedure D: Deprotonations of Ketones Using Carbon-Centred Bases - Reverse Addition Conditions

A Schlenk flask was flame-dried under vacuum (0.005 mbar), purged with argon three times and allowed to cool to room temperature (if LiCl or any other salt was used as additive it was be flame-dried along with the Schlenk tube, taking care not to melt the salts). Following this the additives (any additive in a solution state at room temperature), the ketone and the electrophile were added and stirred at the stated temperature for 5 min. A solution of base (0.5 M solution in THF, 0.5 eq., 0.5 mmol, 1 mL) was added dropwise into the reaction mixture over 5 min and the reaction mixture was then stirred at the stated temperature. After the stated time the reaction mixture was quenched with a saturated solution of $NaHCO_3$ (10 mL) and allowed to warm to room temperature. The mixture was extracted with Et_2O (50, 25, 25 mL) and the organic layers dried over $MgSO_4$. Removal of the solvent *in vacuo* gave an oil which was purified by column chromatography on silica gel using 0-30 % Et_2O in petroleum ether (40-60 °C) to give the desired product.

*5.2.1. Preparation of Carbon Centred Bases **41** and **42***

Experimental procedure **Scheme 1.22**

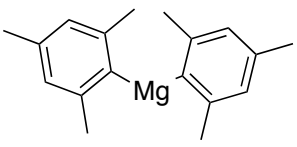

41

To a solution of MesMgBr (1 M solution in THF, 100 mL, 100 mmol) in a Schlenk tube under argon at r.t. was added 1,4-dioxane (1.05 eq., 105 mmol, 9.25 g, 8.95 mL)

steadily over 5 min. The mixture was stirred vigorously for 3 h before discontinuation of the stirring. The mixture (now a dark solution with fine white precipitate) was then left to settle for 72 h. After this time, the precipitate had settled to a thick white layer at the bottom of the Schlenk tube, allowing removal of the yellow Mes_2Mg solution, *via* cannula, to a previously flame-dried and purged pear-shaped flask. Care was taken to avoid withdrawing any of the precipitate. The Mes_2Mg solution was standardised before use using salicylaldehyde phenylhydrazone as the indicator. The molarity of the Mes_2Mg solution was typically 0.5 M (100 % conversion of MesMgBr to Mes_2Mg, yield typically ~ 90 mL, ~ 90%).

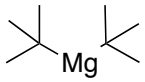

42

To a solution of *t*-BuMgCl (1 M solution in THF, 100 mL, 100 mmol) in a Schlenk tube under argon at r.t. was added 1,4-dioxane (1.05 eq., 105 mmol, 9.25 g, 8.95 mL) steadily over 5 min. The mixture was stirred vigorously for 3 h before discontinuation of the stirring. The mixture (now a dark solution with fine white precipitate) was then left to settle for 72 h. After this time, the precipitate had settled to a thick white layer at the bottom of the Schlenk tube, allowing removal of the yellow *t*-Bu_2Mg solution, *via* cannula, to a previously flame-dried and purged pear-shaped flask. Care was taken to avoid withdrawing any of the precipitate. The *t*-Bu_2Mg solution was standardised before use using salicylaldehyde phenylhydrazone as indicator. The molarity of the $^tBu_2Mg$ solution was typically 0.5 M (100 % conversion of *t*-BuMgCl to *t*-Bu_2Mg, yield typically ~ 90 mL, ~ 90%).

Experimental procedure **Scheme 1.23**

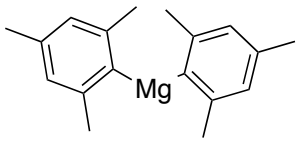

41

A Schlenk flask was flame-dried under vacuum (0.005 mbar), purged three times with argon and allowed to cool to room temperature before the addition of magnesium turnings (1.9 g, 80 mmol). THF (80 mL) was then added, followed by a

dropwise addition of MesBr (15.9 g, 12.24 mL, 80 mmol). A cold finger was quickly swapped with the Suba Seal and the Schlenk flask was heated slowly to 40 °C. After 5 min, a reflux of the THF was observed due to initiation of the Grignard reaction. After 30 min, the end of the reflux was observed and the mixture was stirred at 40 °C for a further 30 min, before being allowed to cool to room temperature. The solution of MesMgBr was standardised with salicylalhdehyde phenylhydrazone, then 1.4-dioxane (1.05 eq., 105 mmol, 9.25 g, 8.95 mL) was added dropwise and the reaction mixture stirred at room temperature. The reaction mixture (now a yellow solution with a fine white precipitate) was then left to settle for 72 h. After this time, the precipitate had settled to a thick white layer at the bottom of the Schlenk tube, allowing removal of the yellow Mes_2Mg solution, *via* cannula, to a previously flame-dried and purged pear-shaped flask. Care was taken to avoid withdrawing any of the precipitate. The Mes_2Mg solution was standardised before use using salicylaldehyde phenylhydrazone as the indicator. The molarity of the Mes_2Mg solution was typically 0.5 M (100 % conversion of MesMgBr to Mes_2Mg, yield typically ~ 90 mL, ~ 90%).

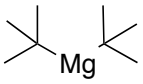

42

A Schlenk flask was flame-dried under vacuum (0.005 mbar), purged three times with argon and allowed to cool to room temperature before the addition of magnesium turnings (1.9 g, 80 mmol). THF (80 mL) was added and the reaction mixture was then cooled to -10 °C, followed by a dropwise addition of *t*-BuMgCl (31.8 g, 24.48 mL, 160 mmol). Great care was taken to avoid warming the reaction mixture by controlling the addition rate. The solution of *t*-BuMgCl was standardised with salicylalhdehyde phenylhydrazone, and 1.4-dioxane (1.05 eq., 105 mmol, 9.25 g, 8.95 mL) was added dropwise to the reaction mixture, which was then stirred at room temperature. The reaction mixture (now a dark solution with fine white precipitate) was then left to settle for 72 h. After this time, the precipitate had settled to a thick white layer at the bottom of the Schlenk tube, allowing removal of the dark *t*-Bu_2Mg solution, *via* cannula, to a previously flame-dried and purged pear-shaped

flask. Care was taken to avoid withdrawing any of the precipitate. The *t*-Bu_2Mg solution was standardised before use using salicylaldehyde phenylhydrazone as indicator. The molarity of the *t*-Bu_2Mg solution was typically 0.25 M.

5.3. Deprotonation Reactions

5.3.1. Benchmark Deprotonation Reaction

Scheme 1.24

Following General Procedure A for the deprotonation reaction, data are presented as (a) Mg base, (b) reaction temperature, (c) additives, (d) amount of additive, (e) amount of TMSCl, (f) ketone, (g) amount of ketone, (h) reaction time, (i) isolated yield.

Entry 1: General Procedure A: (a) Mes_2Mg, (b) 0 °C, (c) LiCl, (d) 84 mg, 2 eq., (e) 0.17 mL, 1 mmol, (f) 4-*tert*-butylcyclohexanone, (g) 154 mg, 1 mmol, (h) 1 h, (i) 177 mg, 78%

Entry 2: General Procedure A: (a) *t*-Bu_2Mg, (b) 0 °C, (c) LiCl, (d) 84 mg, 2 eq., (e) 0.17 mL, 1 mmol, (f) 4-*tert*-butylcyclohexanone, (g) 154 mg, 1 mmol, (h) 1 h, (i) 150 mg, 85%

(4-(*tert*-butyl)cyclohexenyloxy)trimethylsilane,[36] **37**:

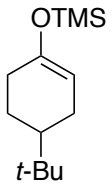

Colorless oil

ν_{max}: 1673 cm^{-1}.

^{1}H NMR (400 MHz, $CDCl_3$): δ 4.83-4.87 (m, 1H, C=CH), 1.95-2.14 (m, 3H, CH, CH_2), 1.75-1.86 (m, 2H, CH_2), 1.17-1.31 (m, 2H, CH_2), 0.87 (s, 9H, $(CH_3)_3$), 0.18 (s, 9H, $Si(CH_3)_3$.
^{13}C NMR (400 MHz, $CDCl_3$): δ 150.4, 104.1, 44.1, 32.2, 31.1, 27.4, 25.2, 24.5, 0.44.

Scheme 1.25

Following general procedure A for the deprotonation reaction, data are presented as (a) Mg base, (b) reaction temperature, (c) additives, (d) amount of additive, (e) amount of $ClP(O)(OPh)_2$, (f) ketone, (g) amount of ketone, (h) reaction time, (i) isolated yield.

Table 1.5

Entry 1: General Procedure A: (a) Mes_2Mg, (b) 0 °C, (c) LiCl, (d) 84 mg, 2 eq., (e) 0.21 mL, 1 mmol, (f) 4-*tert*-butylcyclohexanone, (g) 154 mg, 1 mmol, (h) 8 h, (i) 119 mg, 31%

Entry 2: General Procedure A: (a) Mes_2Mg, (b) 0 °C, (c) LiCl, (d) 84 mg, 2 eq., (e) 0.21 mL, 1 mmol, (f) 4-*tert*-butylcyclohexanone, (g) 154 mg, 1 mmol, (h) 16 h, (i) 112 mg, 29%

Entry 3: General Procedure A: (a) Mes_2Mg, (b) 0 °C, (c) DMPU, (d) 0.24 mL, 2 eq., (e) 0.21 mL, 1 mmol, (f) 4-*tert*-butylcyclohexanone, (g) 154 mg, 1 mmol, (h) 1 h, (i) 116 mg, 30%

Entry 4: General Procedure A: (a) Mes_2Mg, (b) 0 °C, (c) DMPU, (d) 0.24 mL, 2 eq., (e) 0.21 mL, 1 mmol, (f) 4-*tert*-butylcyclohexanone, (g) 154 mg, 1 mmol, (h) 16 h, (i) 127 mg, 33%

Entry 5: General Procedure A: (a) Mes_2Mg, (b) rt, (c) DMPU, (d) 0.24 mL, 2 eq., (e) 0.21 mL, 1 mmol, (f) 4-*tert*-butylcyclohexanone, (g) 154 mg, 1 mmol, (h) 1 h, (i) 228 mg, 59%

Entry 6: General Procedure A: (a) Mes_2Mg, (b) rt, (c) DMPU, (d) 0.24 ml, 2 eq,. (e) 0.21 mL, 1 mmol, (f) 4-*tert*-butylcyclohexanone, (g) 154 mg, 1 mmol, (h) 20 h, (i) 255 mg, 66%

Entry 7: General Procedure A: (a) Mes_2Mg, (b) rt, (c) -, (d)-, (e) 0.21 mL, 1 mmol, (f) 4-*tert*-butylcyclohexanone, (g) 154 mg, 1 mmol, (h) 1 h, (i) 77 mg, 20%

4-(*tert*-butyl)cyclohexenyl diphenyl phosphate[37] **16**:

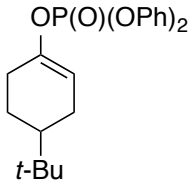

Chiral HPLC analysis: Chiracel OD-H column, 1% IPA in *n*-hexane, 1.4 mL/minute flow rate, 254 nm detector, t_R (+) = 31.65 min and t_R (-) = 33.67 min.
ν_{max}: 1690, 1191, 963 cm^{-1}.
^1H NMR (400 MHz, $CDCl_3$): δ 7.38-7.34 (m, 4H, ArH), 7.26-7.18 (m, 6H, ArH), 5.57-5.55 (m, 1H, C=CH), 2.29-2.25 (m, 2H), 2.09-2.08 (m, 1H), 1.89-1.85 (m, 2H), 1.37-1.29 (m, 2H), 0.88 (s, 9H, $C(CH_3)_3$).
^{13}C NMR (100 MHz, $CDCl_3$): δ 150.2, 147.3, 129.2, 124.8, 119.6, 111.3, 42.7, 31.6, 28.2, 26.8, 24.5, 23.5;
^{31}P NMR (400 MHz, $CDCl_3$): δ -17.4.

Scheme 1.26

Following General Procedure A for the deprotonation reaction, data are presented as (a) Mg base, (b) reaction temperature, (c) additives, (d) amount of additive, (e)

amount of $ClP(O)(OPh)_2$, (f) ketone, (g) amount of ketone, (h) reaction time, (i) isolated yield.

Table 1.6

Entry 1: General Procedure A: (a) *t*-Bu_2Mg, (b) 0 °C, (c) LiCl, (d) 84 mg, 2 eq., (e) 0.21 mL, 1 mmol, (f) 4-*tert*-butylcyclohexanone, (g) 154 mg, 1 mmol, (h) 1 h, (i) 262 mg, 68%

Entry 2: General Procedure A: (a) *t*-Bu_2Mg, (b) 0 °C, (c) DMPU, (d) 0.24 mL, 2 eq., (e) 0.21 mL, 1 mmol, (f) 4-*tert*-butylcyclohexanone, (g) 154 mg, 1 mmol, (h) 1 h, (i) 289 mg, 75%

Entry 3: General Procedure A: (a) *t*-Bu_2Mg, (b) rt, (c) DMPU, (d) 0.24 mL, 2 eq., (e) 0.21 mL, 1 mmol, (f) 4-*tert*-butylcyclohexanone, (g) 154 mg, 1 mmol, (h) 1 h, (i) 247 mg, 64%

Entry 4: General Procedure A: (a) *t*-Bu_2Mg, (b) rt, (c) DMPU, (d) 0.24 mL, 2 eq., (e) 0.21 mL, 1 mmol, (f) 4-*tert*-butylcyclohexanone, (g) 154 mg, 1 mmol, (h) 8 h, (i) 258 mg, 67%

Scheme 1.28

Following General Procedures for the deprotonation reaction, data are presented as (a) Mg base, (b) reaction temperature, (c) additives, (d) amount of additive, (e) amount of $ClP(O)(OPh)_2$, (f) ketone, (g) amount of ketone, (h) reaction time, (i) isolated yield.

Table 1.7

Entry 1: General Procedure B: (a) Mes_2Mg, (b) rt, (c) DMPU, (d) 0.24 mL, 2 eq., (e) 0.21 mL, 1 mmol, (f) 4-*tert*-butylcyclohexanone, (g) 154 mg, 1 mmol, (h) 1 h, (i) 119 mg, 31%

Entry 1: General Procedure C: (a) Mes_2Mg, (b) rt, (c) DMPU, (d) 0.24 mL, 2 eq., (e) 0.21 mL, 1 mmol, (f) 4-*tert*-butylcyclohexanone, (g) 154 mg, 1 mmol, (h) 1 h, (i) 185 mg, 48%

Entry 1: General Procedure D: (a) Mes_2Mg, (b) rt, (c) DMPU, (d) 0.24 mL, 2 eq., (e) 0.21 mL, 1 mmol, (f) 4-*tert*-butylcyclohexanone, (g) 154 mg, 1 mmol, (h) 1 h, (i) 135 mg, 35%

Scheme 1.29

Following General Procedure A for the deprotonation reaction, data are presented as (a) Mg base, (b) reaction temperature, (c) additives, (d) amount of additive, (e) amount of $ClP(O)(OPh)_2$, (f) ketone, (g) amount of ketone, (h) reaction time, (i) isolated yield.

Table 1.8

Entry 1: General Procedure A: (a) Mes_2Mg, (b) rt, (c) DMPU, (d) 0.12 mL, 1 eq., (e) 0.21 mL, 1 mmol, (f) 4-*tert*-butylcyclohexanone, (g) 154 mg, 1 mmol, (h) 1 h, (i) 138 mg, 36%

Entry 2: General Procedure A: (a) Mes_2Mg, (b) rt, (c) DMPU, (d) 0.48 mL, 4 eq., (e) 0.21 mL, 1 mmol, (f) 4-*tert*-butylcyclohexanone, (g) 154 mg, 1 mmol, (h) 1 h, (i) 220 mg, 57%

Entry 3: General Procedure A: (a) Mes_2Mg, (b) rt, (c) DMPU, (d) 0.72 mL, 6 eq., (e) 0.21 mL, 1 mmol, (f) 4-*tert*-butylcyclohexanone, (g) 154 mg, 1 mmol, (h) 1 h, (i) 173 mg, 45%

Entry 4: General Procedure A: (a) Mes_2Mg, (b) rt, (c) DMPU, (d) 0.96 mL, 8eq., (e) 0.21 mL, 1 mmol, (f) 4-*tert*-butylcyclohexanone, (g) 154 mg, 1 mmol, (h) 1 h, (i) 158 mg, 41%

Entry 2: General Procedure A: (a) Mes_2Mg, (b) rt, (c) DMPU, (d) 1.2 mL, 10 eq., (e) 0.21 mL, 1 mmol, (f) 4-*tert*-butylcyclohexanone, (g) 154 mg, 1 mmol, (h) 1 h, (i) 162 mg, 42%

Scheme 1.30

Following General Procedure A for the deprotonation reaction, data are presented as (a) Mg base, (b) reaction temperature, (c) additives, (d) amount of additive, (e) amount of $ClP(O)(OPh)_2$, (f) ketone, (g) amount of ketone, (h) reaction time, (i) isolated yield.

Table 1.9

Entry 1: General Procedure A: (a) Mes_2Mg, (b) rt, (c) DMPU, (d) 0.48 mL, 4 eq., (e) 0.315 mL, 1.5 mmol, (f) 4-*tert*-butylcyclohexanone, (g) 154 mg, 1 mmol, (h) 1 h, (i) 285 mg, 74%

Entry 2: General Procedure A: (a) Mes_2Mg, (b) rt, (c) DMPU, (d) 0.48 mL, 4 eq., (e) 0.42 mL, 2 mmol, (f) 4-*tert*-butylcyclohexanone, (g) 154 mg, 1 mmol, (h) 1 h, (i) 266 mg, 69%

Entry 3: General Procedure A: (a) Mes_2Mg, (b) rt, (c) DMPU, (d) 0.48 mL, 4 eq., (e) 0.84 mL, 4 mmol, (f) 4-*tert*-butylcyclohexanone, (g) 154 mg, 1 mmol, (h) 1 h, (i) 265 mg, 69%

Scheme 1.31

A solution of base (0.75 M solution in THF, 0.75 eq., 0.75 mmol, 1.5 mL) was added to a Schlenk flask which had been flame-dried under vacuum (0.005 mbar) and purged three times with argon then allowed to cool to room temperature. THF (10 mL) was added and the reaction mixture was stirred at room temperature. DMPU (0.48 mL, 4 eq.) and $P(O)(OPh)_2Cl$ (0.21 mL, 1 eq.) were added and stirred for 5 min,

then 4-*tert*-butylcyclohexanone (154 mg, 1 mmol) was added as a solution in THF (2 mL) over 1 h using a syringe pump and the reaction mixture stirred at room temperature. After 1 h the reaction mixture was quenched with a saturated solution of $NaHCO_3$ (10 mL) and allowed to warm to room temperature. The mixture was extracted with Et_2O (50, 25, 25 mL) and the organic layers dried over $MgSO_4$. Removal of the solvent *in vacuo* gave an oil which was purified by column chromatography on silica gel using 0-30 % Et_2O in petroleum ether (40-60 °C) to give the desired product as a colourless oil in 351 mg, 91% yield.

Scheme 1.32

Following General Procedures for the deprotonation reaction, data are presented as (a) Mg base, (b) reaction temperature, (c) additives, (d) amount of additive, (e) amount of $ClP(O)(OPh)_2$, (f) ketone, (g) amount of ketone, (h) reaction time, (i) isolated yield.

Table 1.10

Entry 1: General Procedure C: (a) *t*-Bu_2Mg, (b) 0 °C, (c) DMPU, (d) 0.24 mL, 2 eq., (e) 0.21 mL, 1 mmol, (f) 4-*tert*-butylcyclohexanone, (g) 154 mg, 1 mmol, (h) 1 h, (i) 324 mg, 84%

Entry 2: General Procedure D: (a) *t*-Bu_2Mg, (b) 0 °C, (c) DMPU, (d) 0.24 mL, 2 eq., (e) 0.21 mL, 1 mmol, (f) 4-*tert*-butylcyclohexanone, (g) 154 mg, 1 mmol, (h) 1 h, (i) 309 mg, 80%

Scheme 1.33

Following General Procedure D for the deprotonation reaction, data are presented as (a) Mg base, (b) reaction temperature, (c) additives, (d) amount of additive, (e) amount of $ClP(O)(OPh)_2$, (f) ketone, (g) amount of ketone, (h) reaction time, (i) isolated yield.

Table 1.11

Entry 1: General Procedure D: (a) *t*-Bu_2Mg, (b) rt, (c) DMPU, (d) -, -, (e) 0.21 mL, 1 mmol, (f) 4-*tert*-butylcyclohexanone, (g) 154 mg, 1 mmol, (h) 1 h, (i) 323 mg, 84%

Entry 2: General Procedure D: (a) *t*-Bu_2Mg, (b) rt, (c) DMPU, (d) 0.06 mL, 0.5 eq., (e) 0.21 mL, 1 mmol, (f) 4-*tert*-butylcyclohexanone, (g) 154 mg, 1 mmol, (h) 1 h, (i) 332 mg, 86%

Entry 3: General Procedure D: (a) *t*-Bu_2Mg, (b) rt, (c) DMPU, (d) 0.12 mL, 1 eq., (e) 0.21 mL, 1 mmol, (f) 4-*tert*-butylcyclohexanone, (g) 154 mg, 1 mmol, (h) 1 h, (i) 340 mg, 88%

Entry 4: General Procedure D: (a) *t*-Bu_2Mg, (b) rt, (c) DMPU, (d) 0.18 mL, 1.5 eq., (e) 0.21 mL, 1 mmol, (f) 4-*tert*-butylcyclohexanone, (g) 154 mg, 1 mmol, (h) 1 h, (i) 347 mg, 90%

Entry 5: General Procedure D: (a) *t*-Bu_2Mg, (b) rt, (c) DMPU, (d) 0.24 mL, 2 eq., (e) 0.21 mL, 1 mmol, (f) 4-*tert*-butylcyclohexanone, (g) 154 mg, 1 mmol, (h) 1 h, (i) 351 mg, 91%

Entry 6: General Procedure D: (a) *t*-Bu_2Mg, (b) rt, (c) DMPU, (d) 0.36 mL, 3 eq., (e) 0.21 mL, 1 mmol, (f) 4-*tert*-butylcyclohexanone, (g) 154 mg, 1 mmol, (h) 1 h, (i) 363 mg, 94%

Entry 7: General Procedure D: (a) *t*-Bu_2Mg, (b) rt, (c) DMPU, (d) 0.48 mL, 4 eq., (e) 0.21 mL, 1 mmol, (f) 4-*tert*-butylcyclohexanone, (g) 154 mg, 1 mmol, (h) 1 h, (i) 367 mg, 95%

Entry 8: General Procedure D: (a) *t*-Bu_2Mg, (b) rt, (c) DMPU, (d) 0.6 mL, 5 eq., (e) 0.21 mL, 1 mmol, (f) 4-*tert*-butylcyclohexanone, (g) 154 mg, 1 mmol, (h) 1 h, (i) 359 mg, 93%

*5.3.2. Optimised Conditions Using Mes_2Mg, **41***

Scheme 1.34

Optimised conditions using base **41** (Mes_2Mg)

A solution of base (0.75 M solution in THF, 0.75 eq., 0.75 mmol, 1.5 mL) was added to a Schlenk flask which had been flame-dried under vacuum (0.005 mbar) and purged three times with argon then allowed to cool to room temperature. THF (10 mL) was added and the mixture was stirred at room temperature. DMPU (0.48 mL, 4 eq.) and $P(O)(OPh)_2Cl$ (0.21 mL, 1 eq.) were added and stirred for 5 min, then 4-*tert*-butylcyclohexanone (154 mg, 1 mmol) was added as a solution in THF (2 mL) over 1 h using a syringe pump and the reaction mixture was then stirred at room temperature. After 1 h, the reaction mixture was quenched with a saturated solution of $NaHCO_3$ (10 mL). The mixture was extracted with Et_2O (50, 25, 25 mL) and the organic layers dried over $MgSO_4$. Removal of the solvent *in vacuo* gave an oil which was purified by column chromatography on silica gel using 0-30 % Et_2O in petroleum ether (40-60 °C) to give the desired product as a colourless oil in 352 mg, 91% yield.

*5.3.3. Optimised Conditions Using t-Bu_2Mg, **42***

Optimised conditions using base **42** (*t*-Bu_2Mg)

A Schlenk flask was flame-dried under vacuum (0.005 mbar) and purged three times with argon then allowed to cool to room temperature. Following this, DMPU (0.48 mL, 4 eq.), $P(O)(OPh)_2Cl$ (0.21 mL, 1 eq.), and 4-*tert*-butylcyclohexanone (154 mg, 1 mmol) were added and the mixture stirred at room temperature for 5 min. A solution of base **1.10** (0.5 M solution in THF, 0.5 eq., 0.5 mmol, 1 mL) was added dropwise into the mixture over 5 min and the mixture stirred at room temperature. After 1 h, the reaction mixture was quenched with a saturated solution of $NaHCO_3$

(10 mL). The mixture was extracted with Et_2O (50, 25, 25 mL) and the organic layers dried over $MgSO_4$. Removal of the solvent *in vacuo* gave an oil which was purified by column chromatography on silica gel using 0-30 % Et_2O in petroleum ether (40-60 °C) to give the desired product as a colourless oil in 367 mg, 95% yield.

*5.3.4. Substrate scope using base **42** t-Bu_2Mg*

Scheme 1.35

For the entries in **Scheme 1.35**, each reaction was run twice under identical conditions, and the best yield was presented in the Scheme.

Following General Procedure D for the deprotonation reaction, data are presented as (a) Mg base, (b) reaction temperature, (c) additive, (d) amount of additive, (e) amount of $ClP(O)(OPh)_2$, (f) ketone, (g) amount of ketone, (h) reaction time, (i) yield of run 1, (j) yield of run 2, and (k) appearance.

*Compound **80**:* General Procedure D: (a) *t*-Bu_2Mg (0.5 mmol, 1 mL), (b) rt, (c) DMPU, (d) 0.48 mL, 4 mmol, (e) 0.21 mL, 1 mmol, (f) 4-methylcyclohexanone, (g) 112 mg, 1 mmol, (h) 1 h, (i) 316 mg, 92 %, (j) 323 mg, 94%, and (k) colourless oil.

Diphenyl 4-methylcyclohex-1-enyl phosphate 80:

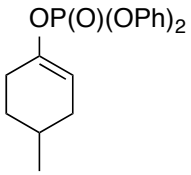

ν_{max}: 1589, 1487, 1296, 1186, 1114, 945 cm^{-1}.

^{1}H NMR (400 MHz, $CDCl_3$): δ 7.39-7.33 (m, 4H, ArH), 7.26-7.18 (m, 6H, ArH), 5.58-5.50 (m, 1H, C=CH), 2.36-2.20 (m, 3H, CH_2), 1.80-1.62 (m, 3H, CH_2, CH), 1.43-1.31 (m, 1H, CH_2), 0.97 (d, J = 6.4 Hz, 3H, CH_3).
^{13}C NMR (100 MHz, $CDCl_3$): δ 150.9, 148.0, 130.1, 125.7, 120.4, 111.6, 32.2, 31.0, 27.9, 27.7, 21.3.
^{31}P NMR (162 MHz, $CDCl_3$): δ -17.46.
HRMS (ESI) Calculated for $C_{19}H_{22}O_4P$ $[M+H]^+$: 345.1250; found: 345.1244.

*Compound **72**:* General Procedure D: (a) *t*-Bu_2Mg (0.5 mmol, 1 mL), (b) rt, (c) DMPU, (d) 0.48 mL, 4 mmol, (e) 0.21 mL, 1 mmol, (f) 4-phenylcyclohexanone, (g) 174 mg, 1 mmol, (h) 1 h, (i) 365 mg, 90 %, (j) 366 mg, 90%, and (k) white solid.

Diphenyl (1,2,3,6-tetrahydro-[1,1'-biphenyl]-4-yl) phosphate 72:

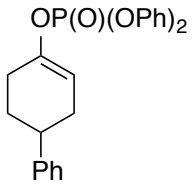

Chiral HPLC analysis: Chiracel OJ-H column, 10% IPA in *n*-hexane, 1.2 mL/minute flow rate, 254 nm detector, t_R (+) = 40 minutes and t_R (-) = 45 minutes.
ν_{max}: 1688, 1587, 1489, 1282, 1188, 1105, 939 cm^{-1}.
^{1}H NMR (400 MHz, $CDCl_3$): δ 7.41-7.34 (m, 4H, ArH), 7.32-7.25 (m, 6H, ArH), 7.24-7.19 (m, 5H, ArH), 5.70-5.65 (m, 1H, C=CH), 2.87-2.77 (m, 1H, CH), 2.54-2.21 (m, 4H, CH_2), 2.07-1.98 (m, 1H, CH_2), 1.97-1.85 (m, 1H, CH_2).
^{13}C NMR (100 MHz, $CDCl_3$): δ 150.7, 147.8, 145.5, 129.9, 128.6, 126.9, 126.4, 125.5, 120.2, 111.6, 39.2, 31.6, 29.7, 28.1.
^{31}P NMR (162 MHz, $CDCl_3$): δ -17.40.
HRMS (ESI) Calculated for $C_{24}H_{24}O_4P$ $[M+H]^+$: 407.1407; found: 407.1408.

*Compound **73**:* General Procedure D: (a) *t*-Bu_2Mg (0.5 mmol, 1 mL), (b) rt, (c) DMPU, (d) 0.48 mL, 4 mmol, (e) 0.21 mL, 1 mmol, (f) 4-methyl-4-

phenylcyclohexanone, (g) 188 mg, 1 mmol, (h) 1 h, (i) 378 mg, 90 %, (j) 374 mg, 89%, and (k) colourless oil.

Diphenyl 1-methyl-1,2,3,6-tetrahydro-[1,1'-biphenyl]-4-yl phosphate 73:

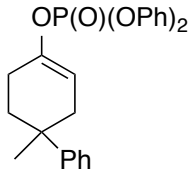

Chiral HPLC analysis: Chiracel OJ-H column, 10% IPA in *n*-hexane, 1. mL/minute flow rate, 254 nm detector, t_R (+) = 21.30 minutes and t_R (-) = 22.56 minutes.
ν_{max}: 1687, 1589, 1487, 1294, 1186, 1114, 943 cm^{-1}.
^1H NMR (400 MHz, $CDCl_3$): δ 7.39-7.29 (m, 8H, ArH), 7.24-7.17 (m, 7H, ArH), 5,7-5.65 (m, 1H, C=CH), 2.67-2.56 (m, 1H, CH_2), 2.32-2.2 (m, 2H, CH_2), 2.11-1.97 (m, 2H, CH_2), 1.91-1.82 (m, 1H, CH_2), 1.31 (s, 3H, CH_3).
^{13}C NMR (100 MHz, $CDCl_3$): δ 150.9, 148.1, 147.6, 130.1, 128.6, 126.2, 125.9, 125.7, 120.4, 110.8, 36.5, 36.0, 35.2, 28.8, 25.9.
^{31}P NMR (162 MHz, $CDCl_3$): δ – 17.64.
HRMS (ESI) Calculated for $C_{25}H_{26}O_4P$ $[M+H]^+$: 421.1563; found: 421.1554.

*Compound **74**:* General Procedure D: (a) *t*-Bu_2Mg, (b) rt, (c) DMPU, (d) 0.48 mL, 4 eq., (e) 0.21 mL, 1 mmol, (f) 4-propylcyclohexanone, (g) 140 mg, 1 mmol, (h) 1 h, (i) 268 mg, 72%, (j) 264 mg, 71%, and (k) colourless oil.

Diphenyl (4-propylcyclohexenyl)phosphate 74:

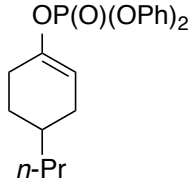

ν_{max}: 1590, 1488, 1301, 1188, 1120, 943 cm^{-1}.

^{1}H NMR (400 MHz, $CDCl_3$): δ 7.37-7.33 (m, 4H, ArH), 7.26-7.18 (m, 6H, ArH), 5.57-5.52 (m, 1H, C=CH), 2.34-2.20 (m, 1H, CH), 2.23-2.12 (m, 2H, CH_2), 1.84-1.68 (m, 2H, CH_2), 1.56-1.49 (m, 1H, CH), 1.39-1.29 (m, 3H, CH_2), 1.28-1.22 (m, 2H, CH_2), 0.93-0.87 (t, J = 7.2 Hz, 3H, CH_3).

^{13}C NMR (100 MHz, $CDCl_3$): δ 150.6, 147.8, 129.7, 125.3, 120.1, 111.3, 37.9, 32.3, 30.0, 28.7, 27.4, 20.2.

^{31}P NMR (162 MHz, $CDCl_3$): δ –17.47.

HRMS (ESI) Calculated for $C_{21}H_{26}O_4P$ $[M+H]^+$: 373.1563; found: 373.1561.

*Compound **81**:* General Procedure D: (a) *t*-Bu_2Mg, (b) rt, (c) DMPU, (d) 0.48 mL, 4 eq., (e) 0.21 mL, 1 mmol, (f) 4-((*tert*-butyldimethylsilyl)oxy)cyclohexanone,[19] (g) 228 mg, 1 mmol, (h) 1 h, (i) 359 mg, 78 %, (j) 368 mg, 80%, and (k) colourless oil.

Diphenyl 4-((*tert*-butyldimethylsilyl)oxy)cyclohexenyl phosphate 81:

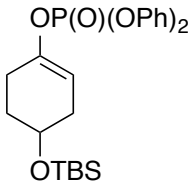

Chiral HPLC analysis: Chiracel OJ-H column, 1% IPA in *n*-hexane, 0.2 mL/minute flow rate, 254 nm detector, t_R (+) = 190 minutes and t_R (-) = 214 minutes.

ν_{max}: 1589, 1489, 1296, 1251, 1188, 1101, 943 cm^{-1}.

^{1}H NMR (400 MHz, $CDCl_3$): δ 7.39-7.32 (m, 4H, ArH), 7.26-7.18 (m, 6H, ArH), 5.47-5.42 (m, 1H, C=CH), 3.96-3.87 (m, 1H, CH), 2.40-2.24 (m, 3H, CH_2), 2.14-2.03 (m, 1H, CH_2), 1.83-1.70 (m, 2H, CH_2), 0.88 (s, 9H, $C(CH_3)_3$), 0.06 (s, 6H, CH_3).

^{13}C NMR (100 MHz, $CDCl_3$): δ 150.9, 147.4, 130.1, 125.8, 120.5, 109.4, 66.5, 33.3, 31.5, 26.2, 26.0, 18.5, - 4.4.

^{31}P NMR (162 MHz, $CDCl_3$): δ -17.62.

HRMS (ESI) Calculated for $C_{24}H_{34}O_5PSi$ $[M+H]^+$: 461.1908; found: 461.1896.

*Compound **82**:* General Procedure D: (a) *t*-Bu_2Mg, (b) rt, (c) DMPU, (d) 0.48 mL, 4 eq., (e) 0.21 mL, 1 mmol, (f) 4-(dimethylamino)cyclohexanone,[35] (g) (g) 141 mg, 1 mmol, (h) 1 h, (i) 280 mg, 75%, (j) 272 mg, 73%, and (k) yellow oil.

Diphenyl 4-(dimethylamino)cyclohexenyl phosphate 82:

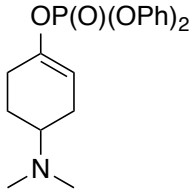

ν_{max}: 1591, 1487, 1222, 1155, 1083, 887 cm^{-1}.

^1H NMR (400 MHz, $CDCl_3$): δ 7.39-7.32 (m, 4H ArH), 7.26-7.18 (m, 6H ArH), 5.54-5.49 (m, 1H C=CH), 2.61-2.46 (m, 2H, CH_2, CH), 2.33 (s, 6H, *N*-CH_3), 2.30-2.21 (m, 2H, CH_2), 2.17-2.06 (m, 1H, CH_2), 2.04-1.96 (m, 1H, CH_2), 1.65-1.53 (m, 1H, CH_2).

^{13}C NMR (100 MHz, $CDCl_3$): δ 150.9, 147.6, 130.2, 129.6, 125.8, 120.4, 59.7, 41.9, 27.8, 25.7, 25.3;

^{31}P NMR (162 MHz, $CDCl_3$): δ – 17.53.

HRMS (ESI) Calculated for $C_{20}H_{25}NO_4P$ $[M+H]^+$: 374.1516; found: 374.1516.

*Compound **83**:* General Procedure D: (a) *t*-Bu_2Mg, (b) rt, (c) DMPU, (d) 0.48 mL, 4 eq., (e) 0.21 mL, 1 mmol, (f) 1,4-dioxaspiro[4.5]decan-8-one, (g) 156 mg, 1 mmol, (h) 1 h, (i) 260 mg, 67%, (j) 261 mg, 67%, and (k) colourless oil.

diphenyl (1,4-dioxaspiro[4.5]dec-7-en-8-yl) phosphate 83:

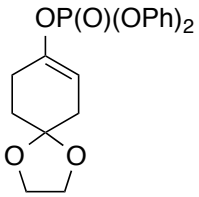

ν_{max}: 1590, 1488, 1220, 1157, 1101, 901 cm^{-1}.

^{1}H NMR (400 MHz, $CDCl_3$): δ 7.38-7.35 (m, 4H, ArH), 7.27-7.18 (m, 6H, ArH), 5.52-5.47 (m, 1H, C=CH), 4.00-3.96 (m, 4H, O-CH_2) 2.48-2.42 (m, 2H, CH_2), 2.36-2.32 (m, 2H, CH_2), 1.89-1.83 (m, 2H, CH_2).

^{13}C NMR (100 MHz, $CDCl_3$): δ 150.6, 145.0, 129.8, 125.4, 120.1, 109.1, 106.8, 64.5, 33.8, 30.9, 26.5.

^{31}P NMR (162 MHz, $CDCl_3$): δ –17.47.

HRMS (ESI) Calculated for $C_{20}H_{22}O_6P$ $[M+H]^+$: 389.1149; found: 389.1145.

*Compound **84**:* General Procedure D: (a) *t*-Bu_2Mg, (b) rt, (c) DMPU, (d) 0.48 mL, 4 eq., (e) 0.21 mL, 1 mmol, (f) (±)-menthone, (g) 154 mg, 1 mmol, (h) 1 h, (i) 227 mg, 59%, (j) 221 mg, 57%, and (k) yellow oil.

NB: Mixture of diastereomers with presence of the C-phosphate compound.

6-isopropyl-3-methylcyclohexenyl diphenyl phosphate, **84**:

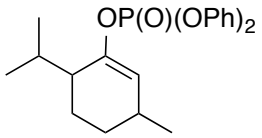

ν_{max}: 1595, 1492, 1296, 1189, 1124, 972 cm^{-1}.

^{1}H NMR (400 MHz, $CDCl_3$): δ 7.4-7.32 (m, 8H, ArH), 7.28-7.19 (m, 12H, ArH), 5.68-5.64 (m, 1H, C=CH), 5.56-5.53 (m, 1H, C=CH), 2.43-2.30 (m, 2H, CH), 2.29-2.18 (m, 2H, CH), 2.13-1.96 (m, 2H, CH), 1.81-1.56 (m, 4H, CH_2), 1.51-1.25 (m, 4H, CH_2), 1.03-0.73 (m, 18H, CH_3).

^{13}C NMR (100 MHz, $CDCl_3$): δ 150.2, 148.0, 129.2, 129.0 124.8, 124.6, 119.6, 119.4, 118.3, 42.1, 34.1, 29.6, 28.7, 27.5, 27.4, 26.5, 25.3, 21.6, 21.4, 20.6, 20.3, 19.9, 19.4, 17.3, 15.9.

^{31}P NMR (162 MHz, $CDCl_3$): δ –17.57, -17.79.

HRMS (ESI) Calculated for $C_{22}H_{28}O_4P$ $[M+H]^+$: 387.1725; found: 387.1726.

*Compound **75**:* General Procedure D: (a) *t*-Bu_2Mg, (b) rt, (c) DMPU, (d) 0.48 mL, 4 eq., (e) 0.21 mL, 1 mmol, (f) acetophenone, (g) 120 mg, 1 mmol, (h) 1 h, (i) 7 mg, 2 %, (j) 21 mg, 6%, and (k) yellow oil.

Diphenyl 1-phenylethen-1-yl phosphate 75:

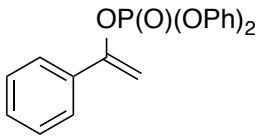

ν_{max}: 1683, 1589, 1487, 1184, 1010, 947 cm^{-1}.

^1H NMR (400 MHz, $CDCl_3$): δ 7.39-7.29 (m, 10H, ArH), 7.25-7.16 (m, 5H, ArH), 5.42-5.39 (m, 1H, C=CH), 5.36-5.34 (m, 1H, C=CH).

^{13}C NMR (100 MHz, $CDCl_3$): δ 152.6, 150.8, 130.2, 130.1, 129.6, 128.8, 125.9, 125.6, 120.5, 98.7.

^{31}P NMR (162 MHz, $CDCl_3$): δ -17.77.

HRMS (ESI) Calculated for $C_{20}H_{17}NaO_4P$ $[M+Na]^+$: 375.0757; found: 375.0757.

*5.3.5. Substrate scope using base **41** Mes_2Mg*

Scheme 1.36

For the entries in **Scheme 1.36**, each reaction was run twice under identical conditions, and the best yield was presented in the Scheme.

Following General Procedure A for the deprotonation reaction, data are presented as (a) Mg base, (b) reaction temperature, (c) additives, (d) amount of additive, (e) amount of $ClP(O)(OPh)_2$, (f) ketone, (g) amount of ketone, (h) reaction time, (i) yield of run 1, (j) yield of run 2, and (k) appearance.

*Compound **75**:* General Procedure A: (a) Mes_2Mg (0.75 mL, 0.75 eq., 0.75 mmol), (b) rt, (c) DMPU, (d) 0.48 mL, 4 eq., (e) 0.21 mL, 1 mmol, (f) acetophenone, (g) 120 mg, 1 mmol, (h) 1 h, (i) 271 mg, 77%, (j) 268 mg, 76%, and (k) colourless oil.

*Compound **85**:* General Procedure A: (a) Mes_2Mg (0.75 mL, 0.75 eq., 0.75 mmol), (b) rt, (c) DMPU, (d) 0.48 mL, 4 eq., (e) 0.21 mL, 1 mmol, (f) 4-bromoacetophenone, (g) 199 mg, 1 mmol, (h) 1 h, (i) 322 mg, 75%, (j) 323 mg, 75%, and (k) colourless oil.

Diphenyl 1-(4-bromophenyl)ethen-1-yl phosphate 85:

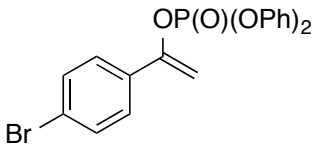

ν_{max}: 1587, 1487, 1184, 1298, 1265, 1211, 1006, 954, 941 cm^{-1}.

^1H NMR (400 MHz, $CDCl_3$): δ 7.46-7.42 (m, 2H, ArH), 7.38-7.33 (m, 6H, ArH), 7.26-7.16 (m, 6H, ArH), 5.41-5.36 (m, 2H, $C=CH_2$).

^{13}C NMR (100 MHz, $CDCl_3$): δ 151.8, 150.8, 131.9, 130.2, 130.6, 127.1, 126.6, 123.9, 120.5, 99.3.

^{31}P NMR (162 MHz, $CDCl_3$): δ -17.80.

HRMS (ESI) Calculated for $C_{20}H_{17}BrO_4P$ $[M+H]^+$: 431.0042/433.0022; found: 431.0035/433.0012.

*Compound **76**:* General Procedure A: (a) Mes_2Mg (0.75 mL, 0.75 eq., 0.75 mmol), (b) rt, (c) DMPU, (d) 0.48 mL, 4 eq., (e) 0.21 mL, 1 mmol, (f) 4-methoxyacetophenone, (g) 120 mg, 1 mmol, (h) 1 h, (i) 290 mg, 76%, (j) 294 mg, 77%, and (k) colourless oil.

Diphenyl 1-(4-methoxyphenyl)ethen-1-yl phosphate 76:

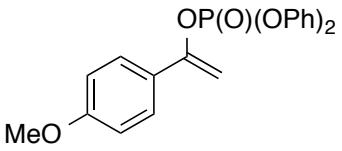

ν_{max}: 1671, 1595, 1489, 1257, 1186, 918 cm^{-1}.

^{1}H NMR (400 MHz, $CDCl_3$): δ 7.47-7.40 (m, 2H, ArH), 7.38-7.32 (m, 4H, ArH), 7.28-7.17 (m, 6H, ArH), 6.87-6.81 (m, 2H, ArH), 5.28-5.21 (m, 2H, C=CH_2), 3.82 (s, 3H, CH_3).

^{13}C NMR (100 MHz, $CDCl_3$): 160.8, 152.6, 150.9, 130.2, 127.1, 125.9, 120.6, 120.5, 114.1, 96.8, 55.7.

^{31}P NMR (162 MHz, $CDCl_3$): δ -17.75.

HRMS (ESI) Calculated for $C_{21}H_{20}O_5P$ $[M+H]^+$: 383.1045; found: 383.1043.

*Compound **78**:* General Procedure A: (a) Mes_2Mg (0.75 mL, 0.75 eq., 0.75 mmol), (b) rt, (c) DMPU, (d) 0.48 mL, 4 eq., (e) 0.21 mL, 1 mmol, (f) 4-cyanoacetophenone, (g) 145 mg, 1 mmol, (h) 1 h, (i) 256 mg, 68%, (j) 257 mg, 68%, and (k) colourless oil.

Diphenyl 1-(4-cyanophenyl)ethen-1-yl phosphate 78:

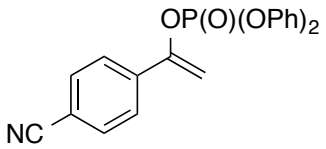

ν_{max}: 2227, 1589, 1487, 1300, 1182, 1093, 1008, 958 cm^{-1}.

^{1}H NMR (400 MHz, $CDCl_3$): δ 7.63-7.54 (m, 4H, ArH), 7.40-7.33 (m, 4H, ArH), 7.26-7.16 (m, 6H, ArH), 5.56-5.50 (m, 2H, C=CH_2).

^{13}C NMR (100 MHz, $CDCl_3$): δ 151.0, 150.7, 138.12, 132.6, 130.30, 126.2, 126.1 120.43, 118.7 113.1, 101.9.

^{31}P NMR (162 MHz, $CDCl_3$): δ -17.78.

HRMS (ESI) Calculated for $C_{21}H_{17}NO_4P$ $[M+H]^+$: 378.0898; found: 378.0888.

*Compound **86**:* General Procedure A: (a) Mes_2Mg (0.75 mL, 0.75 eq., 0.75 mmol), (b) rt, (c) DMPU, (d) 0.48 mL, 4 eq., (e) 0.21 mL, 1 mmol, (f) mesitylethanone, (g) 162 mg, 1 mmol, (h) 1 h, (i) 244 mg, 75%, (j) 296 mg, 62%, and (k) yellow oil.

Diphenyl 1-mesitylethen-1-yl phosphate, **86**:

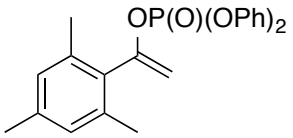

ν_{max}: 1589, 1487, 1296, 1213, 1186, 1161, 1008, 939 cm^{-1}.

^1H NMR (400 MHz, $CDCl_3$): δ 7.39-7.28 (m, 4H, ArH), 7.23-7.15 (m, 6H, ArH), 6.85 (s, 2H, ArH), 5.51-5.47 (m, 1H, C=CH_2), 4.81-4.78 (m, 1H, C=CH_2), 2.31 (s, 6H, CH_3), 2.29 (s, 3H, CH_3).

^{13}C NMR (100 MHz, $CDCl_3$): δ 151.5, 150.8, 139.1, 137.5, 131.8, 130.0, 128.5, 125.7, 120.4, 103.9, 21.4, 20.3.

^{31}P NMR (162 MHz, $CDCl_3$): δ -18.34.

HRMS (ESI) Calculated for $C_{23}H_{24}O_4P$ $[M+H]^+$: 395.1407; found: 395.1403.

Compound 77: General Procedure A: (a) Mes_2Mg (0.75 mL, 0.75 eq., 0.75 mmol), (b) rt, (c) DMPU, (d) 0.48 mL, 4 eq., (e) 0.21 mL, 1 mmol, (f) 4-nitroacetophenone, (g) 165 mg, 1 mmol, (h) 1 h, (i) 8 mg, 2%, (j)15 mg, 4%, and (k) red oil.

Diphenyl 1-(4-nitrophenyl)ethenyl phosphate 77:

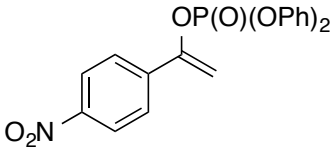

ν_{max}: 1591, 1485, 1456, 1296, 1265, 1222, 1184, 1161, 1128, 1008, 948 cm^{-1}.

^{1}H NMR (400 MHz, $CDCl_3$): δ 7.36-7.31 (m, 4H, ArH), 7.25-7.17 (m, 6H, ArH), 6.94-6.89 (m, 1H, C=CH_2), 6.87-6.83 (m, 2H, ArH), 6.82-6.77 (m, 2H, ArH), 5.32 (s, 1H, C=CH_2).
^{13}C NMR (100 MHz, $CDCl_3$): δ 156.2, 150.9, 146.3, 135.4, 130.1, 129.9, 125.8, 120.8, 120.6, 115.6.
^{31}P NMR (162 MHz, $CDCl_3$): δ -17.23.

Scheme 1.37

Using base **41** (Mes_2Mg)

A solution of base **41** (0.75 M solution in THF, 0.75 eq., 0.75 mmol, 1.5 mL) was added to a Schlenk flask which had been flame-dried under vacuum (0.005 mbar) and purged three times with argon then allowed to cool to room temperature. THF (10 mL) was added and the reaction mixture was stirred at room temperature. DMPU (0.48 mL, 4 eq.) and $P(O)(OPh)_2Cl$ (0.21 mL, 1 eq.) were added and the reaction stirred for 5 min, then 2-methylcyclohexanone (112 mg, 1 mmol) was added as a solution in THF (2 mL) over 1 h using a syringe pump, then the reaction mixture was stirred at room temperature. After 1 h, the reaction mixture was quenched with a saturated solution of $NaHCO_3$ (10 mL). The mixture was extracted with Et_2O (50, 25, 25 mL) and the organic layers dried over $MgSO_4$. Removal of the solvent *in vacuo* gave an oil which was purified by column chromatography on silica gel using 0-30 % Et_2O in petroleum ether (40-60 °C) to give the desired product as a colourless oil in 230 mg, 67% yield.

Using base **42** (*t*-Bu_2Mg)

A Schlenk flask was flame-dried under vacuum (0.005 mbar) and purged three times with argon then allowed to cool to room temperature. Following this, DMPU (0.48 mL, 4 eq.), $P(O)(OPh)_2Cl$ (0.21 mL, 1 eq.), and 2-methylcyclohexan-1-one (112 mg, 1 mmol) were added and the mixture stirred at room temperature for 5 min. A solution of base **1.10** (0.5 M solution in THF, 0.5 eq., 0.5 mmol, 1 mL) was added

dropwise into the reaction mixture over 5 min then the mixture was stirred at room temperature. After 1 h, the reaction mixture was quenched with a saturated solution of $NaHCO_3$ (10 mL). The mixture was extracted with Et_2O (50, 25, 25 mL) and the organic layers dried over $MgSO_4$. Removal of the solvent *in vacuo* gave an oil which was purified by column chromatography on silica gel using 0-30 % Et_2O in petroleum ether (40-60 °C) to give the desired product as a colourless oil in 175 mg, 51% yield.

Diphenyl 6-methylcyclohex-1-en-1-yl phosphate[38] **5**:

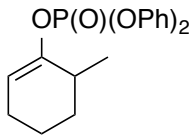

ν_{max}: 1589, 1487, 1294, 1186, 1101, 950 cm^{-1}

^1H NMR (400 MHz, $CDCl_3$): δ 7.39-7.33 (m, 5H, ArH), 7.26-7.33 (m, 5H, ArH), 5.63-5.59 (m, 1H, C=CH), 2.45-2.37 (m, 1H), 2.12-2.06 (m, 2H), 1.87-1.80 (m, 1H), 1.67-1.58 (m, 1H), 1.56-1.48 (m, 1H), 1.47-1.37 (m, 1H), 1.04 (d, J = 7.0 Hz, 3H, CH_3).

^{13}C NMR (100 MHz, $CDCl_3$): δ 152.1, 150.9, 130.1, 125.7, 120.5, 111.7, 32.4, 31.5, 24.5, 19.7, 18.4.

^{31}P NMR (162 MHz, $CDCl_3$): δ -17.52.

HRMS (ESI) Calculated for $C_{19}H_{22}O_4P$ $[M+H]^+$: 345.1250; found: 345.1246

5.3.5.Towards Future Work

Scheme 1.38

Following General Procedures for the deprotonation reaction, data are presented as (a) Mg base, (b) reaction temperature, (c) additives, (d) amount of additive, (e) amount of TESCl, (f) ketone, (g) amount of ketone, (h) reaction time, (i) isolated yield.

Classical conditions

Entry 1: General Procedure A: (a) Mes_2Mg, (b) 0 °C, (c) LiCl, (d) 84 mg, 2 eq., (e) 0.17 mL, 1 mmol, (f) 4-*tert*-butylcyclohexanone, (g) 154 mg, 1 mmol, (h) 16 h, (i) 142 mg, 53%

Entry 2: General Procedure A: (a) *t*-Bu_2Mg, (b) 0 °C, (c) LiCl, (d) 84 mg, 2 eq., (e) 0.17 mL, 1 mmol, (f) 4-*tert*-butylcyclohexanone, (g) 154 mg, 1 mmol, (h) 1 h, (i) no product isolated

Enol phosphate conditions

Entry 1: General Procedure A: (a) Mes_2Mg, (b) rt, (c) DMPU, (d) 0.48 mL, 4 eq., (e) 0.17 mL, 1 mmol, (f) 4-*tert*-butylcyclohexanone, (g) 154 mg, 1 mmol, (h) 1 h, (i) 228 mg, 85%

Entry 2: General Procedure D: (a) *t*-Bu_2Mg, (b) rt, (c) DMPU, (d) 0.48 mL, 4 eq., (e) 0.17 mL, 1 mmol, (f) 4-*tert*-butylcyclohexanone, (g) 154 mg, 1 mmol, (h) 1 h, (i) 171 mg, 64%

((4-(*tert*-butyl)cyclohexenyl)oxy)triethylsilane[39] **88**:

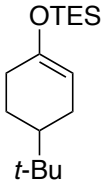

ν_{max}: 2913, 2876, 1673,1364, 1190 cm^{-1}.

^1H NMR (500 MHz, $CDCl_3$) δ 4.85 (dt, *J* = 5.7 Hz, 1.9, 1H), 2.14–2.07 (m, 1H), 2.04–2.02 (m, 1H), 2.00–1.98 (m, 1H), 1.84–1.77 (m, 2H), 1.30– 1.18 (m, 2H), 0.98 (t, *J* = 7.8 Hz, 9H), 0.87 (s, 9H), 0.66 (q, *J* = 8.1 Hz, 6H).

^{13}C NMR (100 MHz, C_6D_6) δ 151.3, 103.4, 44.8, 32.6, 31.8, 27.9, 25.9, 25.2, 7.4, 5.9.

Scheme 1.39

A Schlenk flask was flame-dried under vacuum (0.005 mbar) and purged three times with argon then allowed to cool to room temperature. Following this, DMPU (0.48 mL, 4 eq.), $P(O)(OPh)_2Cl$ (0.21 mL, 1 eq.), and methyl vinyl ketone (0.08 mL, 1 mmol) were added and the mixture stirred at room temperature for 5 min. A solution of base **42** (0.5 M solution in THF, 0.5 eq., 0.5 mmol, 1 mL) was added dropwise into the reaction solution over 5 min and the mixture was then stirred at room temperature. After 1 h, the reaction mixture was quenched with a saturated solution of $NaHCO_3$ (10 mL). The mixture was extracted with Et_2O (50, 25, 25 mL) and the organic layers dried over $MgSO_4$. Removal of the solvent *in vacuo* gave an oil which was purified by column chromatography on silica gel using 0-30 % Et_2O in petroleum ether (40-60 °C) to give the desired product as a colourless oil in 262 mg, 73% yield with an *E*:*Z* selectivity of 1:1.1 (determined by 2D ^1H nOe NMR experiments).

5,5-dimethylhex-2-en-2-yl diphenyl phosphate 90:

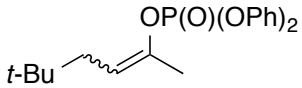

A mixture of diastereomers 1:1.1 is reported.

ν_{max}: 2953, 1689, 1591, 1489, 1298, 1188, 1010, 952 cm^{-1}.

^1H NMR (400 MHz, $CDCl_3$): δ 7.40-7.34 (m, 8H, ArH), 7.31-7.25 (m, 9H, ArH), 7.31-7.25 (m, 4H, ArH), 5.42 (td, *J* = 8.3 Hz, 2.5 Hz, 1H, C=CH), 4.9 (t, *J* = 7.3 Hz, 1H, C=CH), 2.10-2.08 (m, 3.3H, CH_3), 1.96-1.94 (m, 3H, CH_3), 1.91-1.86 (m, 4.4H, CH_2), 0.90 (s, 9H, CH_3), 0.83 (s, 9.9H, CH_3).

^{13}C NMR (100 MHz, $CDCl_3$): δ 129.3, 124.9, 124.8, 119.7, 119.6, 40.3, 38.3, 28.6, 20.0, 16.3, 15.6.

^{31}P NMR (162 MHz, $CDCl_3$): δ (ppm) -17.2, -17.7.

HRMS (ESI) Calculated for $C_{20}H_{26}O_4P$ $[M+H]^+$: 361.1563; found: 361.1561.

Scheme 1.40

Synthesis of **2-methyl-4-phenylcyclohexanone 91**:

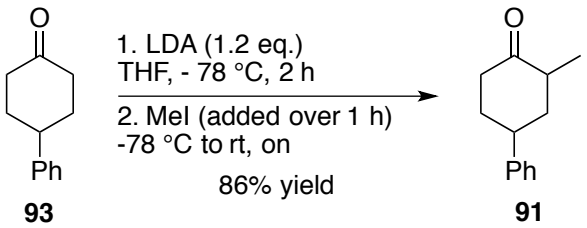

Scheme 1. 41

A round-bottom flask was flame dried under vacuum and purged with argon three times. Di-*iso*-propylamine (0.84 mL, 6 mmol) was added, followed by THF (20 mL), the reaction vessel cooled to -78 °C and stirred for 15 min. To the reaction mixture was added *n*-BuLi (2.5 M in hexanes, 2.4 mL, 6 mmol) dropwise over 10 min and the mixture stirred for a further 5 min, before letting the mixture warm up to room temperature. The mixture was left at room temperature for 5-10 min before cooling it back to -78 °C. After 10 min, 4-phenylcyclohexanone (870 mg, 5 mmol) was added as a solution in THF (5 mL) *via* a syringe pump over 1 h followed by intense stirring for 1 h. Finally, methyl iodide (0.31 mL, 5 mmol) was added *via* a syringe pump over 1 h, and the reaction was left to slowly warm to room temperature overnight before being quenched with saturated NH_4Cl. The aqueous solution was extracted 3 times with diethyl ether (50 mL, 50 mL, 25 mL), and the organic phases combined before being washed with brine and dried over $MgSO_4$. The solvent was removed *in vacuo* and the crude was then was purified by column chromatography on silica gel using 0-30 % Et_2O in petroleum ether (40-60 °C), to give the desired product as a colourless oil in 161 mg, 86% yield with a d.r .1:1.

2-methyl-4-phenylcyclohexanone 91:

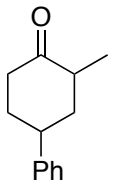

A mixture of diastereomers is reported.

ν_{max}: 2954, 1708, 1494, 1452, 756, 698 cm^{-1}.

^1H NMR (400 MHz, $CDCl_3$): δ 7.38-7.29 (m, 6H, ArH), 7.27-7.21 (m, 4H, ArH), 3.26-3.10 (m, 2H, CH), 2.69-2.49 (m, 5H, CH_2, CH), 2.46-2.37 (m, 1H, CH_2), 2.31-2.07 (m, 6H, CH_2), 2.00-1.91 (m, 2H, CH_2), 1.26 (d, J = 7.2 Hz, 3H, CH_3), 1.08 (d, J = 6.5 Hz, 3H, CH_3).

^{13}C NMR (100 MHz, $CDCl_3$): δ 214.2, 212.2, 128.4, 128.2, 128.1, 127.0, 126.3, 126.2, 126.0, 129.9, 44.3, 42.9, 42.7, 41.0, 39.5, 37.4, 36.5, 34.5, 32.4, 16.3, 13.9.

HRMS (ESI) Calculated for $C_{13}H_{17}O_1$ $[M+H]^+$: 189.1274; found: 189.1273.

Synthesis of **92**:

Conditions A

A round-bottom flask was flame dried under vacuum and purged with argon three times. Di-*iso*-propylamine (0.28 mL, 2 mmol) was added followed by THF (10 mL) and the reaction vessel cooled to -78 °C and stirred for 15 min. To the reaction mixture was added *n*-BuLi (2.5 M in hexanes, 0.8 mL, 2 mmol) dropwise over 10 min and the mixture stirred for a further 5 min, before letting the mixture warm up to room temperature. The mixture was left at room temperature for 5-10 min before cooling it back to -78 °C. After 10 min, ketone **1.47** (376 mg, 2 mmol) was added as a solution in THF (2 mL) *via* a syringe pump over 1 h, followed by intense stirring for 1 h. Finally, diphenyl phosphoryl chloride (0.42 mL, 2 mmol) was added dropwise over 5 minutes, and the reaction was left to slowly warm to room temperature over night before being quenched with saturated NH_4Cl. The aqueous phase was extracted 3 times with diethyl ether (50 mL, 50 mL, 25 mL), and the organic phases combined before being washed with brine and dried over $MgSO_4$. The solvent was removed *in vacuo* and the crude was then was purified by column chromatography on silica gel using 0-30 % Et_2O in petroleum ether (40-60 °C), to give the desired product as a colourless oil in 277 mg, 66% yield with a d.r. 1:1.

Conditions B

Following General Procedures for the deprotonation reaction, data are presented as (a) Mg base, (b) reaction temperature, (c) additives, (d) amount of additive, (e) amount of TESCl, (f) ketone, (g) amount of ketone, (h) reaction time, (i) isolated yield, (j) dr

Classical conditions

Conditions B: General Procedure D: (a) *t*-Bu_2Mg, (b) rt, (c) DMPU, (d) 0.96 mL, 4 eq., (e) 0.42 mL, 2 mmol, (f) **1.47**, (g) 376 mg, 2 mmol, (h) 1 h, (i) 369 mg, 88%, (j) 1:3.3

3-methyl-1,2,3,6-tetrahydro-[1,1'-biphenyl]-4-yl diphenyl phosphate 92:

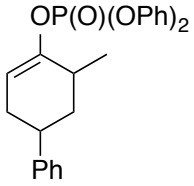

A mixture of diastereomers is reported.

ν_{max}: 2198, 1487, 1296, 1186, 1095, 985 cm^{-1}.

^1H NMR (400 MHz, $CDCl_3$): δ 7.41-7.19 (m, 30H, ArH), 5.71-5.67 (m, 2H, CH), 2.97-2.81 (m, 2H, CH), 2.55-2.48 (m, 2H, CH), 2.42-2.21 (m, 4H, CH_2, CH), 2.14-2.04 (m, 2H, CH_2), 1.78-1.72 (m, 2H, CH_2), 1.17 (d, J = 7.1 Hz, 3H, CH_3), 1.07 (d, J = 6.9 Hz, 3H, CH_3).

^{13}C NMR (100 MHz, $CDCl_3$): δ 150.9, 129.3, 128.0, 126.4, 126.2, 125.8, 124.9, 119.7, 119.6, 110.7, 110.6, 39.3, 39.2, 33.2, 31.9, 17.4.

^{31}P NMR: δ (ppm) -17.5.

HRMS (ESI) Calculated for $C_{25}H_{26}O_4P$ $[M+H]^+$: 421.1569; found: 421.1569.

6. References

1. Lichtenthaler, F. W., *Chem. Rev.*, **1961**, *61* (6), 607.
2. (a) Perkow, W.; Ullerich, K.; Meyer, F., *Naturwissenschaften*, **1952**, *39* (15), 353. (b) Perkow, W., *Chem. Ber.*, **1954**, *87* (5), 755 - 758.
3. Bhattacharya, A. K.; Thyagarajan, G., *Chem. Rev.*, **1981**, *81* (4), 415.
4. Sellars, J. D.; Steel, P. G., *Chem. Soc. Rev.*, **2011**, *40* (10), 5170.
5. Lee, P. H.; Kang, D.; Choi, S.; Kim, S., *Org. Lett.*, **2011**, *13* (13), 3470.
6. Lee, P. H.; Kim, S.; Park, A.; Chary, B. C.; Kim, S. *Angew. Chem. Int. Ed.* **2010**, *49* (38), 6806.
7. You, W.; Li, Y.; Brown, M. K., *Org. Lett.*, **2013**, *15* (7), 1610.
8. Gregson, R. P.; Mirrington, R. N., *J. Chem. Soc. Chem. Commun.*, **1973**, No. 17, 598.
9. Sato, M.; Takai, K.; Oshima, K.; Nozaki, H., *Tetrahedron Lett.*, **1981**, *22* (17), 1609.
10. Rui, Y.; Thompson, D. H., *J. Org. Chem.*, **1994**, *59* (19), 5758.
11. Blaszczak, L.; Winkler, J.; O'Kuhn, S., *Tetrahedron Lett.*, **1976**, *17* (49), 4405.
12. Fuwa, H.; Kainuma, N.; Tachibana, K.; Sasaki, M., *J. Am. Chem. Soc.*, **2002**, *124* (50), 14983.
13. Aggarwal, V. K.; Humphries, P. S.; Fenwick, A*., Angew. Chem. Int. Ed.*, **1999**, *38* (13-14), 1985.
14. Pedzisa, L.; Vaughn, I. W.; Pongdee, R., *Tetrahedron Lett.*, **2008**, *49* (26), 4142.
15. Hansen, A. L.; Ebran, J.-P.; Gøgsig, T. M.; Skrydstrup, T., *J. Org. Chem.*, **2007**, *72* (17), 6464.
16. Gauthier, D.; Beckendorf, S.; Gøgsig, T. M.; Lindhardt, A. T.; Skrydstrup, T., *J. Org. Chem.*, **2009**, *74* (9), 3536.
17. Coe, J. W., *Org. Lett.*, **2000**, *2* (26), 4205.
18. Moore, J.; Stanitski, C.; Jurs, P., *Chemistry: The Molecular Science*; Available Titles OWL Series; Cengage Learning, 2010.
19. (a) Henderson, K. W.; Kerr, W. J.; Moir, J. H., *Chem. Commun.*, **2000**, 479. (b) Henderson, K. W.; Kerr, W. J.; Moir, J. H., *Chem. Commun.*, **2001**, 1722.
20. Watson, A. J. B. *PhD Thesis*; University of Strathclyde; 2007.

21. Henderson, K. W.; Kerr, W. J.; Moir, J. H., *Tetrahedron*, **2002**, *58* (23), 4573.
22. (a) Kerr, W. J.; Watson, A. J. B.; Hayes, D., *Chem. Commun.*, **2007**, 5049. (b) Kerr, W. J.; Watson, A. J. B.; Hayes, D., *Org. Biomol. Chem.*, **2008**, *6*, 1238. (c) Kerr, W. J.; Watson, A. J. B.; Hayes, D., *Synlett*, **2008**, *19* (9), 1386.
23. Clegg, W.; Craig, F. J.; Henderson, K. W.; Kennedy, A. R.; Mulvey, R. E.; O'Neil, P. A.; Reed, D., *Inorg. Chem.*, **1997**, *36* (27), 6238.
24. (a) Shapiro, R, H.; Heath, M, J., *J. Am. Chem. Soc*, **1967**, *89*, 5734 , (b) Weber, T. *PhD Thesis*; University of Strathclyde; 2013.
25. Kerr, W. J.; Morrison, A. J.; Pazicky, M.; Weber, T., *Org. Lett.*, **2012**, *14* (9), 2250.
26. Miller, J. A., *Tetrahedron Lett.*, **2002**, *43* (39), 7111.
27. Corey, E. J.; Gross, A. W., *Tetrahedron Lett.*, **1984**, *25* (5), 495.
28. Bunn, B. J.; Simpkins, N. S.; Spavold, Z.; Crimmin, M. J., *J. Chem. Soc. [Perkin 1]*, **1993**, No. 24, 3113.
29. Bunn, B. J.; Simpkins, N. S., *J. Org. Chem.*, **1993**, *58* (3), 533.
30. Sato, D.; Kawasaki, H.; Shimada, I.; Arata, Y.; Okamura, K.; Date, T.; Koga, K., *J. Am. Chem. Soc.*, **1992**, *114* (2), 761–763.
31. Perrin, D., D.; Armarego, W. L. F., *Purification of Laboratory Chemicals*; Pergaman: Oxford; 1988.
32. Love, B. E.; Jones, E. G., *J. Org. Chem.*, **1999**, *64* (10), 3755.
33. Zimmerman, H. E.; Jones, G., *J. Am. Chem. Soc.*, **1970**, *92* (9), 2753.
34. Carreño, M. C.; Urbano, A.; Di Vitta, C., *J. Org. Chem.*, **1998**, *63* (23), 8320.
35. Guzzo, P. R.; Buckle, R. N.; Chou, M.; Dinn, S. R.; Flaugh, M. E.; Kiefer, A. D.; Ryter, K. T.; Sampognaro, A. J.; Tregay, S. W.; Xu, Y.-C., *J. Org. Chem.*, **2003**, *68* (3), 770.
36. Bennie, L. S.; Kerr, W. J.; Middleditch, M.; Watson, A. J. B., *Chem. Commun.*, **2011**, *47* (8), 2264.
37. Lagerlund, O.; Mantel, M. L. H.; Larhed, M., *Tetrahedron*, **2009**, *65* (36), 7646.
38. Lee, P. H.; Kang, D.; Choi, S.; Kim, S., *Org. Lett.*, **2011**, *13* (13), 3470.
39. Hurlocker, B.; Miner, M. R.; Woerpel, K. A., *Org. Lett.*, **2014**, *16* (16), 4280.

Chapter 2

The Synthesis of Enantioenriched Enol Phosphates

Content

1. Introduction

1.1.Chiral Lithium Amides

1.1.1. The Beginning of a Concept

In the 1980s, Whitesell and Felman first described the proposal that a chiral lithium amide species could deprotonate a prochiral substrate, and subsequently allow an asymmetric transformation to take place.[1] They imagined the opening of a prochiral epoxide, such as **94**, and reasoned that, with a chiral base, the kinetics of the deprotonation process would be different for the two enantiotopic protons and, consequently, this could allow the formation of an enantioenriched allylic alcohol **(*R*)-95**. In order to validate this hypothesis, they used the chiral (*S*,*S*)-bis(phenylethyl)amine-derived lithium amide **(*S*,*S*)-96** to deprotonate the ß-hydrogen of **94** and generate the chiral alcohol **(*R*)-95** (**Scheme 2.1**) in 31% e.e. Although delivering only low levels of selectivity, this result was fundamental to establishing the now widely explored concept of the asymmetric deprotonation reaction. Key to this process is the two possible transition states for the deprotonation reaction having different energies due to their diastereomeric nature, imparted by the chirality of the base, and therefore allowing the preferential kinetic access to one enantiomer over the other.

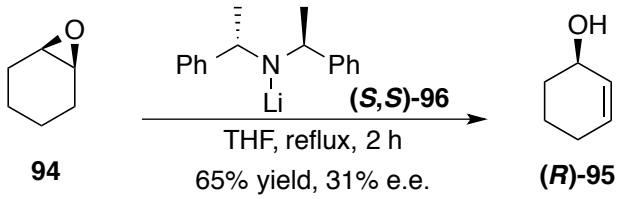

Scheme 2. 1

After this initial discovery, Asami *et* al. later rationalised the enantioselective deprotonation reaction whilst working with a novel, proline-derived lithium amide (**Figure 2.1**).[2] In their model, they realised that the outcome of the epoxide opening

was correlated to the R_2 unit depicted below and therefore, that the epoxide can approach the amide at face A or face B, resulting in two differing interactions.

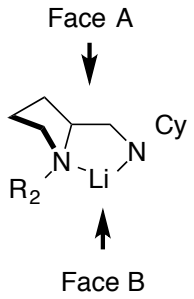

Figure 2. 1

As depicted in **Scheme 2.2**, the use of lithium amide base **(*S*)-97** delivered chiral alcohol **(*R*)-95** in a good 80% yield and with an impressive 78% e.e.

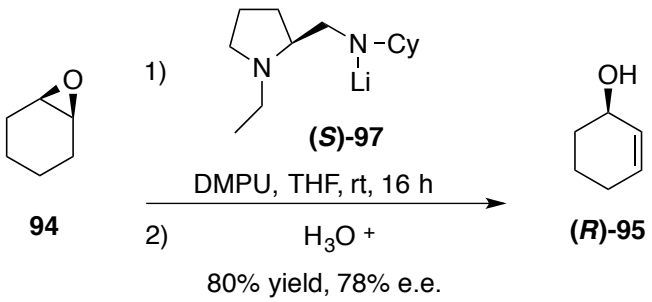

Scheme 2. 2

This result was explained by envisaging two possible transition states along the reaction coordinate. It was proposed that if the epoxide approached from face B, *i.e.* the bottom face of the lithium amide, there would be significant steric interactions between R_2 (ethyl in **(*S*)-97**) and the protons on the carbon α to the epoxide (**Figure 2.2**). As shown below, transition state 1 (T1) is more favoured than transition state 2 (T2), hence the selectivity towards alcohol **(*R*)-95**.

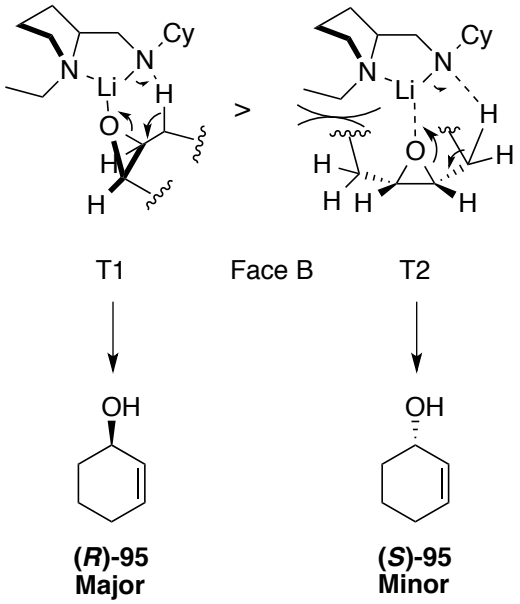

Figure 2. 2

The authors noticed that if a much bulkier R_2 substituent, such as the neopentyl group, was employed, the lithium amide base **(*S*)-98** delivered the opposite enantiomer **(*S*)-95** (**Scheme 2.3**). The opening of epoxide **94** by the lithium amide **(*S*)-97** afforded **(*S*)-95** in a high 77% yield and a good selectivity of 62% e.e.

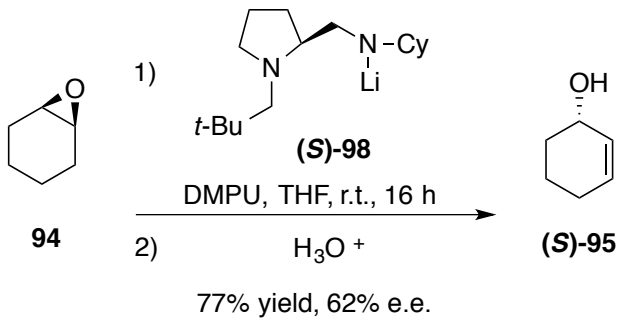

Scheme 2. 3

This inversion in selectivity has been rationalised by the approach of the epoxide switching to face A, *i.e.* the top face of the lithium amide (*c.f.* **Figure 2.1**). The steric bias of a bulky R_2 group (CH_2-*t*-Bu in **(*S*)-98**) now forces an approach on side A; the possible approaches are depicted in **Figure 2.3**. The interaction between the protons on the carbon α to the epoxide and the ring system would therefore favour the transition state T3 over the transition state T4.

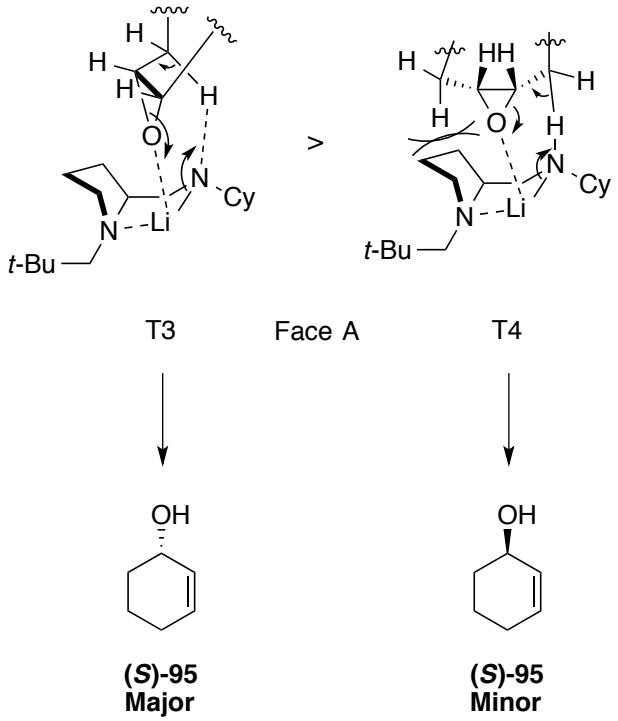

Figure 2. 3

1.1.2. The Desymmetrisation of 4-Substituted Ketones

Having established the concept of asymmetric deprotonation reaction and proposed a rationale for the enantioselectivity observed by subtle variations on the amide, a range of research groups diversified the process by exploring novel substrates.[3] The deprotonation of prochiral compounds, such as 4-substituted cyclohexanones, was thus envisaged. In such substrates, a stereoelectronic preference for the removal of the axial protons α- to the ketone, as opposed to the equatorial protons, exists (**Figure 2.4**). To form an enolate, the σ* orbital of the C-H bond which is broken should be sufficiently aligned with the π* orbital of the carbonyl group. Therefore, in

a conformationally locked cyclohexanone substrate, the axial proton is favoured for deprotonation, giving rise, after trapping with a suitable electrophile, to enantioenriched products when these two prochiral protons can be discriminated.

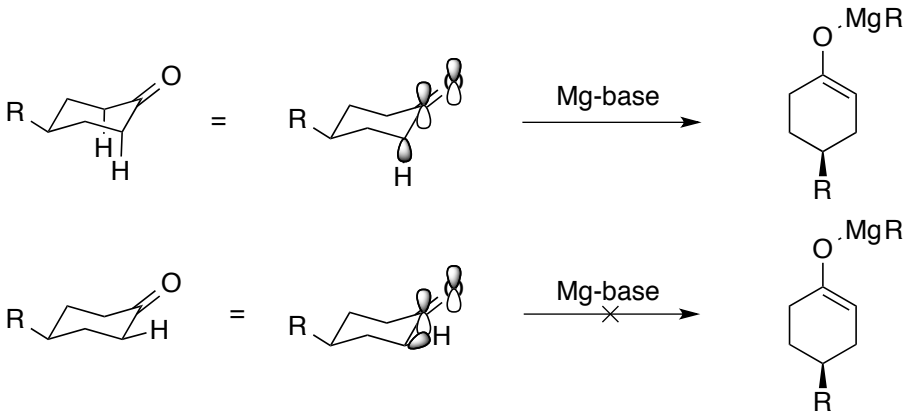

Figure 2. 4

It should be stated that these 4-substituted cyclohexanones are thermodynamically more stable when the 4-substitutent is in the equatorial conformation. As shown in **Figure 2.5**, unfavourable 1,3-diaxial steric interactions occur when the R group is in an axial conformation.

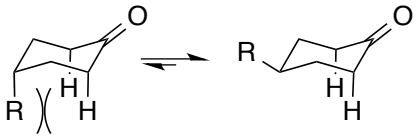

Figure 2. 5

In 1986, Simpkins,[3a,4] using simple C_2-symmetric amines, and Koga[3b], exploring chelating-type amines, reported independently the lithium base-mediated asymmetric deprotonation reaction (**Scheme 2.4**). In order to study the enolate formed, they trapped it with trimethylsilyl chloride (TMSCl) to generate the silyl enol ether product; with the intention of using such compounds as chiral intermediates for further transformations.[5] The standard prochiral ketone used within these reactions was 4-*t*-butylcylclohexanone **35**, which, after asymmetric deprotonation, afforded the enol ether compounds **(*R*)-37** or **(*S*)-37.**

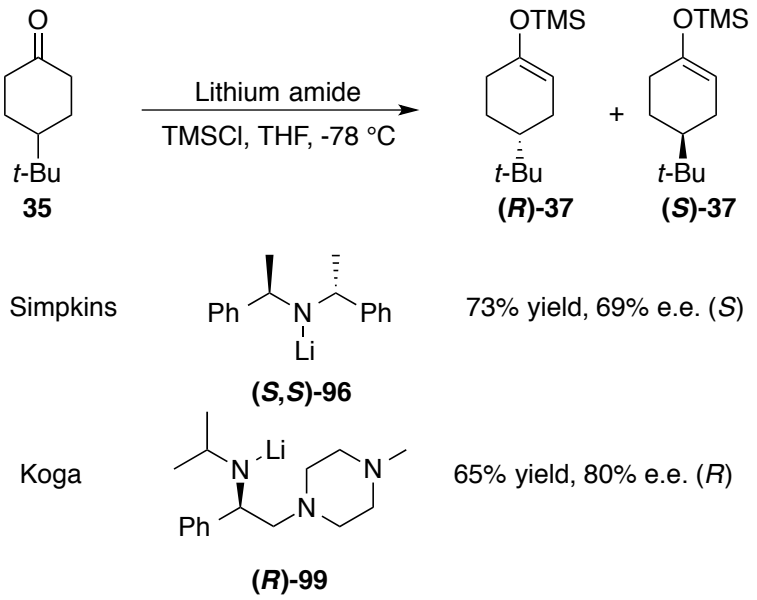

Scheme 2. 4

As shown above, Simpkins's C_2 symmetric base delivered silyl enol ether product **(*S*)-37** in a good 73% yield and in 69% e.e. However, Koga's chelating base **(*R*)-99** delivered the enantioenriched product **(*R*)-37** in a much improved 80% e.e.

In 1984, Koga noticed that the presence of a Lewis base, such as HMPA, increased the reactivity of the lithium species, resulting in a much improved 87% yield and 84% e.e. (**Scheme 2.5).** The author attributed this result to the disaggregation of the organometallic species by HMPA.[6] Compared to their previous results, the presence of HMPA undoubtedly increased the system's reactivity, allowing the improvement to an 87% yield.

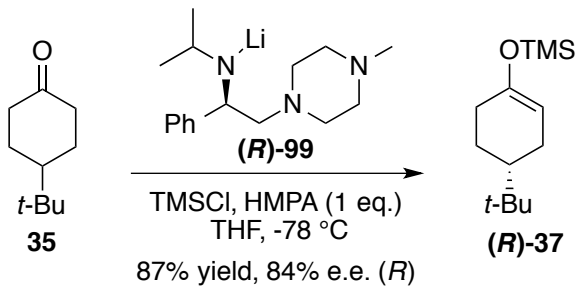

Scheme 2. 5

More interestingly, the selectivity was also increased, from 80% e.e. to 84% e.e. In order to observe the effect of additives on the base, a series of X-ray diffraction, ^{6}Li and ^{15}N NMR spectroscopic studies have been carried out by Koga.[7] The presence of a dimeric form of the lithium amide **(*R*,*R*)-100** was been observed (**Figure 2.6**), and addition of HMPA allowed the formation of a more active species: the chelated monomer **(*R*)-101**. It was also noticed that HMPA de-aggregated the dimeric form **(*R*,*R*)-100** without affecting the chelating bond between the nitrogen and the lithium.

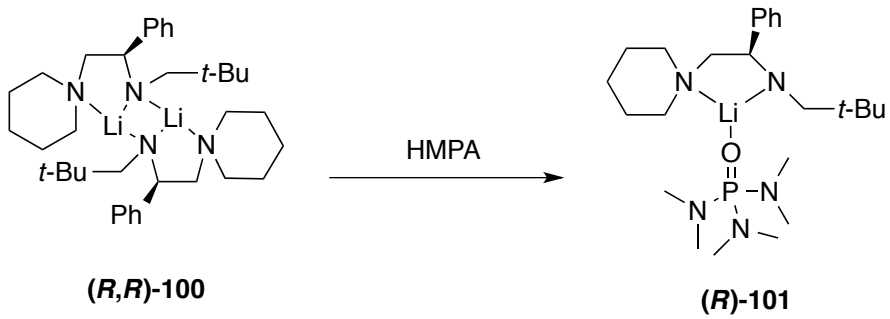

(*R*,*R*)-100 **(*R*)-101**

Figure 2. 6

1.1.3. Introduction to Novel Quench Methods

There has been increasing interest in the use of additives in this field, due to their ability to positively influence the selectivity and reactivity. With this in mind, Simpkins, working on C_2-symmetric bases, explored the effect of salts such as LiCl on the selectivity and reactivity of the C_2-symmetric lithium base **(*R*,*R*)-96** (**Scheme 2.6**).[8] In addition to this, Simpkins investigated the protocol by which these reactions were carried out. At the outset, the reaction was run using an internal quench (IQ) method, *i.e.* the ketone substrate was added slowly to a mixture of all other reagents. Indeed, all the lithium amide base experiments described above were carried out using this method, which was first established by Corey.[9] Employing base **(*R*,*R*)-96**, under the IQ method, the desired product was produced with a moderate 69% e.e. (**Table 2.1**, **Entry 1**). Alternatively, the reaction was studied using an external quench (EQ) protocol, *i.e.* the base and the ketone substrate were mixed together prior to the addition of the electrophile. In this case, a very low enantioselectivity was observed (**Table 2.1, Entry 2**). It is important to note the effect of lithium chloride; carrying out the reaction in the presence of this additive resulted in a high

enantioselectivity being observed (**Table 2.1, Entry 3**). This result has been rationalized by the *in situ* formation of LiCl when the IQ method was applied. In fact, the lithium enolate, formed on deprotonation of the ketone (**35**), was quenched with TMSCl, generating the silyl enol ether **(*S*)-37**, and LiCl salt, which was key in promoting the reaction.

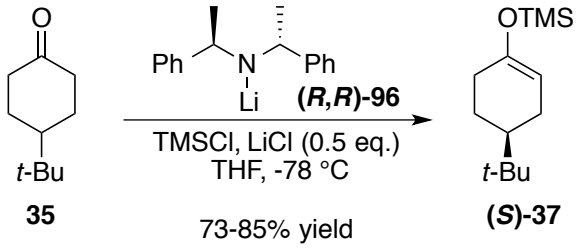

Scheme 2. 6

Entry	Quench	Additive	e.e.
1	IQ	none	69% (*S*)
2	EQ	none	23% (*S*)
3	EQ	LiCl	83% (*S*)

Table 2. 1

In order to establish the effect of LiCl within such processes, Koga conducted X-ray diffraction and NMR experiments using the C_2-symmetric bases.[10] Under EQ conditions, the asymmetric deprotonation was carried out at -78 °C and -114 °C, employing various salts (LiCl, LiBr, LiI) at various loadings (**Scheme 2.7**, **Table 2.2**). Carrying out the reaction using 1.2 equivalents of lithium chloride resulted in a high yield of 87% and a high enantioselectivity of 88% e.e. for compound **(*S*)-37** (**Table 2.2**, **Entry 1**). Moving to lithium bromide as the additive, a comparable yield and enantioselectivity was observed (**Table 2.2**, **Entry 2**). However, upon moving to lithium iodide, whilst the yield was still appreciably high, a much lower 44% e.e. was obtained (**Table 2.2**, **Entry 3**).

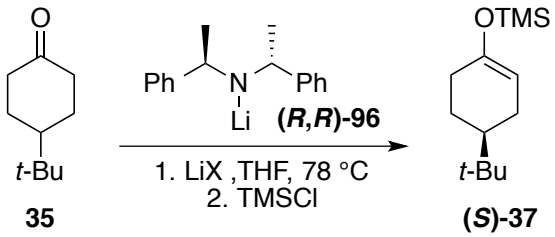

Scheme 2. 7

Entry	Additive (eq.)	Yield %	e.e.
1	LiCl (1.2 eq.)	87	88% (*S*)
2	LiBr (3.6 eq.)	82	86% (*S*)
3	LiI (1.2 eq.)	85	44% (*S*)

Table 2. 2

Based upon NMR spectra (^{6}Li and ^{15}N) of the lithium amide bases, four different lithium species were suggested (**Figure 2.7**). The monomeric lithium amide **A** and the homo-dimer **B** were observed when the base was analysed by NMR spectroscopy without LiCl in the reaction vessel. More surprisingly, the presence of mixed aggregates **C** and **D** were observed upon addition of LiCl salt to the reaction mixture. Although it was not observed as the major species, the mixed dimer **D** was suggested to be the active species, as the amount of this aggregate is lowered in the presence of LiBr, and is non-existent when LiI is the additive. A rapid equilibrium between these different aggregates supports the enantioselectivity observed in the presence of different lithium salts (*c.f.* **Scheme 2.7**, **Table 2.2**). The two species, **B** and **D**, were considered as the active species in solution, allowing high reactivity and selectivity and the *in situ* formation of LiCl.

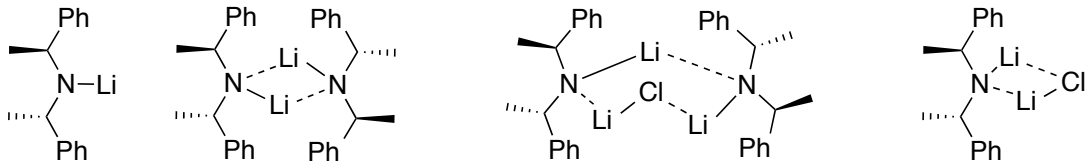

A **B** **C** **D**

Figure 2. 7

1.1.4. Expanding the Substrate Scope

With the additive effect established, exploration of the asymmetric deprotonation was extended to the application of this reaction on a range of substrates. Honda contributed to this area by exploring the reactivity of these bases on varying ring systems.[11] On studying a range of substrates, no general trend could be established, as the reactivity and selectivities obtained were not only substrate dependent but also amide dependant. In these cases, the enolates were quenched with a more stable electrophile, TESCl, as the silyl enol ethers derived from TMSCl could not be isolated. As observed in **Table 2.3** (**Scheme 2.8**) with substrate **2.9** under the optimised conditions, use of lithium base **(*R*,*R*)-96** resulted in a 67% yield and a high 92% e.e. (**Entry 1**), whereas the base **(*R*)-101** afforded a 68% yield but a low 42% e.e. (**Entry 2**).

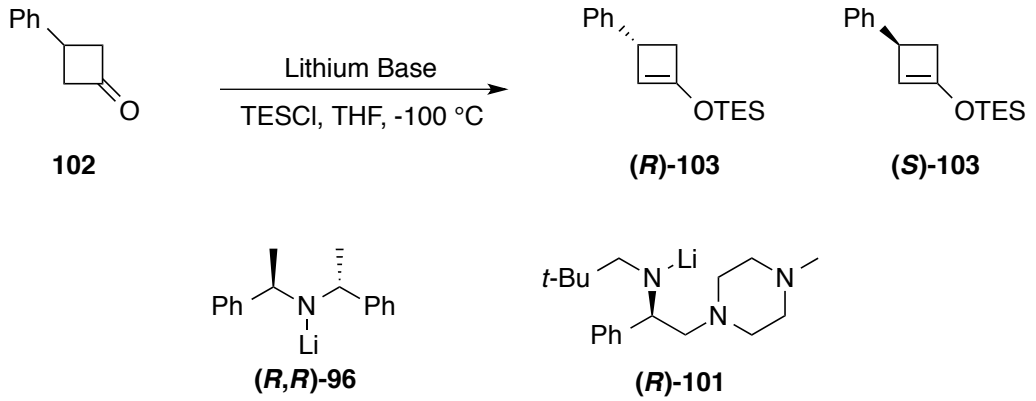

Scheme 2. 8

Entry	Base	Additive	Yield %	e.e.
1	**(*R*,*R*)-96**	-	67	92% (*S*)
2	**(*R*)-101**	HMPA	68	47% (*S*)

Table 2. 3

Meanwhile, substrate **104** (**Scheme 2.9, Table 2.4**) gave a good yield of 85% with the lithium base **(*R*,*R*)-96**, but afforded a poor 12% e.e. (**Entry 1**). In this case, however, the chelating base **(*R*)-101** gave a good 70% yield and a high 72% e.e. of product **(*S*)-105** (**Entry 2**).

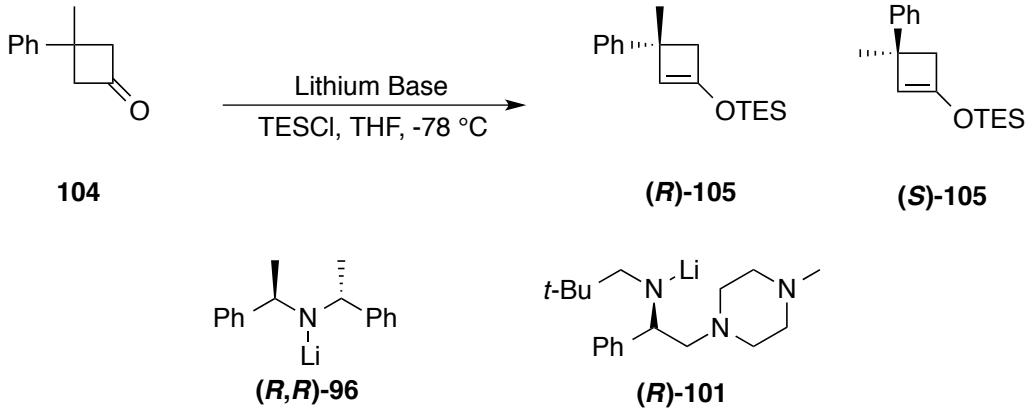

Scheme 2. 9

Entry	Base	Additive	Yield %	e.e.
1	**(*R*,*R*)-96**	-	85	12% (*S*)
2	**(*R*)-101**	HMPA	70	72% (*S*)

Table 2. 4

This example highlights one of the key difficulties with the use of lithium amide bases for asymmetric deprotonation: the reactivity and selectivity can vary depending on many parameters, and this is in part due to the different aggregation states involved with these species. Furthermore no rationalisation was given by the authors regarding the difference in selectivity and reactivity observed.

Although the results are not always predictable with new substrates, the asymmetric deprotonation has been used in the total synthesis of natural products.[12] Recently, Aggarwal applied this strategy towards the synthesis of (+)-anatoxin, where a C_2-symmetric lithium base was used to carry out an asymmetric deprotonation on an eight-membered cyclic ketone. The electrophile chosen to quench the enolate was diphenylphosphoryl chloride (**Scheme 2.10**).[13] An EQ protocol was been applied, with the addition of the amine hydrochloride salt ((**R,R**)-**108**) and 2 eq. of *n*-BuLi thereby generating LiCl *in situ* along with the lithium amide base. This protocol afforded a very good yield of 89%, and an excellent 89% e.e. of the enol phosphate

compound **(*R*)-107**. It should be noted that these levels of selectivity are obtained at the very low temperature of -100 °C.

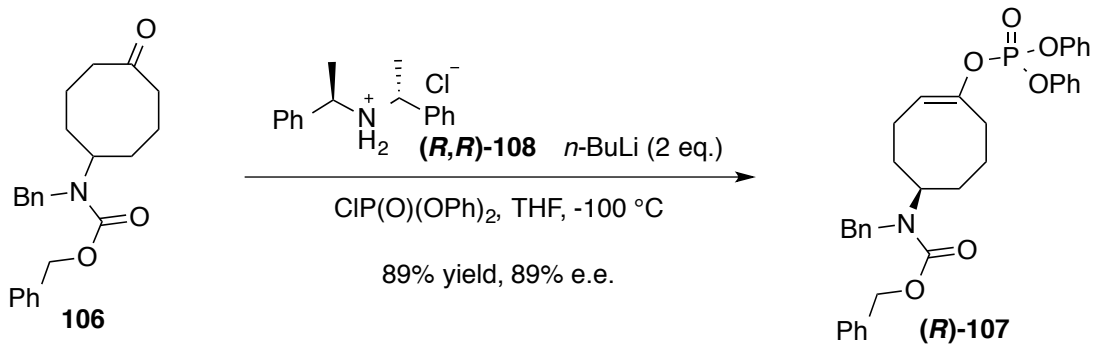

Scheme 2. 10

The asymmetric deprotonation of cyclic ketones is not the only application of chiral lithium amide bases. Clayden et al. reported a selective deprotonation of an amine followed by a dearomatising cyclisation in studies towards the formal total synthesis of (-)-kainic acid.[14] Herein (**Scheme 2.11**), the asymmetric deprotonation is carried out by the C_2-symmetric base **(*R*,*R*)-96**, and the chiral organolithium compound thus generated retains its chirality and reacts in a Michael type addition, followed by a rearrangement, leading to the cyclized compound **111**, afforded in a high enantiomeric excess of 80%.

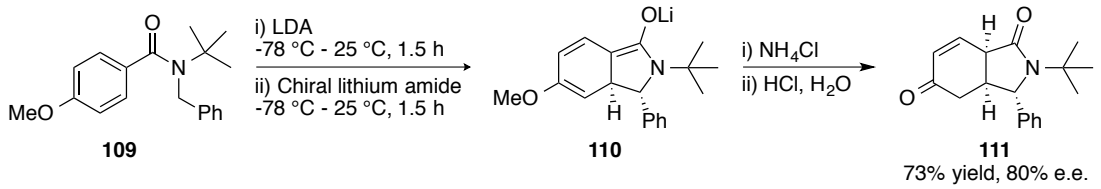

Scheme 2. 11

The body of work established over the past three decades has improved the scope of asymmetric deprotonation using lithium amide bases by improving our understanding of the various aggregation states involved. These chiral lithium amide bases have showed good selectivity and reactivity with a range of different substrates

and electrophiles, allowing the formal synthesis of various natural products. Although the reactivity and selectivities are in many cases high, the predictability of the reaction often suffers due to the influence of many parameters such as aggregation states, additives, bases and electrophiles.

1.2. Chiral Magnesium Bases

So far, lithium bases have delivered very promising results in a range of asymmetric deprotonation reactions, however the temperatures required for the preparation and use of lithium bases are expensive on an industrial scale. The preparation of the chiral lithium amide requires addition of the amine to the organolithium species at -78 °C, then the reaction vessel is brought to room temperature to form the active, thermodynamic aggregate. With the base formed, the reaction mixture is then re-cooled to -78 °C to carry out the asymmetric deprotonation. Although this process does not require a lot of time, it can be seen that such a preparative method would become expensive on an industrial scale (as the variation in temperature of a batch is energy consuming). On the other hand, magnesium bases are know to be more thermally stable than lithium bases.[15]

1.2.1. Advantages of Magnesium amides

One key aspect of magnesium bases was the fact that they present fewer aggregation states in solution than the corresponding lithium species.[16] Crystal structures and NMR spectroscopic studies on magnesium bisamides have showed that, depending on the solvent, the usual aggregation state observed is a homo dimer species **112** (**Figure 2.8**). The equilibrium between the homo dimer and the monomeric species **113** can be displaced by addition of a Lewis base additive such as HMPA. In fact, HMPA coordinates to the homo dimer **112** to form a new chelated species **114**, aiding the disaggregation and forming the monomer **113** and the Lewis base coordinated species **115**.

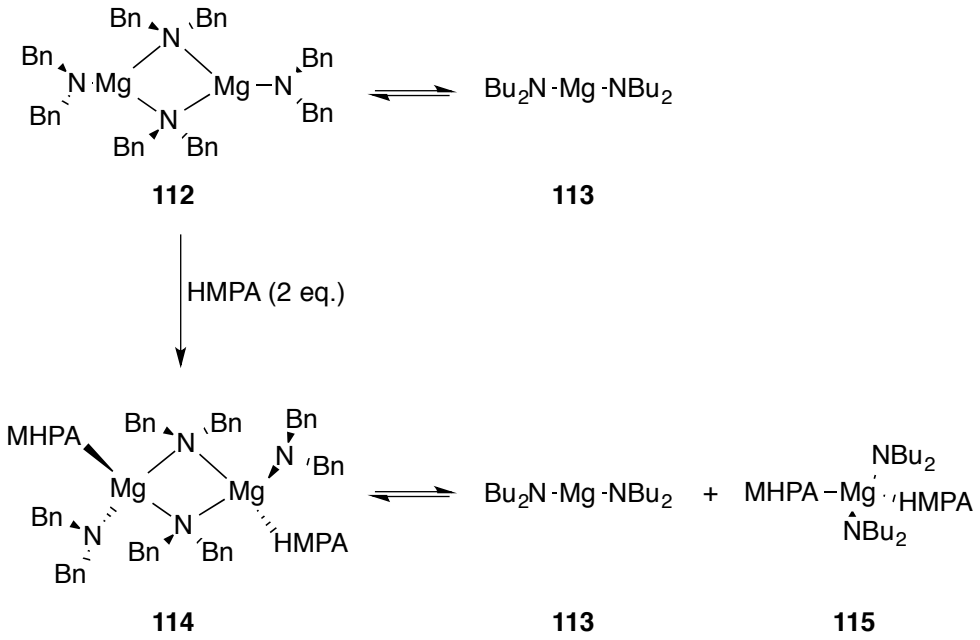

Figure 2. 8

One other advantage of their use is that magnesium species are divalent, which means that heteroleptic species can be formed, increasing the diversity of structures available. Indeed, the reactivity of the base can thus be tailored by varying the nature of the groups present on the magnesium (O, N, S, etc.).[17]

1.2.2. Magnesium Bisamide Bases

The first use of a magnesium bisamide species for asymmetric deprotonation was reported by Evans and Nelson (**Scheme 2.12**).[18] Chiral sulfonamide-derived magnesium base **(*S*,*S*)-118** was employed in a catalytic process to deprotonate compound **116** in an asymmetric manner to afford **(*S*)-117** in high yield and high stereoselectivity. As shown in **Table 2.5**, the variation of the aryl group to Ph (**Entry 1**) afforded a 92% yield of product **(*S*)-117** in an enantiomeric ratio of 93:7. When the aryl unit was changed to a *p*-F-C_6H_5 group (**Entry 2**), this resulted in a high 97% yield and an e.r. of 95:5, whilst changing it to *p*-$CH_3OC_6H_5$ (**Entry 3**) afforded a good 93% yield and an e.r. of 93:7.

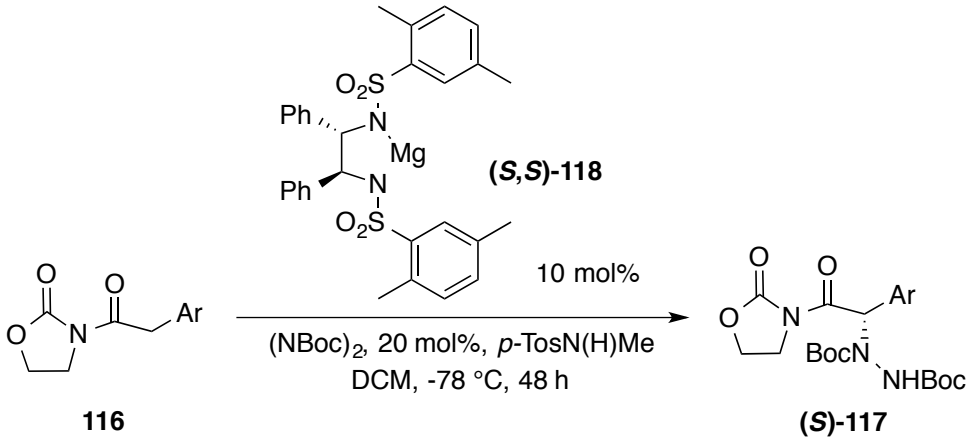

Scheme 2. 12

Entry	Ar	Yield %	e.r. (*S*):(*R*)
1	C_6H_5	92	93:7
2	*p*-F-C_6H_5	97	95:5
3	*p*-CH_3O-C_6H_5	93	93:7

Table 2. 5

Later, Kerr and Henderson developed, from a commercially available, and inexpensive (*R*)-*N*-benzyl-1-phenylethanamine **(*R*)-33**, a magnesium bisamide species (**Scheme 2.13**).[19] The bisamide **(*R*)-119** was formed by heating the amine to reflux in various solvents (Et_2O, THF, hexane or heptane) with the commercially available *n*-Bu_2Mg. It was been observed that no crystals were formed during this process, and that the bisamide remained soluble under these conditions. The formation of the base has been observed by following the N-H signal by ^{1}H NMR spectroscopy.

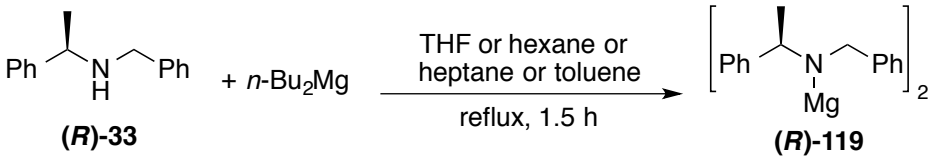

Scheme 2. 13

Kerr and Henderson then carried out studies on the asymmetric deprotonation of 4-*tert*-butylcyclohexanone using base (**(*R*)-119**), and obtained very promising results when the reaction was screened in a small range of solvents (**Scheme 2.14**, **Table 2.6**). As observed in **Entry 1**, the reaction in diethyl ether afforded a good conversion of 83% and a good enantiomeric ratio of 80:20 favouring **(*S*)-37**. When the solvent was switched to DCM (**Entry 2**), only a 40% conversion was observed, with a lower enantiomeric ratio of 72:28. On the other hand, when the reaction was carried out in THF (**Entry 3**), an excellent 94% conversion was obtained, and a high enantioselectivity of 86:14, making this solvent the most effective one for this chemistry.

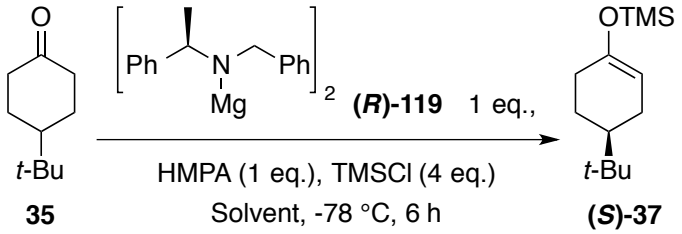

Scheme 2. 14

Entry	Solvent	Conversion %	e.r. (*S*):(*R*)
1	Et_2O	83	80:20
2	CH_2Cl_2	40	72:28
3	THF	94	86:14

Table 2. 6

With the solvent system determined, the importance of HMPA as an additive was then explored (**Scheme 2.15**). As depicted in **Table 2.7**, in the absence of HMPA a good enantiomeric ratio of 90:10 was delivered, but with a poor 33% conversion (**Entry 1**), whereas adding 0.5 eq. of HMPA (**Entry 2**) gave a high 82% conversion with a good e.r. of 91:9. Increasing the HMPA loading to 1 eq. resulted in an increase in conversion to 94% but decreased the enantioselectivity to 86:14.

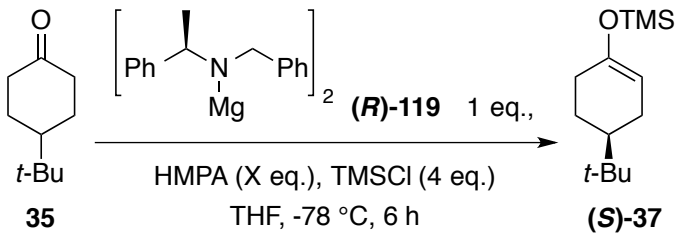

Scheme 2. 15

Entry	HMPA (eq.)	Conversion %	e.r. (*S*):(*R*)
1	0	33	90:10
2	0.5	82	91:9
3	1	94	86:14

Table 2. 7

1.2.3. Expanding the Substrate Scope

This work suggested that the presence of HMPA was indeed important for the selectivity and reactivity, but also that the choice of solvent was also crucial to the reaction. With this methodology in hand, an array of 4-substituted cyclohexanone substrates were converted to their respective silyl enol ethers with high levels of selectivity (**Table 2.8**). Varying the R- group of cyclohexanones the general trend was of high conversions. With a 4-phenyl group (**Entry 2**), a good conversion of 79% was obtained, with an enantiomeric ratio of 87:13; whereas a 4-methyl group (**Entry 3**) afforded an 81% conversion and a 91:9 enantiomeric ratio. As shown in **Entry 4**, the 4-*i*Pr-substituted product was formed in 77% conversion with a high 95:5 of enantiomeric ratio, and as presented in **Entry 5**, the 4-*n*-Pr-substituted product was formed with 88% conversion and an 82:18 er.

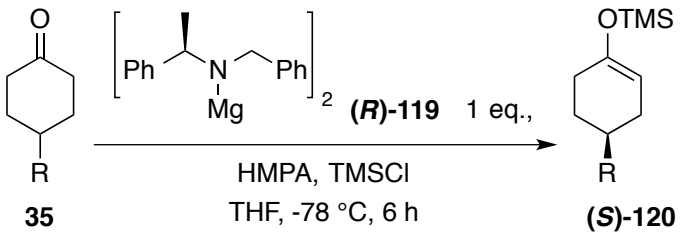

Scheme 2. 16

Entry	R	Conversion %	e.r. (*S*):(*R*)
1	*t*-Bu	82	91:9
2	Ph	79	87:13
3	Me	81	91:9
4	*i*-Pr	77	95:5
5	*n*-Pr	88	82:12

Table 2. 8

Although Evans had shown that the magnesium sulfonamide gave good selectivity in DCM, in the case of the chiral amides studied in our laboratories, THF afforded the best selectivities and conversions. Therefore all further development of the magnesium bases was carried out in THF. When extending the methodology to the asymmetric deprotonation of 2,6-dimethylcyclohexanone, a surprising result was observed.[20] This lead them to study more thoroughly 2,6- substituted cyclohexanones where, both the *trans*- and *cis*-ketone were studied. The first notable feature of this system is the very high selectivities obtained when using the *cis*-ketone (**Scheme 2.17**). The selectivity observed for the deprotonation of compound **121** at -78 °C (**Table 2.9**, **Entry 1**) was 99.5:0.5 e.r. with only a 54% conversion. Although a very high selectivity was obtained, the reaction required higher temperatures to afford complete conversion. At -40 °C (**Table 2.9**, **Entry 2**), a very high 99% conversion was observed with an excellent selectivity of 99.8:0.2 of e.r. At room temperature, the reaction was complete in only 2 h and with a high 91:9 e.r. (**Table 2.9**, **Entry 3**).

Scheme 2. 17

Entry	Temperature	Conversion	e.r. (*S*):(*R*)
1	- 78 °C[a]	54 %	99.5:0.5
2	- 40 °C[b]	99 %	98.8:1.2
3	rt[c]	100 %	91:9

a = reaction time 39 h, b = reaction time 6 h, c = reaction time 2 h

Table 2. 9

To understand the high selectivity obtained in the *cis*- case, the corresponding *trans*-ketone, **123**, was also studied. Interestingly, in this case, the deprotonation allowed the kinetic resolution of **(*R*,*R*)-123** to generate an enantiomeric ratio of 79:21 of product **(*S*)-124**. This result can be explained by considering the mechanism of asymmetric deprotonation.

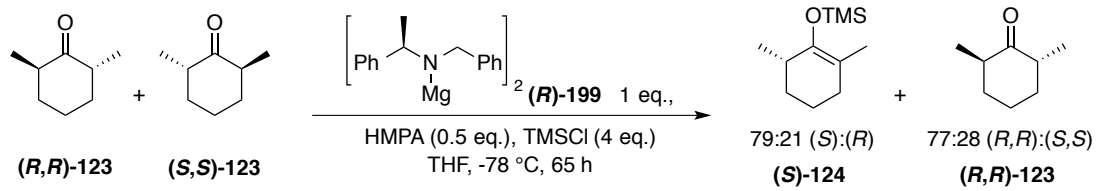

Scheme 2. 18

As shown in **Figure 2.9**, only one proton in each isomer could be deprotonated, in accordance with the stereoelectronic requirements of the deprotonation. As described previously, the σ∗ orbital of the C-H should be aligned with the π* orbital of C-O bond, in order to generate an enolate. Therefore, in chair **A** and **B**, only the proton in the equatorial conformation can be deprotonated. The asymmetric deprotonation involves a diastereomeric transition state, resulting in one deprotonation taking place much more rapidly than the other and therefore allowing a kinetic resolution.

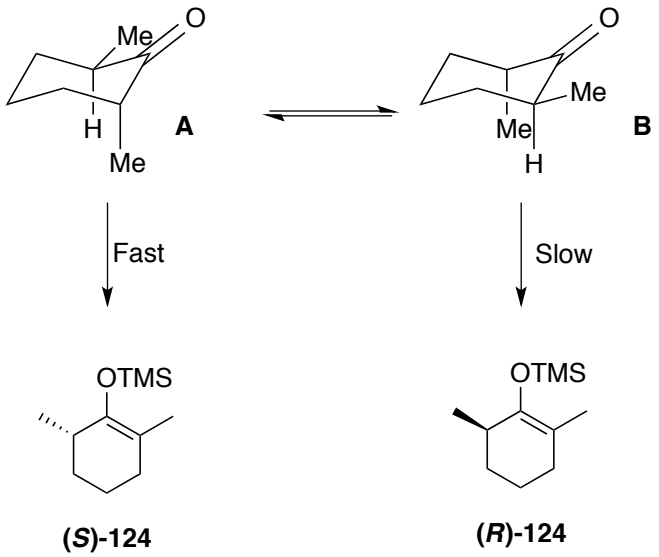

Figure 2. 9

Following these results, a range of chiral amines were synthesised by the Kerr group in order to further study the asymmetric deprotonation reaction. Preliminary work on the structure-reactivity relationship showed that the selectivity of the asymmetric deprotonation could be improved by using C_2-symmetric and *pseudo*-C_2-symmetric amines. It should also be mentioned that this work, carried out within our laboratory over the past decade, also focused on chelating amides. Herein, only the simple chiral amide systems will be described, in line with the work carried out on this project.

1.2.4. Towards C_2- and Pseudo-C_2-Symmetric Bases

Since the C_2-symmetric lithium bases developed by Simpkins afforded good selectivities and yields, the Kerr group opted to study the asymmetric deprotonation using a C_2-symmetric magnesium bisamide, **(*R*,*R*)-125**.[21] The asymmetric deprotonation was carried out, following conditions presented in **Scheme 2.19**, and as shown in **Table 2.10**, the reaction carried out at -78 °C (**Entry 1**) afforded a high 93% yield and a high 93:7 enantiomeric ratio. More encouraging, however, was the excellent yield (93 %) and selectivity (88:12) obtained at a more accessible temperature of -20 °C (**Entry 2**). This result represents one of the mildest selective asymmetric deprotonations reported to date, furthermore this process utilised the

DMPU, which is a safer additive than HMPA. The substrate scope showed also demonstrated the high general enantioselectivity of this reaction.

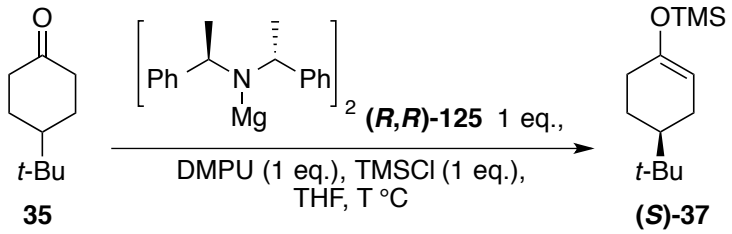

Scheme 2. 19

Entry	Temperature	Yield %	er (*S*):(*R*)
1	-78 °C	93	93:7
2	-20 °C	93	88:12

Table 2. 10

As depicted in **Table 2.11**, following the conditions described in **Scheme 2.20**, various 4-subsituted cyclohexanones afforded enantiomeric ratios up to 95:5, and yield up to 96%. With a 4-*n*-Pr- substituent (**Entry 1**) a high 92% yield was obtained with an e.r. 94:6. The 4-*i*-Pr (**Entry 2**) or 4-Me (**Entry 3**) analogues were both obtained in 96% yield, with a 93:5 e.r. for the *i*-Pr derivative and a 95:5 e.r. for the Me derivative. The presence of the OTBS functional group at the 4-position (**Entry 4**) resulted in a 91% yield with an e.r. of 92:8.

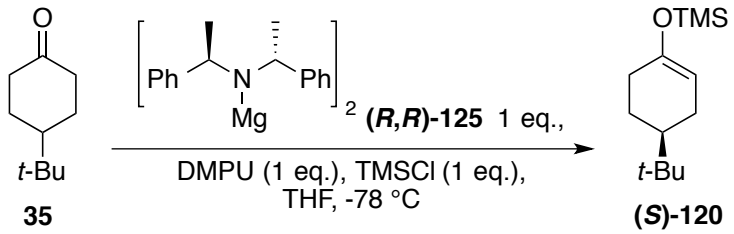

Scheme 2. 20

Entry	R	Yield %	e.r. (*S*):(*R*)
1	*n*-Pr	92	94:6
2	*i*-Pr	96	93:7
3	Me	96	95:5
4	OTBS	91	92:8

Table 2. 11

With these excellent results in hand, a series of C_2-symmetric and *pseudo*-C_2-symmetric bases were explored within the Kerr group. Under otherwise standard conditions (**Scheme 2.21**), the reaction was carried out with different amines, at both -78 °C and -20 °C.[22]

As depicted in **Figure 2.10**, the use of C_2- and *pseudo*-C_2-symmetric bases derived from their parent amines was explored over two different temperature conditions. At first, bulkier C_2-symmetric bases were constructed by extending the methyl group to ethyl (**(*S*,*S*)-126**), and by extending the phenyl group to naphthyl (**(*R*,*R*)-127**). At –78 °C, these bases displayed good selectivities, 12:88 using **(*S*,*S*)-126** and 93:7 using **(*R*,*R*)-127**, however the yields (71% for **(*S*,*S*)-126**, 70% for **(*R*,*R*)-127**) and selectivities obtained were lower than with amine **(*R*,*R*)-125** (*c.f.* **Scheme 2.19**). At -20 °C, use of **(*R*,*R*)-127** gave a good 79% yield and 82:18 selectivity.

Next, a wide range of *pseudo*-C_2-symmetric magnesium bases were explored. The *pseudo*-C_2-symmetric structures were designed by maintaining one α-methylbenzyl unit, while modifying the aryl and alkyl portions of the second unit whilst keeping the absolute stereochemistry consistent. Increasing the bulk of the alkyl group from a methyl unit to an ethyl unit **(*R*,*R*)-128** gave the same order of reactivity (71% yield) and selectivity (94:6) as obtained with **(*R*,*R*)-125**, whereas if the alkyl group was too bulky *i.e. iso*-propyl, as in **(*R*,*R*)-129**, the reactivity drops off, affording only a 21%

yield, and the selectivity is decreased to 86:14. With this result in mind, variation of the aryl unit was thus the main focus going forward.

The importance of the aromatic group was explored by replacing the phenyl group with a cyclohexyl group, in **(*R*,*R*)-134**. At -78 °C, only a 47% yield was observed, with a low selectivity of 85:15, and at -20 °C the yield was increased to 76%, but still with a low selectivity of 70:30. Therefore, the aromaticity was maintained from this point on, and the phenyl group was modified. The addition of a methyl group to the 2-position of the phenyl ring (**(*R*,*R*)-130**) resulted in, at -78 °C, a low 42% yield but a high e.r. of 95:5. At -20 °C, the reactivity was increased to 79% yield with a good selectivity of 90:10. Extending this concept, an ethyl group was added to the 2-position of the phenyl ring (**(*R*,*R*)-138**), delivering a 58% yield and a high e.r. of 96:4 at -78 °C, while at -20 °C, this base afforded an excellent 90% yield with a selectivity of 90:10. With the same idea, the substituent at the 2-position of the phenyl ring was replaced by a methoxy group to give amine **(*R*,*R*)-131**, but the yield obtained with the corresponding base was 42%, and with a low selectivity of 78:22. Placing a phenyl group at the 2-position of the phenyl ring (**(*R*,*R*)-132**) resulted in a good yield of 68%, and a high selectivity of 96:4 at -78 °C, while at -20 °C a good yield of 78% was obtained, with a selectivity of 87:13. When this phenyl group was moved to the 4-position of the phenyl ring (**(*R*,*R*)-133**), only a 48% yield was obtained, with a selectivity of 94:6 at -78 °C, whereas at -20 °C a good 83% yield resulted, with a selectivity of 87:13.

Structurally more elaborate 1- and 2-naphthyl groups were next used instead of the phenyl group, in amines (**(*R*,*R*)-135** and **(*R*,*R*)-136**)**.** With this variation, a yield of only 58% was observed with **(*R*,*R*)-135** whereas 72% was observed with **(*R*,*R*)-136**. The change in structure lead to a slight change in selectivity, with a 96:4 e.r. using **(*R*,*R*)-136** and a 94:6 e.r. using **(*R*,*R*)-135** at -78 °C. At -20 °C, **(*R*,*R*)-135** gave a 72% yield with a selectivity of 84:16, and **(*R*,*R*)-136** delivered a 78 % yield and a selectivity of 89:11. Following this short structure-activity study, simultaneous variation of both the alkyl group and the aryl group was carried out. Compound **(*R*,*R*)-137**, featuring an ethyl group as the alkyl unit and a naphthyl group as the aryl unit, gave a good yield of 80 % and a selectivity of 82:18. Surprisingly, at -20 °C, only a 75% yield and a poor 69:31e.r. was observed with **(*R*,*R*)-137**.

The final structural variation of the amine was to introduce rigidity by joining the alkyl and aryl group, generating a cyclic species. The five membered analogue **(*R*,*R*)-139** afforded an 83% yield but only a selectivity of 74:26 at -78 °C, with the six membered variant **(*R*,*R*)-140** giving only a 62% yield and a selectivity of 82:18 at -78 °C, while at -20 °C a yield of 73% and a selectivity of 74:26 was obtained. Finally, the seven membered ring amine **(*R*,*R*)-141** delivered a good 87% yield, but only a selectivity of 79:21 at -78 °C.

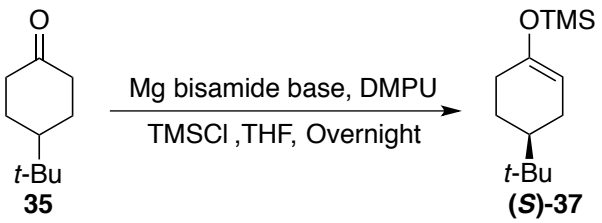

Scheme 2. 21

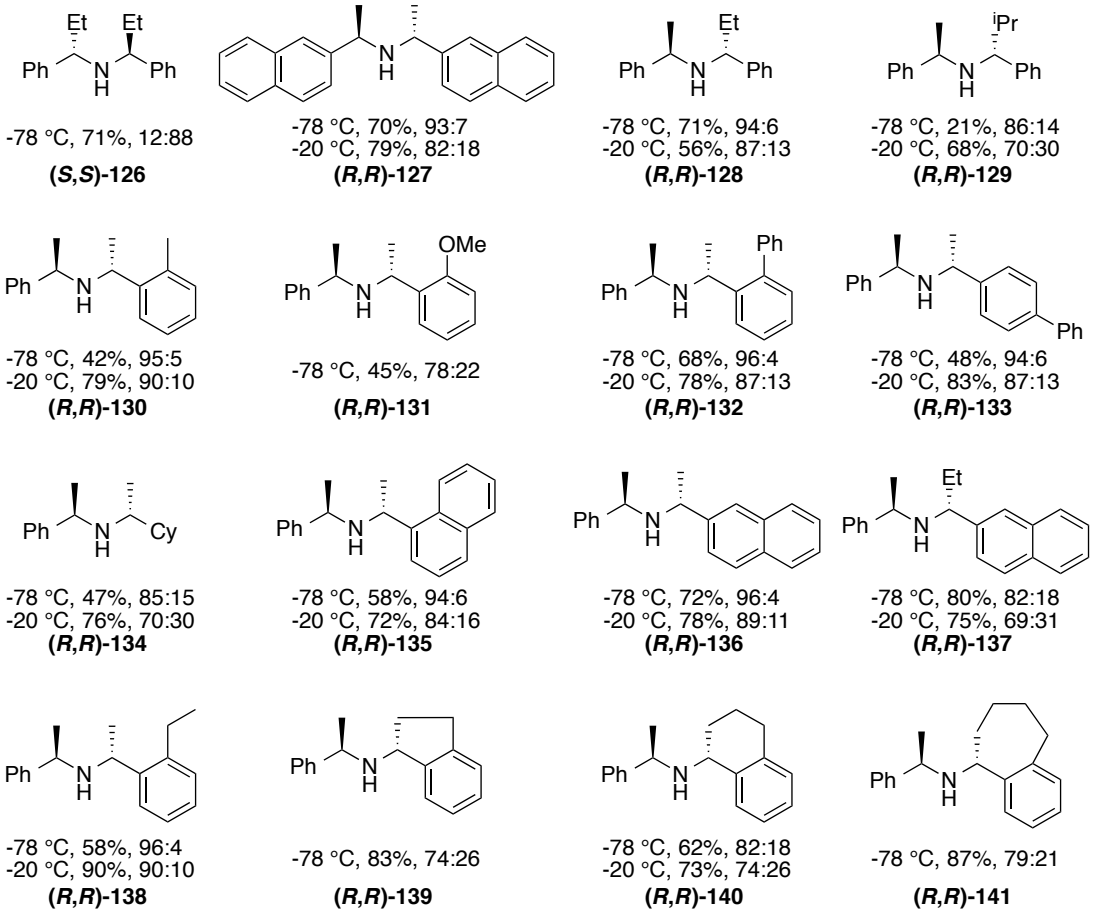

Figure 2. 10

1.2.5. Exploring a Novel Electrophile

Whilst exploring the reactivity and enantioselectivity of the C_2-symmetric bases, the use of diphenylphosphoryl chloride as electrophile was also studied. The resulting enol phosphates display better stability towards acidic aqueous work-up and chromatography compared to the corresponding silyl enol ethers, and therefore this class of functional group represents a useful extension of the methodology. As presented in **Scheme 2.22** a good 74% yield was obtained with a high selectivity of 96:4 for the formation of the enol phosphate from 4-*t*-butylcyclohexanone **35**.[22a] It

should be noted that this result was unoptimised, and therefore further work on this single example was needed. Furthermore, the absolute stereochemistry of the product was not established, as no literature data was available on this compound, and the absolute stereochemistry was only postulated by analogy to the previous work on the formation of enol silanes.

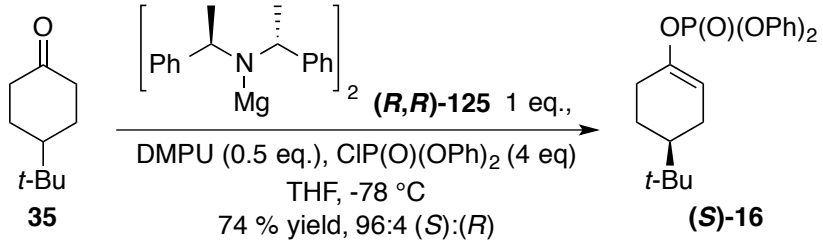

Scheme 2. 22

With this encouraging result in hand, the potential for the formation of chiral enol phosphates using the chiral magnesium base chemistry with phosphoryl electrophiles was explored.

2. Proposed work

Although the scope of magnesium-based amide has been extensively studied in the Kerr group, the substrate- and electrophile scope had the potential to be explored further. So far, some outstanding results, in terms of selectivity and reactivity, had been achieved using chiral magnesium amides, by studying the selectivity induced by different groups on the chiral amine. These studies led to a novel range of C_2-and *pseudo* C_2-symmetric magnesium amide bases.

The use of amines **(*R*,*R*)-126**, **(*R*,*R*)-132**, **(*R*,*R*)-135**, **(*R*,*R*)-136 and (*R*,*R*)-142** to form the corresponding bisamide bases, has resulted in high levels of selectivity and reactivity in the formation of enantioenriched silyl enol ether **(*S*)-37**. We were interested in exploring the asymmetric preparation of enol phosphates with the use of selected magnesium bisamide bases, and to further expand the substrate scope of the reaction through the synthesis and analysis of a range of enol phosphate substrate, such as **(*S*)-72**, **(*S*)-73**, **(*S*)-81** and **(*S*)-82** (**Scheme 23**).

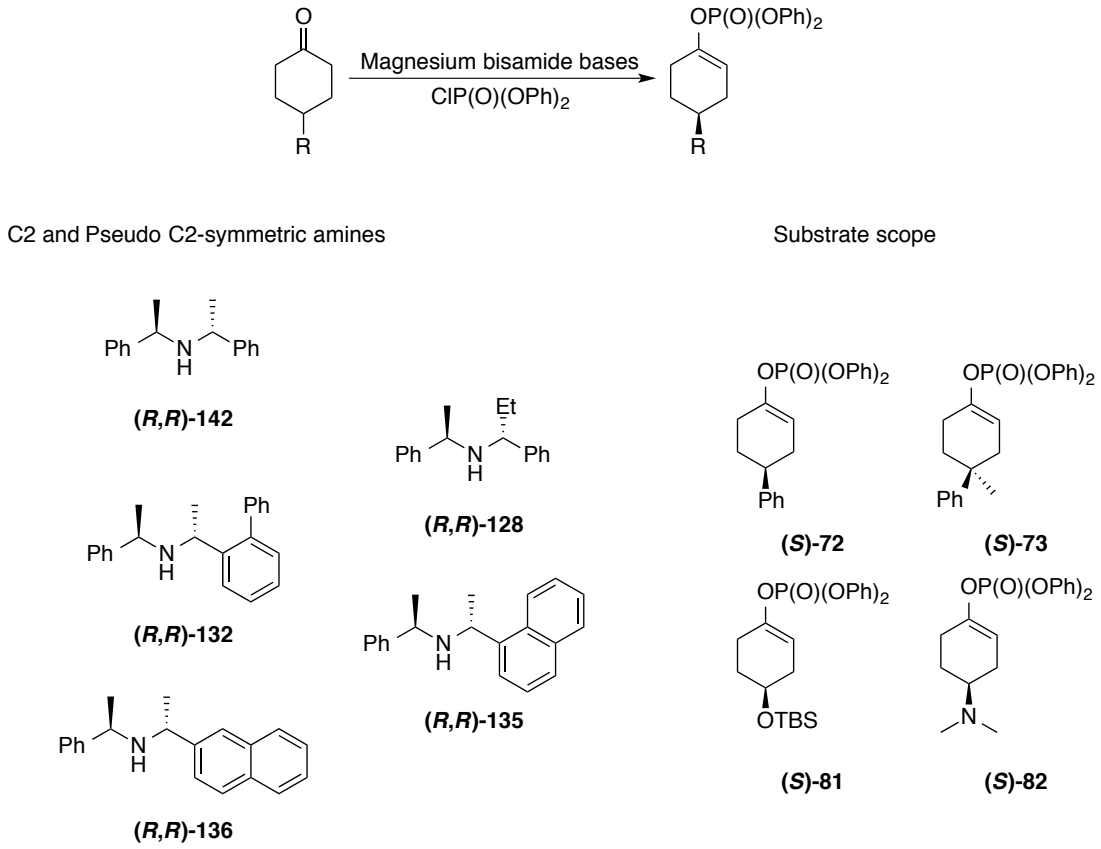
O
R
Magnesium bisamide bases
ClP(O)(OPh)2
OP(O)(OPh)2
R
C2 and Pseudo C2-symmetric amines
Substrate scope
Ph
N
H
Ph
(R,R)-142
Et
Ph
N
H
Ph
(R,R)-128
Ph
Ph
N
H
(R,R)-132
Ph
N
H
(R,R)-135
Ph
N
H
(R,R)-136
OP(O)(OPh)2
Ph
(S)-72
OP(O)(OPh)2
Ph
(S)-73
OP(O)(OPh)2
OTBS
(S)-81
OP(O)(OPh)2
N
(S)-82

Scheme 2. 23

3. Results and Discussions

3.1. Synthesis of Chiral C2 and pseudo C2 symmetric amines

In order to study the reactivity of the new electrophile (the diphenyl phosphoryl chloride) it was decided to use the C_2-symmetric and *pseudo*-C_2-symmetric bases developed previously within the group. Therefore, the first step was the synthesis of the requisite amines in enantiomerically pure form.

Using Alexakis's procedure[23] the requisite amines were synthesised using enantiopure (*R*)-1-phenylethanamine **(*R*)-143** and the corresponding ketone in a reductive amination reaction (**Scheme 2.24**). The reactants were mixed neat under 45 psi of H_2 over three days, with titanium isopropoxide as Lewis acid and palladium on charcoal as catalyst. After work up and recrystallization of the parent acid salt, the enantiopure amine was obtained after neutralising the diastereomerically pure salt obtained. Following the preparation the various *pseudo*-C_2-symmetric and C_2-symmetric amines (**(*R*,*R*)-128**, **(*R*,*R*)-132**, **(*R*,*R*)-135**, **(*R*,*R*)-136** and **(*R*,*R*)-125**) were prepared (**Figure 2.11**), by employing the corresponding ketone with **(*R*)-143**. Although the yield for the synthesis and extraction of these enantiopure *pseudo*-C_2-symmetric amines was low, the quantities obtained were sufficient to carry out the proposed studies.

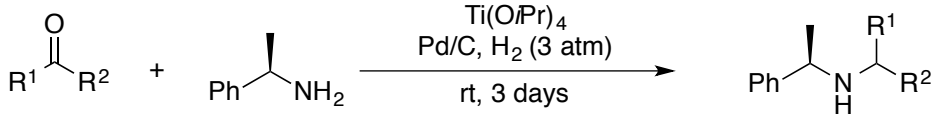

(*R*)-143

R^1= methyl or ethyl
R^2= phenyl, napthyl or 2-phenyl-phenyl

Scheme 2. 24

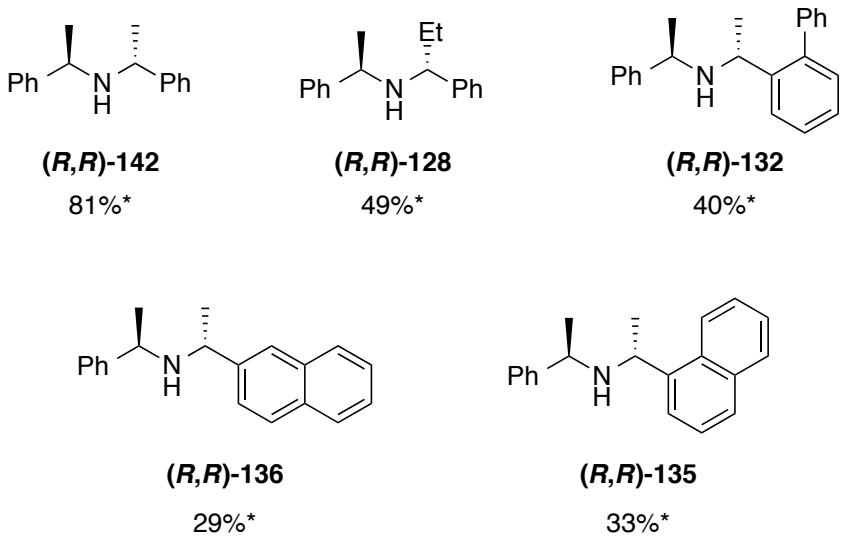

Figure 2. 11

With the synthesis of the most effective C_2- and *pseudo*-C_2-symmetric amines in hand, attention turned to the asymmetric deprotonation using the new electrophile, diphenylphosphoryl chloride. The amines were distilled before use, and the reactions carried out on the benchmark ketone 4-*t*-butylcyclohexanone **35**.

3.2. Asymmetric Deprotonation Using Magnesium Bisamide Base

Before attempting optimisation and a study of the scope, the first objective was to carry out the deprotonation on the standard ketone and obtain the same level of selectivity and yield (**Scheme 2.25**) as obtained previously within the group (*c.f.* **Scheme 2.22**).[22a] With the benchmark reaction successfully reproduced, attention was next turned towards optimization of the asymmetric deprotonation.

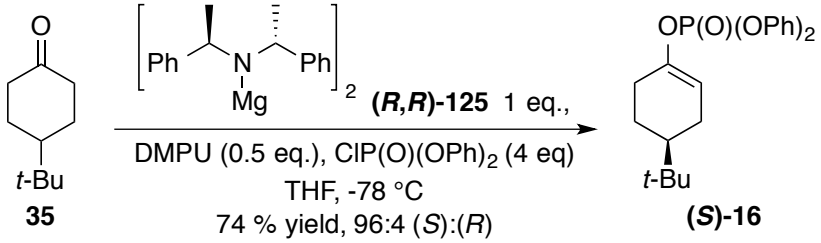

Scheme 2. 25

3.2.1. Electrophile Loading

It was decided to begin the optimisation by studying the electrophilic loading, not only because this reagent is important in terms of environmental and waste considerations, but also because diphenylphosphoryl chloride has been described as more reactive than the previously used electrophiles, leading to concerns about side-reactions related to reaction of the magnesium species with the electrophile. Having stated this, our carbon-centred base studies (Chapter 1) showed that a stoichiometric amount of the electrophile was enough to enable an efficient reaction. As shown below (**Table 2.12**), the amount of electrophile was gradually lowered from 4 eq. to 1 eq., otherwise using the conditions described previously in **Scheme 2.26**. By reducing the electrophile loading, an increase in yield was observed with 3 eq. (**Entry 1**) and 2 eq. (**Entry 2**), while maintaining the same levels of enantioselectivity. The use of a stoichiometric amount of the electrophile gave a slightly lower yield (**Entry 3**, 84 %) when compared to the result obtained in **Entry 2** (91%). According to these results, the optimum loading was between 1 eq. and 2 eq. of electrophile, and therefore a slight excess of electrophile required. Pleasingly, a slight excess of electrophile was enough to obtain a high yield. With 1.1 eq. (**Entry 4**) of electrophile, high yields in the range 88-91 were obtained. Whereas with 1.2 eq. of electrophile, a consistent yield of 95% was observed over two runs (**Entry 2**). Thus, the optimum electrophile loading was determined to be 1.2 equivalents.

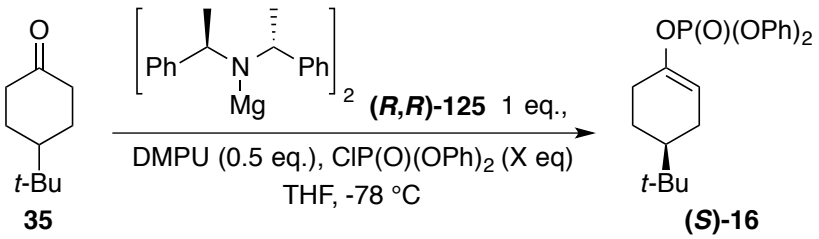

Scheme 2. 26

Entry	X	Yield %	er (*S*):(*R*)
1	3	92	95:5
2	2	91	95:5
3	1	84	95:5
4	1.1	91	95:5
5	1.2	95	95:5

Table 2. 12

With these results in hand, the next parameter to study was the reaction time.

3.2.2. Reaction Time

Using the previously optimised electrophile loading, the reaction time was studied. As a reference, from Chapter 1, using carbon-centred bases, the enol phosphate formation was complete in only 1 h.

Pleasingly, in the current study with the bisamide base, an excellent 92% yield was obtained after only 1 h of reaction time (**Entry 1**, **Table 2.13**). Following this optimal result, shorter reaction times were then studied. Thus, the reaction was carried out and quenched after 30 min, giving a slightly decreased 89% yield (**Entry 2**, **Table 2.13**). Further studies showed that longer reaction times did not allow for any substantial increase in reactivity; and with this in mind, it was been decided to set the optimum reaction time as 1 h.

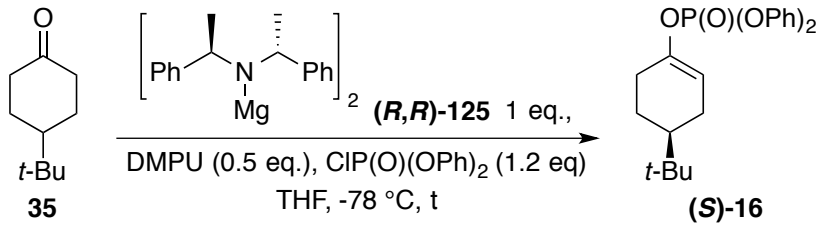

Scheme 2. 27

Entry	t (min)	Yield %	e.r. (*S*):(*R*)
1	60	92	95:5
2	30	89	95:5

Table 2. 13

Next, it was decided to study the importance of the DMPU additive. As mentioned previously, DMPU is a Lewis base, and aids the disaggregation of the magnesium bisamide bases.[10] c

3.2.3. Additive Loading

Lewis base and salt additives have been extensively studied in the past to increase the selectivity and reactivity of the chiral magnesium amide bases. The role played by additives in the formation of enol phosphates should therefore be worthy of study. Starting from the current optimal conditions (**Scheme 2.28**), the reaction was studied with both an increase and decrease in additive loading. As shown in **Table 2.14**, without DMPU in the reaction mixture (**Entry 1**), a surprisingly high yield of 92% was observed, accompanied with a slight decrease in selectivity, whereas the increase to 1 eq. of DMPU (**Entry 2**) resulted in a slight decrease in yield without loss in selectivity.

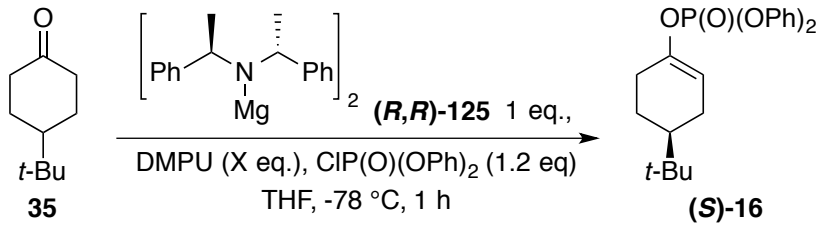

Scheme 2. 28

Entry	DMPU	Yield %	e.r. (*S*):(*R*)
1	0 eq	92	94:6
2	1 eq	85	95:5

Table 2. 14

The results observed are surprising but can be rationalised. In the past, the most used Lewis base was HMPA, and for health reasons it has now been replaced by the less harmful DMPU. It should however be noted that both HMPA and diphenylphosphoryl chloride have a P=O bond, which could act as a Lewis base and therefore activate the base. Thus, the base could be disaggregated by either the diphenylphosphoryl chloride or even the *in situ* formed enol phosphate product. The slight excess of electrophile required might tend to favour the diphenylphosphoryl chloride in breaking down the aggregation state of the magnesium bisamide. It should also be noted that LiCl was briefly studied as an additive, and it was noted that although the selectivity of the reaction was unchanged, the reactivity dropped drastically.

So far, outstanding levels of reactivity and selectivity have been established in the formation of chiral enol phosphates, with lowered reaction time, low amounts of electrophile and without the need for any additive, whilst maintaining the levels of selectivity and reactivity observed previously for the formation of enantioenriched silyl enol ethers. Having optimised the reaction conditions at -78 °C, we were next keen to exploring milder and more process efficient temperatures.

3.2.4. Temperature Control

The temperature study was based on employing the best conditions for reactivity and selectivity found for the reaction at -78 °C. Therefore, the reaction was carried out as described in **Scheme 2.29** while varying the temperature. Prior to the results presented below, a range of temperatures were explored during this study to establish the overall reactivity and selectivity observed while raising the temperature. Only the reactions at -20 °C are presented here, as they allow direct comparison with the previous work on silyl enol ethers, and at room temperature, which would represent the ideal higher temperature which can be used as a benchmark. As shown in **Table 2.15** below, when the reaction was carried out at -20 °C (**Entry 1**), a 69% yield was obtained with a selectivity of 86:14; whereas at room temperature only a 23% yield with a selectivity of 74:26 was observed (**Entry 2**). In fact, a linear trend of loss of both reactivity and selectivity was observed along the temperature gradient between -75 °C and room temperature. Having observed previously that the reaction displayed a mild increase in selectivity when the DMPU was used as an additive, the same range of temperatures were studied in its presence. As shown in **Entry 3**, at -20 °C, the reaction afforded a lowered yield of 65% and an increased selectivity of 88:12. This trend was also observed at room temperature (**Entry 5**, 20% yield, 80:20 selectivity).

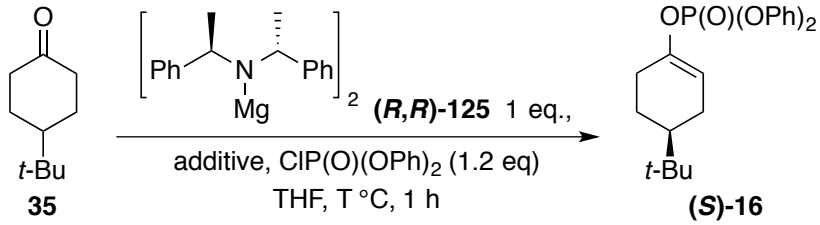

Scheme 2. 29

Entry	Additive	Temperature	Yield %	e.r. (*S*):(*R*)
1	-	- 20 °C	69	86:14
2	-	rt	23	74:26
3	DMPU (0.5 eq.)	-20 °C	65	88:12
4	DMPU (0.5 eq.)	r.t.	20	80:20

Table 2. 15

This decrease in yield was attributed to a side reaction, specifically nucleophilic attack of the amide onto the electrophile, generating compound **(*R*,*R*)-144** (**Figure 2.12**). Unfortunately, however, the isolation and identification of this by-product again proved difficult.

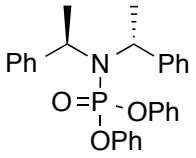

(*R*,*R*)-144

Figure 2. 12

With these results in hand, various quench methodologies could now be explored, as they could allow higher levels of reactivities and/or selectivities. In particular, the quench protocol could have a profound effect on any side-reactions responsible for the decrease in reaction efficiency.

3.2.5. Quench Conditions

As described in Chapter 1 (**Figure 1.2**), there exists a broad range of quench methodologies, and we were keen on exploring them to improve our process at higher temperatures. In order to elicit the biggest improvement in the process, it was decided to explore the various quench options at room temperature, as it was under such conditions that the lowest levels of reactivity were. It should also be noted that among the 3 other quench conditions presented in Chapter 1 (External quench, co-addition, and reverse addition) the reverse addition method was not explored in this case, as the chiral base was freshly prepared for each reaction and, being air- and moisture-sensitive, transferring it into another vessel would introduce the potential for more impurities to form.

As presented below, when the reaction was carried out as shown in **Scheme 2.30**, the external quench methodology afforded a high 77% yield and a selectivity of 79:21 (**Entry 1**, **Table 2.16**). In contrast, the use of the co-addition protocol resulted in a 74% yield with a selectivity of 88:12 (**Entry 2**, **Table 2.16**). The results obtained

through changing the quench conditions are interesting, as in both cases, a much higher improvement in reactivity was observed. The external quench delivered the highest yield observed at such a mild temperature, but the selectivity observed was slightly lower compared to the standard internal quench. On the other hand, the co-addition protocol resulted in a moderate 74% yield, being only slightly lower than the external quench, but with the highest selectivity observed yet at room temperature.

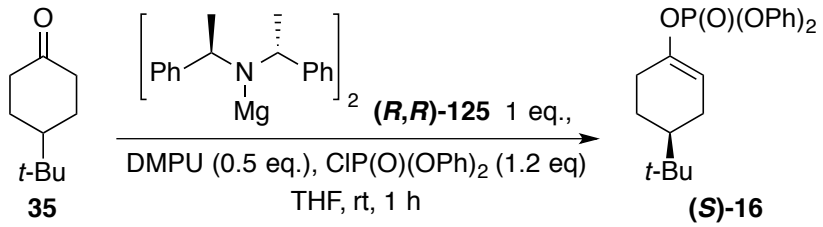

Scheme 2. 30

Entry	Quench	Yield %	e.r. (*S*):(*R*)
1	External	77	79:21
2	Co-addition	74	82:18

Table 2. 16

We were pleased to observe that our hypothesis of nucleophilic attack of the base onto the electrophile was indeed viable, as both these methodologies resulted in an improved yield. In fact, both methodologies only present the electrophile under low loadings in the presence of the base, as in the external quench the electrophile was added slowly after the enolate was formed, and for the co-addition, only a stoichiometric amount of electrophile was added to the reaction mixture, making the concentration of electrophile present constant over time.

With these results in hand, the reaction temperature was again studied, with reactions ranging from room temperature to -78 °C carried out using the co-addition protocol. Following conditions presented in **Scheme 2.31**, the various results are depicted in **Table 2.17**. At 0 °C, a 73% yield and 86:14 e.r. was obtained (**Entry 1**), and when carried out at -20 °C, a high 89% yield and a selectivity of 89:11 resulted (**Entry 2**). Finally, at -40 °C, a 91% yield and 92:8 e.r. was delivered. It should also be

mentioned that at -78 °C, the co-addition protocol afforded the same results as the classical internal quench.

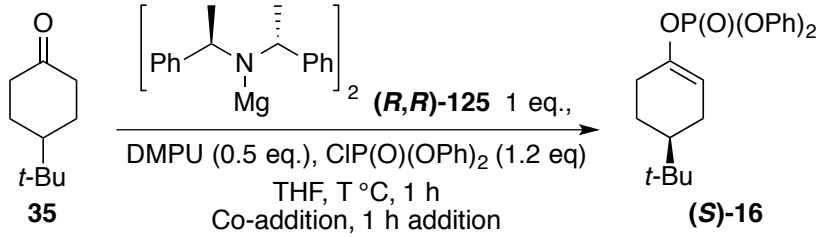

Scheme 2. 31

Entry	Temperature (°C)	Yield %	e.r. (*S*):(*R*)
1	0	73	86:14
2	-20	89	89:11
3	-40	91	92:8

Table 2. 17

Following these results, a reaction temperature of -20 °C was chosen as a good compromise between, reactivity, selectivity and energy efficiency. Furthermore, the results obtained for the formation of enol phosphates at this temperature were similar to those obtained for the formation of silyl enol ethers, which reinforces our proposal that chiral magnesium amide bases are more robust in general than lithium amide bases. To further extend this methodology, we next chose to investigate the *pseudo*-C_2-symmetric amides synthesised previously.

3.2.6. Pseudo-C_2-Symmetric Amines

As described earlier, a series of *pseudo*-C_2-symmetric amines were reported previously as generating high levels of reactivity and selectivity for the synthesis of enantioenriched silyl enol ethers. In order to verify the consistency of results obtained through the use of chiral magnesium bases, we were keen to apply these chiral amides for the asymmetric synthesis of enol phosphates, using our optimised conditions. As shown below, when using the conditions described in **Scheme 2.32**, the use of **(*R*,*R*)-145** resulted in a 95% yield with a 95:5 e.r., while **(*R*,*R*)-146**

provided a 92% yield with an e.r. of 94:6. Interestingly, when the naphthyl derivatives were used, **(*R*,*R*)-147** delivered a 94% yield and a 94:6 e.r., whereas **(*R*,*R*)-148** provided only an 86 % yield and a mildly higher e.r. of 95:5. Although most results obtained for the formation of enantioenriched silyl enol ethers are similar in selectivity and higher in reactivity to those obtained below, it was interesting to note that in the case of the naphthyl-derived amines, the best selectivity obtained for silyl enol ethers was using **(*R*,*R*)-147**, whereas for enol phosphates it was **(*R*,*R*)-148**.[22a]

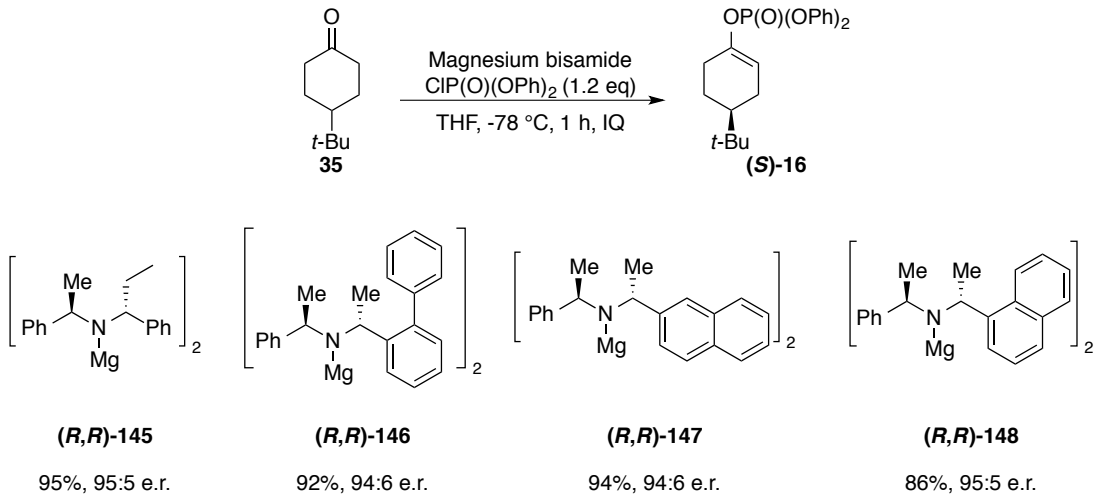

Scheme 2. 32

Furthermore, we have also applied these amines to our -20 °C conditions using the co-addition protocol. As shown in **Scheme 2.33** below, **(*R*,*R*)-146** provided the product in 90% yield, whereas the other amides, **(*R*,*R*)-145**, **(*R*,*R*)-147**, and **(*R*,*R*)-148** delivered a 95% yield of product. In terms of selectivity, **(*R*,*R*)-145** gave an 89:11 e.r., **(*R*,*R*)-146** an 88:12 e.r., and for the naphthyl derivatives **(*R*,*R*)-147** and **(*R*,*R*)-148** selectivities of 86:14 and 87:13 were observed, respectively. Herein, the results obtained are higher in reactivity and similar in selectivity to those observed for the silyl enol ethers, but again it was interesting to note that the naphthyl-derived amides allowed mild differences in the results obtained. It could be hypothesised that the phosphoryl electrophile, bearing aromatic groups, could possibly interact with the

naphthyl units by π-stacking, altering the selectivities observed, since such variations only occurred with these more extended aromatic systems.

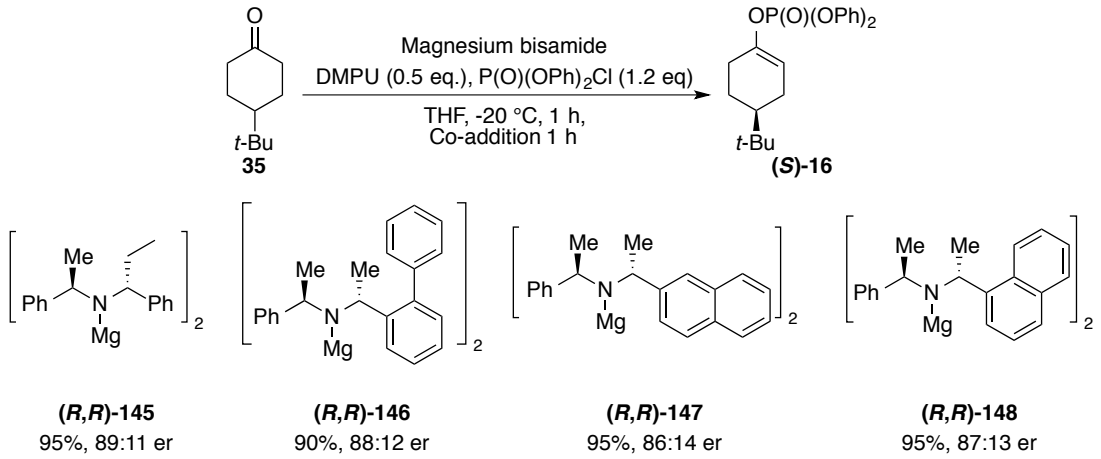

Scheme 2. 33

With these extremely pleasing optimisation results in hand, we then moved to exploring the substrate scope of the enol phosphate formation.

3.2.7. Substrate Scope

We have so far shown that the use of chiral magnesium bisamide bases affords high levels of reactivity, at -78 °C as well as at -20 °C, with a range of both C_2- and pseudo-C_2-symmetric bases. To provide further evidence for the utility of our bases, we were interested in exploring their activity with a range of 4-susbtituted cyclohexanones. One of the major issues encountered while expanding the substrate scope was that chiral HPLC separation conditions were required for the determination of enantiomeric ratios. Thus far, the chiral silyl enol ethers were characterised using chiral GC, and unfortunately the high boiling point of these enol phosphates required the use of chiral HPLC instead. Due to these technical limitations only 4 substrates were successfully characterised.

As shown in **Scheme 2.34**, following the optimised conditions developed for reaction at -78 °C, presented below are a range of substrates that provided new, enantioenriched enol phosphate products. While the 4-phenyl derivative afforded the

enol phosphate **(*S*)-72** in an excellent 92% yield and a selectivity of 97:3 e.r., the 4-OTBS derivative **(*S*)-81** was obtained in a moderate 77% yield, with a selectivity of 88:12. We were delighted to establish that the quaternary centre-containing 4-Me-4-Ph derivative could also be formed in a high 95% yield and with a good selectivity of 87:13 at -78 °C (**(*S*)-73**). In fact, this molecule was our first example of a desymmetrised prochiral quaternary centre. Finally, extending the scope of our system further, we examined the 4-dimethylamino analogue. With this particular unit, we were curious as to the behaviour of our chiral magnesium bases with substrates containing a potentially co-ordinating group. As depicted below, the use of this substrate still resulted in a good 80% isolated yield of the compound **(*S*)-82**. During the synthesis of this enol phosphate, it was realised that the product was not separable by HPLC, and, moreover, the product was not stable and in fact degraded overnight at room temperature. Having encountered a range of difficulties with this substrate, the selectivity was eventually determined through cross coupling of the enol phosphate product with MeMgBr and comparing the optical rotation of the product with that reported in the literature,[24] allowing us to define the selectivity of the enol phosphate formation at an e.r. of 93:7. Although it presented numerous challenges, this substrate allowed us to establish two important points related to this methodology: firstly, the presence of the co-ordinating group did not alter the selectivity obtained through the asymmetric deprotonation, as the results match with those observed with the standard 4-*tert*-butyl system (95:5 er); and secondly, through comparison with the literature optical rotation value, we were able to assign the major enantiomer as (*S*). Up to this point, the absolute stereochemistry could only be assumed to be (*S*) based on previous work on the synthesis of silyl enol ethers. With this confirmation, and with the range of satisfying results obtained, we turned our attention towards the optimised conditions at -20 °C.

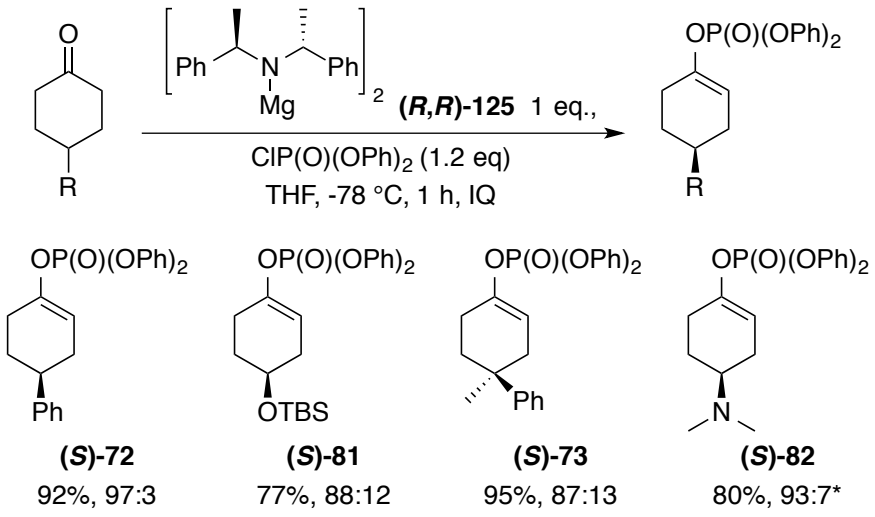

* Selectivity defined after derivatisation (*see experimental*)

Scheme 2. 34

As shown in **Scheme 2.35** below, when the optimised conditions for -20 °C were applied to the range of substrates, similar results were observed. The 4-Ph derivative **(*S*)-72** was obtained in 94% yield and 90:10 e.r., while the 4-OTBS-derived enol phosphate **(*S*)-81** was obtained in 82% yield and an e.r. of 80:20. It was interesting to note that the drop in selectivity for the quaternary centre-bearing substrate (**(*S*)-73**) was less than compared to other groups, forming in an e.r. of 80:20 with a 93% yield. On the other hand, enol phosphate **(*S*)-82** was obtained with 84% yield and 86:14 selectivity.

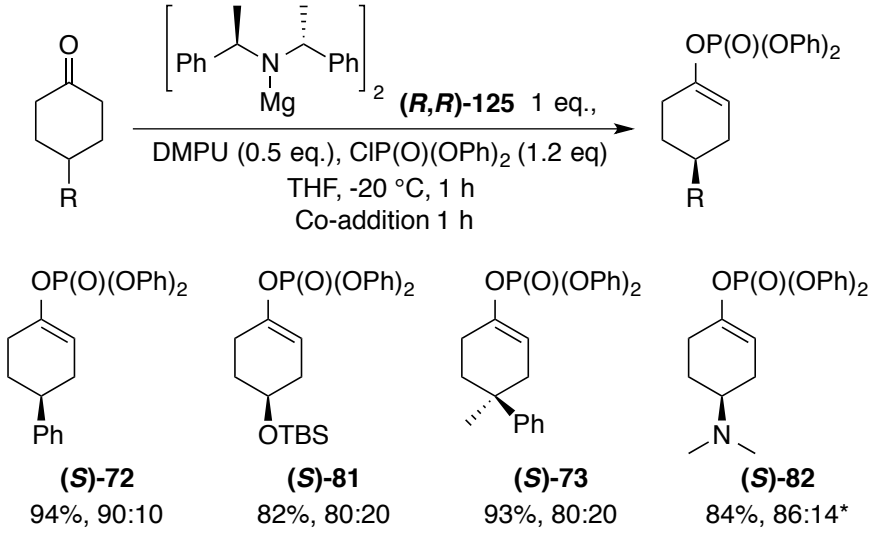

* Selectivity defined after derivatisation (*see experimental*)

Scheme 2. 35

To summarise, a novel methodology for the synthesis of enantioenriched enol phosphates using chiral magnesium bisamide bases has been developed. These bases performed outstandingly, providing high selectivity and reactivity at both lower (-78 °C) and higher (-20 °C) temperatures. The stability and reliability of our magnesium bisamide system was then explored through the use of a range of *pseudo*-C_2-symmetric amides and by examining a range of substrates, which provided consistently excellent levels of reactivity and enantioselectivity.

3.3. Future Work

3.3.1. Asymmetric Shapiro Reaction

We have established, within our laboratories, a broad range of experience in various metal-based chemistries, among which are the applications of chiral bisamides and the carbon-centred bases in organic synthesis. The carbon-centred bases have been particularly efficient in interesting transformations such as the Shapiro reaction, whereas the bisamide bases have been effective in the desymmetrisation of prochiral ketones, and especially 4-substituted cyclohexanones. We were interested in merging both the Shapiro reaction and the asymmetric deprotonation to generate enantioenriched olefins.

We therefore sought to carry out preliminary investigations regarding this transformation by firstly employing a chiral magnesium amide base. After synthesis of the 4-*tert*-butyl hydrazine derivative **149**, this substrate was treated with the chiral bisamide base **(*R*,*R*)-125** and was then left for 1 h at either room temperature or -78 °C, followed by quenching with water. The resulting olefin was well documented in the literature and therefore would represent a viable substrate for primary work.[25] Unfortunately no reaction occurred and only starting material was recovered.

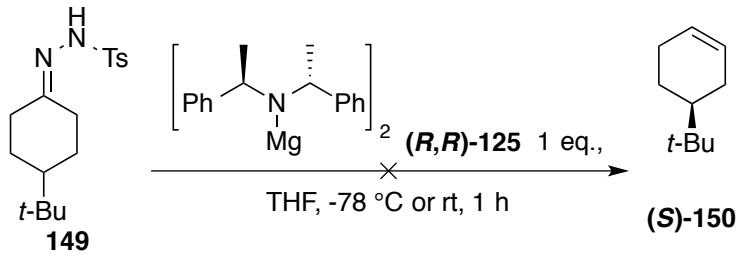

Scheme 2. 36

Having since gathered more information on the nature of the magnesium species in solution and their formation, the lack of reactivity could be explained by the absence of an active base species. Indeed, the most active species, the amide, would deprotonate the most acidic proton, with no other active base left to carry out the second deprotonation. We have therefore envisaged promoting the first deprotonation by using a lithium base such as *n*-BuLi, followed by addition of the chiral magnesium amide base. Under these conditions, the reaction now afforded a substantial yield of product at room temperature following overnight reaction. As show below, the reaction at room temperature afforded 58% yield of the desired product, but unfortunately little selectivity was observed, as only a 52:48 e.r. was obtained, as determined by optical rotation.

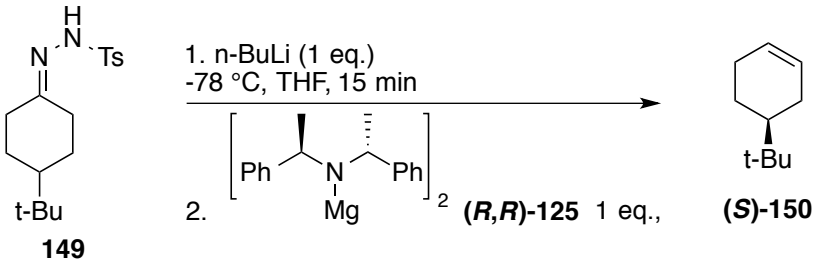

Scheme 2. 37

Entry	Temperature	Time	Yield %
1	-78 °C to rt	16 h	-
2*	rt	16 h	58

Table 2. 18

* No enantioenrichment of **(*S*)-150** was observed.

Although a low level of selectivity was observed, we were delighted to observe a good yield of 58%. It should also be noted that when the addition of the base species were reversed under the conditions described in **Entry 2**, **Table 2.18** (*i.e.* addition of alkylmagnesium amide then addition of *n*-BuLi), only a trace amount of the desired product was isolated. This latter result has implications for the active base species in solution. With this in mind we have studied a range of reaction conditions, such as the use of a Grignard reagent instead of *n*-BuLi, use of Hauser bases and other alkylmagnesium amide bases, but low levels of reaction were observed in all cases. Although unsuccessful so far, further understating of the active species may allow an asymmetric Shapiro reaction to be developed using chiral magnesium bases.

3.3.2. Alkylmagnesium Amides

During early optimisation studies, an interesting result was observed when varying the stoichiometry of the amine versus the dialkylmagnesium. Specifically, (**Scheme 2.38**) the formation of the base was modified when only one equivalent of the chiral amine **(*R*,*R*)-142** was reacted with *n*-Bu_2Mg. The (presumed) heteroleptic alkylmagnesium amide base thus formed was then subjected to the reaction mixture and to our great surprise; the reaction afforded a high 77% yield of product with an excellent selectivity of 95:5.

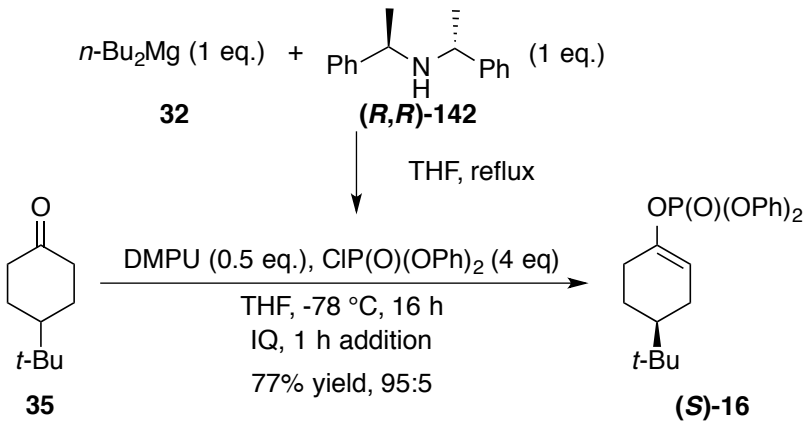

Scheme 2. 38

Further work on the exploration of this new active species, the optimisation and the determination of the nature of the active base species in solution is discussed further in Chapter 3.

4. Summary

Herein we have developed a novel methodology for the synthesis of enantioenriched enol phosphates using our chiral magnesium amide bases. The use of a range of chiral C_2- (**(*R*,*R*)-125**) and *pseudo*-C_2-symmetric amides (**(*R*,*R*)-145**, **(*R*,*R*)-146**, **(*R*,*R*)-147**, and **(*R*,*R*)-148**), which resulted in excellent levels of reactivity and selectivity for the synthesis of enol silanes, also provided exceptional results for the formation of enol phosphate compounds in the present study. Furthermore, these reagents display high levels of reactivity at -78°C without the requirement of any additive, while a more subtle co-addition protocol significantly improved the reactivity and the selectivity observed for such transformations at higher temperatures such as -20 °C. We have also explored a range of substrates which all afford impressive levels of reactivity and selectivity at both -78 °C and -20 °C. Among the substrates explored for the first time are a quaternary centre-containing substrate which led to the enantioenriched enol phosphate (**(*S*)-73**). We have, by this work, demonstrated the utility of the asymmetric deprotonation reaction mediated by chiral magnesium bisamide bases.

5. Experimental

5.1. General

All reagents were obtained from commercial suppliers (Aldrich, Lancaster, Alfa-aesar or Acros) and used without further purification, unless otherwise stated. Purification was carried out according to standard laboratory methods.[26]

- Dichloromethane, diethyl ether, hexane and toluene were obtained from an Innovative Technology, Pure Solv, SPS-400-5 solvent purification system.
- Tetrahydrofuran was dried by heating to reflux over sodium wire, using benzophenone ketyl as an indicator, then distilled under nitrogen.
- TMSCl, was distilled from CaH_2 under argon and was stored over 4Å molecular sieves under argon.
- Acetophenone was purified by distillation over CaH_2 at 88 °C, 18 mbar.
- DMPU and diphenylphosphoryl chloride were distilled from CaH_2 under high vacuum and were stored over 4 Å molecular sieves under argon.
- Organometallic reagents were standardised using salicylaldehyde phenylhydrazone.[27]
- 4-*tert*-Butylcyclohexanone, 4-phenylcyclohexanone, and 4-methyl-4-phenylcyclohexanone,[28] were purified by recrystallization from hexane and were dried by storing under vacuum (0.005 mbar) for 16 h.
- 4-((*tert*-butyldimethylsilyl)oxy)cyclohexanone,[29] and 4-(dimethylamino)cyclohexanone,[30] were dried by distillation over $CaCl_2$ and were stored under argon over 4 Å molecular sieves.

Thin layer chromatography was carried out using CamLab silica plates, coated with fluorescent indicator UV_{254}, and analysed using a Mineralight UVGL-25 lamp.

Flash column chromatography was carried out using Prolabo silica gel (230-400 mesh).

IR spectra were recorded on a SHIMADZU IRAFFINITY-1 spectrophotometer.

^{1}H, ^{13}C and ^{31}P NMR spectra were recorded on a Bruker DPX 400 spectrometer at 400 MHz, 100 MHz, and 162 MHz, respectively. Chemical shifts are reported in ppm. Coupling constants are reported in Hz and refer to $^{3}J_{H\text{-}H}$ interactions unless otherwise specified.

5.2. General Procedures

General Procedure A: preparation of magnesium bisamides

A solution of *n*-Bu_2Mg in heptane was transferred to a Schlenk flask, which had been flame-dried under vacuum (0.005 mbar) and allowed to cool under an atmosphere of argon, and the heptane was removed *in vacuo* (0.005 mbar) until a white solid was revealed. THF (10 mL) was then added, followed by the requisite amine, and the solution was heated at reflux for 1.5 h, assuming quantitative formation of the magnesium bisamide. Data are presented as (a) amount of *n*-Bu_2Mg, (b) amine used, and (c) amount of amine.

General Procedure B: asymmetric deprotonation using Mg bases with IQ

A solution of the magnesium base in THF, prepared *via* General Procedure A, was cooled under nitrogen to the appropriate temperature. A Schlenk flask was then charged with the additives (when used), followed by $P(O)(OPh)_2Cl$, and the reaction mixture was stirred for 10 min at the stated temperature. The requisite ketone was then added as a solution in THF (2 mL) over 1 h using a syringe pump. The reaction mixture was stirred at the temperature stated for the required time before being quenched with a saturated solution of $NaHCO_3$ (10 mL) and allowed to warm to room temperature. The aqueous phase was extracted with Et_2O (50, 25, 25 mL) and

the organic phases were combined and washed with 1 M HCl (2 × 10 mL) to recover the amine. The removal of the solvent *in vacuo* gave an oil which was purified by column chromatography on silica gel using 0-30% Et_2O in petroleum ether (40-60 °C) to give the desired product as a colourless oil. The enantiomeric ratio of the product was determined by analysis using chiral HPLC with a CHIRALCEL OD or OJ column.

General Procedure C: asymmetric deprotonation using Mg bases with EQ

A solution of magnesium base in THF, prepared *via* General Procedure A, was cooled under nitrogen to the appropriate temperature. A Schlenk flask was then charged with the additives (when used), and the reaction mixture was stirred for 10 min at the temperature stated. The requisite ketone was then added dropwise over 5 min as a solution in THF (1 mL). After the stated reaction time, the electrophile was diluted in THF to form an overall solution of 2mL and added over 1 h using a syringe pump. The reaction mixture was stirred at the temperature stated for the required time before being quenched with a saturated solution of $NaHCO_3$ (10 mL) and allowed to warm to room temperature. The aqueous phase was extracted with Et_2O (50, 25, 25 mL) and the organic phases were combined and washed with 1M HCl(2 × 10 mL) to recover the amine. The removal of the solvent *in vacuo* gave an oil, which was purified by column chromatography on silica gel using 0-30% Et_2O in petroleum ether (40-60 °C) to give the desired product as a colourless oil. The enantiomeric ratio of the product was determined by analysis using chiral HPLC with a CHIRALCEL OD or OJ column.

General Procedure D: asymmetric deprotonation using Mg bases in a co-addition protocol

A solution of magnesium base in THF, prepared *via* General Procedure A, was cooled under nitrogen to the appropriate temperature. A Schlenk flask was then charged with the additive (when used) and the reaction mixture was stirred for 10

min at the temperature stated. The requisite ketone and $P(O)(OPh)_2Cl$ were then added as a solution in THF (2 mL) over 1 h using a syringe pump. The reaction mixture was stirred at the temperature stated for the required time before being quenched with a saturated solution of $NaHCO_3$ (10 mL) and allowed to warm to room temperature. The aqueous phase was extracted with Et_2O (50, 25, 25 mL) and the organic phases were combined and washed with 1M HCl (2 × 10 mL) to recover the amine. The removal of the solvent *in vacuo* gave an oil which was purified by column chromatography on silica gel using 0-30% Et_2O in petroleum ether (40-60 °C) to give the desired product as a colourless oil. The enantiomeric ratio of the product was determined by analysis using chiral HPLC with a CHIRALCEL OD or OJ column.

General Procedure E: Scheme 2.24 - Preparation of C_2- and *pseudo*-C_2-symmetric amines[42]

(*R*)-1-Phenylethylamine **(*R*)-143**, the requisite ketone and titanium tetra-*iso*-propoxide were stirred for 30 min before addition of palladium on charcoal. The reaction mixture was then hydrogenated using a hydrogenation apparatus under a pressurised H_2 atmosphere (3 atm) with stirring for 72 h before addition of a minimal amount of H_2O. Once the reaction was quenched (formation of a white solid), EtOAc was added to dilute the cake, and the mixture was filtered through Celite. The organic phase was dried over Na_2SO_4 and concentrated *in vacuo* to give a yellow oil. The d.r. was determined as 87:13 by ^1H NMR analysis. The crude product was converted to its HCl salt and purified by recrystallisation from IPA. The diastereomerically pure, free amine was then obtained by dissolving the salt in 2M NaOH (500 mL), followed by extraction with EtOAc (3 × 300 mL). The organic phase was dried over Na_2SO_4, and concentrated *in vacuo* to yield the desired amine.

5.3. Asymmetric Deprotonation Reactions

5.3.1. Synthesis of Chiral Amines

Figure 2.24

Following General Procedure E for the synthesis of chiral amines, data are presented as (a) ketone, (b) amount of ketone, (c) amount of **(*R*)-143**, (d) amount of palladium on charcoal, (e) isolated yield, (f) purification

Synthesis of **(*R*,*R*)-142**: General Procedure E: (a) acetophenone, (b) 19.8 g (165 mmol), (c) 20.0 g (165 mmol), (d) 720 mg, (e) 81% (30 g), (f) heated at 50 °C over CaH_2 *in vacuo* (0.4 mbar) for 16 h before being distilled *in vacuo* (98 °C, 0.4 mbar).

(*R*,*R*)-bis(1-phenylethyl)amine[23] **(*R*,*R*)-142**:

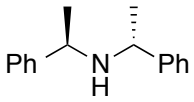

$\nu_{max}(CDCl_3)$: 2962 cm^{-1}.
^1H NMR (400 MHz, $CDCl_3$): δ 7.34-7.23 (m, 10H, ArH), 3.56 (q, J = 6.7 Hz, 2H, $N(CH)_2$), 1.33 (d, J = 6.7 Hz, 6H, $N(CHCH_3)2$).
Peaks used to deduce d.r. of crude amine from 1H NMR (400 MHz, $CDCl_3$):
(*R*,*R*): δ 3.54 (q, 1H, CH).
(*R*,*S*): δ 3.82 (q, 1H, CH).
^{13}C NMR (100 MHz, $CDCl_3$): δ (ppm) 145.9, 128.5, 126.8, 126.7, 55.2, 25.1.

Synthesis of **(*R*,*R*)-128**: General Procedure E: (a) propiophenone, (b) 22.1 g (165 mmol), (c) 20.0 g (165 mmol), (d) 720 mg, (e) 49% (19.3 g), (f) dried over Kugelroho at 100 °C under vacuum (0.1 mbar) for 2 h and stored over 4 A molecular sieves under argon

(*R*)-1-phenyl-*N*-((*R*)-1-phenylethyl)propan-1-amine[22a] **(*R*,*R*)-128** :

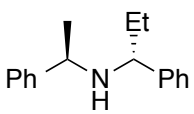

ν_{max}(DCM): 2982 cm^{-1}.

^{1}H NMR (400 MHz, $CDCl_3$): δ 7.39-7.21 (m, 10H, ArH), 3.54 (q, *J* = 6.7 Hz, 1H, $CHCH_3$), 3.26 (t, *J* = 7.0 Hz, 1H, $CHCH_2$), 1.74-1.56 (m, 3H, CH_2CH_3 and NH), 1.30 (d, *J* = 6.7 Hz, 3H, $CHCH_3$), 0.80 (t, *J* = 7.4 Hz, 3H, CH_2CH_3).

Peaks used to deduce d.r. of crude amine from 1H NMR (400 MHz, $CDCl_3$):
(*R*,*R*): δ 1.30 (d, 3H, CH_3).
(*R*,*S*): δ 1.38 (d, 3H, CH_3).

^{13}C NMR (100 MHz, $CDCl_3$): δ 146.0, 144.6, 128.4, 128.3, 127.4, 126.8, 61.8, 55.0, 31.5, 25.2, 11.0.

Synthesis of **(*R*,*R*)-132**: General Procedure E: (a) 1-([1,1'-biphenyl]-2-yl)ethanone,[31] (b) 25 g (165 mmol), (c) 20.0 g (165 mmol), (d) 720 mg, (e) 40% (19.9 g), (f) the white solid was dried over high vacuum (0.1 mbar) for 5 h and stored under argon.

(*R*)-1-(biphenyl-2-yl)-*N*-((*R*)-1-phenylethyl)ethanamine,[22a] **(*R*,*R*)-132**:

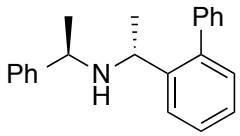

Melting point = 52-54 °C.
ν_{max}(DCM): 2982 cm^{-1}.
^{1}H NMR (400 MHz, $CDCl_3$): δ (ppm) 7.65 (d, *J* = 7.8 Hz, 1H, ArH), 7.44 (td, *J* = 7.5 and 1.3 Hz, 1H, ArH), 7.32-7.15 (m, 8H, ArH), 7.14-7.08 (m, 2H, ArH), 6.95 (d, *J* = 6.6 Hz, 2H, ArH), 3.80 (q, *J* = 6.6 Hz, 1H, CH), 3.58 (q, *J* = 6.6 Hz, 1H, CH), 1.58 (brs, 1H, NH), 1.26 (d, *J* = 6.7 Hz, 3H, CH_3), 1.17 (d, *J* = 6.6 Hz, 3H, CH_3).

Peaks used to deduce d.r. of crude HCl salt from ^{1}H NMR (400 MHz, $CDCl_3$):
(*R*,*R*): δ 1.85 (d, 3H, CH_3).

(*R*,*S*): δ 2.01 (d, 3H, CH_3).

^{13}C NMR (100 MHz, $CDCl_3$): δ (ppm) 145.9, 143.3, 141.8, 141.1, 130.1, 129.2, 128.4, 127.9, 127.8, 126.6, 126.6, 126.2, 125.6, 55.2, 50.7, 25.4, 25.2.

Synthesis of **(*R*,*R*)-136**: General Procedure E: (a) 2-acetonaphtone, (b) 28 g (165 mmol), (c) 20.0 g (165 mmol), (d) 720 mg, (e) 29% (13.1 g), (f) heated at 50 °C over CaH_2 *in vacuo* (0.4 mbar) for 16 h before being distilled *in vacuo* (141 °C, 0.001 mbar).

(*R*)-1-(naphthalen-2-yl)-*N*-((*R*)-1-phenylethyl)ethanamine[32] **(*R*,*R*)-136**:

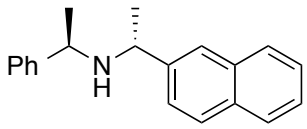

$\nu_{max}(CDCl_3)$: 2962 cm^{-1}.
^1H NMR (400 MHz, $CDCl_3$): δ 7.86-7.81 (m, 3H, ArH), 7.61 (s, 1H, ArH), 7.51-7.44 (m, 3H, ArH), 7.38-7.34 (m, 2H, ArH), 7.30-7.26 (m, 1H, ArH), 7.25-7.23 (m, 2H, ArH), 3.70 (q, *J* = 6.6 Hz, 1H, CH), 3.55 (q, *J* = 6.6 Hz, 1H, CH), 1.67 (brs, 1H, NH), 1.37 (d, *J* = 6.6 Hz, 3H, CH_3), 1.31 (d, *J*= 6.6 Hz, 3H, CH_3).

Peaks used to deduce d.r. of crude HCl salt from 1H NMR (400 MHz, $CDCl_3$):
(*R*,*R*): δ 3.70 (q, 1H, CH).
(*R*,*S*): δ 3.81 (q, 1H, CH).

^{13}C NMR (100 MHz, $CDCl_3$): δ 144.8, 142.2, 132.4, 131.8, 127.4, 127.2, 126.7, 126.6, 125.8, 125.6, 124.9, 124.4, 124.3, 123.8, 54.2, 54.1, 24.0, 23.9.

Synthesis of **2.(*R*,*R*)-135**: General Procedure E: (a) 1-acetonaphtone, (b) 28 g (165 mmol), (c) 20.0 g (165 mmol), (d) 720 mg, (e) 33% (15 g), (f) heated at 50 °C over CaH_2 *in vacuo* (0.4 mbar) for 16 h before being distilled *in vacuo* (98 °C, 0.4 mbar).

(*R*)-1-(naphthalen-1-yl)-*N*-((*R*)-1-phenylethyl)ethan-1-amine,[33] **(*R*,*R*)-135**:

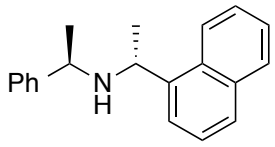

ν_{max} (DCM): 2982 cm^{-1}.

^1H NMR (400 MHz, $CDCl_3$): δ (ppm) 7.97-7.88 (m, 2H, ArH), 7.81 (d, J = 8.1 Hz, 1H, ArH), 7.74 (d, J = 6.9 Hz, 1H, ArH), 7.57 (t, J = 7.3 Hz, 1H, ArH), 7.48 (td, J = 6.8 and 1.0 Hz, 1H, ArH), 7.43 (td, J = 8.6 and 1.4 Hz, 1H, ArH), 7.38-7.25 (m, 3H, ArH), 7.24-7.18 (m, 2H, ArH), 4.46 (q, J = 6.6 Hz, 1H, CH_3CH), 3.65 (q, J = 6.6 Hz, 1H, CH_3CH), 0.85 (brs, 1H, NH), 1.44 (d, J = 6.7 Hz, 3H, CH_3), 1.39 (d, J = 6.7 Hz, 3H, CH_3).

Peaks used to deduce d.r. of crude HCl salt from 1H NMR (400 MHz, CDCl3):
(*R*,*R*): δ 1.75 (d, 3H, CH_3).
(*R*,*S*): δ 1.89 (d, 3H, CH_3).

^{13}C NMR (100 MHz, CDCl3): δ (ppm) 128.9, 128.4, 127.1, 126.9, 126.7, 125.8, 125.6, 125.3, 123.2, 122.8, 55.4, 50.8, 24.8, 24.7.

5.3.2. Synthesis of Enantioenriched Enol Phosphates

Scheme 2.25

Following General Procedure A for the preparation of magnesium base, data are presented as (a) amount of *n*-Bu_2Mg, (b) amine used, and (c) amount of amine.
Following General Procedure B for the asymmetric deprotonation reaction, data are presented as (a) Mg base, (b) reaction temperature, (c) additives, (d) amount of

additive, (e) amount of $ClP(O)(OPh)_2$, (f) ketone, (g) amount of ketone, (h) reaction time, (i) isolated yield, (e) e.r. (*S*):(*R*)

General Procedure A: (a) 1.00 M, 1 mmol, 1 mL (b) **(*R,R*)-142** and (c) 0.44 mL, 2mmol. General Procedure B (a) **(*R,R*)-125**, (b) -78 °C, (c) DMPU, (d) 0.06 mg, 0.5 eq., (e) 0.84 mL, 4 mmol, (f) 4-*tert*-butylcyclohexanone, (g) 123 mg, 0.8 mmol, (h) 16 h, (i) 228 mg, 74%, (e) 96:4

Scheme 2.26

Following General Procedure A for the preparation of magnesium base, data are presented as (a) amount of *n*-Bu_2Mg, (b) amine used, and (c) amount of amine.
Following General Procedure B for the asymmetric deprotonation reaction, data are presented as (a) Mg base, (b) reaction temperature, (c) additives, (d) amount of additive, (e) amount of $ClP(O)(OPh)_2$, (f) ketone, (g) amount of ketone, (h) reaction time, (i) isolated yield, (e) e.r. (*S*):(*R*)

Table 2.12

Entry 1: General Procedure A: (a) 1.00 M, 1 mmol, 1 mL (b) **(*R,R*)-142** and (c) 0.44 mL, 2mmol. General Procedure B: (a) **(*R,R*)-125**, (b) -78 °C, (c) DMPU, (d) 0.06 mg, 0.5 eq., (e) 0.63 mL, 3 mmol, (f) 4-*tert*-butylcyclohexanone, (g) 123 mg, 0.8 mmol, (h) 16 h, (i) 284 mg, 92%, (e) 95:5

Entry 2: General Procedure A: (a) 1.00 M, 1 mmol, 1 mL (b) **(*R,R*)-142** and (c) 0.44 mL, 2mmol. General Procedure B: (a) **(*R,R*)-125**, (b) -78 °C, (c) DMPU, (d) 0.06 mg, 0.5 eq., (e) 0.42 mL, 2 mmol, (f) 4-*tert*-butylcyclohexanone, (g) 123 mg, 0.8 mmol, (h) 16 h, (i) 281 mg, 91%, (e) 95:5

Entry 3: General Procedure A: (a) 1.00 M, 1 mmol, 1 mL (b) **(*R,R*)-142** and (c) 0.44 mL, 2mmol. General Procedure B: (a) **(*R,R*)-125**, (b) -78 °C, (c) DMPU, (d) 0.06 mg,

0.5 eq., (e) 0.21 mL, 1 mmol, (f) 4-*tert*-butylcyclohexanone, (g) 123 mg, 0.8 mmol, (h) 16 h, (i) 259 mg, 84%, (e) 95:5

Entry 4: General Procedure A: (a) 1.00 M, 1 mmol, 1 mL (b) **(*R,R*)-142** and (c) 0.44 mL, 2mmol. General Procedure B: (a) **(*R,R*)-125**, (b) -78 °C, (c) DMPU, (d) 0.06 mg, 0.5 eq., (e) 0.23 mL, 1.1 mmol, (f) 4-*tert*-butylcyclohexanone, (g) 123 mg, 0.8 mmol, (h) 16 h, (i) 281 mg, 91%, (e) 95:5

Entry 5: General Procedure A: (a) 1.00 M, 1 mmol, 1 mL (b) **(*R,R*)-142** and (c) 0.44 mL, 2mmol. General Procedure B: (a) **(*R,R*)-125**, (b) -78 °C, (c) DMPU, (d) 0.06 mg, 0.5 eq., (e) 0.25 mL, 1.2 mmol, (f) 4-*tert*-butylcyclohexanone, (g) 123 mg, 0.8 mmol, (h) 16 h, (i) 293 mg, 95%, (e) 95:5

Scheme 2.27

Following General Procedure A for the preparation of magnesium base, data are presented as (a) amount of *n*-Bu_2Mg, (b) amine used, and (c) amount of amine.
Following General Procedure B for the asymmetric deprotonation reaction, data are presented as (a) Mg base, (b) reaction temperature, (c) additives, (d) amount of additive, (e) amount of $ClP(O)(OPh)_2$, (f) ketone, (g) amount of ketone, (h) reaction time, (i) isolated yield, (e) e.r. (*S*):(*R*)

Table 2.13

Entry 1: General Procedure A: (a) 1.00 M, 1 mmol, 1 mL (b) **(*R,R*)-142** and (c) 0.44 mL, 2mmol. General Procedure B: (a) **(*R,R*)-125**, (b) -78 °C, (c) DMPU, (d) 0.06 mg, 0.5 eq., (e) 0.25 mL, 1.2 mmol, (f) 4-*tert*-butylcyclohexanone, (g) 123 mg, 0.8 mmol, (h) 1 h, (i) 284 mg, 92%, (e) 95:5

Entry 2: General Procedure A: (a) 1.00 M, 1 mmol, 1 mL (b) **(*R,R*)-142** and (c) 0.44 mL, 2mmol. General Procedure B: (a) **(*R,R*)-125**, (b) -78 °C, (c) DMPU, (d) 0.06 mg,

0.5 eq., (e) 0.25 mL, 1.2 mmol, (f) 4-*tert*-butylcyclohexanone, (g) 123 mg, 0.8 mmol, (h) 0.5 h, (i) 275 mg, 89%, (e) 95:5

Scheme 2.28

Following General Procedure A for the preparation of magnesium base, data are presented as (a) amount of *n*-Bu_2Mg, (b) amine used, and (c) amount of amine.
Following General Procedure B for the asymmetric deprotonation reaction, data are presented as (a) Mg base, (b) reaction temperature, (c) additives, (d) amount of additive, (e) amount of $ClP(O)(OPh)_2$, (f) ketone, (g) amount of ketone, (h) reaction time, (i) isolated yield, (e) e.r. (*S*):(*R*)

Table 2.14

Entry 1: General Procedure A: (a) 1.00 M, 1 mmol, 1 mL (b) **(*R,R*)-142** and (c) 0.44 mL, 2mmol. General Procedure B: (a) **(*R,R*)-125**, (b) -78 °C, (c) -, (d) -, (e) 0.25 mL, 1.2 mmol, (f) 4-*tert*-butylcyclohexanone, (g) 123 mg, 0.8 mmol, (h) 1 h, (i) 284 mg, 92%, (e) 94:6

Entry 2: General Procedure A: (a) 1.00 M, 1 mmol, 1 mL (b) **(*R,R*)-142** and (c) 0.44 mL, 2mmol. General Procedure B: (a) **(*R,R*)-125**, (b) -78 °C, (c) DMPU, (d) 0.12 mg, 1 eq., (e) 0.25 mL, 1.2 mmol, (f) 4-*tert*-butylcyclohexanone, (g) 123 mg, 0.8 mmol, (h) 1 h, (i) 262 mg, 85%, (e) 95:5

Scheme 2.29

Following General Procedure A for the preparation of the magnesium base, data are presented as (a) amount of *n*-Bu_2Mg, (b) amine used, and (c) amount of amine.
Following General Procedure B for the asymmetric deprotonation reaction, data are presented as (a) Mg base, (b) reaction temperature, (c) additives, (d) amount of

additive, (e) amount of $ClP(O)(OPh)_2$, (f) ketone, (g) amount of ketone, (h) reaction time, (i) isolated yield, (e) e.r. (*S*):(*R*)

Table 2.15

Entry 1: General Procedure A: (a) 1.00 M, 1 mmol, 1 mL (b) **(*R,R*)-142** and (c) 0.44 mL, 2mmol. General Procedure B: (a) **(*R,R*)-125**, (b) -20 °C, (c) -, (d) -, (e) 0.25 mL, 1.2 mmol, (f) 4-*tert*-butylcyclohexanone, (g) 123 mg, 0.8 mmol, (h) 1 h, (i) 213 mg, 69%, (e) 86:14

Entry 2: General Procedure A: (a) 1.00 M, 1 mmol, 1 mL (b) **(*R,R*)-142** and (c) 0.44 mL, 2mmol. General Procedure B: (a) **(*R,R*)-125**, (b) rt, (c) -, (d) -, (e) 0.25 mL, 1.2 mmol, (f) 4-*tert*-butylcyclohexanone, (g) 123 mg, 0.8 mmol, (h) 1 h, (i) 71 mg, 23%, (e) 74:26

Entry 3: General Procedure A: (a) 1.00 M, 1 mmol, 1 mL (b) **(*R,R*)-142** and (c) 0.44 mL, 2mmol. General Procedure B: (a) **(*R,R*)-125**, (b) -20 °C, (c) DMPU, (d) 0.06 mg, 0.5 eq., (e) 0.25 mL, 1.2 mmol, (f) 4-*tert*-butylcyclohexanone, (g) 123 mg, 0.8 mmol, (h) 1 h, (i) 200 mg, 65%, (e) 88:12

Entry 4: General Procedure A: (a) 1.00 M, 1 mmol, 1 mL (b) **(*R,R*)-142** and (c) 0.44 mL, 2mmol. General Procedure B: (a) **(*R,R*)-125**, (b) rt, (c) DMPU, (d) 0.06 mg, 0.5 eq., (e) 0.25 mL, 1.2 mmol, (f) 4-*tert*-butylcyclohexanone, (g) 123 mg, 0.8 mmol, (h) 1 h, (i) 61 mg, 20%, (e) 80:20

Scheme 2.30

Following General Procedure A for the preparation of magnesium base, data are presented as (a) amount of *n*-Bu_2Mg, (b) amine used, and (c) amount of amine.
Following General Procedure B for the asymmetric deprotonation reaction, data are presented as (a) Mg base, (b) reaction temperature, (c) additives, (d) amount of

additive, (e) amount of $ClP(O)(OPh)_2$, (f) ketone, (g) amount of ketone, (h) reaction time, (i) isolated yield, (e) e.r. (*S*):(*R*)

Table 2.16

Entry 1: General Procedure A: (a) 1.00 M, 1 mmol, 1 mL (b) **(*R,R*)-142** and (c) 0.44 mL, 2mmol. General Procedure C: (a) **(*R,R*)-125**, (b) rt, (c) DMPU, (d) 0.06 mg, 0.5 eq., (e) 0.25 mL, 1.2 mmol, (f) 4-*tert*-butylcyclohexanone, (g) 123 mg, 0.8 mmol, (h) 1 h, (i) 238 mg, 77%, (e) 79:21

Entry 2: General Procedure A: (a) 1.00 M, 1 mmol, 1 mL (b) **(*R,R*)-142** and (c) 0.44 mL, 2mmol. General Procedure D: (a) **(*R,R*)-125**, (b) rt, (c) DMPU, (d) 0.06 mg, 0.5 eq., (e) 0.25 mL, 1.2 mmol, (f) 4-*tert*-butylcyclohexanone, (g) 123 mg, 0.8 mmol, (h) 1 h, (i) 228 mg, 74%, (e) 82:18

Scheme 2.31

Following General Procedure A for the preparation of magnesium base, data are presented as (a) amount of *n*-Bu_2Mg, (b) amine used, and (c) amount of amine.
Following General Procedure B for the asymmetric deprotonation reaction, data are presented as (a) Mg base, (b) reaction temperature, (c) additives, (d) amount of additive, (e) amount of $ClP(O)(OPh)_2$, (f) ketone, (g) amount of ketone, (h) reaction time, (i) isolated yield, (e) e.r. (*S*):(*R*)

Table 2.17

Entry 1: General Procedure A: (a) 1.00 M, 1 mmol, 1 mL (b) **(*R,R*)-142** and (c) 0.44 mL, 2mmol. General Procedure D: (a) **(*R,R*)-125**, (b) 0 °C, (c) DMPU, (d) 0.06 mg, 0.5 eq., (e) 0.25 mL, 1.2 mmol, (f) 4-*tert*-butylcyclohexanone, (g) 123 mg, 0.8 mmol, (h) 1 h, (i) 225 mg, 73%, (e) 86:14

Entry 2: General Procedure A: (a) 1.00 M, 1 mmol, 1 mL (b) **(*R*,*R*)-142** and (c) 0.44 mL, 2mmol. General Procedure D: (a) **(*R*,*R*)-125**, (b) -20 °C, (c) DMPU, (d) 0.06 mg, 0.5 eq., (e) 0.25 mL, 1.2 mmol, (f) 4-*tert*-butylcyclohexanone, (g) 123 mg, 0.8 mmol, (h) 1 h, (i) 275 mg, 89%, (e) 89:11

Entry 3: General Procedure A: (a) 1.00 M, 1 mmol, 1 mL (b) **(*R*,*R*)-142** and (c) 0.44 mL, 2mmol. General Procedure D: (a) **(*R*,*R*)-125**, (b) -40 °C, (c) DMPU, (d) 0.06 mg, 0.5 eq., (e) 0.25 mL, 1.2 mmol, (f) 4-*tert*-butylcyclohexanone, (g) 123 mg, 0.8 mmol, (h) 1 h, (i) 281 mg, 91%, (e) 92:8

5.3.3. Scope of Pseudo-C_2-Symmetric Bases at -78 °C

Scheme 2.32

Following General Procedure A for the preparation of the magnesium base, data are presented as (a) amount of *n*-Bu_2Mg, (b) amine used, and (c) amount of amine.
Following General Procedure B for the asymmetric deprotonation reaction, data are presented as (a) Mg base, (b) reaction temperature, (c) additives, (d) amount of additive, (e) amount of $ClP(O)(OPh)_2$, (f) ketone, (g) amount of ketone, (h) reaction time, (i) isolated yield, (e) er (*S*):(*R*)

Use of *pseudo- C_2*-symmetric amide **(*R*,*R*)-145**
General Procedure A: (a) 1.00 M, 1 mmol, 1 mL (b) **(*R*,*R*)-128** and (c) 0.48 mL, 2 mmol. General Procedure B: (a) **(*R*,*R*)-145**, (b) -78 °C, (c) -, (d) -, (e) 0.25 mL, 1.2 mmol, (f) 4-*tert*-butylcyclohexanone, (g) 123 mg, 0.8 mmol, (h) 1 h, (i) 293 mg, 95%, (e) 95:5

Use of *pseudo- C_2*-symmetric amide **(*R*,*R*)-146**
General Procedure A: (a) 1.00 M, 1 mmol, 1 mL (b) **(*R*,*R*)-132** and (c) 600 mg, 2 mmol. General Procedure B: (a) **(*R*,*R*)-146**, (b) -78 °C, (c) -, (d) -, (e) 0.25 mL, 1.2 mmol, (f) 4-*tert*-butylcyclohexanone, (g) 123 mg, 0.8 mmol, (h) 1 h, (i) 284 mg, 92%, (e) 94:6

Use of *pseudo*- C_2-symmetric amide **(*R*,*R*)-147**

General Procedure A: (a) 1.00 M, 1 mmol, 1 mL (b) **(*R*,*R*)-136** and (c) 0.55 mL, 2 mmol. General Procedure B: (a) **(*R*,*R*)-147**, (b) -78 °C, (c) -, (d) -, (e) 0.25 mL, 1.2 mmol, (f) 4-*tert*-butylcyclohexanone, (g) 123 mg, 0.8 mmol, (h) 1 h, (i) 290 mg, 94%, (e) 94:6

Use of *pseudo*- C_2-symmetric amide **(*R*,*R*)-148**

General Procedure A: (a) 1.00 M, 1 mmol, 1 mL (b) **(*R*,*R*)-135** and (c) 0.55 mL, 2mmol. General Procedure B: (a) **(*R*,*R*)-148**, (b) -78 °C, (c) -, (d) -, (e) 0.25 mL, 1.2 mmol, (f) 4-*tert*-butylcyclohexanone, (g) 123 mg, 0.8 mmol, (h) 1 h, (i) 265 mg, 86%, (e) 95:5

5.3.4. Scope of Pseudo-C_2-Symmetric Bases at -20 °C

Scheme 2.33

Following General Procedure A for the preparation of magnesium base, data are presented as (a) amount of *n*-Bu_2Mg, (b) amine used, and (c) amount of amine.

Following General Procedure B for the asymmetric deprotonation reaction, data are presented as (a) Mg base, (b) reaction temperature, (c) additives, (d) amount of additive, (e) amount of $ClP(O)(OPh)_2$, (f) ketone, (g) amount of ketone, (h) reaction time, (i) isolated yield, (e) e.r. (*S*):(*R*)

Use of *pseudo C2*-symmetric amide **(*R*,*R*)-145**

General Procedure A: (a) 1.00 M, 1 mmol, 1 mL (b) **(*R*,*R*)-128** and (c) 0.48 mL, 2mmol. General Procedure D: (a) **(*R*,*R*)-145**, (b) -20 °C, (c) DMPU, (d) 0.06 mg, 0.5 eq., (e) 0.25 mL, 1.2 mmol, (f) 4-*tert*-butylcyclohexanone, (g) 123 mg, 0.8 mmol, (h) 1 h, (i) 293 mg, 95%, (e) 89:11

Use of *pseudo C2*-symmetric amide **(*R*,*R*)-146**

General Procedure A: (a) 1.00 M, 1 mmol, 1 mL (b) **(*R*,*R*)-132** and (c) 600 mg, 2mmol. General Procedure D: (a) **(*R*,*R*)-146**, (b) -20 °C, (c) DMPU, (d) 0.06 mg, 0.5 eq., (e) 0.25 mL, 1.2 mmol, (f) 4-*tert*-butylcyclohexanone, (g) 123 mg, 0.8 mmol, (h) 1 h, (i) 278 mg, 90%, (e) 88:12

Use of *pseudo C2*-symmetric amide **(*R*,*R*)-147**

General Procedure A: (a) 1.00 M, 1 mmol, 1 mL (b) **(*R*,*R*)-136** and (c) 0.55 mL, 2mmol. General Procedure D: (a) **(*R*,*R*)-147**, (b) -20 °C, (c) DMPU, (d) 0.06 mg, 0.5 eq., (e) 0.25 mL, 1.2 mmol, (f) 4-*tert*-butylcyclohexanone, (g) 123 mg, 0.8 mmol, (h) 1 h, (i) 294 mg, 95%, (e) 86:14

Use of *pseudo C2*-symmetric amide **(*R*,*R*)-148**

General Procedure A: (a) 1.00 M, 1 mmol, 1 mL (b) **(*R*,*R*)-135** and (c) 0.55 mL, 2mmol. General Procedure D: (a) **(*R*,*R*)-148**, (b) -20 °C, (c) DMPU, (d) 0.06 mg, 0.5 eq., (e) 0.25 mL, 1.2 mmol, (f) 4-*tert*-butylcyclohexanone, (g) 123 mg, 0.8 mmol, (h) 1 h, (i) 293 mg, 95%, (e) 87:13

5.3.5. Substrate Scope at -78 °C

Scheme 2.34

Following General Procedure A for the preparation of the magnesium base, data are presented as (a) amount of *n*-Bu_2Mg, (b) amine used, and (c) amount of amine.

Following General Procedure B for the asymmetric deprotonation reaction, data are presented as (a) Mg base, (b) reaction temperature, (c) additives, (d) amount of additive, (e) amount of $ClP(O)(OPh)_2$, (f) ketone, (g) amount of ketone, (h) reaction time, (i) isolated yield, (e) e.r. (*S*):(*R*)

Synthesis of **(*S*)-72**

General Procedure A: (a) 1.00 M, 1 mmol, 1 mL (b) **(*R*,*R*)-142** and (c) 0.44 mL, 2mmol. General Procedure B: (a) **(*R*,*R*)-125**, (b) -78 °C, (c) -, (d) -, (e) 0.25 mL, 1.2

mmol, (f) 4-phenylcyclohexanone, (g) 139 mg, 0.8 mmol, (h) 1 h, (i) 299 mg, 92%, (e) 97:3

Synthesis of **(*S*)-81**

General Procedure A: (a) 1.00 M, 1 mmol, 1 mL (b) **(*R,R*)-142** and (c) 0.44 mL, 2mmol. General Procedure B: (a) **(*R,R*)-125**, (b) -78 °C, (c) -, (d) -, (e) 0.25 mL, 1.2 mmol, (f) 4-((*tert*-butyldimethylsilyl)oxy)cyclohexanone, (g) 0.18 mL, 0.8 mmol, (h) 1 h, (i) 283 mg, 77%, (e) 88:12

Synthesis of **(*S*)-73**

General Procedure A: (a) 1.00 M, 1 mmol, 1 mL (b) **(*R,R*)-142** and (c) 0.44 mL, 2mmol. General Procedure B: (a) **(*R,R*)-125**, (b) -78 °C, (c) -, (d) -, (e) 0.25 mL, 1.2 mmol, (f) 4-methyl-4-phenylcyclohexanone, (g) 150 mg, 0.8 mmol, (h) 1 h, (i) 319 mg, 95%, (e) 87:13

Synthesis of **(*S*)-82**

General Procedure A: (a) 1.00 M, 1 mmol, 1 mL (b) **(*R,R*)-142** and (c) 0.44 mL, 2mmol. General Procedure B: (a) **(*R,R*)-125**, (b) -78 °C, (c) -, (d) -, (e) 0.25 mL, 1.2 mmol, (f) 4-(dimethylamino)cyclohexanone, (g) 0.11 mL, 0.8 mmol, (h) 1 h, (i) 238 mg, 80%, (e) 93:7

Defining the selectivity by derivatisation.

To an oven-dried flask under argon was added **(*S*)-82**, followed by Peppsi SiPr catalyst (3 mg, 1 mol%) and dry Et_2O (2 mL) at room temperature. The mixture was stirred at room temperature for 5 min before addition of a solution of methylmagnesium bromide (0.5 mL, 1.5 eq., 3M in THF) and the reaction left for 1 h before quenching the reaction with water. The mixture was extracted with Et_2O (5 mL, 5 mL, 5 mL) the organic phase was dried over Na_2SO_4 and the solvent was removed *in vacuo*, giving a yellow oil. The crude material was purified by column

chromatography on silica gel using 0-100% Et_2O in petroleum ether (40-60 °C) to give the desired product as a colourless oil in (22 mg) 20% yield. The enantiomeric ratio of the product was determined by optical rotation.
$[\alpha]_D^{27}$ = -82.1 ° (c=1.00, $CHCl_3$). Lit: $[\alpha]_D^{27}$ = -95.5° (-)-(*S*) (c=1.00, $CHCl_3$)[24b]
e.r. 93:7 (*S*):(*R*)

5.3.6. Substrate Scope at -20 °C

Scheme 2.35

Following General Procedure A for the preparation of magnesium base, data are presented as (a) amount of *n*-Bu_2Mg, (b) amine used, and (c) amount of amine.
Following General Procedure B for the asymmetric deprotonation reaction, data are presented as (a) Mg base, (b) reaction temperature, (c) additives, (d) amount of additive, (e) amount of $ClP(O)(OPh)_2$, (f) ketone, (g) amount of ketone, (h) reaction time, (i) isolated yield, (e) e.r. (*S*):(*R*)

Synthesis of **(*S*)-72**

General Procedure A: (a) 1.00 M, 1 mmol, 1 mL (b) **(*R,R*)-142** and (c) 0.44 mL, 2mmol. General Procedure D: (a) **(*R,R*)-125**, (b) -20 °C, (c) DMPU, (d) 0.06mL, 0.5 eq., (e) 0.25 mL, 1.2 mmol, (f) 4-phenylcyclohexanone, (g) 139 mg, 0.8 mmol, (h) 1 h, (i) 305 mg, 94%, (e) 90:10

Synthesis of **(*S*)-81**

General Procedure A: (a) 1.00 M, 1 mmol, 1 mL (b) **(*R,R*)-142** and (c) 0.44 mL, 2mmol. General Procedure D: (a) **(*R,R*)-125**, (b) -20 °C, (c) DMPU, (d) 0.06mL, 0.5 eq., (e) 0.25 mL, 1.2 mmol, (f) 4-((*tert*-butyldimethylsilyl)oxy)cyclohexanone, (g) 0.18 mL, 0.8 mmol, (h) 1 h, (i) 301 mg, 82%, (e) 80:20

Synthesis of **(*S*)-73**

General Procedure A: (a) 1.00 M, 1 mmol, 1 mL (b) **(*R,R*)-142** and (c) 0.44 mL, 2mmol. General Procedure D: (a) **(*R,R*)-125**, (b) -20 °C, (c) DMPU, (d) 0.06mL, 0.5 eq., (e) 0.25 mL, 1.2 mmol, (f) 4-methyl-4-phenylcyclohexanone, (g) 150 mg, 0.8 mmol, (h) 1 h, (i) 312 mg, 93%, (e) 80:20

Synthesis of **(*S*)-82**

General Procedure A: (a) 1.00 M, 1 mmol, 1 mL (b) **(*R,R*)-142** and (c) 0.44 mL, 2mmol. General Procedure D: (a) **(*R,R*)-125**, (b) -20 °C, (c) DMPU, (d) 0.06mL, 0.5 eq., (e) 0.25 mL, 1.2 mmol, (f) 4-(dimethylamino)cyclohexanone, (g) 0.11 mL, 0.8 mmol, (h) 1 h, (i) 250 mg, 84%, (e) 86:14

Defining the selectivity by derivatisation.
To an oven-dried flask under argon was added **(*S*)-82**, Peppsi SiPr catalyst (3 mg, 1 mol%) and dry Et_2O (2 mL). The mixture was stirred at room temperature for 5 min before addition of a solution of methylmagnesium bromide (0.5 mL, 1.5 eq., 3M in THF) and the reaction stirred for 1 h before quenching with water. The mixture was extracted with Et_2O (5 mL, 5 mL, 5 mL), the organic phase was dried over Na_2SO_4 and the solvent was removed *in vacuo*, giving a yellow oil. The crude material was purified by column chromatography on silica gel using 0-100% Et_2O in petroleum ether (40-60 °C) to give the desired product as a colourless oil in (33 mg) 30% yield. The enantiomeric ratio of the product was determined by optical rotation.

$[\alpha]_D^{27}$ = -68.7 ° (c=1.00, $CHCl_3$). Lit: $[\alpha]_D^{27}$ = -95.5° (-)-(*S*) (c=1.00, $CHCl_3$)[24b]
e.r. 86:14 (*S*):(*R*)

5.3.7.Towards Future Work

Scheme 2.36

Following General Procedure A for the preparation of magnesium base, data are presented as (a) amount of *n*-Bu_2Mg, (b) amine used, and (c) amount of amine.

Following General Procedure B for the asymmetric deprotonation reaction, data are presented as (a) Mg base, (b) reaction temperature, (c) hydrazine, (d) amount of hydrazine, (e) reaction time, (f) isolated yield, (g) e.r. (*S*):(*R*)

Shapiro reaction

General Procedure A: (a) 1.00 M, 1 mmol, 1 mL (b) **(*R,R*)-142** and (c) 0.44 mL, 2mmol. General Procedure B: (a) **(*R,R*)-125**, (b) -78 °C, (c) *N*'-(4-(*tert*-butyl)cyclohexylidene)-4-methylbenzenesulfonohydrazide, (d) 129 mg, 0.4 mmol, (e) 1 h, (f) - (g) -

Scheme 2.37

***Entry 1*, Table 2.18**

Part 1

A solution of *n*-Bu_2Mg (1.00 M, 1 mmol, 1 mL) in heptane was transferred to a Schlenk flask, which had been flame-dried under vacuum (0.005 mbar) and allowed to cool under an atmosphere of argon, and the heptane was removed *in vacuo* (0.005 mbar) until a white solid was obtained. THF (10 mL) was then added, followed by the chiral amine **(*R,R*)-142** (0.44 mL, 2 mmol), and the solution was heated at reflux for 1.5 h, assuming quantitative formation of the magnesium bisamide. The solution was stored at room temperature.

Part 2

o a Schlenk tube which had been flame-dried under vacuum, and purged with argon, was added *N*'-(4-(*tert*-butyl)cyclohexylidene)-4-methylbenzenesulfonoylhydrazide (129 mg, 0.4 mmol), followed by THF (10 mL). The mixture was stirred for 5 min at room temperature before cooling it down to -78 °C. After a further 15 min was added dropwise *n*-BuLi (0.16 mL, 0.4 mmol, 2.5 M in hexanes) was added dropwise and the reaction left stirred for a further 15 min. To this solution was added slowly over 30 min the chiral magnesium bisamide base formed in Part 1. The stirred reaction was left to warm to room temperature overnight before being quenched with water. The aqueous phase was extracted with Et_2O (50, 25, 25 mL) and the organic phases were combined and washed with 1 M HCl (2 × 10 mL) to recover the amine.

Removal of the solvent *in vacuo* (n.b. care should be taken at this step due to the low boiling point of the product) gave an oil, Analysis by ^{1}H NMR spectroscopy and TLC showed the absence of the desired compound.

***Entry 2*, Table 2.7**

Part 1

A solution of *n*-Bu_2Mg (1.00 mL, 1 mmol) in heptane was transferred to a Schlenk flask, which had been flame-dried under vacuum (0.005 mbar) and allowed to cool under an atmosphere of argon, and the heptane was removed *in vacuo* (0.005 mbar) until a white solid was obtained. THF (10 mL) was then added, followed by the chiral amine **(*R,R*)-142** (0.44 mL, 2 mmol), and the solution was heated at reflux for 1.5 h, assuming quantitative formation of the magnesium bisamide. The solution was stored at room temperature.

Part 2

To a Schlenk tube which had been flame-dried under vacuum, and purged with argon, was added *N*'-(4-(*tert*-butyl)cyclohexylidene)-4-methylbenzenesulfonylhydrazide (129 mg, 0.4 mmol), followed by THF (10 mL). The mixture was stirred for 5 min at room temperature before dropwise addition of *n*-BuLi (0.16 mL, 0.4 mmol, 2.5 M in hexanes) left for a further 15 min. To this solution was added slowly over 30 min the chiral magnesium bisamide base formed in Part 1. The stirred reaction was left to warm to room temperature overnight before being quenched with water. The aqueous phase was extracted with Et_2O (50, 25, 25 mL) and the organic phases were combined and washed with 1M HCl (2 × 10 mL) to recover the amine. Removal of the solvent *in vacuo* (n.b. care should be taken at this step due to the low boiling point of the product) gave an oil which was purified by column chromatography on silica gel using 0-1% Et_2O in petroleum ether (30-40 °C) to give the desired product as a colourless oil in (32 mg) 58% yield.

$[\alpha]_D^{20} = 4.2$ ° (c=1.00, $CHCl_3$). Lit: $[\alpha]_D^{20} = -105°$ (-)-(*S*) (c=1.00, $CHCl_3$)[25]

4-(*tert*-butyl)cyclohexene[34] **(*S*)-150**:

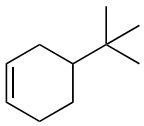

ν_{max}(DCM): 3022, 2955, 2359, 1726, 1656, 1477, 1437, 1365, 1228 cm^{-1};
^{1}H NMR (400 MHz): δ 5.78-5.63 (m, 2 H, C=CH), 2.18-1.98 (m, 3 H, CH_2), 1.87-1.77 (m, 2 H, CH_2), 1.35-1.26 (m, 1 H, CH), 1.23-1.13 (m, 1 H, CH_2), 0.88 (s, CH_3);
^{13}C NMR (125 MHz): δ 127.40, 126.9, 44.16, 32.3, 27.18, 26.83, 26.76, 23.97.

Scheme 2.38

A solution of *n*-Bu_2Mg (1.00 M, 1 mmol, 1ml) in heptane was transferred to a Schlenk flask, which had been flame-dried under vacuum (0.005 mbar) and allowed to cool under an atmosphere of argon, and the heptane was removed *in vacuo* (0.005 mbar) until a white solid was obtained. THF (10 mL) was then added, followed by the chiral amine **(*R,R*)-142** (0.12 mL, 1 mmol), and the solution was heated at reflux for 1.5 h.
The prepared base was cooled under nitrogen to -78 °C then charged with DMPU (0.06 mL, 0.5 eq.) and $ClP(O)(OPh)_2$ (0.84 mL, 4 eq.), and the reaction mixture was stirred for 10 min. Then, 4-*t*-butylcyclohexanone (123 mg, 0.8 mmol) was added as a solution in THF (2 mL) over 1 h using a syringe pump. The reaction mixture was stirred at -78 °C for 16 h for before being quenched with a saturated solution of $NaHCO_3$ (10 mL) and allowed to warm to room temperature. The aqueous phase was extracted with Et_2O (50, 25, 25 mL) and the organic phases were combined and washed with 1M HCl (2 × 10 mL) to recover the amine. The removal of the solvent *in vacuo* gave an oil, which was purified by column chromatography on silica gel using 0-30% Et_2O in petroleum ether (40-60 °C) to give the desired product **0.(*S*)-16** as a colourless oil in (297 mg) 77% yield and an e.r. of 95:5. The enantiomeric ratio of the product was determined by analysis using chiral HPLC with a CHIRALCEL OD or OJ column

6. References

1. Whitesell, J. K.; Felman, S. W., *J. Org. Chem.*, **1980**, *45* (4), 755.
2. Asami, M.; Kirihara, H., *Chem. Lett.*, **1987**, *16* (2), 389.
3. (a) Simpkins, N. S., *J. Chem. Soc. Chem. Commun.*, **1986**, 88. (b) Shirai, R.; Tanaka, M.; Koga, K., *J. Am. Chem. Soc.*, **1986**, *108* (3), 543.
4. (a) Cain, C. M.; Cousins, R. P. C.; Coumbarides, G.; Simpkins, N. S., *Tetrahedron*, **1990**, *46* (2), 523. (b) Cousins, R. P. C.; Simpkins, N. S., *Tetrahedron Lett.*, **1989**, *30* (51), 7241.
5. Simpkins, N. S., *Chem. Soc. Rev.* **1990**, *19* (3), 335.
6. Tomioka, K.; Ando, K.; Takemasa, Y.; Koga, K., *Tetrahedron Lett.*, **1984**, *25* (49), 5677.
7. Sato, D.; Kawasaki, H.; Shimada, I.; Arata, Y.; Okamura, K.; Date, T.; Koga, K., *J. Am. Chem. Soc.*, **1992**, *114* (2), 761–763.
8. (a) Bunn, B. J.; Simpkins, N. S.; Spavold, Z.; Crimmin, M. J., *J. Chem. Soc. Perkin Trans. 1*, **1993**, No. 24, 3113. (b) Bunn, B. J.; Simpkins, N. S., *J. Org. Chem.*, **1993**, *58* (3), 533.
9. Corey, E. J.; Gross, A. W., *Tetrahedron Lett.*, **1984**, *25* (5), 495.
10. Sugasawa, K.; Shindo, M.; Noguchi, H.; Koga, K., *Tetrahedron Lett.*, **1996**, *37* (41), 7377.
11. Honda, T.; Kimura, N.; Tsubuki, M., *Tetrahedron Asymmetry*, **1993**, *4* (1), 21.
12. Honda, T.; Kimura, N., *J. Chem. Soc. Chem. Commun.*, **1994**, No. 1, 77.
13. Aggarwal, V. K.; Humphries, P. S.; Fenwick, A., *Angew. Chem. Int. Ed.*, **1999**, *38* (13-14), 1985–1986
14. Clayden, J.; Menet, C. J.; Mansfield, D. J., *Chem. Commun.*, **2002**, No. 1, 38.
15. (a) Allan, J. F.; Henderson, K. W.; Kennedy, A. R., *Chem Commun*, **1999**, No. 14, 1325. (b) Eaton, P. E.; Lee, C. H.; Xiong, Y., *J. Am. Chem. Soc.*, **1989**, *111* (20), 8016.
16. Clegg, W.; Craig, F. J.; Henderson, K. W.; Kennedy, A. R.; Mulvey, R. E.; O'Neil, P. A.; Reed, D., *Inorg. Chem.*, **1997**, *36* (27), 6238.
17. Watson, A. J. B. *PhD Thesis*; University of Strathclyde; 2007.
18. Evans, D. A.; Nelson, S. G., *J. Am. Chem. Soc.*, **1997**, *119* (27), 6452.

19. Henderson, K. W.; Kerr, W. J.; Moir, J. H., *Chem. Commun.*, **2000**, 479.
20. Henderson, K. W.; Kerr, W. J.; Moir, J. H., *Tetrahedron*, **2002**, *58* (23), 4573
21. Bennie, L. S.; Kerr, W. J.; Middleditch, M.; Watson, A. J. B., *Chem. Commun.*, **2011**, *47* (8), 2264.
22. (a) Bennie, L. S., *PhD Thesis*; University of Strathclyde; 2012. (b) Middleditch, M., *Postdoctoral Report*; University of Strathclyde.
23. Alexakis, A.; Gille, S.; Prian, F.; Rosset, S.; Ditrich, K., *Tetrahedron Lett.*, **2004**, *45* (7), 1449.
24. (a) Cane, D. E.; Yang, G.; Coates, R. M.; Pyun, H. J.; Hohn, T. M., *J. Org. Chem.*, **1992**, *57* (12), 3454. (b) McGeady, P.; Pyun, H.-J.; Coates, R. M.; Croteau, R., *Arch. Biochem. Biophys*,. **1992**, *299* (1), 63.
25. Sadozai, S. K.; Lepoivre, J. A.; Dommisse, R. A.; Alderweireldt, F. C., *Bull. Soc. Chim. Belg.*, **1980**, *89* (8), 637
26. Perrin, D., D.; Armarego, W. L. F., *Purification of Laboratory Chemicals*; Pergaman: Oxford; 1988.
27. Love, B. E.; Jones, E. G., *J. Org. Chem.*, **1999**, *64* (10), 3755.
28. Zimmerman, H. E.; Jones, G. *J. Am. Chem. Soc.* **1970**, *92* (9), 2753.
29. Carreño, M. C.; Urbano, A.; Di Vitta, C., *J. Org. Chem.*, **1998**, *63* (23), 8320.
30. Guzzo, P. R.; Buckle, R. N.; Chou, M.; Dinn, S. R.; Flaugh, M. E.; Kiefer, A. D.; Ryter, K. T.; Sampognaro, A. J.; Tregay, S. W.; Xu, Y.-C., *J. Org. Chem.*, **2003**, *68* (3), 770.
31. Dorra, M.; Gomann, K.; Guth, M.; Kirmse, W., *J. Phys. Org. Chem.*, **1996**, *9* (9), 598.
32. Qian, H.; Yan, S.; Cui, X.; Pi, C.; Liu, C.; Wu, Y., *Chin. J. Chem.*, **2013**, *31* (8), 992.
33. Yamada, H.; Kawate, T.; Nishida, A.; Nakagawa, M., *J. Org. Chem.*, **1999**, *64* (24), 8821.
34. Imboden, C.; Villar, F.; Renaud, P., *Org. Lett.*, **1999**, *1* (6), 873.

Chapter 3

A Structural and Practical Study of Alkylmagnesium Amides

Content

1. Introduction

We have demonstrated that magnesium base species mediate a range of valuable transformations under energy efficient conditions. Specifically, carbon-centred bases have been to permit the synthesis of kinetic silyl enol ethers at 0 °C,[1] and enol phosphates at room temperature. These mild conditions mean that such bases are viable for application in industrial settings. On the other hand, the use of chiral magnesium bisamide bases provides high levels of reactivity and selectivity even at milder temperatures for the asymmetric synthesis of both silyl enol ethers[2] and enol phosphates.

1.1. An Unexpected Observation

In the course of optimising the asymmetric deprotonation reaction using magnesium bisamide bases, we encountered an unexpected result. As shown below in **Scheme 3.1**, while using only 1 eq. of the chiral amine **(*R*,*R*)-142** for the preparation of the base, using the methodology developed for magnesium bisamide species, a high yield of 77% yield was observed, with a 95:5 selectivity. Within our laboratory, we have pursued the aim of reducing the amount of chiral amine required for these reactions, and in the past the Kerr group have explored the use of 1 eq. of chiral amine (alkylmagnesium amide and Hauser bases) and also attempted catalytic (in amine) deprotonation reactions. Nevertheless, such levels of reactivity under these specific conditions were unprecedented, and this observation merited further investigation.

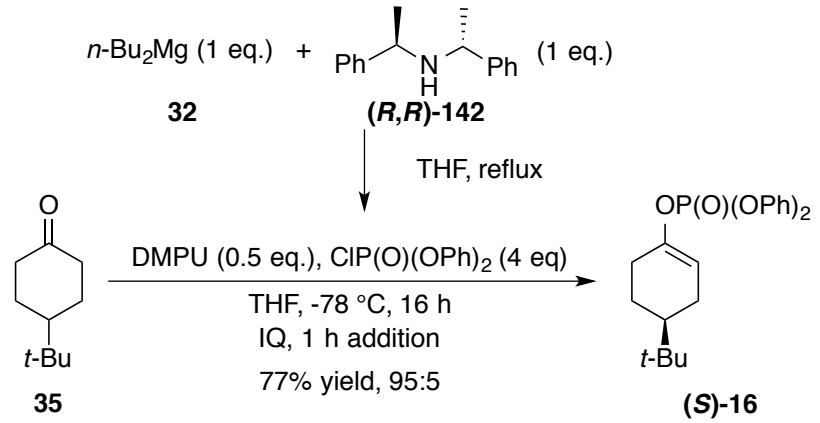

Scheme 3. 1

1.2. Alkylmagnesium Amide Bases

Alkylmagnesium amides are well-described species that have been studied for a range of transformation over many years. These species are formed from the reaction of one equivalent of amine with one equivalent of dialkylmagnesium reagent. Such reagents have been used in transformations such as the alkylation of carbonyl compounds,[3] enantioselective conjugate additions,[4] and reduction of ketones through ß-hydride transfer.[5] Furthermore, within the area of asymmetric deprotonation reactions, a range of processes have also been described.[6] Within our laboratory we have investigated the use of chiral amines for the synthesis and application of alkylmagnesium amide bases.[7]

1.2.1. Synthesis and Primary Work

As shown below (**Scheme 3.2**), the reaction of chiral amine **(*R*)-33** with di-*n*-butylmagnesium **32** at room temperature afforded the desired alkylmagnesium amide base **(*R*)-34** in only 1.5 h at room temperature.

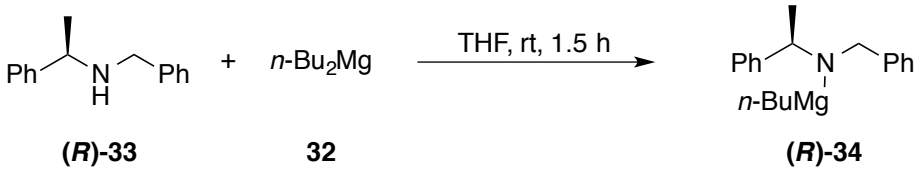

Scheme 3. 2

With the alkyl magnesium amide **(*R*)-34** in hand, a range of temperatures and deprotonation conditions were then explored. **Scheme 3.3** shows the difference in reactivity and selectivity between bis amide base **(*R*)-119** and alkylmagnesium amide **(*R*)-34** in the formation of silyl enol ethers. Specifically, the use of alkylmagnesium amide **(*R*)-34** provided a high level of conversion (88%) with a moderate selectivity of 84:16,[7b] whereas magnesium bisamide base **(*R*)-119** afforded a slightly lower level of conversion (82%), but with a higher e.r. of 91:9.[8] The formation of the base has been studied *via* ^{1}H NMR spectroscopy, where analysis of reaction aliquots in d_8-THF showed the disappearance of the NH signal.[7a]

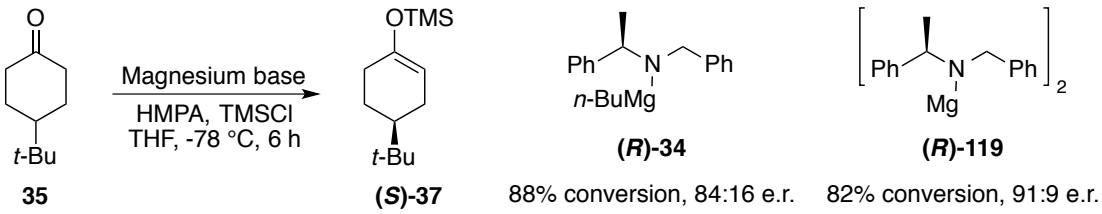

Scheme 3. 3

1.2.2. Varying the Alkyl Moiety

One of the advantages presented by such alkylmagnesium amide bases was the potential to readily tune the alkyl component of the complex. In order to investigate this parameter, the more hindered di-*tert*-butylmagnesium was employed for the synthesis of the base. As shown below in **Scheme 3.4**, when *n*-Bu_2Mg was used to form base **(*R*)-34**, a high 80% conversion was observed with 86:14 of selectivity (N. B. the use of DMPU rather than HMPA afforded a higher selectivity with a lowered reactivity). In contrast, when *t*-Bu_2Mg (**42**), generated from the transmetallation reaction of *t*-BuLi, was used for the synthesis of base **(*R*)-151**, the same 86:14 selectivity was observed, along with a slightly higher conversion to **(*S*)-37** of 90%.[7a] On the other hand, when the same base **(*R*)-151** was formed using *t*-Bu_2Mg derived via the methodology described in Chapter 1 (*c.f.* **Scheme 1.13**) only a poor 6%

conversion was observed, with a selectivity of 72:29. This contrast in results could be explained by the presence of a range of salts, such as LiCl, in the former case, and the generation of ate complexes. Further variation of the alkyl portion of the magnesium complex resulted in a broad variation of the reaction outcome, as using the *iso*-propyl derived base **(*R*)-152** provided the enol ether in 89% conversion with a lowered selectivity of 82:18,[9] while the use of Mes_2Mg (**41**), affording the base **(*R*)-153**, not only provided a poor conversion of 47%, but moreover resulted in no stereoselectivity in the formation of **37**.[9] It was also shown that the use of various salts, such as LiCl, could greatly influence the selectivity and reactivity of the desired transformation.[9]

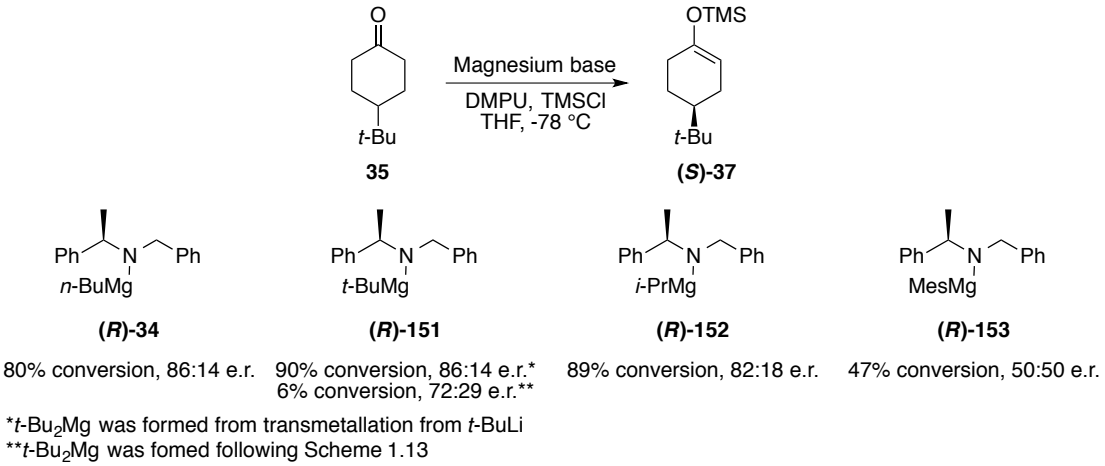

Scheme 3. 4

1.2.3. Addition of Additives

Although most of this preliminary work was carried out with the aim of developing a catalytic asymmetric deprotonation reaction, studies have also focussed on further improve the stoichiometric alkylmagnesium amide process. The alkylmagnesium amide bases were fully explored in an additive study where it was shown that excellent levels of reactivity and selectivity could be obtained with the use of crown ethers.[9] As shown below (**Scheme 3.5**), the desired asymmetric deprotonation reaction was performed with the use of LiCl and 18-c-6, which dramatically enhanced the reactivity and selectivity of the transformation. Thus, use of the first developed alkylmagnesium amide, **(*R*)-34**, afforded a high 94% yield with a

selectivity of 90:10, whereas the C_2-symmetric amide **(*R*,*R*)-154** allowed an excellent 91% yield and 95:5 e.r. in the formation of silyl enol ether **(*S*)-37**. Importantly, this was the first time that such levels of selectivity and reactivity were achieved using only 1 equivalent of the chiral amine.

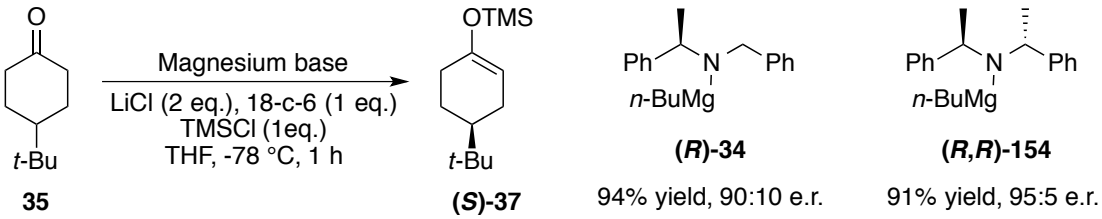

Scheme 3. 5

It was proposed that the presence of crown ether in the solution allowed the formation of either a threaded complex or a more simple edge-on interaction with the magnesium species (**Figure 3.1**) leading to an enhancement of both reactivity and selectivity.[9]

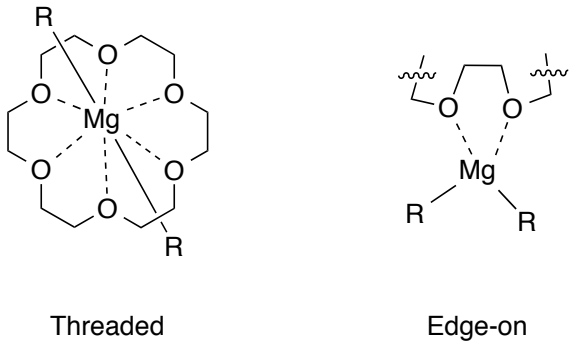

Figure 3. 1

With the development of alkylmagnesium amides, more simple Grignard reagents were also used to access chiral magnesium complexes for asymmetric deprotonation reactions, while still employing only one equivalent of chiral amine.

1.3. Hauser bases

1.3.1. Synthesis and Application

Hauser bases are magnesium complexes that result from the reaction of Grignard reagents and with amines, and therefore they are often considered the magnesium equivalent of lithium amide reagents.[10] The development of Hauser bases for the synthesis of silyl enol ethers under non-asymmetric conditions has been described within the literature.[11] However, the use of such species in asymmetric deprotonation reactions was first investigated within our laboratories. As shown below (**Scheme 3.6**), in initial studies with chiral Hauser bases, a high conversion was observed (98%), but with very low levels of enantioselectivity (58:49).[7a]

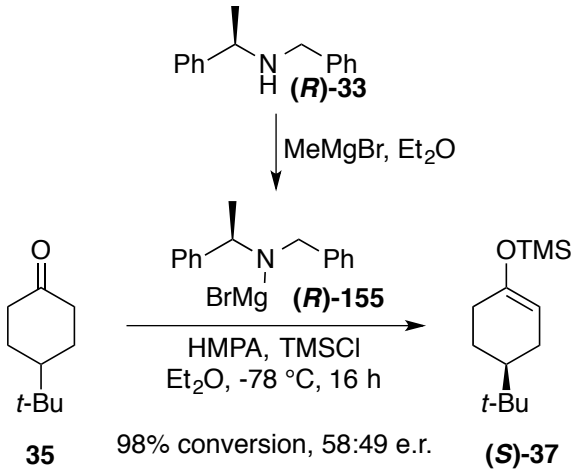

Scheme 3. 6

1.3.2. Additive and Halogen Effect

Encouraged by positive results obtained with the use of crown ethers for the asymmetric deprotonation reaction with alkylmagnesium amides, the chiral Hauser bases were also subjected to such additive conditions. Further optimisation of the reaction conditions improved the outcome of the reaction such that a 92% yield and 90:10 selectivity was obtained when base **(*R*)-156** was used (**Scheme 3.7**). Interestingly, the use of the C_2-symmetric amine-derived Hauser base **(*R*)-157** afforded a low 48% yield, but a higher selectivity of 92:8. It should be noted that the C_2-symmetric amine **(*R*,*R*)-142**, when converted to a Hauser base **(*R*,*R*)-157**, delivered a lower selectivity than when used as an alkylmagnesium amide base **(*R*,*R*)-154** (*c.f.* **Scheme 3.5**).

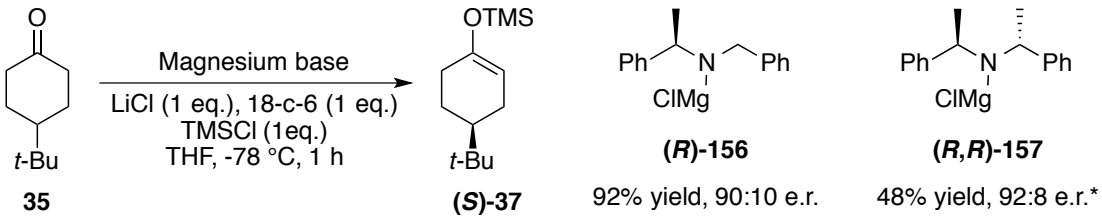

Scheme 3. 7

Furthermore, was also shown that the nature of the halide in the Hauser base had a drastic effect on the reactivity; but no general trend could be established in terms of selectivity. Overall, the size of the halide may explain the reactivity observed, as the presence of a bromide decrease the reactivity to 80% yield, whereas an iodide provided only 39% yield (**Scheme 3.8**). In terms of selectivity, bromide complex **(*R*)-158** afforded an 83:17 e.r., whereas iodide complex **(*R*)-159** generated a high 90:10 e.r., comparable to the result obtained with the use of the chloride derivative **(*R*)-157**.

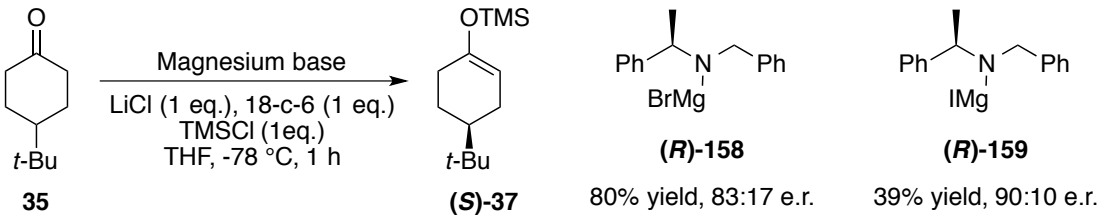

Scheme 3. 8

This Hauser base methodology resulted in further conditions for the asymmetric deprotonation reaction where only one equivalent of the chiral amine is used. Nevertheless, the reactivity and selectivity presented by the alkylmagnesium amide or the Hauser bases were never comparable to those observed with the corresponding magnesium bisamide base. In addition, the bisamide bases also display good levels of selectivity and high reactivity at milder temperatures. Such milder conditions were also explored with the Hauser bases, but only low levels of conversion were

observed. As seen below (**Scheme 3.9**), at -40 °C, a 55% yield with a selectivity of 86:14 was observed, and at 0 °C, a higher 66% yield, with a poor 70:30 e.r., was obtained in the formation of silyl enol ether of **(*S*)-37**.

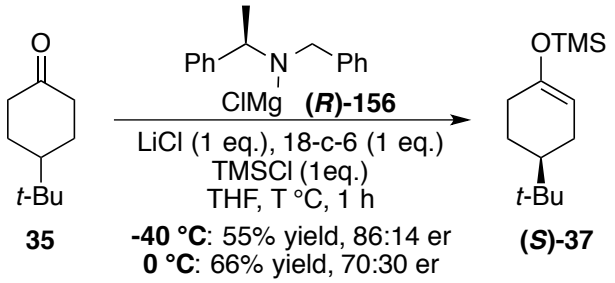

Scheme 3. 9

So far, two distinct methodologies that have been developed have demonstrated the possibilty of accessing enantioenriched silyl enol ethers with only one equivalent of the chiral amine employed. The scope and limitations of both alkylmagnesium amide bases and Hauser bases have been revealed, as they both require the presence of additives and low temperatures to perform efficiently. Currently, these two processes represent the most efficient method in terms of the amount of chiral amine required, but the lower yields and selectivities, coupled with the additives required, makes them less viable than the magnesium bisamide bases. However, the result depicted in **Scheme 3.1** shows a process where only one equivalent of the chiral amine is used, and yet a high 95:5 level of selectivity is observed, without the use of crown ether additives. We were therefore interested in further exploring this observation in order to understand this efficient, alkylmagnesium amide-mediated process.

2. Proposed Work

The interesting outcome of the reaction presented in **Scheme 3.1** could be exploited to further improve the asymmetric deprotonation reaction. Although apparently highly promising, a range of questions arose form this transformation:

- What is the nature of the base involved in this transformation? (*i.e.* alkylmagnesium amide or magnesium bisamide base, or an *in situ* generated Hauser base)
- Is it possible to enhance the efficiency of this transformation without altering the selectivity?
- Can we improve the overall process without the use of additives, and therefore develop a more environmentally favourable transformation?
- Can we access higher temperatures with the species formed in solution, and therefore directly compare this system with the milder conditions used with magnesium bisamide bases?

3. Results and Discussions

Our studies began with the unexpected result depicted in **Scheme 3.1**, when only one equivalent of amine was added to *n*-Bu_2Mg, and, following reflux in THF, the base species used to carry out the asymmetric deprotonation reaction afforded a high 77% isolated yield. More surprisingly, the reaction repeatedly afforded a high e.r. of 95:5.

3.1. Theoretical Approach

Another unexpected feature of this transformation was the fact that more than 50% isolated yield of product was obtained. In **Figure 3.2** below is presented various options for the theoretical outcome of this base formation. The presence of one equivalent of chiral amine **(*R*,*R*)-142**, when reacted with one equivalent of *n*-Bu_2Mg **1.1**, could follow either **Pathway I**, affording 50% of bisamide **(*R*,*R*)-125**, and 50% of unreacted base **32**, or, on the other hand, by following **Pathway II**, afford 100% of the alkylmagnesium amide **(*R*,*R*)-154**.

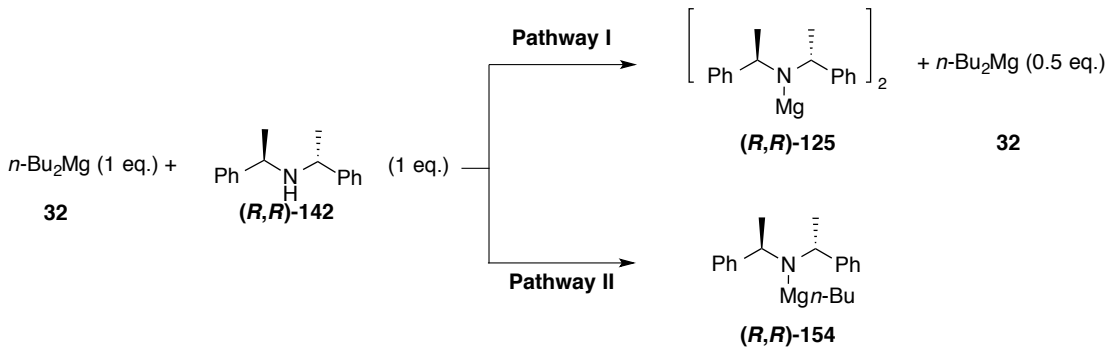

Figure 3. 2

A mixture of both Pathways I and II, generating all three components **(*R*,*R*)-125**, **(*R*,*R*)-154** and **32** in the reaction mixture, is also possible. Among these three active species, a range of proposals can be made, which will guide the studies in this area:

Postulate 1) Given the selectivity obtained (95:5), which was the highest observed with the use of magnesium bases derived from **(*R*,*R*)-142**, only amide species **(*R*,*R*)-125**, and/or **(*R*,*R*)-154** are involved in the reaction. Indeed, previous work on the development of a catalytic cycle has shown that, when the carbon-centred base was involved in the deprotonation reaction, a loss in selectivity was observed (*c.f.* **Scheme 1.11** and **1.12** in Chapter 1). Generally, it was established that *n*-Bu_2Mg was unreactive in the deprotonation reaction at -78 °C.[9]

Postulate 2) Our previous observations have shown that alkylmagnesium amide **(*R*,*R*)-154** was highly efficient (*i.e.* 95:5 e.r.) only when a crown ether and LiCl were present in the reaction mixture.[9] Additionally, it was also observed that the second amide moiety on the magnesium bisamide base **(*R*,*R*)-125** was totally unreactive, hence the requirement for 1 equivalent of bisamide for the asymmetric deprotonation reaction of 0.8 equivalents of 4-*tert*-butylcyclohexanone **35**.[12]

3.1.1. An Electrophile Effect

With these two postulates in mind, the first issue to consider should be the influence of the diphenylphosphoryl chloride electrophile. Indeed, studies should determine if the enhancement in reactivity is due to the presence of a more reactive electrophile containing a coordinating group. We have already established that the use of this electrophile does not require additives such as DMPU to enable high levels of reactivity and selectivity (see Chapter 2), and attributed this to the P=O bond in either the phosphoryl electrophile or the enol phosphate product. With this in mind, and the presence of two possible active species, *i.e.* the alkylmagnesium amide base **(*R*,*R*)-125**, and bisamide base **(*R*,*R*)-154**, in the reaction mixture, it can be proposed that the formation of enol phosphates is facilitated by one of these two species (**Figure 3.3**).

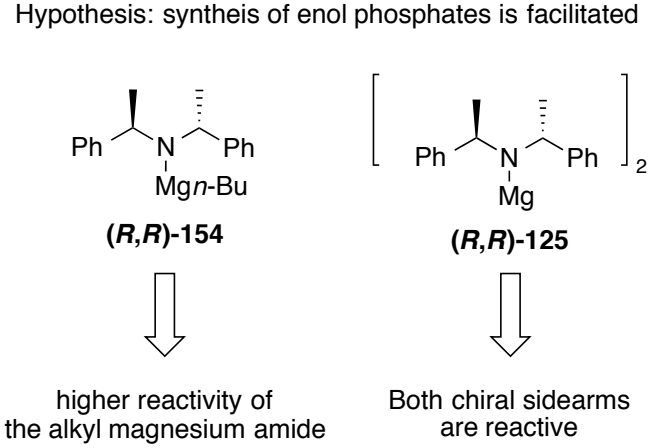

Figure 3. 3

In order to examine the possibility of a higher reactivity of the alkylmagnesium amide base **(*R*,*R*)-154** in the presence of a P=O containing species, the base was formed using conditions previously described in the literature.[9] Specifically, 1 eq. of *n*-Bu_2Mg **32**, and 1 eq. of **(*R*,*R*)-142** were stirred at room temperature for 1.5 h, whereas in **Scheme 3.1**, the active species had been formed by refluxing these reactants for 1 h in THF. Under these conditions, the reaction now afforded a low 38% yield, with a slight erosion of selectivity of 93:7 e.r. (**Scheme 3.10**).

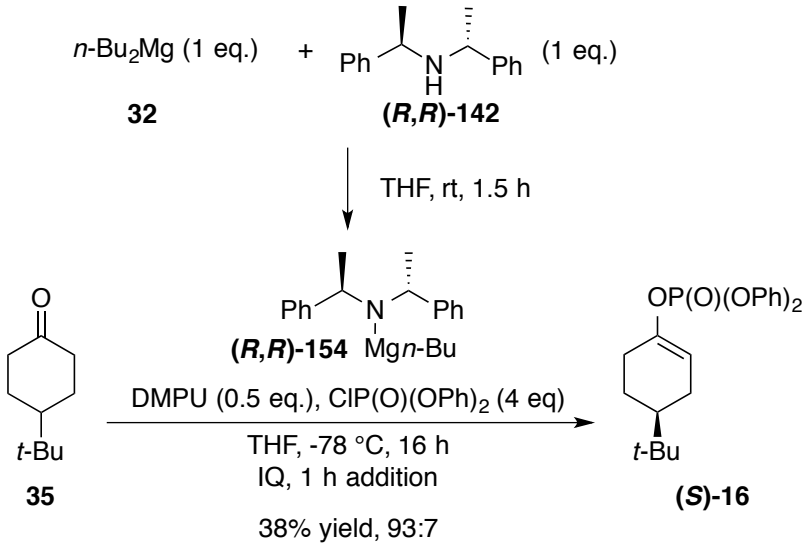

Scheme 3. 10

This result eliminated the possibility of a higher reactivity of the alkylmagnesium amide base in the formation of enol phosphates. In order to test the second hypothesis, which stated that both amides of the magnesium bisamide base **(*R*,*R*)-125** perform the deprotonation reaction during the synthesis of enol phosphates, the reaction in **Scheme 3.11** was carried out, where 0.5 eq. of magnesium bisamide base **(*R*,*R*)-125** was utilised under the standard reaction conditions.

As observed below in **Scheme 3.11**, under such conditions a low 42% yield was observed, with a high e.r. of 96:4. If both amides were able to act as a base, then a yield >50% should be observed. With the reaction below, we have demonstrated that in the case of the magnesium bisamide base, only one amide is involved in the asymmetric deprotonation reaction.

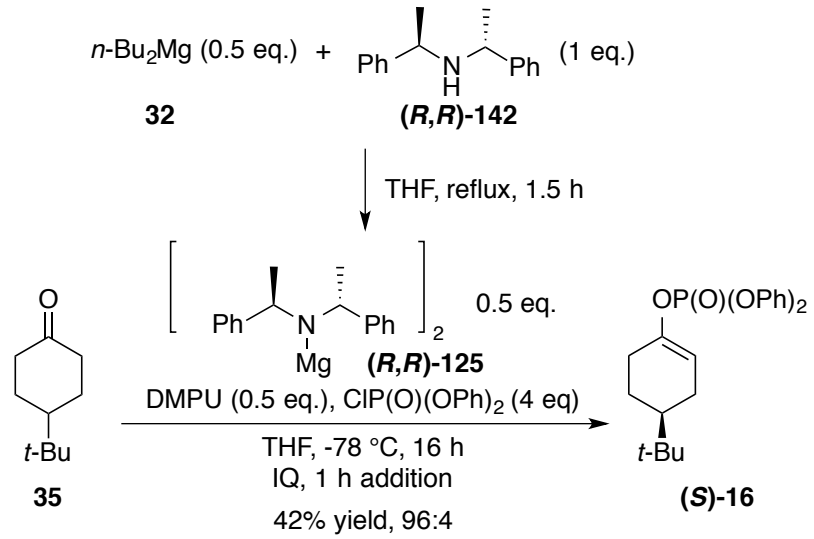

Scheme 3. 11

The low levels of reactivity observed in these two experiments suggest that neither of the two hypotheses regarding the active species can explain the high reactivity observed (77%) in the initial reaction. Furthermore, the use of diphenylphosphoryl chloride as electrophile was shown not to enhance the reactivity of the base species present in solution.

3.1.2. The Effect of Multiple Species

One further possibility would be the formation of a novel, so far unproposed species under the reaction conditions. As mentioned earlier, while describing **Figure 3.2**, the ratio of magnesium species present in solution should lead to a mixture of all three components **(*R*,*R*)-125**, **(*R*,*R*)-154** and **32**. We were interested in exploring the hypothesis in which a mixture of two of these species would enhance the reactivity of the base. As shown below in **Scheme 3.12**, we first prepared 0.5 eq. of the magnesium bisamide base **(*R*,*R*)-125**, to which was added 0.5 eq. of *n*-Bu_2Mg at -78 °C, (which would represent **Pathway I** in **Figure 3.2**). Under these conditions, a 42% isolated yield was obtained, with a selectivity of 96:4 (**Table 3.1**), which was the same outcome as observed in **Scheme 3.11**. This result, although disappointing, indicated that *n*-Bu_2Mg was only a spectator species under the reaction conditions, supporting our *Postulate 1*. It was also envisaged that the presence of a mixture of magnesium bisamide species **(*R*,*R*)-125** and alkylmagnesium amide species **(*R*,*R*)-154**, may be responsible for the enhanced reactivity. Therefore we prepared separately 0.5 eq. of **(*R*,*R*)-125** and 0.5 eq. of **(*R*,*R*)-154**, mixed both species at -78 °C, and carried out the reaction under the conditions presented below (**Scheme 3.12**). Under such conditions, only 61% yield was observed with a selectivity of 94:6. Although delivering a higher yield, the result did not correspond to the theoretical yield of 80% (*i.e.* added yields of the reactions in **Schemes 3.10** and **3.11**). This outcome provided evidence that the mixture of species was not responsible for the high yield observed in the first reaction (**Scheme 3.1**).

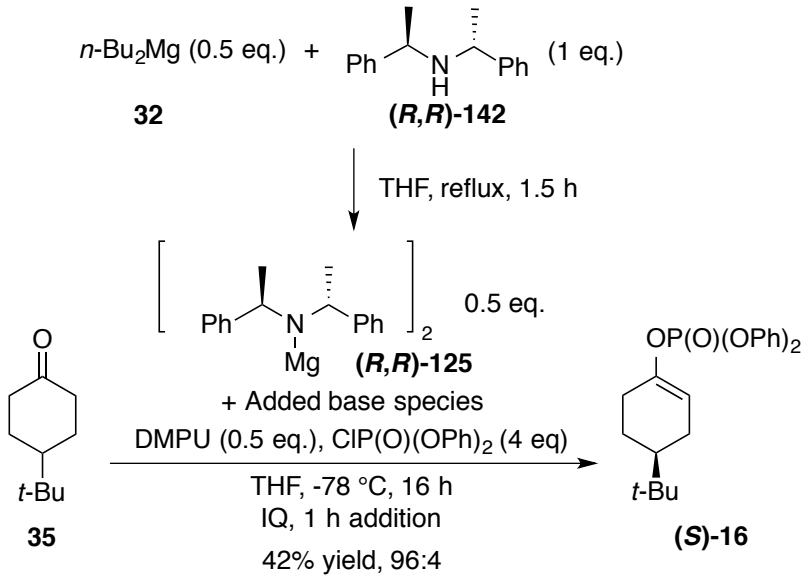

Scheme 3. 12

Entry	Added base species	Yield %	e.r. (*S*):(*R*)
1	**32** (0.5 eq.)	42	96:4
2	**(*R*,*R*)-154** (0.5 eq.)	61	94:6

Table 3. 1

With the parameters explored so far, we have demonstrated that the high singular abilities displayed by the novel electrophile could not possibly explain the high reactivity observed, nor could the unique mixture of species present in solution. Further explorations involved the addition of 1,4-dioxane, deoxygenation of the reaction solution, and sonication; in all cases these attempts did not afford the reactivity obtained in **Scheme 3.1**. As a further possibility, the key element in this initial process was the employment of reflux conditions for the base formation, which could be responsible for the emergence of a novel magnesium aggregate species.

3.1.3. Formation of a New Magnesium Aggregate

As shown below in **Scheme 3.13**, the alkylmagnesium amide **(*R*,*R*)-154** was described to be quantitatively formed after stirring for 90 min at room temperature,[7a,9,13] and further heating of the alkylmagnesium amide might provide a novel undefined magnesium aggregate species **(*R*,*R*)-160**. In our initial reaction

conditions (**Scheme 3.1**), directly heating the reaction mixture may have increased the rate of formation of **(*R*,*R*)-154** and driven the magnesium amide species to form a novel aggregate.

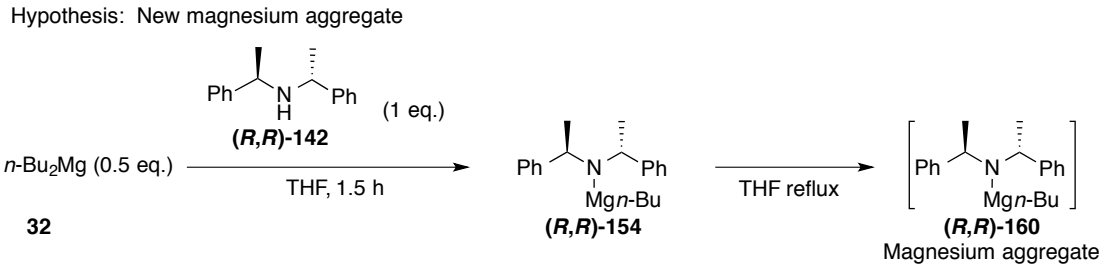

Scheme 3. 13

To validate such a hypothesis, a range of test reactions were carried out starting with the hypothetical aggregate formation. As shown below (**Scheme 3.14**), base **(*R*,*R*)-160** was prepared by first forming the alkylmagnesium amide base **(*R*,*R*)-154**, which was then refluxed in THF for a further 1.5 h. Interestingly, the same levels of reactivity (77% yield, *c.f.* **Scheme 3.1**) was observed whilst maintaining the high levels of selectivity (96:4). (N.B. the exploration of the active species described in Chapter 3 was carried out simultaneously with the optimisation of the magnesium bisamide base in Chapter 2, and therefore the reaction conditions were adapted accordingly)

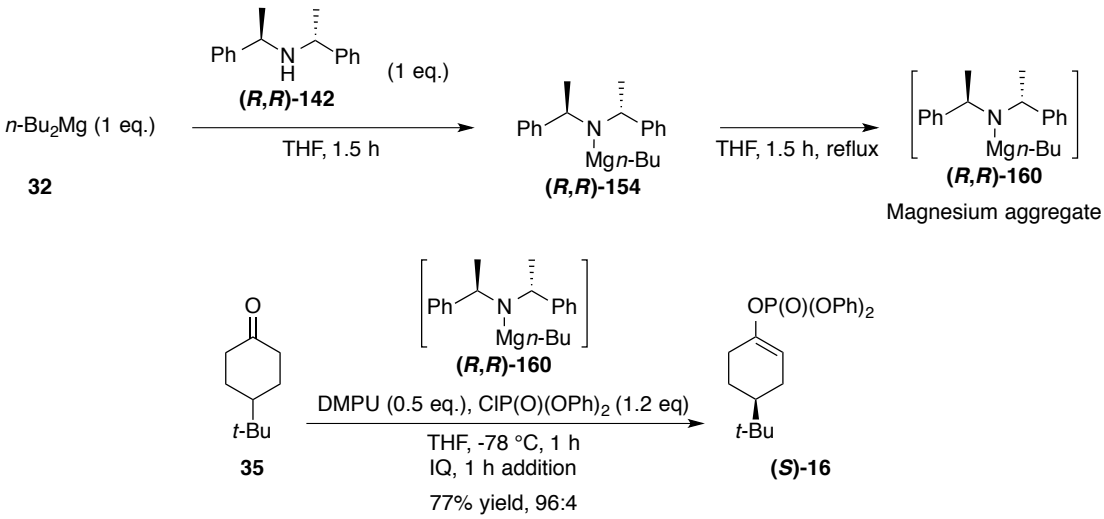

Scheme 3. 14

Although this first result on its own did not validate the aggregation state theory, it does not disapprove it. Indeed, this base afforded a higher level of conversion than the alkylmagnesium amide base **(*R*,*R*)-154** alone (*cf.* **Scheme 3.10**) and suggests that the reflux conditions provided a more reactive base. With this hypothesis in mind, we proposed that further improvement of the reactivity required the full conversion of the alkylmagnesium amide **(*R*,*R*)-154** to the more reactive aggregate species **(*R*,*R*)-160**. We first envisaged that a prolonged reflux time of 3 h might favour the overall transformation, but as observed in **Scheme 3.15** below, only a slight improvement was observed (79% yield, 96:4 e.r.).

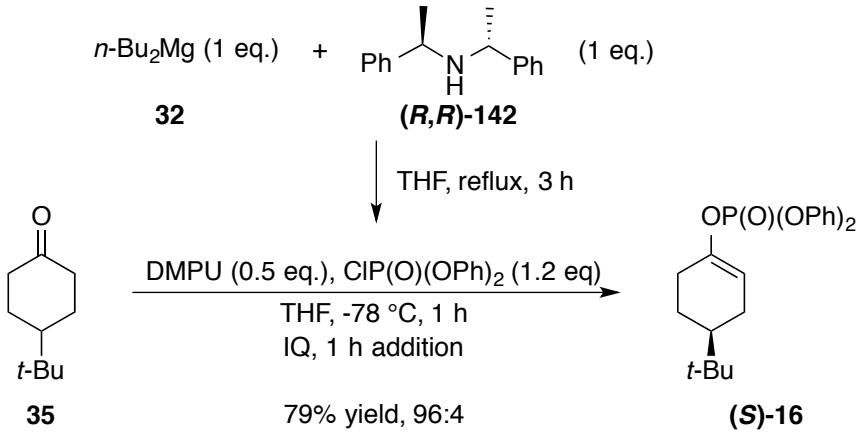

Scheme 3. 15

With the low improvement in yield, we envisaged that the kinetics of formation of the alkylmagnesium amide **(*R*,*R*)-154** might be important; therefore it was decided to carry out the reaction with an excess of *n*-Bu_2Mg, as this would increase the theoretical $k_{[alkylmagnesium\ amide]}$. As shown below (**Scheme 3.16**), by doubling the initial amount of *n*-Bu_2Mg to 2 eq. (N.B. we have previously shown that unreacted *n*-Bu_2Mg was a spectator in the reaction mixture) the reaction afforded an excellent 93% isolated yield towards the desired product **(*S*)-16** with an excellent selectivity of 96:4.

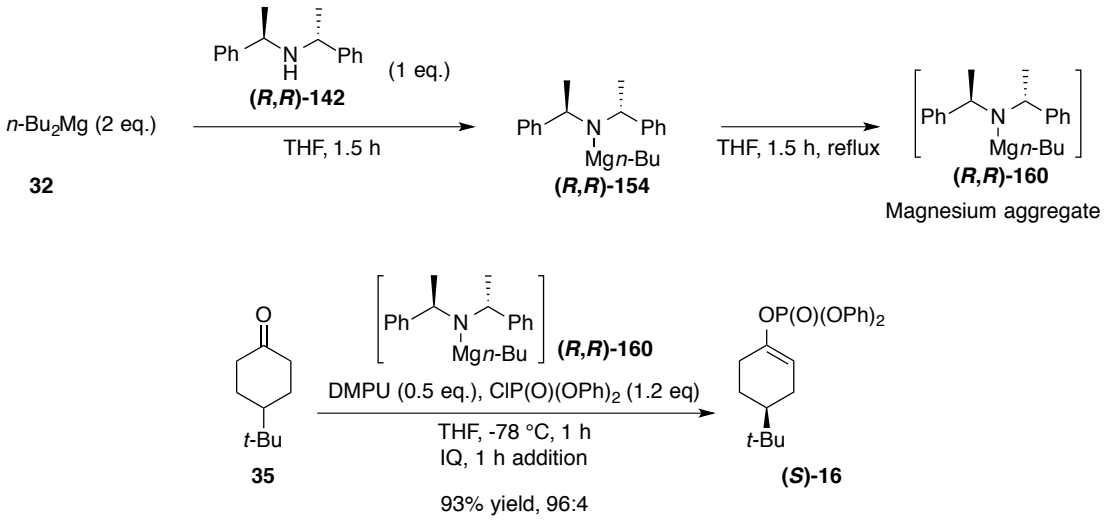

Scheme 3. 16

3.2. Improving the Reaction Conditions

Since, concurrently, the reaction conditions for the magnesium bisamide mediated formation of enol phosphates were now optimised (Chapter 2), it was therefore decided to compare those finding to this novel and efficient alkylmagnesium amide species, **(*R*,*R*)-160**. To this end, and as shown below in **Scheme 3.17**, the benchmark deprotonation reaction was carried out. In **Table 3.2**, **Entry 1** are represented the optimised conditions for the asymmetric deprotonation reaction at -78 °C, where the novel alkylmagnesium amide base **(*R*,*R*)-160** afforded an excellent 90% yield with a selectivity of 95:5, comparable with that observed in Chapter 2 (*c.f.* **Entry 1**, **Table 2.14**). Furthermore, under the optimised conditions at -20 °C, the novel base

performed at a good level, affording an 81% yield and 88:12 e.r. (**Entry 2**, **Table 3.2**). Although affording good results at higher temperatures, the reactivity observed was lower than that observed with the use of the magnesium bisamide base **(*R*,*R*)-125** (*c.f.* **Entry 2**, **Table 2.17**). This reaction showed the limitations of the current developed conditions and suggested that further investigations were required to optimise the base formation. Indeed, the presence of an excess of *n*-Bu_2Mg, although a spectator at -78 °C, could lead to side reactions at higher temperatures, as previous studies have shown that higher temperatures allow these species to be active by either allowing a kinetic deprotonation reaction or even an addition into the substrate carbonyl group.[9] Finally, to prove the concept of the new aggregate by comparison to a more simple alkylmagnesium amide, base **(*R*,*R*)-154** was employed under the optimised conditions at -78 °C. As shown in **Entry 3**, **Table 3.2**, the reaction afforded only a 34% yield, and a reduced selectivity of 84:16, suggesting that the species present under the conditions employed for the formation of **(*R*,*R*)-160** were different and highly reactive.

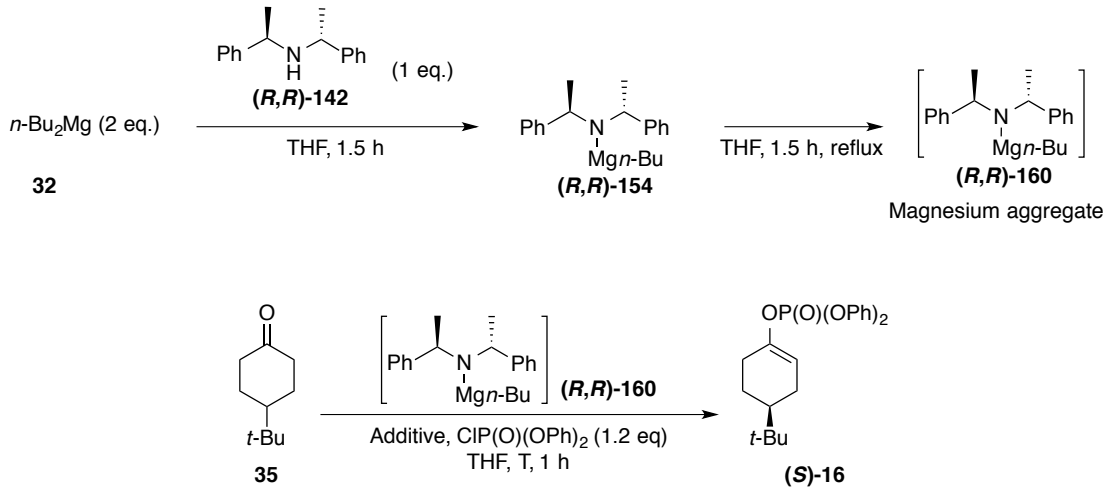

Scheme 3. 17

Entry	Temperature	Base formation	Quench	Additive	Yield %	e.r. (*S*):(*R*)
1	-78 °C	**(*R*,*R*)-160**	IQ	-	90	96:4
2	-20 °C	**(*R*,*R*)-160**	Co-addition	DMPU 0.5 eq.	81	88:12
3	-78 °C	**(*R*,*R*)-154**	IQ	-	34	84:16

Table 3. 2

3.2.1. Optimisation of the Base Formation

With promising results in hand, we first explored the importance of the time required at both room temperature and under reflux conditions for the base formation. To establish a trend in reactivity we first fixed the time for the room temperature base formation at 0.5 h, followed by increasing the time of the reflux temperature. As shown below in **Table 3.3**, under the conditions depicted in **Scheme 3.18**, increasing the reflux time, from 30 min (**Entry 1**) to 1 h (**Entry 2**), and finally to 1.5 h (**Entry 3**), resulted in a slight increase in the overall yield from 87% to 93%, with consistent levels of selectivity. Finally, when the room temperature reaction time was increased to 1.5 h followed by 1 h of reflux ($t_1 > t_2$), a lower 87% yield was observed (**Entry 4**).

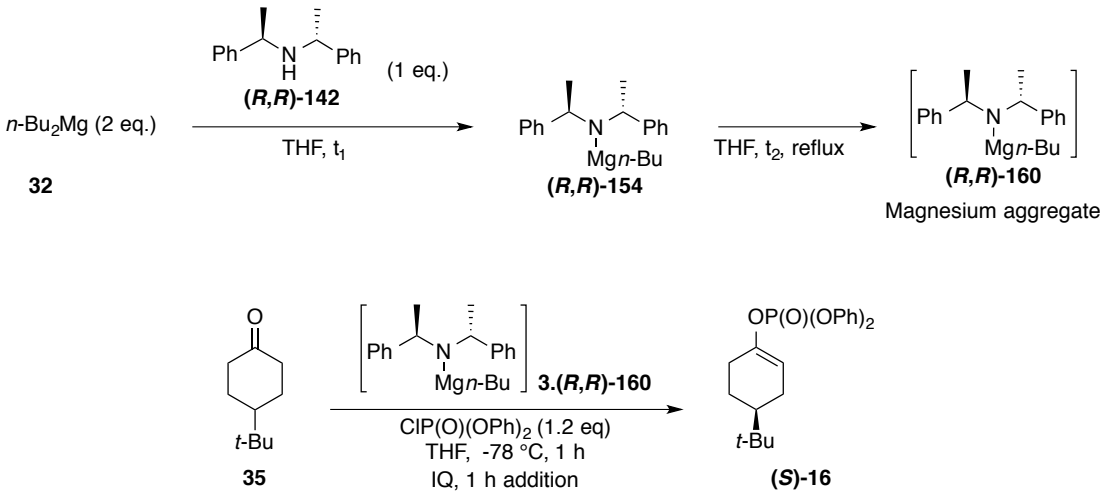

Scheme 3. 18

Entry	rt (t_1)	reflux (t_2)	Yield %	e.r. (*S*):(*R*)
1	0.5 h	0.5 h	87	95:5
2	0.5 h	1 h	90	95:5
3	0.5 h	1.5 h	93	95:5
4	1.5 h	1 h	86	95:5

Table 3. 3

The conditions obtained in **Entry 3**, **Table 3.3** were therefore defined as the optimised conditions for the formation of the base **(*R*,*R*)-160**.

With these results in hand, we next turned our attention to the charge of *n*-Bu_2Mg, as this would impact on the reactivity, especially at higher temperatures. As shown below in **Scheme 3.19**, the optimised conditions for the base formation were employed for 1 equivalent (**Entry 1**, **Table 3.4**) and 1.1 equivalents (**Entry 2**, **Table 3.4**) of *n*-Bu_2Mg. Interestingly, under stoichiometric conditions, a slightly improved 81% yield was observed and using only a slight excess of the base, a high 90% yield was obtained, with in both cases a selectivity of 95:5. Interestingly, increasing the *n*-Bu_2Mg equivalents to 1.2 provided similar results, allowing an 89% isolated yield with an e.r. of 95:5 (**Entry 3**, **Table 3.4**).

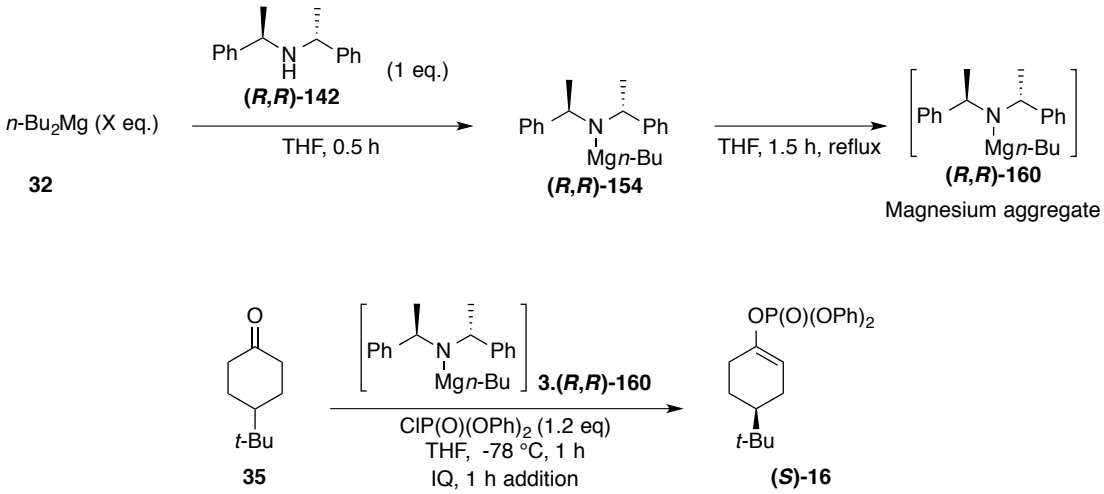

Scheme 3. 19

Entry	*n*-Bu_2Mg (eq.)	Yield %	e.r. (*S*):(*R*)
1	1	81%	95:5
2*	1.1	90%	95:5
3	1.2	89%	95:5

Table 3. 4

*repeated result

With the optimised conditions defined for the base formation, this base was employed for the optimised conditions at -20 °C, as described in Chapter 2 (**Entry 2**, **Table 2.17**). As shown below in **Scheme 3.20**, the reaction allowed a high 95% yield with a selectivity of 88:12 towards compound **(*S*)-16**. This result was consistent with that observed when the magnesium bisamide base was used in the reaction process.

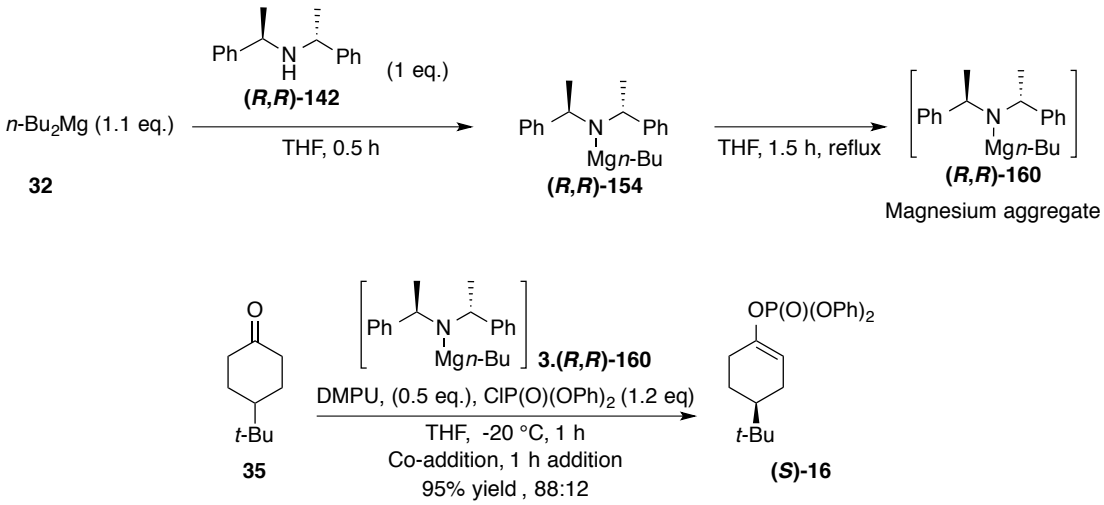

Scheme 3. 20

3.2.2. Optimised Conditions

Since the initial, unexpected result described in **Scheme 3.1**, which resulted in a good reactivity and selectivity with only one equivalent of the chiral amine, this reaction has been studied thoroughly, resulting, finally, in the hypothesis of a novel magnesium aggregate **(*R*,*R*)-160**, formed under reflux in THF (**Scheme 3.21**). In fact, this species was easily formed, with only a slight excess of the *n*-Bu_2Mg, and moreover performed to the same levels of reactivity and selectivity as those obtained with the chiral magnesium bisamide base over the benchmark asymmetric deprotonation reaction. The optimised conditions for both -78 °C and -20 °C are showed below in **Scheme 3.22**.

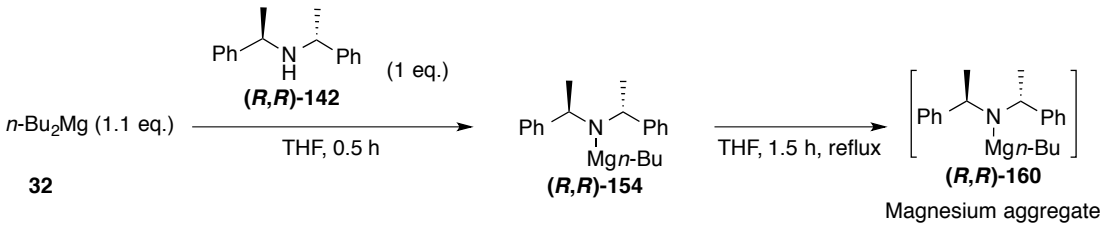

Scheme 3. 21

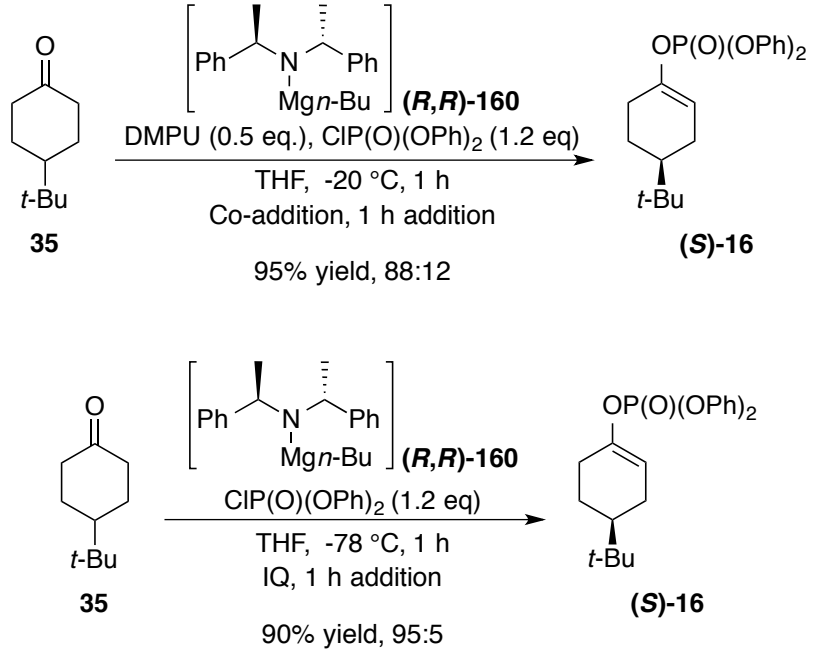

Scheme 3. 22

Having successfully achieved a positive outcome with this base, we were interested in further exploring the reaction mechanism to define the state of the novel aggregate. In fact, with most of the work carried out previously within the group on the use of alkylmagnesium amides and Hauser bases, good levels of reactivity and selectivity were obtained at -78 °C, and, more importantly, required the use of crown ethers as additives. Furthermore, the same levels of reactivity and selectivity had never been observed at more accessible temperatures, such as -20 °C. In the above case, we have not only developed a simpler base, but one which allowed reproducible results at higher temperatures, making these bases directly comparable to lithium amide bases.

3.3. Exploration of the Aggregate Species

Intrigued by the high reactivity displayed by the new aggregate, we studied the generation of such species under various conditions and compared the reactivities and selectivities observed to the standard reaction conditions described in **Scheme 3.22**.

3.3.1. Using Carbon Centred Bases as Initial Species

Among the first experiments was carried out was the use of our later developed carbon centred bases, Mes_2Mg and *t*-Bu_2Mg in forming the alkylmagnesium amide. Following the base formation described in **Scheme 3.21**, the asymmetric deprotonation reaction was carried out, using both bases, **41** and **42**, to form the aggregate base, which was then employed an asymmetric deprotonation reaction (**Scheme 3.23**). We were intrigued to discover that, when base **41 (**Mes_2Mg) was used, a low 9% of the desired enol phosphate **(*S*)-16** was obtained, with a poor selectivity of 67:33 (**Entry 1**, **Table 3.5**). Even more surprisingly, the use of *t*-Bu_2Mg (**42**) under the same conditions did not afford any transformation at all (**Entry 2**, **Table 3.5**), with the starting material recovered in both cases.

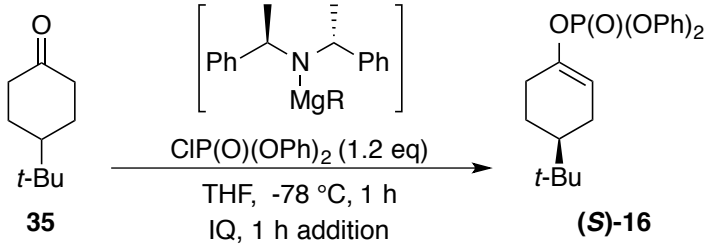

Scheme 3. 23

Entry	R	Yield %	e.r. (*S*):(*R*)
1	Mes (**3.(*R*,*R*)-161**)	9	67:33
2	*t*-Bu (**3.(*R*,*R*)-162**)	-	

Table 3. 5

Both results were surprising, due to the very low, or completely absent, levels of reactivity. From these results, we can conclude that the size and nature of the carbon-based unit on the magnesium species might have an impact on the reactivity.

3.3.2. Exploring Hauser Base Chemistry

We therefore turned our attention towards Hauser bases, in order to verify if similar reactivities (and, by extension, aggregates) could occur. Firstly, we investigated the use of *n*-BuMgCl as the Grignard reagent component in the reaction mixture to directly compare the results to our developed system. As shown below in **Scheme 3.24**, the Grignard reagent was subjected to base formation as described in **Scheme 3.21**. Under such conditions, the reaction afforded a moderate 58% yield, with a high selectivity of 95:5 (**Entry 1**, **Table 3.6**). On the other hand, when the Hauser base was formed under classical conditions (at room temperature), only a low 26% yield, with a slightly lowered 93:7 selectivity, was obtained (**Entry 2**, **Table 3.6**). Overall, the reactivity was lowered but the selectivity mostly remained, and more importantly the reflux conditions did increase the reactivity and selectivity of the overall reaction, when compared to the classical room temperature Hauser base formation. To increase the reactivity of the Hauser base, we attempted a reaction where the Grignard reagent loading was increased to 1.5 equivalents. Under such conditions (**Entry 3**, **Table 3.6**), only a slight increase of the reactivity to 67% was observed along with a slight loss in selectivity (92:8). Further attempts at increasing the reaction time did not result in any change in reactivity. In order to compare a range of Grignard reagents, the bulkier *t*-BuMgCl was also utilised under the standard conditions. Interestingly, when base **(*R*,*R*)-163** was formed by this route, no reactivity was observed (**Entry 4**, **Table 3.6**), but under room temperature Hauser conditions, a low level of reactivity (8%) was observed (**Entry 5**, **Table 3.6**). Unfortunately, the purity and amount of product obtained meant we were unable to define the enantioselectivity. We continued our studies with the use of a smaller Grignard reagent, methylmagnesium chloride. When base **(*R*,*R*)-163** was formed with MeMgCl, a moderate 71% yield was observed (**Entry 6**, **Table 3.6**), whereas under room temperature Hauser conditions, base **(*R*,*R*)-157** only provided a 42% yield (**Entry 7**, **Table 3.6**), with, in both cases, the selectivity being at its highest

(95:5). It should be noted that under the conditions shown in **Entry 7**, a higher amount of addition product (addition into the ketone and addition into the electrophile) was detected. Since the two methods of Hauser base formation led to different reactivities, it seems logical to conclude that differing aggregates are formed under these conditions.

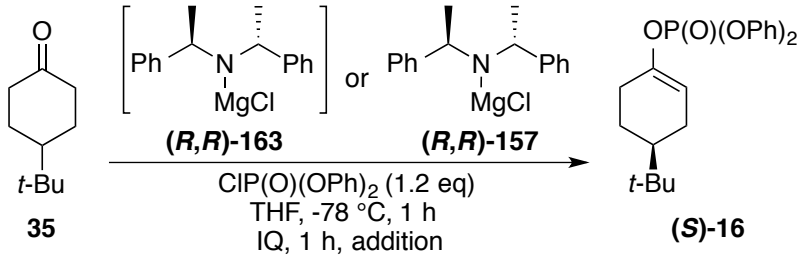

(*R*,*R*)-157 base formation: 2 h rt
(*R*,*R*)-163 base formation: 0.5 h rt, 1.5 h reflux

Scheme 3. 24

Entry	Grignard	Base	Yield %	e.r. (*S*:*R*)
1	*n*-BuMgCl	**(*R*,*R*)-163**	58	95:5
2	*n*-BuMgCl	**(*R*,*R*)-157**	26	93:7
3	*n*-BuMgCl (1.5 eq.)	**(*R*,*R*)-163**	67	92:8
4	*t*-BuMgCl	**(*R*,*R*)-163**	-	
5	*t*-BuMgCl	**(*R*,*R*)-157**	8	-
6	MeMgCl	**(*R*,*R*)-163**	71	95:5
7	MeMgCl	**(*R*,*R*)-157**	42	95:5

Table 3. 6

Furthermore, a novel hypothesis was also envisaged, which was that the size of the Grignard reagent species affected the amide formation. Although it has always been assumed that the formation of the amide was highly facile due the difference in pK_a between the alkyl unit (45-50 in DMSO) and the amide (36 in THF), simply observing the experimental results in **Table 3.6** suggests that such hypothesis is plausible, and the amide formation is not as straightforward as assumed.

3.3.3. Additive Effect

With all these interesting results in hand, and more generally intrigued by the high results obtained when the new base formation methodology was employed for the formation of Hauser bases, we wanted to further explore the influence on the reactivity of LiCl as an additive (**Scheme 3.25**). We were intrigued by LiCl in particular, as work done by Knochel has showed that the -*ate* species formed in solution with the corresponding organomagnesium species enhanced the overall reactivity.[14] As shown below, under the modified base formation methodology, the use of LiCl (1 eq.) allowed a high 72% yield, with a selectivity of 91:9 (**Entry 1**, **Table 3.7**). We also studied the reactivity with higher and lower loadings of LiCl, but this modification did not result in any overall trend, and consistently provided the same levels of reactivity and selectivity. On the other hand, the use of Hauser base conditions (*i.e.* **(*R*,*R*)-157**), with the presence of LiCl (1 eq.) only provided a 25% yield and a selectivity of 92:8, which was similar results to previous results without the salt additive. It should be noted that, in both cases, LiCl was present during the base formation and not only present for the asymmetric deprotonation reaction.

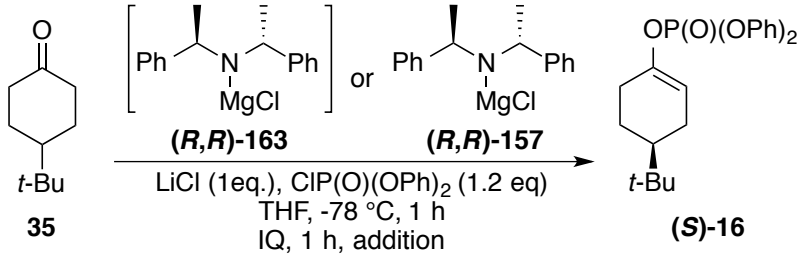

(*R*,*R*)-157 base formation: 2 h rt
(*R*,*R*)-163 base formation: 0.5 h rt, 1.5 h reflux

Scheme 3. 25

Entry	Base	Yield %	e.r. (*S*:*R*)
1	**(*R*,*R*)-163**	72	91:9
2	**(*R*,*R*)-157**	26	92:8

Table 3. 7

Interestingly, the addition of LiCl as additive had a positive impact on the reactivity and also increased the reactivity. Although, the reactivity obtained was lower than compared to the use of *n*-Bu_2Mg, the concept of aggregation or a more reactive species in the reaction mixture seems to be present with the chiral Hauser bases as well. To further explore the importance of additives with the formation of this highly reactive species, we have carried out a range of reactions employing both DMPU and LiCl as additives, with addition both before and after the base formation. Unfortunately, no general trend was observed and similar reactivities and selectivities were observed in all cases.

3.3.4. One Pot Procedure

During studies aimed at further the understanding of the reaction mechanism and searching for evidence of the aggregate, a placement in an industrial laboratory required several modifications to the developed experimental procedure. In particular, the first step of the standard process, the removal of heptane from the commercial solution of *n*-Bu_2Mg, before dissolution in THF, required modification. Furthermore, experimental work has shown that the presence of heptane during the base formation provided lower reactivities when magnesium bisamide was used. We therefore envisaged a one-pot formation of the base from the commercial Grignard reagent. As the corresponding Hauser base did not allow the same levels of reactivity, the methodology developed for the formation of carbon-centred bases was used, which consisted in the addition of 1,4-dioxane to disproportionate the Grignard reagent to the dialkylmagnesium *via* the Schlenk equilibrium. The *in situ* generated *n*-Bu_2Mg was then subjected to the novel base formation (**Scheme 3.21**), in order to perform the asymmetric deprotonation reaction. As shown below in **Scheme 3.26**, we were pleased to discover that the reaction afforded high levels of reactivity and selectivity with the use of this one-pot methodology. Moreover, the use of a sealed microwave vial made the reaction process facile and, more importantly, did not require the use of Schlenk conditions or other rigorous air-sensitive techniques.

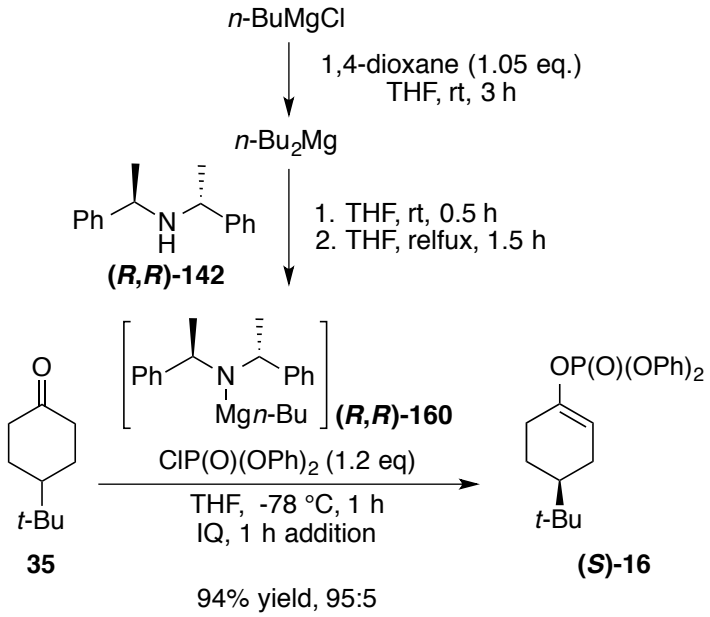

Scheme 3. 26

With a range of experimental results in hand, we have clearly identified that the reflux in THF afforded a more reactive base, and, more importantly, the species created had a direct correlation with the size of the Grignard reagent employed in the alkylmagnesium amide formation. So far, our main hypothesis is based on the formation of a novel thermodynamic magnesium aggregate in solution. In order to define such a novel, active species, further analytical studies were required.

3.3.5. Comparison with Lithium Amides

Thus far, we have described our studies to further develop a novel and highly efficient asymmetric deprotonation reaction using chiral magnesium amide bases. The chiral lithium amide bases described by Simpkins or Koga[15] have always been the benchmark for such transformations. We were therefore interested to compare our new system with lithium amide bases for the synthesis of enantioenriched enol phosphates.

Having stated this, unfortunately there exists no literature study on this transformation, using chiral lithium amides. Therefore, we briefly studied the reactivity of the chiral lithium bases in the preparation of enol phosphates by employing the conditions described by Simpkins[15a,16] for the formation of silyl enol

ethers, while using diphenylphosphoryl chloride as electrophile. As shown below, under the conditions described in **Scheme 3.27**, when the reaction was carried out using the external quench methodology, a moderate 52% yield, and a selectivity of 92:8, was observed (**Entry 1**, **Table 3.8**). On the other hand, at the higher temperature of -20 °C, although affording an improved 73% yield, only a selectivity of 83:17 was recorded. It should also be noted that these results represent the best results observed with the use of the lithium amide base. This transformation has also been studied using the internal quench methodology, but only trace amounts of the desired product were obtained.

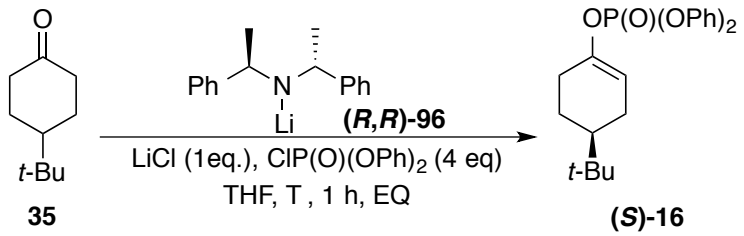

Scheme 3. 27

Entry	T °C	Yield %	e.r. (*S*):(*R*)
1	-78	52	92:8
2	-20	73	83:17

Table 3. 8

Thus, we were pleased to note that the best results for this transformation were obtained with the use of chiral magnesium amide bases, in terms of both reactivity and selectivity at both low and mild temperatures (*c.f.* **Scheme 3.26**). Furthermore, with the development of the novel magnesium amide base **(*R*,*R*)-160**, every aspect of the lithium amide base methodology has been improved upon. However, it should still be noted that the magnesium amide bases require twice the amount of the chiral reagent than do the corresponding lithium bases, and this represents one slight disadvantage over the existing lithium-based methodology.

3.4. Spectroscopic Studies

With the hypothesis of a novel aggregate formation in mind, we have optimised the reaction conditions in order to deliver high levels of reactivity and selectivity. However, in order to understand what species are present in solution, spectroscopic analysis would be required. Having observed a slight change in colour of the solution after base formation, we first investigated the use of UV-Vis spectroscopy to quantify the formation of the active species. Although an extremely small shift in the absorbance was observed, the resolution of the signal did not allow further quantification of the novel species. We therefore turned our attention to NMR spectroscopy for further studies.

3.4.1. DOSY NMR Experiments

We envisaged that the use of modern techniques, such as ^{1}H DOSY, would provide information on the different species present in solution and, more importantly, would allow us to find an approximate mass of the unknown aggregate formed, and, by extension, allow us to propose a structure.[26–28] With this in mind, we first examined the ^{1}H NMR spectrum of the magnesium bisamide base in d_8-THF. As shown below in **Figure 3.4**, a range of remarkable peaks were observed, such as the protons at -0.4 ppm, probably corresponding to protons attached to a carbon bonded to magnesium, doublets for the 3H corresponding to the CH_3 unit on C_2 at 1.3 ppm, a complex aromatic region containing 10H, and, more importantly, the presence of two or more species around 3.5 ppm, corresponding to the CH protons at C_1, *i.e.* α- to N. Since we were unable to determine the number of species present in solution, we elected to concentrate on the well-defined signals of the ^{1}H protons on C_1 for preliminary study.

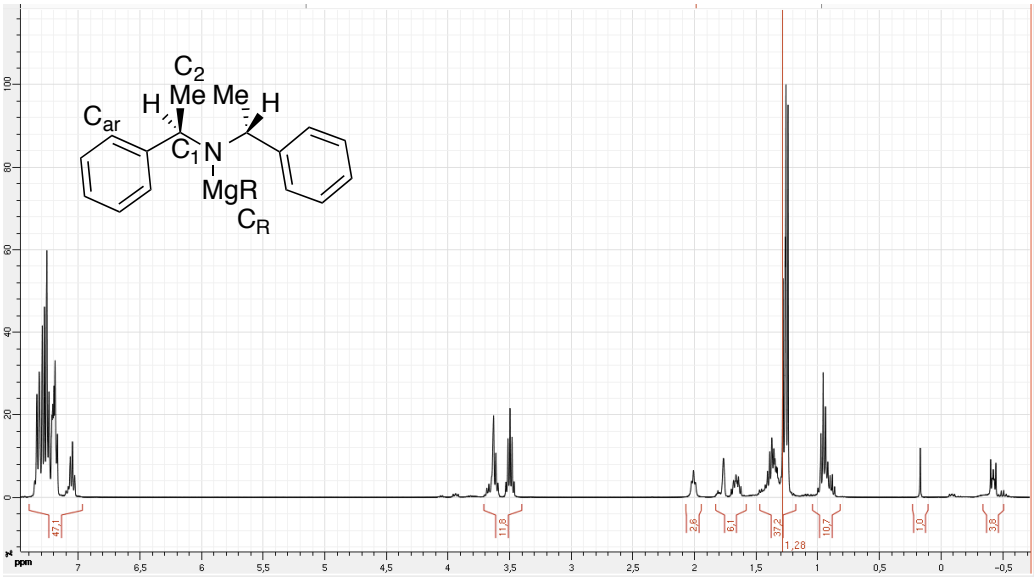

Figure 3. 4

Presented below are a range of NMR experiments in d_8-THF where only the protons on C1 are shown (**Figure 3.5**). We were at first interested in defining a number of known species, in order to compare them to the mixture obtained when the new conditions were employed (**Scheme 3.21**). While examining the free amine **(*R*,*R*)-142**, the expected quartet signal at 3.45 ppm was detected. Under the classical alkyl magnesium amide synthesis conditions (**(*R*,*R*)-154**),[9] the quartet changed to a more complex multiplet. We further continued our investigation by employing the procedure for the synthesis of **(*R*,*R*)-160** and as shown below, we observed the emergence of a new signal at 3.59 ppm. Unfortunately, being close to residual THF, the analysis and quantification of this signal was problematic; nevertheless, the newly formed signal appeared to have a greater intensity that the preceding multiplet at 3.4 ppm. Such a modification suggested us that this peak corresponded to the novel magnesium aggregate. We then examined the ^{1}H NMR spectrum of the magnesium bisamide base **(*R*,*R*)-125**, and, upon comparison of the ^{1}H signals with the previous results, we were surprised by the profile observed. In fact, the range of major signals detected were similar to the one obtained for the formation of base **(*R*,*R*)-154**. Confused by the current observation, we questioned the formation of the

bisamide base itself and in order to verify the current trend we have sought reference from the primary synthesis of the magnesium bisamide base (on an achiral magnesium bisamide species) as reported by Mulvey *et al*.[29] Under their conditions, the magnesium bisamide was primarily generated by refluxing hexanes of 2 eq. of the amine with *n*-Bu_2Mg. We therefore followed this procedure by refluxing **(*R*,*R*)-142** with *n*-Bu_2Mg, and, upon removal of the solvent and analysis in d_8-THF, we were surprised to see the appearance of a quartet at 3.83 ppm. Although the full spectrum is not presented herein, it should be noted that a new, significantly deshielded doublet corresponding to the 3H of the methyl group of C_2 was also observed.

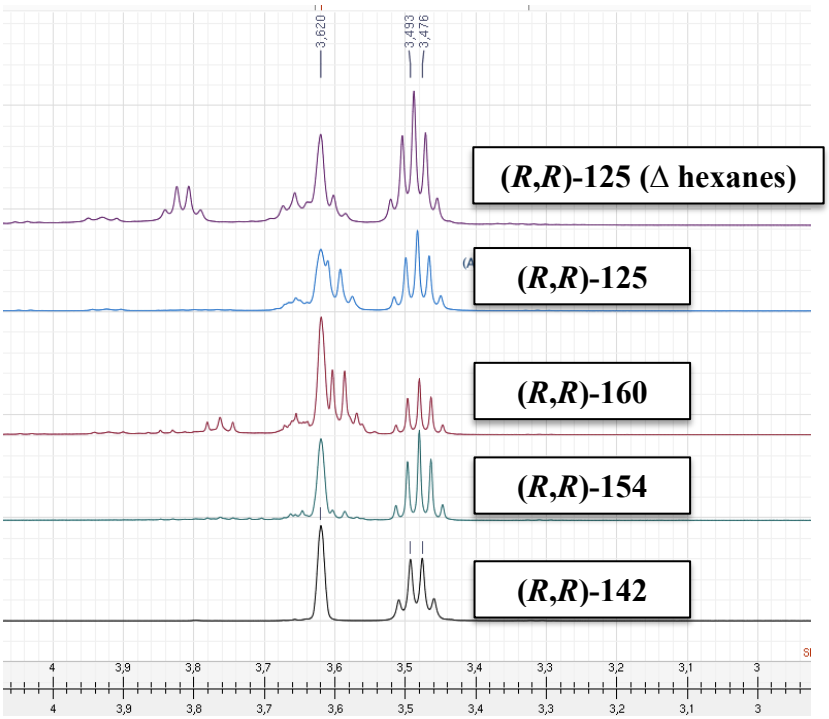

Figure 3. 5

Intrigued by the observed results, we consulted Dr J. Parkinson, the NMR spectroscopist in the Department of Pure and Applied Chemistry. With his help, we were first able to address the multiplicity of the signal presented at 3.45 ppm. The first observation made was that the signal showed no coupling with any of the methyl protons appearing at 1.25 ppm (see **Figure 3.6**). Furthermore, the signal was actively correlated to a signal at 1.97 ppm. We proposed that the signal at 1.97 ppm

corresponded to the NH proton in d_8-THF, and to verify this, a ^{1}H - ^{13}C HSQC - TOCSY experiment was carried out, which removed the signal. In fact, the magnetisation transfer only allows recovery of the signals of protons attached to a carbon (^{13}C), and any proton signal attached to a heteroatom is lost. This was indeed the case with the proton signal at 1.97 ppm, suggesting that this signal corresponded to an NH proton. Furthermore, this experiment defined the multiplicity observed in the signal at 3.45 ppm as a quintet, where the 2 CH protons coupled with the 6 CH_3 protons and the NH proton. Such a change in signal between the quartet observed in **Figure 3.5** for **(*R*,*R*)-142** and the quintet observed after addition of the *n*-Bu_2Mg was explained by the total absence of water. Although all the ^{1}H NMR analysis were carried out under anhydrous conditions, trace levels of water present would be sufficient to make the NH signal exchangeable, therefore explaining the observed quartet.

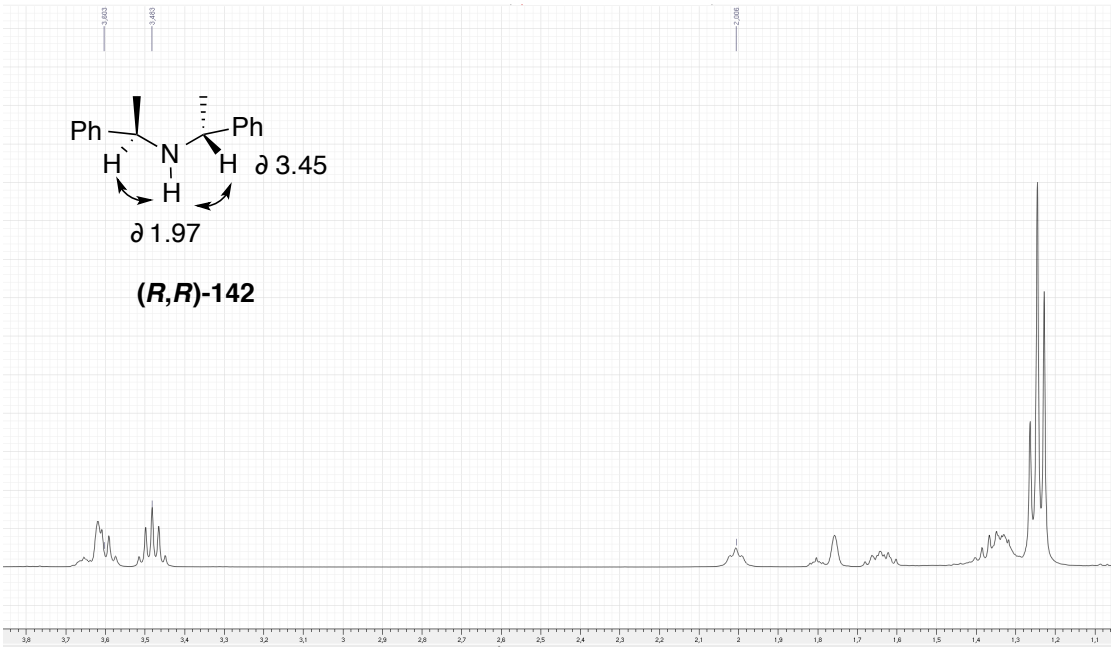

Figure 3. 6

We then turned our attention to the novel signal formed at 3.59 ppm, when conditions for the formation of **3.(*R*,*R*)-10** and **(*R*,*R*)-125** were employed. An in-

depth nOe experiment revealed that this quartet was the result of an alkylmagnesium amide species. In fact, the multiplicity observed was due to the coupling of the 2 CH protons with the 6 protons of the methyl group at C_2, and hydride protons detected at -0.49 ppm on the alkyl fragment C_R (**Figure 3.7**). It was proposed that these species were less likely to be in an aggregated state, but further evidence was necessary in order to be more certain of this claim.

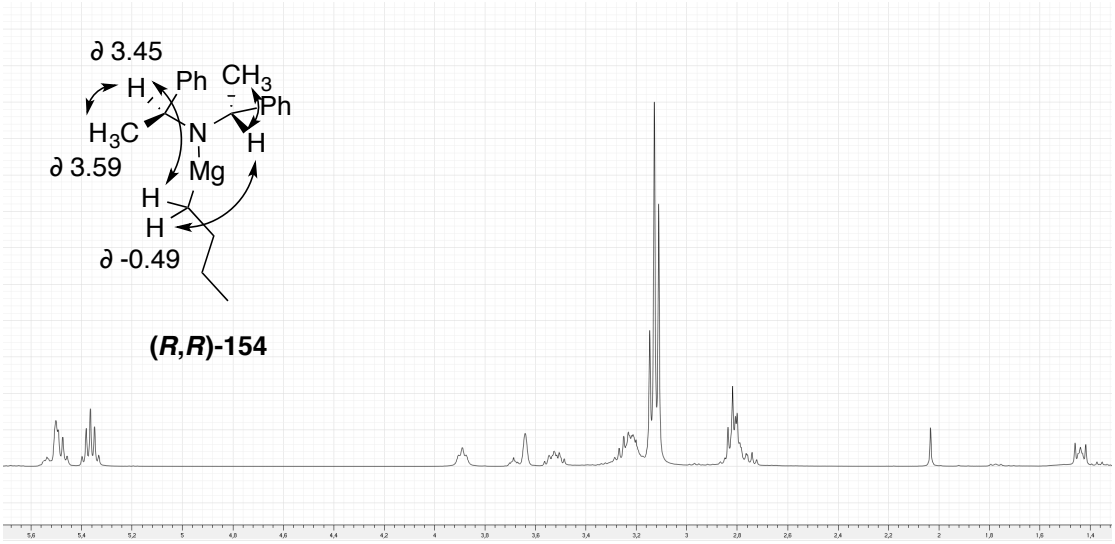

Figure 3. 7

Following these findings, we were extremely surprised by this first series of analytical results. In fact, thorough ^{1}H NMR spectroscopic analysis suggested that when the *C*$_2$-symmetric chiral amine **(*R*,*R*)-142**, was stirred at room temperature with *n*-Bu_2Mg in THF, the alkylmagnesium amide **(*R*,*R*)-154** was not formed, but, instead, only free amine was present in the reaction mixture. Furthermore under reflux conditions in THF, using either one equivalent of the chiral amine **(*R*,*R*)-142** (intending formation of base **(*R*,*R*)-160**), or two equivalents of the chiral amine **(*R*,*R*)-142** (intending formation of base **(*R*,*R*)-125**) in both cases only resulted in the generation of the alkylmagnesium amide **(*R*,*R*)-154**. The experimental evidence agrees with this observation to a certain degree, as the optimised conditions defined

for the synthesis of enantioenriched bases using base **(*R*,*R*)-125** was directly used with base **(*R*,*R*)-160** providing similar results. In order to obtain more evidence, we initiated ^{1}H DOSY NMR studies.[17] This experiment produces a 2D NMR spectrum where the ^{1}H proton NMR spectrum is correlated with the diffusion of the different species present in solution. With the diffusion of compounds being mass dependant, we were able to establish the mass of the observed species through their diffusion value. To be able to reference the relative diffusion rates, we established a correlation curve in d_8-THF with compounds of known molecular weight.[19] It has to be noted that the diffusion parameter was calculated by the intensity (integration) of each signal and therefore the average diffusion rate of one established species allowed us to predict the mass of the species in solution.

3.4.2. Defining the Active Species

As Shown below in **Figure 3.8**, the correlation curve, with a R^2 of 0.985, allowed a good approximation of the results. Among the different values presented are the blue spots corresponding to the 5 known compounds which were used to generate the correlation curve. The 3 red spots under compounds A, B and C correspond to the three different signals that were observed from the ^{1}H NMR spectroscopy studies. To relay this to the signals depicted in **Figure 3.5**, compound A corresponds to the signal at 3.45 ppm, compound B corresponds to the signal at 3.59 ppm and, finally, compound C corresponds to the new signal at 3.83 ppm (**(*R*,*R*)-125** formation in hexanes). To these experimental diffusion rates we have inferred the mass of the corresponding species A, B and C through the graph, and suggested structures (represented as green triangle) of compounds bearing this mass.

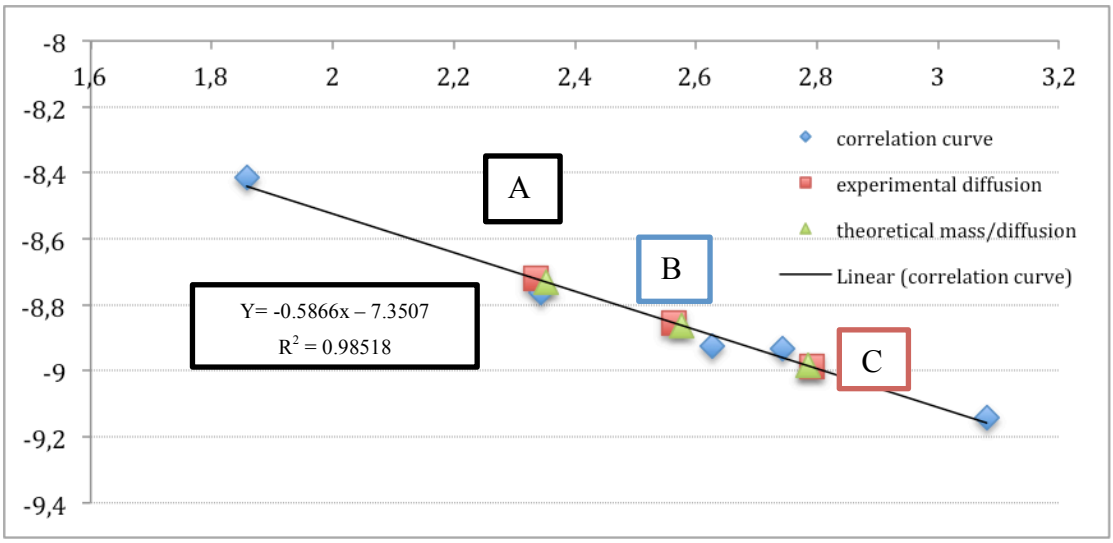

Figure 3. 8

Depicted in **Figure 3.9** below are the structures of the compounds A, B and C, as suggested by the DOSY experiment. As predicted by the ^{1}H NMR spectroscopic experiment carried out earlier, the signal at 3.45 ppm correlates with the mass of the free amine **(*R*,*R*)-142**. Furthermore, compound B, responsible for the signal at 3.59 ppm, corresponds to the mass of an alkylmagnesium amide base with two molecules of THF co-ordinated (**(*R*,*R*)-154.2THF**). Finally, we were intrigued by the novel signal that appeared when the magnesium bisamide was formed under reflux conditions in hexanes. The mass of this compound corresponds to the dimer of the magnesium bisamide species **(*R*,*R*)-164**. Interestingly, Mulvey *et al*. described this type of structure (magnesium bisamide dimer) in their initial work.

Compound A **Compound B** **Compound C**

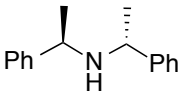

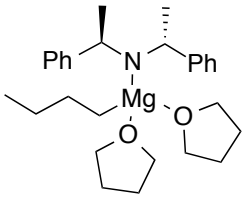

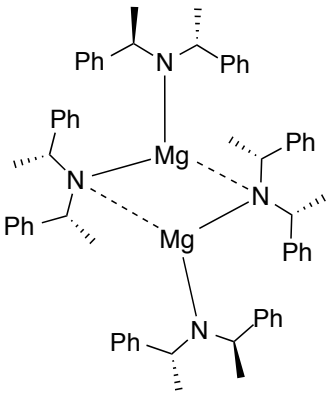

(*R*,*R*)-142 **(*R*,*R*)-154.2THF** **(*R*,*R*)-164**

Scheme 3. 28

These NMR experiments revealed some ground-breaking results, as they clearly showed the formation of several base species, which would be unexpected in an assumed quantitative reaction. In fact, in the present case, the preparation of alkylmagnesium amide **(*R*,*R*)-154** required harsher reflux conditions in THF. Furthermore, the desired bisamide base was only formed in hexanes and not in THF. In order to have enhanced insight into our previous work, we also carried out the DOSY experiment on the first chiral amine used in this work, **(*R*)-33**.

As depicted below in **Figure 3.10**, when the simple chiral amine was refluxed in hexane or in THF, a more deshielded set of signals were observed. For example, the multiplet at 3.9 ppm (corresponding to the CH signals) or the doublet at 1.32 ppm (corresponding to CH_3 signals) were similar in both cases and were not present in high levels when the amine was stirred at room temperature. Unfortunately, the DOSY experiment predicted a mass of compound close to a MW 440 g/mol, which does not correspond to the dimer of the bisamide base. This could either correspond to the alkylmagnesium amide with two molecules of THF complexed (**(*R*)-34**.**2THF**), having a MW of 436 g/mol, or the magnesium bisamide monomer (**(*R*,*R*)-119**) with MW 444 g/mol (**Figure 3.11**).

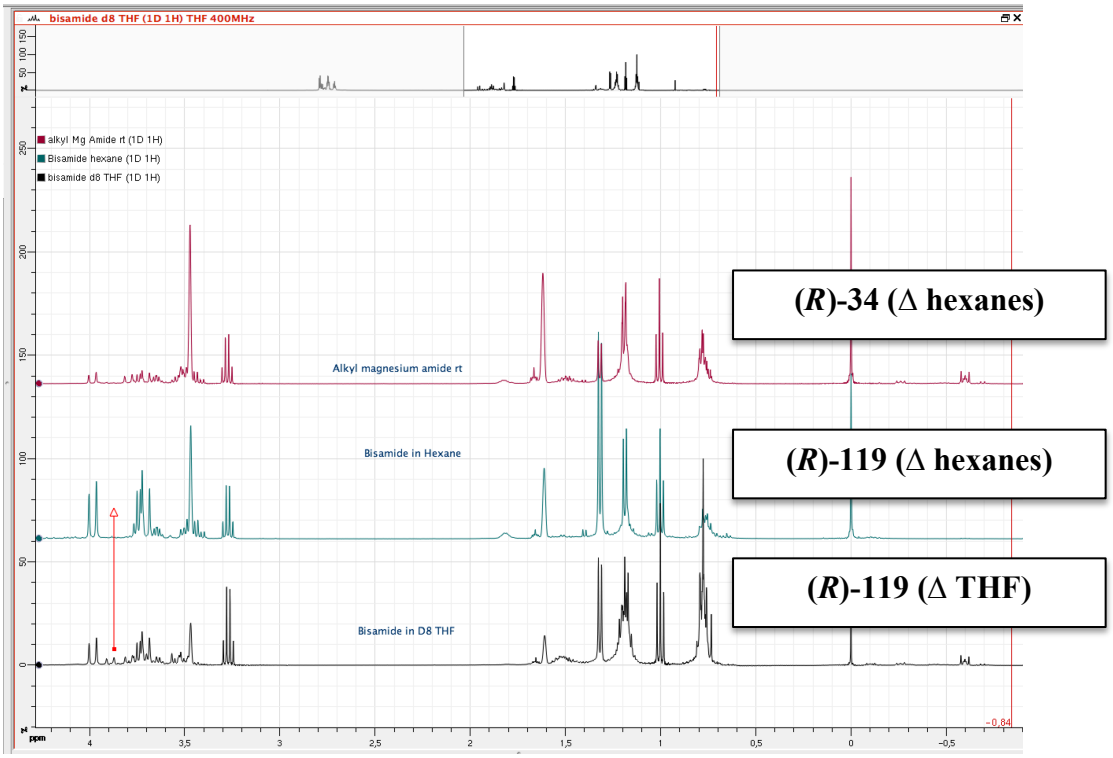

Figure 3. 9

By comparing these results, we suggest that the compound formed was the magnesium bisamide base **(*R*,*R*)-119**, as the chemical shifts of both the CH signal (3.9 ppm) and CH_3 (1.32 ppm) are close to those observed for the bisamide base **(*R*,*R*)-164** with the CH protons appearing at 3.83 ppm and the CH_3 signals appearing at 1.45 ppm. These well defined and deshielded signals suggest that with the base derived from chiral amine **(*R*)-33**, the magnesium bisamide base was indeed formed.

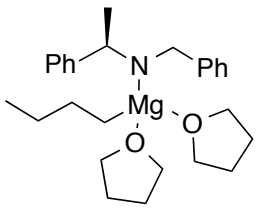

(*R*,*R*)-34.2THF

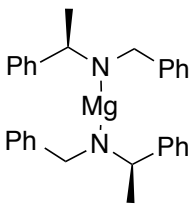

(*R*,*R*)-119

Figure 3. 10

Reassured by the present findings, we were intrigued by the unique trend displayed by the use of the C_2-symmetric amine in the formation of the magnesium bisamide base. Earlier, while exploring the Hauser bases, we proposed a hypothesis suggesting

that the size of the Grignard reagent used to form Hauser base had a considerable impact on the reactivity in the asymmetric deprotonation reaction. This proposal can also be translated to the formation of the bisamide base in a highly coordinating solvent such as THF, where steric hindrance of the co-ordinated solvent might increase the energetic barrier to formation of the bisamide base. With the present statement in mind, we were interest in studying the synthesis and quantification of the magnesium amide bases.

3.5. Future work

As described above, this range of studies led to the revelation that the alkylmagnesium amide base was responsible for the asymmetric deprotonation reaction. More precisely, when C_2-symmetric amines were used, access to the bisamide base was difficult, thus leading us to question the efficacy of the base formation. In fact, our previous work on the structure-reactivity relationship of C_2- and *pseudo* C_2-symmetric bases[13] led us to choose a range of chiral amines of interest which presented the best ratio of yield/selectivity, but in these cases, the base formation was assumed and not quantified. If the hypothesis that the formation of the magnesium amide base is influenced by its size, then the reactivity observed for the silyl enol ether formation ought to be revisited.

In fact, the quantification of amide base formation was difficult, as only spectroscopic methods permitted the observation of such species. Moreover, as observed with the experiments carried out above, although providing a simpler spectrum, C_2-symmetric amide base signals were overlapping with various other proton signals, rendering the quantification inaccurate. One solution would be the use of a novel methodology: ^{1}H Pure Shift DOSY.[19] The Pure Shift methodology has the advantage of simplifying the spectrum observed by presenting simple peaks instead of the coupling pattern of ^{1}H spectrum signals.[20] This would not only allow us to quantify the amount of amide formed for different amines, but also allow us to verify the base formation using different magnesium species. In fact we have observed in this Chapter 3 (and more generally in previous work) that the size of the

Grignard reagent (for generation of the Hauser base), or carbon-centred magnesium species (for generation of the alkyl magnesium amide) greatly influenced the outcome of the asymmetric deprotonation. Unfortunately, this result could be attributed to either the amide formation or the ability of the amide to process the deprotonation reaction. Quantifying the amide formation would clarify our concerns in this area and, moreover, allow us to revisit the catalytic cycle where the key step is the formation of a reactive magnesium amide species (alkylmagnesium amide or Hauser base).

4. Summary

Herein we have exploited the unexpected result observed while optimising the asymmetric deprotonation reaction with magnesium bisamide bases. We realised that the use of only one equivalent of the chiral amine afforded good levels of reactivity and selectivity in the enol phosphate formation. Base on previous knowledge built on the use of chiral magnesium amide species, we speculated on the formation of a novel magnesium aggregate species, and optimised the base formation. This base allowed us to access the same levels of reactivity and selectivity to those observed when the magnesium bisamide base was used to perform the similar reaction. Finally, upon NMR spectroscopic analysis, we have revealed that the magnesium species responsible for this high activity was a simple alkylmagnesium amide base, and, moreover, the magnesium bisamide base was not formed under reflux conditions in THF. Further studies have shown that on the other hand, the simple *pseudo*-C_2-symmetric amine primarily allowed the ready formation of the bisamide base in THF. This result, coupled with the range of work on Hauser bases, suggests that the bulk of the magnesium species and the amine both influence the reactivity.

5. Experimental

5.1. General

All reagents were obtained from commercial suppliers (Aldrich, Lancaster, Alfa-aesar or Acros) and used without further purification, unless otherwise stated. Purification was carried out according to standard laboratory methods.[21]

- Dichloromethane, diethyl ether, hexane and toluene were obtained from an Innovative Technology, Pure Solv, SPS-400-5 solvent purification system.
- Tetrahydrofuran and d_8-tetrahydrofurane were dried by heating to reflux over sodium wire, using benzophenone ketyl as an Indicator, then distilled under nitrogen.
- DMPU and diphenylphosphoryl chloride were distilled from CaH_2 under high vacuum and were stored over 4 Å molecular sieves under argon.
- Organometallic reagents were standardised using salicylaldehyde phenylhydrazone.[22]
- 4-*tert*-butylcyclohexanone, was purified by recrystallization from hexane and was dried by storing under vacuum (0.005 mbar) for 16 h.
- the amines (*R,R*)-bis(1-phenylethyl)amine and (*R*)-*N*-benzylphenylethanamine[8] were distilled over CaH_2 and distilled under vacuum.

Thin layer chromatography was carried out using CamLab silica plates, coated with fluorescent indicator UV_{254}, and analysed using a Mineralight UVGL-25 lamp.

Flash column chromatography was carried out using Prolabo silica gel (230-400 mesh).

IR spectra were recorded on a SHIMADZU IRAFFINITY-1 spectrophotometer.

^{1}H, ^{13}C and ^{31}P NMR spectra were recorded on a Bruker DPX 400 spectrometer at 400 MHz, 100 MHz, and 162 MHz, respectively. Chemical shifts are reported in ppm. Coupling constants are reported in Hz and refer to $^{3}J_{H\text{-}H}$ interactions unless otherwise specified.

5.2. General Procedures

General Procedure A: formation of alkylmagnesium amides

A solution of *n*-Bu_2Mg in heptane was transferred to a Schlenk flask, which had been flame-dried under vacuum (0.005 mbar) and allowed to cool under an atmosphere of argon, and the heptane was removed *in vacuo* (0.005 mbar) until a white solid was obtained. THF (10 mL) was then added, followed by the required amine, and the solution was stirred at room temperature for 1.5 h, assuming quantitative formation of the alkylmagnesium amide species. Data are presented as (a) amount of *n*-Bu_2Mg, (b) amine used, and (c) amount of amine.

General Procedure B: preparation of magnesium bisamides

A solution of *n*-Bu_2Mg in heptane was transferred to a Schlenk flask, which had been flame-dried under vacuum (0.005 mbar) and allowed to cool under an atmosphere of argon, and the heptane was removed *in vacuo* (0.005 mbar) until a white solid was obtained. THF (10 mL) was then added, followed by the required amine, and the solution was heated at reflux for 1.5 h, assuming quantitative formation of the magnesium bisamide. Data are presented as (a) amount of *n*-Bu_2Mg, (b) amine used, and (c) amount of amine.

General Procedure C: asymmetric deprotonation using Mg bases with IQ

A solution of the magnesium base in THF, prepared *via* a General Procedure, was cooled under nitrogen to the appropriate temperature. The Schlenk flask was then

charged with the required additives, followed by $P(O)(OPh)_2Cl$, and the reaction mixture was stirred for 10 min at the temperature stated. The desired ketone was then added as a solution in THF (2 mL) over 1 h using a syringe pump. The reaction mixture was stirred at the temperature stated for the required time before being quenched with a saturated solution of $NaHCO_3$ (10 mL) and allowed to warm to room temperature. The aqueous phase was extracted with Et_2O (50, 25, 25 mL) and the organic phases were combined and washed with 1M HCl (2 × 10 mL) to recover the amine. Removal of the solvent *in vacuo* gave an oil, which was purified by column chromatography on silica gel using 0-30% Et_2O in petroleum ether (40-60 °C) to give the desired product as a colourless oil. The enantiomeric ratio of the product was determined by analysis using chiral HPLC with a CHIRALCEL OD or OJ column.

General Procedure D: Preparation of alkylmagnesium amide bases (novel aggregation state theory)

A solution of *n*-Bu_2Mg in heptane was transferred to a Schlenk flask, which had been flame-dried under vacuum (0.005 mbar) and allowed to cool under an atmosphere of argon, and the heptane was removed *in vacuo* (0.005 mbar) until a white solid was obtained. THF (10 mL) was then added, followed by the required amine, and the solution was stirred at the time and temperature stated, and the base used for the asymmetric deprotonation reaction. Data are presented as (a) amount of *n*-Bu_2Mg, (b) amine used, (c) amount of amine (d) time and temperature of stage 1, and (e) time and temperature of stage 2.

General Procedure E: asymmetric deprotonation using Mg bases in a co-addition protocol

A solution of the magnesium base in THF, prepared *via* a General Procedure, was cooled under nitrogen to the appropriate temperature. The Schlenk flask was then charged with the required additives and the reaction mixture was stirred for 10 min at the temperature stated. The desired ketone and $P(O)(OPh)_2Cl$ were then added as a

solution in THF (2 mL) over 1 h using a syringe pump. The reaction mixture was stirred at the temperature stated for the required time before being quenched with a saturated solution of $NaHCO_3$ (10 mL) and allowed to warm to room temperature. The aqueous phase was extracted with Et_2O (50, 25, 25 mL) and the organic phases were combined and washed with 1M HCl (2 × 10 mL) to recover the amine. The removal of the solvent *in vacuo* gave an oil, which was purified by column chromatography on silica gel using 0-30% Et_2O in petroleum ether (40-60 °C) to give the desired product as a colourless oil. The enantiomeric ratio of the product was determined by analysis using chiral HPLC with a CHIRALCEL OD or OJ column.

General Procedure F: Formation of Hauser base

A solution of the requisite Grignard reagent in THF was transferred to a Schlenk flask, which had been (charged with LiCl if used then) flame-dried under vacuum (0.005 mbar) and allowed to cool under an atmosphere of argon. THF (9 mL) was then added, followed by the required amine, and the solution was stirred at room temperature for 1.5 h, assuming quantitative formation of the Hauser base. Data are presented as (a) Grignard reagent and quantity, (b) amine used, and (c) amount of amine.

General Procedure G: Formation of Hauser base (novel aggregation state theory)

A solution of the requisite Grignard reagent in THF was transferred to a Schlenk flask, which had been (charged with LiCl if used then) flame-dried under vacuum (0.005 mbar) and allowed to cool under an atmosphere of argon. THF (9 mL) was then added, followed by the required amine, and the solution was stirred at room temperature for 0.5 h, followed by 1.5 h at reflux in THF, and used as active base. Data are presented as (a) Grignard reagent and quantity, (b) amine used, and (c) amount of amine.

5.3. Asymmetric Deprotonation Reactions

Scheme 3.10

Following General Procedure A for the preparation of the magnesium base, data are presented as (a) amount of *n*-Bu_2Mg, (b) amine used, and (c) amount of amine.
Following General Procedure C for the asymmetric deprotonation reaction, data are presented as (a) Mg base, (b) reaction temperature, (c) additives, (d) amount of additive, (e) amount of $P(O)(OPh)_2Cl$, (f) ketone, (g) amount of ketone, (h) reaction time, (i) isolated yield, (e) e.r. (*S*):(*R*)

General Procedure A: (a) 1.0 M, 1 mmol, 1mL (b) **(*R*,*R*)-142** and (c) 0.22 mL, 1 mmol. General Procedure C: (a) **(*R*,*R*)-154**, (b) -78 °C, (c) DMPU, (d) 0.06 mg, 0.5 eq., (e) 0.84 mL, 4 mmol, (f) 4-*tert*-butylcyclohexanone, (g) 123 mg, 0.8 mmol, (h) 16 h, (i) 147 mg, 38%, (e) 93:7

Scheme 3.11

Following General Procedure B for the preparation of magnesium base, data are presented as (a) amount of *n*-Bu_2Mg, (b) amine used, and (c) amount of amine.
Following General Procedure C for the asymmetric deprotonation reaction, data are presented as (a) Mg base, (b) reaction temperature, (c) additives, (d) amount of additive, (e) amount of $ClP(O)(OPh)_2$, (f) ketone, (g) amount of ketone, (h) reaction time, (i) extracted yield, (e) e.r. (*S*):(*R*)

General Procedure B: (a) 1.0 M, 0.5 mmol, 0.5 mL (b) **(*R*,*R*)-142** and (c) 0.22 mL, 1 mmol. General Procedure C: (a) **(*R*,*R*)-125**, (b) -78 °C, (c) DMPU, (d) 0.06 mg, 0.5 eq., (e) 0.84 mL, 4 mmol, (f) 4-*tert*-butylcyclohexanone, (g) 123 mg, 0.8 mmol, (h) 16 h, (i) 162 mg, 42%, (e) 96:4

Scheme 3.12

Table 3.1

Following a General Procedure for the preparation of the magnesium base, data are presented as (a) amount of *n*-Bu_2Mg, (b) amine used, and (c) amount of amine.
Following General Procedure C for the asymmetric deprotonation reaction, data are presented as (a) Mg base, (b) reaction temperature, (c) additives, (d) amount of additive, (e) amount of $P(O)(OPh)_2Cl$, (f) ketone, (g) amount of ketone, (h) reaction time, (i) isolated yield, (e) e.r. (*S*):(*R*)

Entry 1:
Generation of the primary base was carried out using General Procedure B: (a) 1.0 M, 0.5 mmol, (b) **(*R*,*R*)-142** and (c) 0.22 mL, 1 mmol.
Generation of the added base species: *n*-Bu_2Mg in heptane was transferred to a Schlenk flask, which had been flame-dried under vacuum (0.005 mbar) and allowed to cool under an atmosphere of argon, and the heptane was removed *in vacuo* (0.005 mbar) until a white solid was obtained, then THF (5 mL) was added. This species was then transferred into the principal reaction mixture at -78 °C.
General Procedure C: (a) **(*R*,*R*)-125**, (b) -78 °C, (c) DMPU, (d) 0.06 mg, 0.5 eq., (e) 0.84 mL, 4 mmol, (f) 4-*tert*-butylcyclohexanone, (g) 123 mg, 0.8 mmol, (h) 16 h, (i) 162 mg, 42%, (e) 96:4

Entry 2:
Generation of the primary base was carried out using General Procedure B: (a) 1.0 M, 0.5 mmol, 0.5 mL (b) **(*R*,*R*)-142** and (c) 0.22 mL, 1 mmol.
Generation of the added base species was carried out using General Procedure A: (a) 1.0 M, 1 mmol, 1 mL (b) **(*R*,*R*)-142** and (c) 0.22 mL, 1 mmol. This species was then transferred into the principal reaction mixture at -78 °C.
General Procedure C: (a) **(*R*,*R*)-125**, (b) -78 °C, (c) DMPU, (d) 0.06 mg, 0.5 eq., (e) 0.84 mL, 4 mmol, (f) 4-*tert*-butylcyclohexanone, (g) 123 mg, 0.8 mmol, (h) 16 h, (i) 236 mg, 61%, (e) 94:6

Scheme 3.14

Following General Procedure D for the preparation of magnesium base, data are presented as (a) amount of *n*-Bu_2Mg, (b) amine used, (c) amount of amine (d) time and temperature of stage 1, and (e) time and temperature of stage 2.

Following General Procedure C for the asymmetric deprotonation reaction, data are presented as (a) Mg base, (b) reaction temperature, (c) additives, (d) amount of additive, (e) amount of $ClP(O)(OPh)_2$, (f) ketone, (g) amount of ketone, (h) reaction time, (i) isolated yield, (e) e.r. (*S*):(*R*)

General Procedure D: (a) 1.0 M, 1 mmol, 1 mL (b) **(*R*,*R*)-142**, (c) 0.22 mL, 1 mmol, (d) 1.5 h at room temperature, and (e) 1.5 h at reflux in THF. General Procedure C: (a) **(*R*,*R*)-150**, (b) -78 °C, (c) DMPU, (d) 0.06 mg, 0.5 eq., (e) 0.25 mL, 1.2 mmol, (f) 4-*tert*-butylcyclohexanone, (g) 123 mg, 0.8 mmol, (h) 1 h, (i) 297 mg, 77%, (e) 96:4

Scheme 3.15

Following General Procedure B for the preparation of magnesium base, data are presented as (a) amount of *n*-Bu_2Mg, (b) amine used, and (c) amount of amine (d) reflux time.

Following General Procedure C for the asymmetric deprotonation reaction, data are presented as (a) Mg base, (b) reaction temperature, (c) additives, (d) amount of additive, (e) amount of $ClP(O)(OPh)_2$, (f) ketone, (g) amount of ketone, (h) reaction time, (i) isolated yield, (e) e.r. (*S*):(*R*)

General Procedure B: (a) 1.0 M, 1 mmol, 1 mL (b) **(*R*,*R*)-142**, (c) 0.22 mL, 1 mmol, (d) 3 h. General Procedure C: (a) **(*R*,*R*)-160**, (b) -78 °C, (c) DMPU, (d) 0.06 mg, 0.5 eq., (e) 0.25 mL, 1.2 mmol, (f) 4-*tert*-butylcyclohexanone, (g) 123 mg, 0.8 mmol, (h) 1 h, (i) 305 mg, 79%, (e) 96:4

Scheme 3.16

Following General Procedure D for the preparation of magnesium base, data are presented as (a) amount of *n*-Bu_2Mg, (b) amine used, (c) amount of amine (d) time and temperature of stage 1, and (e) time and temperature of stage 2.
Following General Procedure C for the asymmetric deprotonation reaction, data are presented as (a) Mg base, (b) reaction temperature, (c) additives, (d) amount of additive, (e) amount of $ClP(O)(OPh)_2$, (f) ketone, (g) amount of ketone, (h) reaction time, (i) isolated yield, (e) e.r. (*S*):(*R*)

General Procedure D: (a) 1.0 M, 2 mmol, 2 mL (b) **(*R*,*R*)-142**, (c) 0.22 mL, 1 mmol, (d) 1.5 h at room temperature, and (e) 1.5 h at reflux in THF. General Procedure C: (a) **(*R*,*R*)-160**, (b) -78 °C, (c) DMPU, (d) 0.06 mg, 0.5 eq., (e) 0.25 mL, 1.2 mmol, (f) 4-*tert*-butylcyclohexanone, (g) 123 mg, 0.8 mmol, (h) 1 h, (i) 359 mg, 93%, (e) 96:4

Scheme 3.17

Table 3.2

Following General Procedure D for the preparation of the magnesium base, data are presented as (a) amount of *n*-Bu_2Mg, (b) amine used, (c) amount of amine (d) time and temperature of stage 1, and (e) time and temperature of stage 2.
Following General Procedure C for the asymmetric deprotonation reaction, data are presented as (a) Mg base, (b) reaction temperature, (c) additives, (d) amount of additive, (e) amount of $ClP(O)(OPh)_2$, (f) ketone, (g) amount of ketone, (h) reaction time, (i) isolated yield, (e) e.r. (*S*):(*R*)

Entry 1: General Procedure D: (a) 1.0 M, 2 mmol, 2 mL (b) **(*R*,*R*)-142**, (c) 0.22 mL, 1 mmol, (d) 1.5 h at room temperature, and (e) 1.5 h at reflux in THF. General Procedure C: (a) **(*R*,*R*)-160**, (b) -78 °C, (c) -, (d) -, (e) 0.25 mL, 1.2 mmol, (f) 4-*tert*-butylcyclohexanone, (g) 123 mg, 0.8 mmol, (h) 1 h, (i) 347 mg, 90%, (e) 96:4

Entry 2: General Procedure D: (a) 1.0 M, 2 mmol, 2 mL (b) **(*R*,*R*)-142**, (c) 0.22 mL, 1 mmol, (d) 1.5 h at room temperature, and (e) 1.5 h at reflux in THF. General Procedure E: (a) **(*R*,*R*)-160**, (b) -20 °C, (c) DMPU, (d) 0.06 mg, 0.5 eq., (e) 0.25 mL, 1.2 mmol, (f) 4-*tert*-butylcyclohexanone, (g) 123 mg, 0.8 mmol, (h) 1 h, (i) 312 mg, 81%, (e) 88:12

Entry 3: General Procedure A: (a) 1.0 M, 1 mmol, 1mL (b) **(*R*,*R*)-142** and (c) 0.22 mL, 1 mmol. General Procedure C: (a) **(*R*,*R*)-160**, (b) -78 °C, (c) -, (d) -, (e) 0.25 mL, 1.2 mmol, (f) 4-*tert*-butylcyclohexanone, (g) 123 mg, 0.8 mmol, (h) 1 h, (i) 131 mg, 34%, (e) 84:16

Scheme 3.18

Table 3.3

Following General Procedure D for the preparation of magnesium base, data are presented as (a) amount of *n*-Bu_2Mg, (b) amine used, (c) amount of amine (d) time and temperature of stage 1, and (e) time and temperature of stage 2.
Following General Procedure C for the asymmetric deprotonation reaction, data are presented as (a) Mg base, (b) reaction temperature, (c) additives, (d) amount of additive, (e) amount of $ClP(O)(OPh)_2$, (f) ketone, (g) amount of ketone, (h) reaction time, (i) isolated yield, (e) e.r. (*S*):(*R*)

Entry 1: General Procedure D: (a) 1.0 M, 2 mmol, 2 mL (b) **(*R*,*R*)-142**, (c) 0.22 mL, 1 mmol, (d) 0.5 h at room temperature, and (e) 0.5 h at reflux in THF. General Procedure C: (a) **(*R*,*R*)-160**, (b) -78 °C, (c) -, (d) -, (e) 0.25 mL, 1.2 mmol, (f) 4-*tert*-butylcyclohexanone, (g) 123 mg, 0.8 mmol, (h) 1 h, (i) 336 mg, 87%, (e) 95:5

Entry 2: General Procedure D: (a) 1.0 M, 2 mmol, 2 mL (b) **(*R*,*R*)-142**, (c) 0.22 mL, 1 mmol, (d) 0.5 h at room temperature, and (e) 1 h at reflux in THF. General Procedure C: (a) **(*R*,*R*)-160**, (b) -78 °C, (c) -, (d) -, (e) 0.25 mL, 1.2 mmol, (f) 4-*tert*-butylcyclohexanone, (g) 123 mg, 0.8 mmol, (h) 1 h, (i) 347 mg, 90%, (e) 95:5

Entry 3: General Procedure D: (a) 1.0 M, 2 mmol, 2 mL (b) **(*R*,*R*)-142**, (c) 0.22 mL, 1 mmol, (d) 0.5 h at room temperature, and (e) 1.5 h at reflux in THF. General Procedure C: (a) **(*R*,*R*)-160**, (b) -78 °C, (c) -, (d) -, (e) 0.25 mL, 1.2 mmol, (f) 4-*tert*-butylcyclohexanone, (g) 123 mg, 0.8 mmol, (h) 1 h, (i) 359 mg, 93%, (e) 95:5

Entry 4: General Procedure D: (a) 1.0 M, 2 mmol, 2 mL (b) **(*R*,*R*)-142**, (c) 0.22 mL, 1 mmol, (d) 1.5 h at room temperature, and (e) 1 h at reflux in THF. General Procedure C: (a) **(*R*,*R*)-160**, (b) -78 °C, (c) -, (d) -, (e) 0.25 mL, 1.2 mmol, (f) 4-*tert*-butylcyclohexanone, (g) 123 mg, 0.8 mmol, (h) 1 h, (i) 332 mg, 86%, (e) 95:5

Scheme 3.19

Following General Procedure D for the preparation of magnesium base, data are presented as (a) amount of *n*-Bu_2Mg, (b) amine used, (c) amount of amine (d) time and temperature of stage 1, and (e) time and temperature of stage 2.
Following General Procedure C for the asymmetric deprotonation reaction, data are presented as (a) Mg base, (b) reaction temperature, (c) additives, (d) amount of additive, (e) amount of $ClP(O)(OPh)_2$, (f) ketone, (g) amount of ketone, (h) reaction time, (i) isolated yield, (e) e.r. (*S*):(*R*)

Entry 1: General Procedure D: (a) 1.0 M, 1 mmol, 1 mL (b) **(*R*,*R*)-142**, (c) 0.22 mL, 1 mmol, (d) 0.5 h at room temperature, and (e) 1.5 h at reflux in THF. General Procedure C: (a) **(*R*,*R*)-160**, (b) -78 °C, (c) -, (d) -, (e) 0.25 mL, 1.2 mmol, (f) 4-*tert*-butylcyclohexanone, (g) 123 mg, 0.8 mmol, (h) 1 h, (i) 312 mg, 81%, (e) 95:5

Entry 2: General Procedure D: (a) 1.0 M, 1.1 mmol, 1.1 mL (b) **(*R*,*R*)-142**, (c) 0.22 mL, 1 mmol, (d) 0.5 h at room temperature, and (e) 1.5 h at reflux in THF. General Procedure C: (a) **(*R*,*R*)-160**, (b) -78 °C, (c) -, (d) -, (e) 0.25 mL, 1.2 mmol, (f) 4-*tert*-butylcyclohexanone, (g) 123 mg, 0.8 mmol, (h) 1 h, (i) 347 mg, 90%, (e) 95:5

Entry 3: General Procedure D: (a) 1.0 M, 1.2 mmol, 1.2 mL (b) **(*R*,*R*)-142**, (c) 0.22 mL, 1 mmol, (d) 0.5 h at room temperature, and (e) 1.5 h at reflux in THF. General Procedure C: (a) **(*R*,*R*)-160**, (b) -78 °C, (c) -, (d) -, (e) 0.25 mL, 1.2 mmol, (f) 4-*tert*-butylcyclohexanone, (g) 123 mg, 0.8 mmol, (h) 1 h, (i) 343 mg, 89%, (e) 95:5

Scheme 3.20

Following General Procedure D for the preparation of the magnesium base, data are presented as (a) amount of *n*-Bu_2Mg, (b) amine used, (c) amount of amine (d) time and temperature of stage 1, and (e) time and temperature of stage 2.
Following General Procedure C for the asymmetric deprotonation reaction, data are presented as (a) Mg base, (b) reaction temperature, (c) additives, (d) amount of additive, (e) amount of $ClP(O)(OPh)_2$, (f) ketone, (g) amount of ketone, (h) reaction time, (i) extracted yield, (e) e.r. (*S*):(*R*)

General Procedure D: (a) 1.0 M, 1.1 mmol, 1.1 mL (b) **(*R*,*R*)-142**, (c) 0.22 mL, 1 mmol, (d) 0.5 h at room temperature, and (e) 1.5 h at reflux in THF. General Procedure E: (a) **(*R*,*R*)-160**, (b) -20 °C, (c) DMPU, (d) 0.06 mg, 0.5 eq., (e) 0.25 mL, 1.2 mmol, (f) 4-*tert*-butylcyclohexanone, (g) 123 mg, 0.8 mmol, (h) 1 h, (i) 367 mg, 95%, (e) 88:12

5.3.1. Optimised Base Formation

Scheme 3.21

Following General Procedure D for the preparation of magnesium base, data are presented as (a) amount of *n*-Bu_2Mg, (b) amine used, (c) amount of amine (d) time and temperature of stage 1, and (e) time and temperature of stage 2.

General Procedure D: (a) 1.0 M, 1.1 mmol, 1.1 mL (b) **(*R*,*R*)-142**, (c) 0.22 mL, 1 mmol, (d) 0.5 h at room temperature, and (e) 1.5 h at reflux in THF.

5.3.2. Optimised Deprotonation Conditions

Scheme 3.22

Following General Procedure D for the preparation of magnesium base, data are presented as (a) amount of *n*-Bu_2Mg, (b) amine used, (c) amount of amine (d) time and temperature of stage 1, and (e) time and temperature of stage 2.
Following General Procedure C for the asymmetric deprotonation reaction, data are presented as (a) Mg base, (b) reaction temperature, (c) additives, (d) amount of additive, (e) amount of $ClP(O)(OPh)_2$, (f) ketone, (g) amount of ketone, (h) reaction time, (i) isolated yield, (e) e.r. (*S*):(*R*)

Entry 1: General Procedure D: (a) 1.0 M, 1.1 mmol, 1.1 mL (b) **(*R*,*R*)-142**, (c) 0.22 mL, 1 mmol, (d) 0.5 h at room temperature, and (e) 1.5 h at reflux in THF. General Procedure E: (a) **(*R*,*R*)-160**, (b) -20 °C, (c) DMPU, (d) 0.06 mg, 0.5 eq., (e) 0.25 mL, 1.2 mmol, (f) 4-*tert*-butylcyclohexanone, (g) 123 mg, 0.8 mmol, (h) 1 h, (i) 367 mg, 95%, (e) 88:12

Entry 2: General Procedure D: (a) 1.0 M, 1.1 mmol, 1.1 mL (b) **(*R*,*R*)-142**, (c) 0.22 mL, 1 mmol, (d) 0.5 h at room temperature, and (e) 1.5 h at reflux in THF. General Procedure C: (a) **(*R*,*R*)-160**, (b) -78 °C, (c) -, (d) -, (e) 0.25 mL, 1.2 mmol, (f) 4-*tert*-butylcyclohexanone, (g) 123 mg, 0.8 mmol, (h) 1 h, (i) 347 mg, 90%, (e) 95:5

Scheme 3.23

Table 3.5
Entry 1

A solution of magnesium base **41** in THF (1 M, 1 mmol, 1 mL), prepared *via* the General Procedure in Chapter 1, **Scheme 1.23**, was added to a Schlenk flask which had been flame-dried under vacuum and purged with argon. To this base was added THF (9 mL), followed by $P(O)(OPh)_2Cl$ (0.25 mL, 1.2 mmol), and the reaction mixture was stirred for 10 min at -78 °C. 4-*tert*-Butylcylcohexanone (123 mg, 0.8 mmol) was then added as a solution in THF (2 mL) over 1 h using a syringe pump.

The reaction mixture was stirred at -78 °C for 1 h before being quenched with a saturated solution of $NaHCO_3$ (10 mL) and allowed to warm to room temperature. The aqueous phase was extracted with Et_2O (50, 25, 25 mL) and the organic phases were combined and washed with 1 M HCl (2 × 10 mL) to recover the amine. Removal of the solvent *in vacuo* gave an oil which was purified by column chromatography on silica gel using 0-30% Et_2O in petroleum ether (40-60 °C) to give the desired product as a colourless oil in 9% yield and with an e.r. of 67:33.

Entry 2

A solution of magnesium base **42** in THF (1 M, 1 mmol, 1 mL), prepared *via* the General Procedures Chapter 1, **Scheme 1.23** was added to a Schlenk flask which had been flame-dried under vacuum and purged with argon. To this base was added 9 mL of THF, followed, followed by $ClP(O)(OPh)_2$ (0.25 mL, 1.2 mmol), and the reaction mixture was stirred for 10 min at -78 °C. 4-*tert*-Butylcylcohexanone (123 mg, 0.8 mmol) was then added as a solution in THF (2 mL) over 1 h using a syringe pump. The reaction mixture was stirred at -78°C for 1 h before being quenched with a saturated solution of $NaHCO_3$ (10 mL) and allowed to warm to room temperature. The aqueous phase was extracted with Et_2O (50, 25, 25 mL) and the organic phases were combined and washed with 1M HCl (2 × 10 mL) to recover the amine. The removal of the solvent *in vacuo* gave an oil, which, upon analysis by ^1H NMR spectroscopy, revealed only trace levels of the desired product.

Scheme 3.24

Table 3.6

Following General Procedure F or G for the preparation of magnesium base, data are presented as (a) Grignard and amount of Grignard, (b) amine used, and (c) amount of amine.

Following General Procedure C for the asymmetric deprotonation reaction, data are presented as (a) Mg base, (b) reaction temperature, (c) additives, (d) amount of additive, (e) amount of $ClP(O)(OPh)_2$, (f) ketone, (g) amount of ketone, (h) reaction time, (i) isolated yield, (e) er (*S*):(*R*)

Entry 1: General Procedure F: (a) *n*-BuMgCl, 1.0 M, 1.0 mmol, 1.0 mL (b) **(*R*,*R*)-142**, and (c) 0.22 mL, 1 mmol. General Procedure C: (a) **(*R*,*R*)-163**, (b) -78 °C, (c) -, (d) -, (e) 0.25 mL, 1.2 mmol, (f) 4-*tert*-butylcyclohexanone, (g) 123 mg, 0.8 mmol, (h) 1 h, (i) 234 mg, 58%, (e) 95:5

Entry 2: General Procedure G: (a) *n*-BuMgCl, 1.0 M, 1.0 mmol, 1.0 mL (b) **(*R*,*R*)-142**, and (c) 0.22 mL, 1 mmol. General Procedure C: (a) **(*R*,*R*)-157**, (b) -78 °C, (c) -, (d) -, (e) 0.25 mL, 1.2 mmol, (f) 4-*tert*-butylcyclohexanone, (g) 123 mg, 0.8 mmol, (h) 1 h, (i) 100 mg, 26%, (e) 93:7

Entry 3: General Procedure F: (a) *n*-BuMgCl, 1.0 M, 1.5 mmol, 1.5 mL (b) **(*R*,*R*)-142**, and (c) 0.22 mL, 1 mmol. General Procedure C: (a) **(*R*,*R*)-163**, (b) -78 °C, (c) -, (d) -, (e) 0.25 mL, 1.2 mmol, (f) 4-*tert*-butylcyclohexanone, (g) 123 mg, 0.8 mmol, (h) 1 h, (i) 258 mg, 67%, (e) 92:8

Entry 4: General Procedure F: (a) *t*-BuMgCl, 1.0 M, 1.0 mmol, 1.0 mL (b) **(*R*,*R*)-142**, and (c) 0.22 mL, 1 mmol. General Procedure C: (a) **(*R*,*R*)-163**, (b) -78 °C, (c) -, (d) -, (e) 0.25 mL, 1.2 mmol, (f) 4-*tert*-butylcyclohexanone, (g) 123 mg, 0.8 mmol, (h) 1 h, (i) -, (e) -

Entry 5: General Procedure G: (a) *t*-BuMgCl, 1.0 M, 1.0 mmol, 1.0 mL (b) **(*R*,*R*)-142**, and (c) 0.22 mL, 1 mmol. General Procedure C: (a) **(*R*,*R*)-157**, (b) -78 °C, (c) -, (d) -, (e) 0.25 mL, 1.2 mmol, (f) 4-*tert*-butylcyclohexanone, (g) 123 mg, 0.8 mmol, (h) 1 h, (i) 30 mg, 8%, (e) -

Entry 6: General Procedure F: (a) MeMgCl, 3.00 M, 1.0 mmol, 0.33 mL (b) **(*R*,*R*)-142**, and (c) 0.22 mL, 1 mmol. General Procedure C: (a) **(*R*,*R*)-163**, (b) -78 °C, (c) -, (d) -, (e) 0.25 mL, 1.2 mmol, (f) 4-*tert*-butylcyclohexanone, (g) 123 mg, 0.8 mmol, (h) 1 h, (i) 274 mg, 71%, (e) 95:5

Entry 7: General Procedure G: (a) MeMgCl, 1.0 M, 1.0 mmol, 0.33 mL (b) **(*R*,*R*)-142**, and (c) 0.22 mL, 1 mmol. General Procedure C: (a) **(*R*,*R*)-157**, (b) -78 °C, (c) -, (d) -, (e) 0.25 mL, 1.2 mmol, (f) 4-*tert*-butylcyclohexanone, (g) 123 mg, 0.8 mmol, (h) 1 h, (i) 162 mg, 42%, (e) 95:5

Scheme 3.25

Table 3.7

Following General Procedure F or G for the preparation of magnesium base, data are presented as (a) Grignard and amount of Grignard, (b) amine used, and (c) amount of amine.

Following General Procedure C for the asymmetric deprotonation reaction, data are presented as (a) Mg base, (b) reaction temperature, (c) additives, (d) amount of additive, (e) amount of $ClP(O)(OPh)_2$, (f) ketone, (g) amount of ketone, (h) reaction time, (i) isolated yield, (e) e.r. (*S*):(*R*)

Entry 1: General Procedure F: (a) *n*-BuMgCl, 1.0 M, 1.0 mmol, 1.0 mL (b) **(*R*,*R*)-142**, and (c) 0.22 mL, 1 mmol. General Procedure C: (a) **(*R*,*R*)-163**, (b) -78 °C, (c) LiCl, (d) 42 mg,1 mmol, (e) 0.25 mL, 1.2 mmol, (f) 4-*tert*-butylcyclohexanone, (g) 123 mg, 0.8 mmol, (h) 1 h, (i) 278 mg, 72%, (e) 91:9

Entry 2: General Procedure G: (a) *n*-BuMgCl, 1.0 M, 1.0 mmol, 1.0 mL (b) **(*R*,*R*)-142**, and (c) 0.22 mL, 1 mmol. General Procedure C: (a) **(*R*,*R*)-157**, (b) -78 °C, (c) LiCl, (d) 42 mg,1 mmol, (e) 0.25 mL, 1.2 mmol, (f) 4-*tert*-butylcyclohexanone, (g) 123 mg, 0.8 mmol, (h) 1 h, (i) 100 mg, 26%, (e) 92:8

5.3.3. One Pot Procedure

Scheme 3.26

An oven dried and sealed 25 mL microwave vial was purged with argon and charged with *n*-BuMgCl (1 M, 2.2 mmol, 2.2 mL) followed by THF (9 mL). The mixture was stirred at room temperature and 1,4-dioxane (0.17 mL, 2.1 mmol) was added dropwise and the reaction mixture left at room temperature for 3 h. The solution was

then charged with the desired amine **(*R*,*R*)-142** (0.22 mL, 1 mmol), and the solution stirred for a further 0.5 h before heating to reflux for a further 1.5 h. Assuming the base had formed, the base was first cooled to room temperature before further cooling to -78°C and stirring for 5 min before the addition of $P(O)(OPh)_2Cl$ (0.25 mL, 1.2 mmol). To this solution was then added 4-*tert*-butylcyclohexanone (123 mg, 0.8 mmol) as a solution in THF (2 mL) over 1 h *via* a syringe pump. The reaction mixture was stirred at -78°C for 1 h before being quenched with a saturated solution of $NaHCO_3$ (10 mL) and allowed to warm to room temperature. The aqueous phase was extracted with EtOAc (50, 25, 25 mL) and the organic phases were combined and washed with 1 M HCl (2 × 10 mL) to recover the amine. The removal of the solvent *in vacuo* gave an oil, which was purified through a silica cartridge using 0-30% EtOAc in cyclohexane (40-60 °C) to give the desired product as a colourless oil in 94% yield (363 mg) and 95:5 selectivity.

Scheme 3.27
Table 3.8, **Entry 1**

An oven-dried Schlenk flask was charged with LiCl (42 mg, 1 mmol) and the flask was flame-dried under vacuum then purged with argon three times. THF (10 mL) and the desired amine **(*R*,*R*)-142** (0.22 mL, 1 mmol) were added to the flask before cooling the solution to -78 °C and stirring for 10 min. A solution of *n*-BuLi (0.4 mL, 2.5 M in hexanes, 1 mmol,) was slowly added and the mixture was stirred for a further 15 min before allowing the flask warm to room temperature. After the flask had reached room temperature (approximately 20 min) it was stirred for 15 min before cooling the reaction back to -78 °C. To this solution was added 4-*tert*-butylcyclohexanone (123 mg, 0.8 mmol) dropwise as a solution in THF (2 mL). The reaction mixture was stirred at -78°C for 1 h before addition of $P(O)(OPh)_2Cl$ (0.84 mL, 4 mmol) and the stirring continued for a further 15 min, before being quenched with a saturated solution of $NaHCO_3$ (10 mL) and allowed to warm to room temperature. The aqueous phase was extracted with EtOAc (50, 25, 25 mL) and the organic phases were combined and washed with 1M HCl (2 × 10 mL) to recover the amine. The removal of the solvent *in vacuo* gave an oil, which was purified through

a silica cartridge using 0-30% Et_2O in petroleum ether (40-60 °C) to give the desired product as a colourless oil in 52% (201 mg) and 92:8 selectivity.

Table 3.8, **Entry 2**

An oven-dried Schlenk flask was charged with LiCl (42 mg, 1 mmol) and the flask was flame-dried under vacuum and purged with argon three times. THF (10 mL) and the desired amine **(*R*,*R*)-142** (0.22 mL, 1 mmol) were added to the flask before cooling the solution to -78 °C and stirring for 10 min. A solution of *n*-BuLi (0.4 mL, 2.5 M in hexanes, 1 mmol) was slowly added and the mixture was stirred for a further 15 min before allowing the flask warm to room temperature. After the flask had reached room temperature (approximately 20 min) it was stirred for 15 min before cooling the reaction back to -20 °C. To this solution was added 4-*tert*-butylcyclohexanone (123 mg, 0.8 mmol) as a solution in THF (2 mL) dropwise. The reaction mixture was stirred at -20°C for 1 h before addition of $P(O)(OPh)_2Cl$ (0.84 mL, 4 mmol) and the stirring continued for a further 15 min before being quenched with a saturated solution of $NaHCO_3$ (10 mL) and allowed to warm to room temperature. The aqueous phase was extracted with EtOAc (50, 25, 25 mL) and the organic phases were combined and washed with 1 M HCl (2 × 10 mL) to recover the amine. The removal of the solvent *in vacuo* gave an oil, which was purified through a silica cartridge using 0-30% Et_2O in petroleum ether (40-60 °C) to give the desired product as a colourless oil in 73% (282 mg) and 83:17 selectivity.

5.4. Spectroscopic Experiment

5.4.1. Preparation of NMR Samples

(*R*,*R*)-142

An oven-dried flask (25 mL) was flame-dried under vacuum and purged with argon three times followed by the addition of amine **(*R*,*R*)-142** (0.11 mL, 0.5 mmol) and by d_8-THF (2 mL). This mixture was stirred for 5 min at room temperature, then 0.4 mL

of the solution was added to an oven-dried and flame-dried (under vacuum) NMR tube, which had been purged with argon and cooled. The sample was then sealed, taking care to not let any air in, and was analysed immediately.

(*R*,*R*)-154

A solution of *n*-Bu_2Mg (1M, 0.5 mmol, 0.5 mL) in heptane was transferred to a Schlenk flask, which had been flame-dried under vacuum (0.005 mbar) and allowed to cool under an atmosphere of argon, and the heptane was removed *in vacuo* (0.005 mbar) until a white solid was obtained. d_8-THF (5 mL) was then added, followed by the required amine **(*R*,*R*)-142** (0.11 mL, 0.5 mmol), and the solution was stirred at room temperature for 1.5 h, assuming quantitative formation of the alkylmagnesium amide species. A 0.4 mL aliquot of the solution was added to an oven-dried and flame-dried (under vacuum) NMR tube, which had been purged with argon and cooled. The sample was sealed, taking care to not let any air in, and analysed immediately.

(*R*,*R*)-160

A solution of *n*-Bu_2Mg (1M, 0.5 mmol, 0.5 mL) in heptane was transferred to a Schlenk flask, which had been flame-dried under vacuum (0.005 mbar) and allowed to cool under an atmosphere of argon, and the heptane was removed *in vacuo* (0.005 mbar) until a white solid was obtained. d_8-THF (5 mL) was then added, followed by the required amine **(*R*,*R*)-142** (0.11 mL, 0.5 mmol), and the solution was stirred at room temperature for 1.5 h followed by heating at reflux for 1.5 h, assuming quantitative formation of the desired base species. A 0.4 mL aliquot of the solution was added to an oven-dried and flame-dried (under vacuum) NMR tube, which had been purged with argon and cooled. The sample was sealed, taking care to not let any air in, and analysed immediately.

(*R*,*R*)-125

A solution of *n*-Bu_2Mg (1M, 0.5 mmol, 0.5 mL) in heptane was transferred to a Schlenk flask, which had been flame-dried under vacuum (0.005 mbar) and allowed to cool under an atmosphere of argon, and the heptane was removed *in vacuo* (0.005 mbar) until a white solid was obtained. d_8-THF (5 mL) was then added, followed by the required amine **(*R*,*R*)-142** (0.22 mL, 1 mmol), and the solution was heated at reflux for 1.5 h, assuming quantitative formation of the alkylmagnesium amide species. A 0.4 mL aliquot of the solution was added to an oven-dried and flame-dried (under vacuum) NMR tube, which had been purged with argon and cooled. The sample was sealed, taking care to not let any air in, and was analysed immediately.

(*R*,*R*)-125 (in hexanes)

A solution of *n*-Bu_2Mg (1M, 0.5 mmol, 0.5 mL) in heptane was transferred to a Schlenk flask, which had been flame-dried under vacuum (0.005 mbar) and allowed to cool under an atmosphere of argon, and the heptane was removed *in vacuo* (0.005 mbar) until a white solid was obtained. Hexanes (5 mL) was then added, followed by the required amine **(*R*,*R*)-142** (0.22 mL, 1 mmol), and the solution was heated at reflux for 1.5 h, assuming quantitative formation of the alkylmagnesium amide species. The hexane was removed *in vacuo* (0.005 mbar) for 1 h, with heating of the flask to 40 °C follwed by an argon purge. Following this d_8-THF (5 mL) was added to the yellow oil and stirred for a further 10 min at room temperature before a 0.4 mL aliquot of the solution was added to an oven-dried and flame-dried (under vacuum) NMR tube, which had been purged with argon and cooled. The sample was sealed taking, care to not let any air in, and was analysed immediately.

5.4.2. DOSY NMR Analysis

^{1}H NMR data were acquired on a Bruker AVANCE 400 MHz NMR spectrometer operating at a magnetic field strength of 9.4 T, equipped with a 5 mm BBFO-z-atm probehead equilibrated at a constant temperature of 298 K by virtue of a BCU-05 cooling unit and operating under Topspin (version 2.1, Bruker, Karlsruhe, Germany) on a HP-XW3300 workstation within a Windows XP operating environment.

One-dimensional (1D) 1H NMR data were acquired with 4 transients over a frequency width of 12 ppm (acquisition time aq = 3.42 s) and centred at 5 ppm using a single pulse-acquire pulse programme. Diffusion Ordered NMR data were acquired with 4 or 8 transients over the same observation frequency window using a double stimulated echo pulse sequence with bipolar gradients for diffusion encoding (dstebpgp3s) according to the method of Jerschow and Müller[10,11] to compensate for the effects of laminar flow caused by convection. Diffusion encoding gradients (16 values) were distributed between values of 5% and 95% of maximum according to the square of the gradient value. Diffusion coefficients were calculated directly by fitting the experimental data to the standard Stejskal-Tanner expression relating diffusion coefficient to signal intensity and diffusion encoding gradient strength. Diffusion coefficient data were determined for all reference compounds in an identical manner. Alignment of data sets was carried out by virtue of the common presence of THF as both solvent and internal reference point for chemical shift and diffusion coefficient, D (average value measured over seven reference data sets D = $38.6 \pm 0.08 \times 10^{-10}$ m^2/s).

5.4.3. Calibration Curve

Figure 3.8

Diffusion coefficient values were determined for reference compounds over the molecular weight range 72 – 1203 g/mol to establish a calibration curve against which NMR diffusion data from the various amides could be assessed (**Table exp 3.1**). The calibration curve plotted as log *D vs* log MW showed a linear fit to the expression log D = -0.5866 log MW – 7.3507 (R^2 = 0.98518) over a molecular weight range covering two orders of magnitude (blue diamonds).

Diffusion coefficients measured for the Chiral amine A (**(*R*,*R*)-142**) (MW = 231 g/mol, $D_{(R,R)\text{-}142}$ = 18.3 x 10^{-10} m^2/s) was consistent with the molecular weight 225 g/mol, $D_{calculated}$ =18.6 x 10^{-10} m^2/s.

Diffusion coefficients measured for the Alkylmagnesium amide B (**(*R*,*R*)-154.2THF**) ($MW_{measured}$ = 444 g/mol, $D_{measured}$ = 12.5 x 10^{-10} m^2/s) was consistent with the molecular weight 450 g/mol, $D_{calculated}$ =12.4 x 10^{-10} m^2/s.

Diffusion coefficients measured for the magnesium bisamide C ((***R*,*R*)-164**) ($MW_{measured}$ = 908 g/mol, $D_{measured}$ = 8.2 x 10^{-10} m^2/s) was consistent with the molecular weight 944.9 g/mol, $D_{calculated}$ =8.01 x 10^{-10} m^2/s.

Compounds	MW (g/mol)	Log MW	10^{-10} *D* (m^2/s)	Log *D*
THF	72.11	1.858	38.6	-8.413
BHT	220.35	2,343	17.2	-8,763
squalene	422.72	2,626	11.9	-8,924
dppf	554.39	2,744	11.7	-8,932
Cyclosporin A	1202.61	3,080	72.1	-9,142

Table Exp 3. 1

Figure 3.8

Using the diffusion coefficient values determined for reference compounds above in Table exp 3.1, NMR diffusion data from the various amides were assessed.

Diffusion coefficients measured for the magnesium bisamide **(*R*,*R*)-119** ($MW_{measured}$ = 440 g/mol, $D_{measured}$ = 12.5 x 10^{-10} m^2/s) was consistent with the molecular weight 444.9 g/mol, $D_{calculated}$ = 12.4 x 10^{-10} m^2/s.

6. References

1. (a) Kerr, W. J.; Watson, A. J. B.; Hayes, D., *Org. Biomol. Chem.*, **2008**, *6*, 1238. (b) Kerr, W. J.; Watson, A. J. B.; Hayes, D., *Synlett,* **2008**, *19* (9), 1386.
2. Bennie, L. S.; Kerr, W. J.; Middleditch, M.; Watson, A. J. B., *Chem. Commun.*, **2011**, *47* (8), 2264.
3. (a) Yong, K. H.; Taylor, N. J.; Chong, J. M., *Org. Lett.*, **2002**, *4* (21), 3553. (b) Ashby, E. C.; Willard, G. F., *J. Org. Chem.*, **1978**, *43* (21), 4094.
4. Sibi, M. P.; Asano, Y., *J. Am. Chem. Soc.*, **2001**, *123* (39), 9708
5. Henderson, K. W.; Allan, J. F.; Kennedy, A. R. *Chem. Commun.* **1997**, No. 12, 1149.
6. (a) Eaton, P. E.; Zhang, M.-X.; Komiya, N.; Yang, C.-G.; Steele, I.; Gilardi, R., *Synlett*, **2003**, *2003* (09), 1275. (b) Zhang, M.-X.; Eaton, P. E., *Angew. Chem. Int. Ed.*, **2002**, *41* (12), 2169.
7. (a) Carswell, E. L. *PhD Thesis*; University of Strathclyde; 2005. (b) Carswell, E. L.; Hayes, D.; Henderson, K. W.; Kerr, W. J.; Russell, C. J., *Synlett*, **2003**, *14* (7), 1017.
8. Henderson, K. W.; Kerr, W. J.; Moir, J. H., *Chem. Commun.*, **2000**, 479.
9. Watson, A. J. B., *PhD Thesis*; University of Strathclyde; 2007.
10. Wakefield, B. J., In *Organomagnesium Methods in Organic Synthesis*; Wakefield, B. J., Ed.; Best Synthetic Methods; Academic Press: London, 1995.
11. (a) Krafft, M. E.; Holton, R. A., *Tetrahedron Lett.*, **1983**, *24* (13), 1345. (b) Bunnage, M. E.; Davies, S. G.; Goodwin, C. J.; Walters, I. A. S., *Tetrahedron Asymmetry*, **1994**, *5* (1), 35.
12. Moir, J. H., *PhD Thesis*; University of Strathclyde; 2002.
13. Bennie, L. S., *PhD Thesis*; University of Strathclyde; 2012.
14. (a) Krasovskiy, A.; Knochel, P., *Angew. Chem. Int. Ed.*, **2004**, *43* (25), 3333. (b) Piller, F. M.; Bresser, T.; Fischer, M. K. R.; Knochel, P., *J. Org. Chem.*, **2010**, *75* (13), 4365. (c) Piller, F. M.; Appukkuttan, P.; Gavryushin, A.; Helm, M.; Knochel, P., *Angew. Chem. Int. Ed.,* **2008**, *47* (36), 6802.
15. (a) Cousins, R. P. C.; Simpkins, N. S., *Tetrahedron Lett.*, **1989**, *30* (51), 7241. (b) Shirai, R.; Tanaka, M.; Koga, K., *J. Am. Chem. Soc.*, **1986**, *108* (3), 543.

16. (a) Bunn, B. J.; Simpkins, N. S.; Spavold, Z.; Crimmin, M. J., *J. Chem. Soc. Perkin Trans. 1*, **1993**, No. 24, 3113. (b) Sugasawa, K.; Shindo, M.; Noguchi, H.; Koga, K., *Tetrahedron Lett.*, **1996**, *37* (41), 7377.
17. (a) Li, D.; Keresztes, I.; Hopson, R.; Williard, P. G., *Acc. Chem. Res.*, **2009**, *42*, 270; (b) Garcia-Alvarez,P.; Mulvey, R. E.; Parkinson, J. A., *Angew. Chem. Int. Ed.*, **2011**, *50*, 9668.
18. Jolly, P. I.; Zhou, S.; Thomson, D. W.; Garnier, J.; Parkinson, J. A.; Tuttle, T.; Murphy, J., A. *Chem. Sci.*, **2012**, *3* (5), 1675.
19. Hamdoun, G.; Sebban, M.; Cossoul, E.; Harrison-Marchand, A.; Maddaluno, J.; Oulyadi, H., *Chem. Commun.*, **2014**, *50* (31), 4073.
20. Nilsson, M.; Morris, G. A., *Chem Commun*, **2007**, No. 9, 933.
21. Perrin, D., D.; Armarego, W. L. F. *Purification of Laboratory Chemicals*; Pergaman: Oxford; 1988.
22. Love, B. E.; Jones, E. G., *J. Org. Chem.*, **1999**, *64* (10), 3755.
23. (a) Jerschow A.; Müller N., *J. Magn. Reson. Ser. A*, **1996**, *123*, 222. (b) Jerschow A.; Müller N., *J. Magn. Reson. Ser. A*, **1997**, *125*, 372.

Part II: Application of Enol Phosphates

Chapter 4

The Total Synthesis of (+)-Sporochnol

Content

1. Introduction

1.1. Isolation and biological study of Sporochnol

Having successfully developed a highly efficient methodology for the synthesis of enantioenriched enol phosphate products, we were eager to apply this methodology with the context of the total synthesis of a natural product. In this regard, we turned our attention towards the synthesis of (+)-sporochnol (**(*S*)-165**), a monoterpene containing an all carbon chiral centre (**Figure 4.1**).

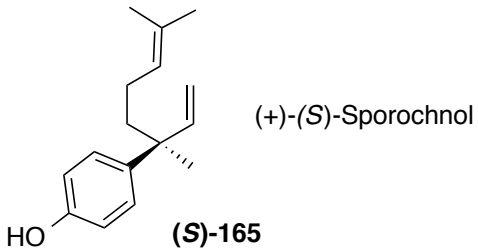

Figure 4. 1

In the early 1990s, Fenical reported the isolation of three novel prenylated phenols from the Caribbean marine alga, *Sporochnus bolleanus*.[1] The major metabolite, sporochnol A, exhibited a substantial feeding deterrence in herbivorous fish. The group showed that in the case of the parrotfish, the consumption of algae decreased by up to 27% when sporochnol A was used. Although we did not intend to study the biological aspects of such a family of compounds, our aim was to develop a novel strategy for the construction of the all-carbon chiral quaternary centre present in the molecule.

1.2. Previous Syntheses of Sporochnol

1.2.1. First Synthesis

Since the isolation of sporochnol A, a wide range of synthetic application have emerged to facilitate the synthesis of racemic sporochnol.[2] More importantly, within

this, a concise synthesis of the all-carbon quaternary centre also presents a considerable challenge. Since its discovery, over 8 total syntheses of sporochnol have been reported in the literature. Ogasawara reported the first synthesis, which also defined the absolute configuration of the stereogenic centre in the natural product.[3] To achieve this, the synthesis began with the commercially-available chiral material, (*S*)-epichlorohydrin (**(*S*)-166**). Through functional group modification, (*R*)-sporochnol (**Scheme 4.1**) was accessed in 12 steps and 14% overall yield. Optical rotation data matched to Fenical's findings, except in the sign of the specific rotation. Thus, the group concluded that the natural product (+)-sporochnol A possessed the *S* configuration.

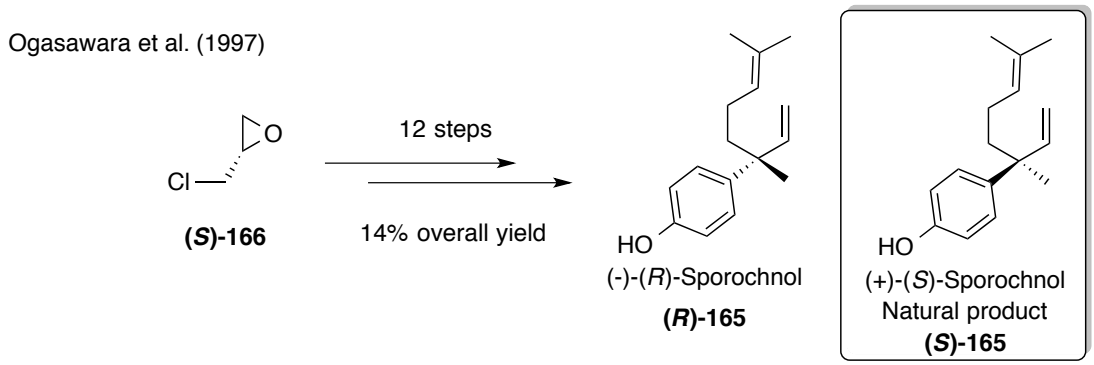

Scheme 4. 1

1.2.2. Enzymatic Approach

Following this work, a number of research groups have used (+)-sporochnol as a target molecule to showcase novel techniques developed within their laboratories. One of the first methodologies employed for the generation of the quaternary chiral centre was carried out with the use of enzymes. In 1999, Fadel used pig liver esterase (PLE) to demonstrate an enantioselective enzymatic hydrolysis on a prochiral dimethyl malonate (**167**).[4] This process allowed the generation of chiral acid ester **(*R*)-168** in high enantioselectivity (85% e.e., 97% e.e. after recrystallisation), which was then subjected to a series of chemical transformations to afford the unnatural isomer (*R*)-sporochnol in 8 steps and an overall yield of 52%. Several years later, Ohira employed the same strategy, using porcine pancreatic lipase (PPL) on a

prochiral acetate **169**.[5] In this case, PPL permitted an enzymatic resolution, allowing the separation of both enantiomers in quantitative yield (50%). With both enantiomers in hand, the group successfully completed the synthesis of the natural product (*S*)-sporochnol over 23 chemical steps and in an overall yield of 7.5%. The use of enzymes in asymmetric synthesis has several advantages, such as ease of set up and high selectivity, but on the other hand they also present some disadvantages. In the case of PLE, although all the material has been transformed towards a chiral product, the required absolute stereochemistry was not obtained. With the use of PPL, only half of the racemate was consumed in a classical kinetic resolution, resulting in an inefficient step, decreasing the overall efficiency of the synthesis.

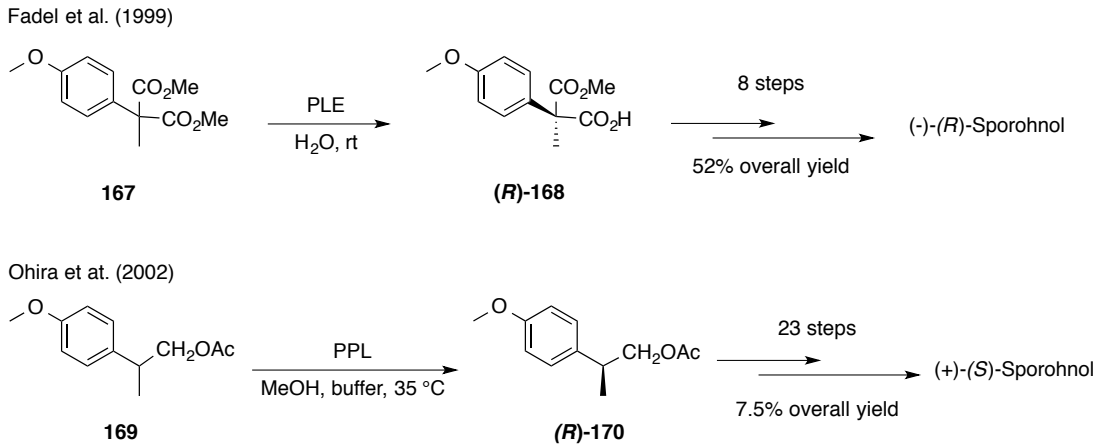

Scheme 4. 2

1.2.3. Using a Chiral Epoxide

In 2001, Kita reported a remarkably elegant strategy, using the efficient rearrangement of an epoxide (**Scheme 4.3**).[6] Kita proposed that the use of an aluminium reagent on a chiral epoxy acylate such as **171** would result in a subtle rearrangement, allowing the construction of quaternary carbon centres and the subsequent ketone **172**. This strategy allowed Kita to complete the synthesis by obtaining optically pure (*S*)-sporochnol. The rest of the synthesis relied on two well-developed strategies, using selective reduction of an enone, followed by a stereoselective Sharpless epoxidation reaction. Although high levels of selectivities were obtained, the reaction required a range of demanding steps, and a total of 13 steps afforded a low 7.8% overall yield.

Kita et al. (2001)

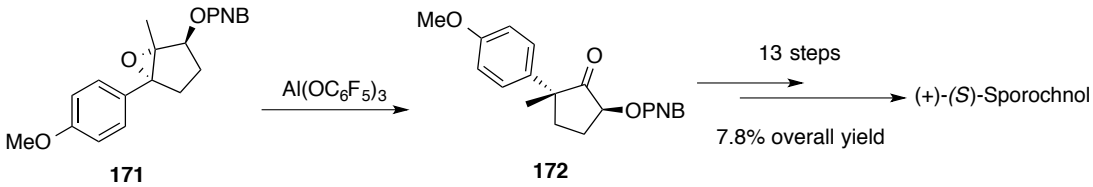

Scheme 4. 3

1.2.4. Using a Chiral Auxiliary

In 2001, Hoveyda developed a new approach towards the formation of the chiral quaternary centre, as shown below in **Scheme 4.4**.[7] Specifically, Hoveyda used the chiral peptide ligand **174** to perform a copper-catalysed allylic substitution on the allylic phosphate **173**, which afforded directly the required stereogenic centre of (*R*)-sporochnol A. Although the synthesis of the precursor was not described, the key step afforded the unnatural isomer with an overall 82% yield and 82% e.e. A few years later, a modified set of conditions was presented, with the use of chiral NHC ligand **177**, which allowed an asymmetric allylic alkylation of the allyl phosphate **176** from an *in situ* generated arylaluminium species from the parent aryl bromide **175**. Under the presented conditions, only a poor 57% e.e. was obtained favouring the unnatural (*R*)-sporochnol, even if the authors described such methodology as a more efficient and easy process.

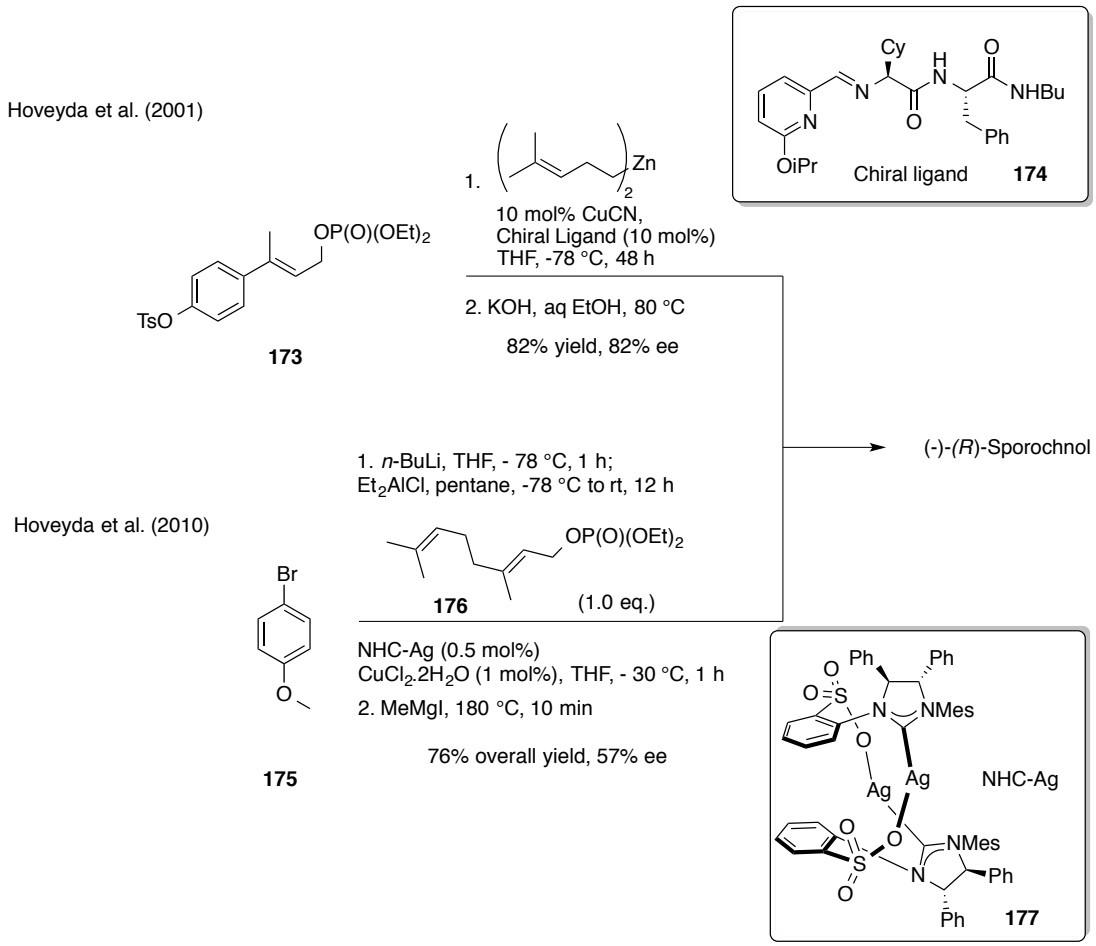
Hoveyda et al. (2001)
1.
Zn
2
10 mol% CuCN,
Chiral Ligand (10 mol%)
THF, -78 °C, 48 h
OP(O)(OEt)2
TsO
173
2. KOH, aq EtOH, 80 °C
82% yield, 82% ee
Cy
H
N
O
NHBu
N
N
O
Ph
OiPr
Chiral ligand
174
(-)-(R)-Sporochnol
1. n-BuLi, THF, - 78 °C, 1 h;
Et2AlCl, pentane, -78 °C to rt, 12 h
Hoveyda et al. (2010)
OP(O)(OEt)2
176
(1.0 eq.)
Br
O
175
NHC-Ag (0.5 mol%)
CuCl2.2H2O (1 mol%), THF, - 30 °C, 1 h
2. MeMgI, 180 °C, 10 min
76% overall yield, 57% ee
Ph
Ph
O
O
S
N
NMes
O
Ag
Ag
NHC-Ag
O
O
NMes
S
N
Ph
O
Ph
177

Scheme 4. 4

1.2.5. Homologation of a Chiral Borane

More recently, in 2011, Aggarwal reported a novel methodology (**Scheme 4.5**), which allows the stereospecific homologation of tertiary boronic esters.[8] To demonstrate the application of this process, Aggarwal completed the synthesis of the natural product (*S*)-sporochnol in an impressively short 5 steps and with an excellent enantioselectivity of 94% e.e. The key step in this synthesis was the homologation of a chiral boronic ester, using a simple Grignard reagent, with retention of starting chiral compound (aryl carbamate) was obtained through the well-precedented asymmetric reduction of aryl ketones reported by Noyori.[9]

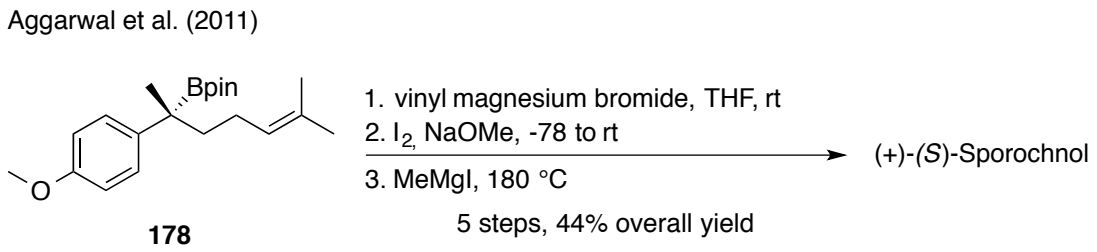

Scheme 4. 6

1.2.6. Desymmetrisation Approach

One other synthesis of optically active sporochnol has been reported, by Busque in 2006 (**Scheme 4.6**).[10] Although this strategy does not represent the most effective synthesis to date, it was still of great interest as it involved the desymmetrization of prochiral 1,4-diketone **178** using (*R*,*R*)-hydrobenzoin to generate the chiral monoketal **179**. Following further transformations, the unnatural product (*R*)-sporochnol was synthesised in a 15% overall yield in only 5 steps. Although the synthesis was concise and accessed an enantiopure compound, two weak points could be identified. Firstly, the key step, which required mono-protection of the diketone, was low yielding due to a large amount of di-ketal by-product. A second issue was the chromatographic separation of diastereomer **180**, which allowed the

enhancement enantioselectivity of the final compound, but decreased the overall yield.

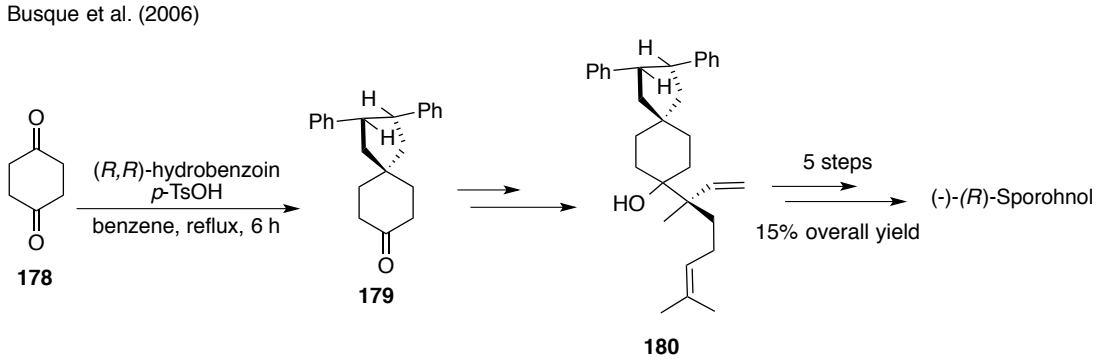

Scheme 4. 7

This last synthesis was particularly interesting, as it established the benchmark for a synthesis of sporochnol through a desymmetrization strategy, and therefore allowed us to compare our methodology to this synthesis.

1.3. From an Asymmetric Deprotonation Reaction

1.3.1. Cyclobutanone as Starting Material

As shown in previous chapters, the use of magnesium bisamide bases has allowed high levels of reactivity and selectivity towards enantioenriched "trapped-enolate" (*i.e.* silyl enol ethers and enol phosphates) products. We were interested in demonstrating the scope of our chemistry through synthesis of a natural product, and we our attention focussed on Sporochnol A. In terms of a synthetic strategy, we were inspired by a publication by Harrity in 2001.[11] As shown below **Scheme 4.7** Harrity attempted the target synthesis with the key step being the ring opening metathesis reaction of a 2,2-disubstituted cyclobutene, **182**, using the Grubbs II catalyst **183**. The di-olefinated product obtained was further advanced through three chemical steps to generate the desired compound (methoxy-sporochnol). In their proposed synthetic route, the authors envisaged the use of a cyclobutanone precursor **181** to generate the olefin **182**. This specific route was preferred as it could be rendered

enantioselective by an asymmetric deprotonation reaction to generate the enantioenriched intermediate **185**, allowing the synthesis of optically-active sporochnol.

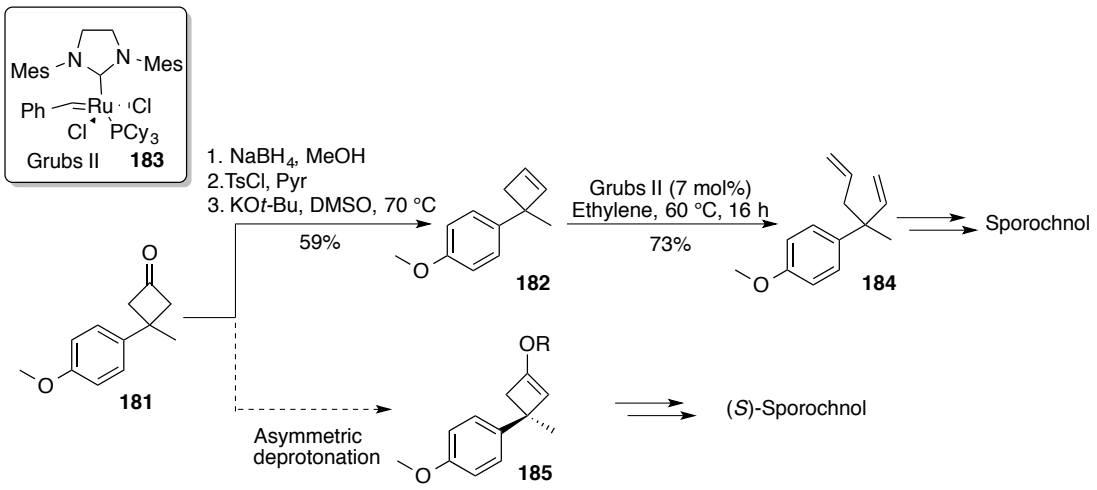

Scheme 4. 8

With the strategy disclosed by Harrity, The Kerr group envisaged an asymmetric deprotonation reaction using the group's chiral magnesium bisamide bases to deprotonate cyclobutanone **181**, to generate an enantioenriched silyl enol ether **(*S*)-186**, followed by application of the well-precedented ring opening metathesis methodology to generate the silyl enol ether **(*S*)-187** (**Scheme 4.8**).[12] Our approach had the advantage of not only delivering an optically active compound but also allowing for chemical differentiation of the two newly formed olefins, which is essential in rapidly accessing the natural product.

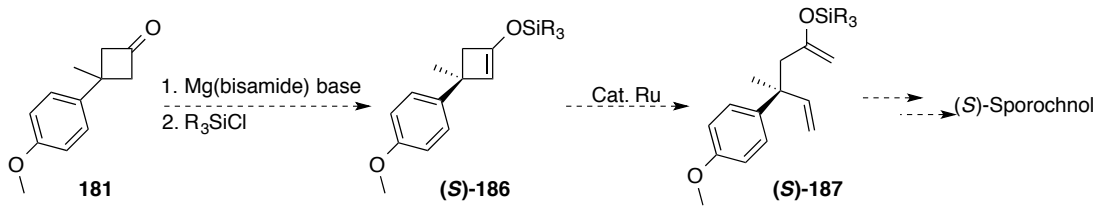

Scheme 4. 9

Unfortunately, early studies towards the synthesis of silyl enol ether **(*S*)-186**, resulted only in low yielding processes which did not afford any enantioenrichment.

1.3.2. Novel Approach Using a Cyclohexanone Derivative

With the first synthesis of enol phosphate products evolving at the same time, and the observation of high levels of selectivity and reproducibility observed when phosphoryl chlorides were used (Part 1),[13] a range of projects within the field of asymmetric deprotonation reaction within our laboratories adopted phosphoryl chlorides as viable trapping electrophiles. The Kerr group therefore proposed a novel synthetic approach to (*S*)-sporochnol (**Scheme 4.9**) where the key step would consist of the asymmetric deprotonation of a 4-substituted cyclohexanone **188**, to generate enol phosphate **(*S*)-189**, based on the excellent reactivity and selectivity observed when 4-*t*-butylcyclohexanone was used to form enantioenriched enol phosphate products.[14] Following this, a palladium-catalysed cross-coupling reaction was envisaged to generate an enantioenriched olefin **(*S*)-190**.

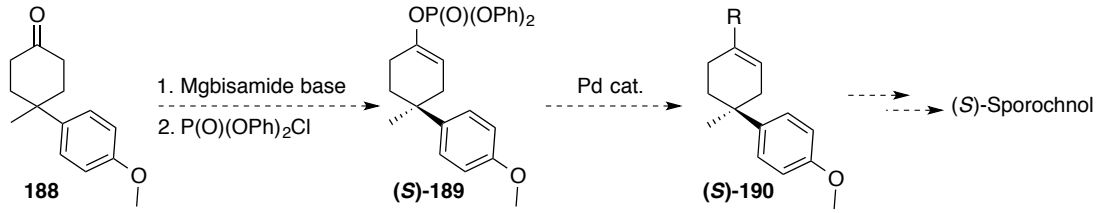

Scheme 4. 10

With this key step in mind, the novel approach had two major challenges, namely the synthesis of the precursor ketone **188**, and conversion of the desymmetrised product to (*S*)-sporochnol.

1.3.3. Primary Approach Towards the Ketone

The first challenge was accomplished as shown below in **Scheme 4.10**. From commerically available esters **191** and **192**, a one-pot, tandem Michael addition/Dieckmann condensation was carried out to generate the ß-ketoester **193** in quantitative yield.[15] With the required scaffold in hand, a simple decarboxylation allowed the synthesis of ketone **194** in a good 77% yield. Reduction of the ester, using $LiAlH_4$, required acetal protection of the ketone,[16] which was achieved in an excellent 92% isolated yield over two steps, to generate alcohol **195**. Further reduction of the alcohol was envisaged *via* conversion of the hydroxyl to a leaving group. Among the various leaving groups studied, the mesylate derivative produced a more stable and reliable intermediate.[17] Following optimisation of the conditions, the mesylate intermediate **196** vas synthesised in quantitative yield. The use of Super-Hydride for the mesylate displacement allowed the synthesis of the protected ketone **197** in a good 77% isolated yield.[18] Finally, deprotection of the acetal[19] resulted in the formation of the desired ketone **188**, in seven steps and with an overall 55% isolated yield. This routed was preferred as it contained only three steps which required chromatographic separation, and was readily scaled up to 200 mmol.

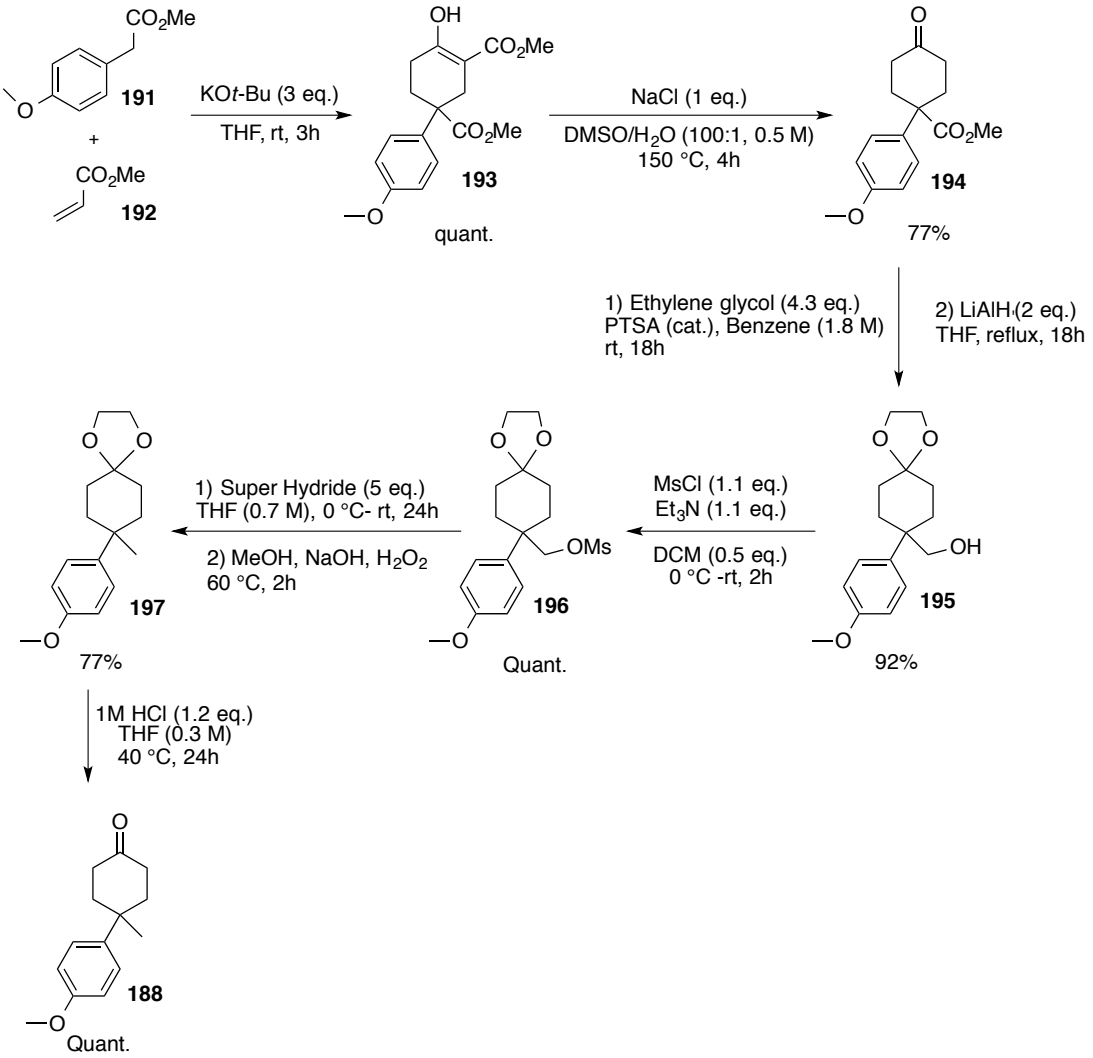

Scheme 4. 11

1.3.4. Synthesis of The Desired Enol Phosphate

With the desired ketone in hand, the next steps towards (*S*)-sporochnol were engaged, starting with the key asymmetric deprotonation reaction. As shown below (**Scheme 4.11**), rapid optimisation of the deprotonation process using the C_2-symmetric magnesium bisamide base **(*R*,*R*)-125** permitted the formation of the required **(*S*)-189** in a high 90% isolated yield and an enantioselectivity of 88:12. At this point, the absolute configuration was unconfirmed, but the major enantiomer was predicted to be the (*S*)-enantiomer by analogy with our work on silyl enol ethers.[14]

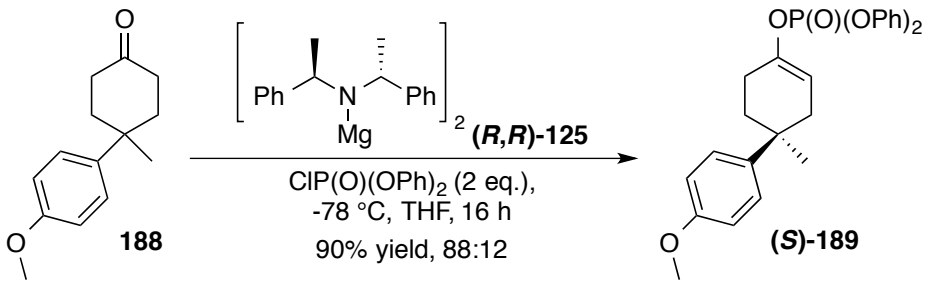

Scheme 4. 12

1.3.5. Towards the Natural Product

Pleased by the success of this first key step, formation of the enol phosphate product, further elaboration of this chiral intermediate towards (*S*)-sporochnol was begun. The strategy involved a palladium-catalysed cross coupling reaction to generate olefin **(*S*)-198**. This newly-formed olefin could be opened through a simple reductive ozonolysis to generate diol **199**, which could be dehydrated to generate the methoxy-protected sporochnol **(*S*)-200**. Final deprotectation to complete the total synthesis is well precedented through previous studies.[3]

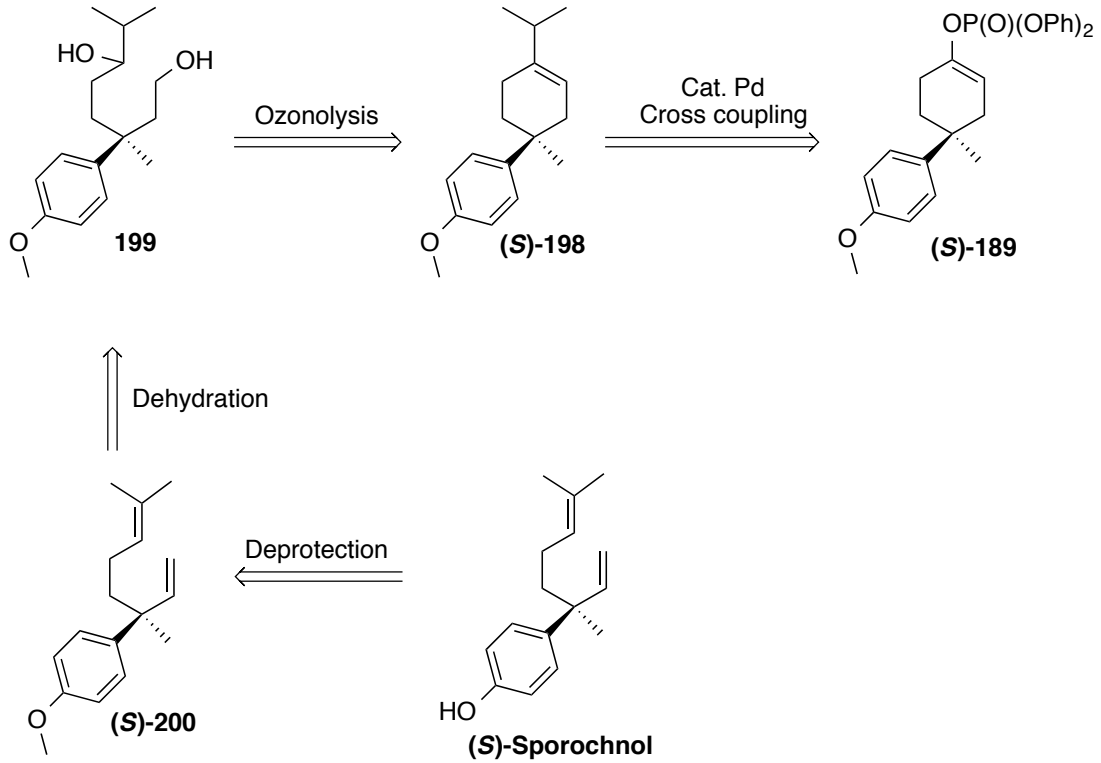

Scheme 4. 13

Having successfully synthesised the required enol phosphate, a range of palladium-catalysed transformations was envisaged to accomplish the cross-coupling reaction to generate the required *i*-propyl unit (**Scheme 4.13**). Unfortunately, no direct cross coupling of the *i*-propyl unit to give **(*S*)-198** was observed when literature-precedented conditions were employed,[20] and instead a major isomerised and non-separable by-product was generated.[14] To overcome this disappointing issue, a cross coupling reaction using an alkenyl Grignard reagent was attempted;[21] and this successfully allowed the synthesis of the diene product **(*S*)-201** in quantitative yield. Finally, after briefly screening various condition for selective reduction of the terminal olefin, Wilkinson's catalyst[22] was found to reduce the diene **(*S*)-201** to afford the desired olefin in **(*S*)-198** in an excellent 82% yield.

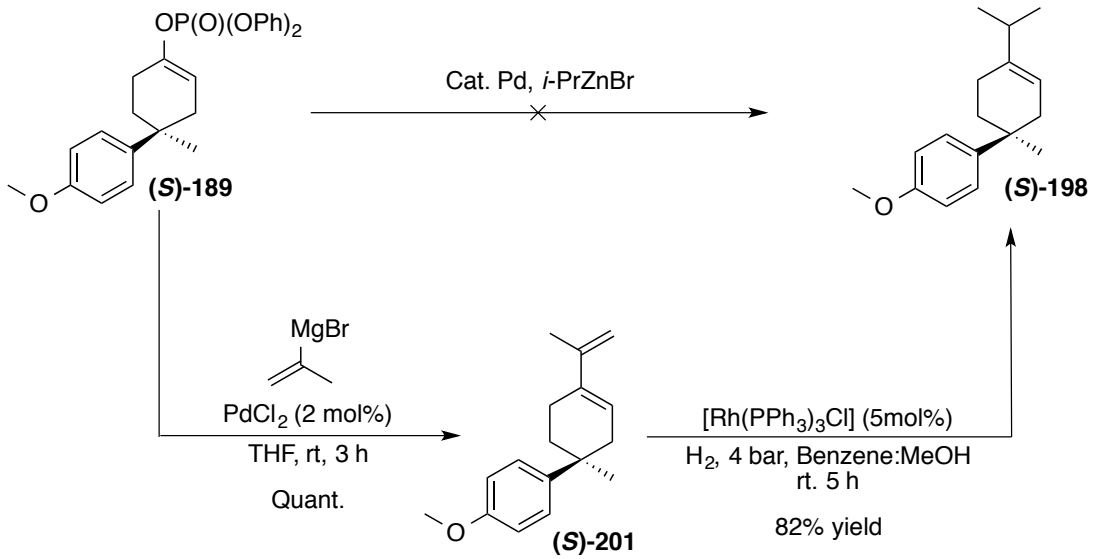

Scheme 4. 14

For the following step, ozonolysis was envisaged using literature precedented conditions (**Scheme 4.14**).[23] Unfortunately, no desired product was isolated, and due to a lack of time and material the synthesis was stopped at this stage.

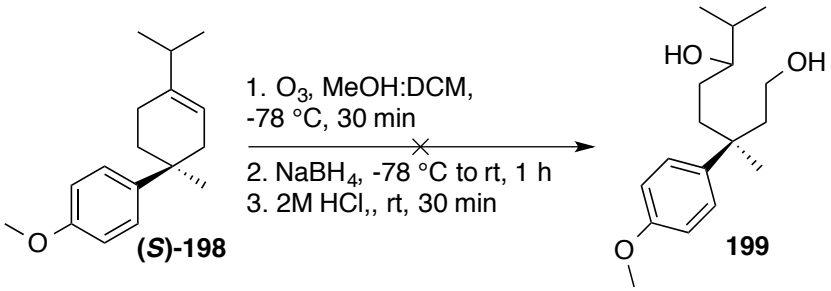

Scheme 4. 15

Although the synthesis of the natural product was not completed, key steps in the proposed route have been established. Specifically, the key asymmetric deprotoantion reaction was sucesfully carried out, proving the viability of our magnesium based process.

2. Proposed Work

As discussed, the synthesis of (*S*)-sporochnol A has been of great interest to a number of synthetic organic chemists ever since its discovery in the early 1990s. After the first synthesis by Ogasawara,[3] which also established the absolute configuration of the natural product, a range of laboratories have used this seemingly simple natural product to highlight their novel methodologies. Within our laboratory, we wished to compare our approach for the efficient synthesis of the natural product. After the group's first unsuccessful attempts at the synthesis of an enantioenriched silyl enol ether derived from a prochiral cyclobutanone species,[12] the asymmetric deprotonation reaction of a cyclohexanone derivative to afford the enol phosphate product was successfully realised.[14] With this positive result in hand, it was decided to base the synthesis of the natural product around this intermediate. Nevertheless, a series of low-yielding and troublesome steps followed the synthesis of the enol phosphate. Previous results have shown that the direct cross coupling of the *i*-propyl moiety did not allow the efficient formation of required alkene, and the first attempt at the reductive ozonolysis did not result in the formation of the desired product. Finally, the synthesis of the prochiral ketone required a total of 7 steps, with only a 55% overall yield, and, although representing a scalable route, it was nonetheless expensive and time-consuming. Furthermore, a short and scalable route would allow study of all the remaining steps and provide enough material to quickly explore a wide variety of synthetic methodologies.

Work on this second generation synthesis began with a new route to the symmetric ketone **204**. The synthesis of this ketone was dramatically simplified with application of a published transformation derived from a Robinson annulation (**Scheme 4.15**). We have previously reported the synthesis of a closely identical substrate, which was obtained from a two-step process, from extremely cheap starting materials.[24] The use of methyl vinyl ketone (**89**) with aldehyde **202** allowed, under basic conditions, the synthesis of the required eneone **203** in a low 35% isolated yield. Even though we were unable to achieve the levels of isolated yields reported (74%), the quantity of material obtained through this method was extremely high. Further reduction of the

enone using palladium on charcoal was achieved quantitatively, to furnish the required ketone **204**.[25] Unfortunately the corresponding *p*-methoxy-functionalised aldehyde was not commercially available, and hence a different approach had to be adopted from previous work (**Scheme 4.10**).

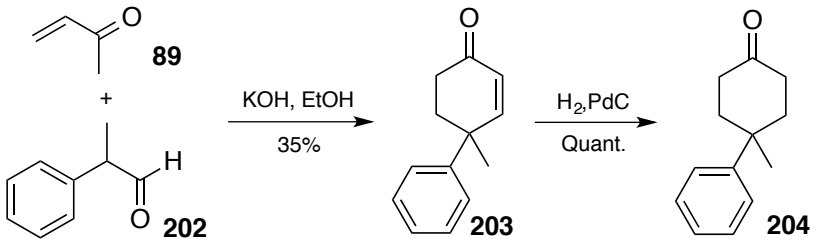

Scheme 4. 16

This strategy has the advantage of being extremely short when compared to the previous synthesis; nevertheless the installation of the *p*-hydroxy group, essential for the synthesis of sporochnol, might become problematic in later steps. Therefore, new strategies could be explored for the synthesis of *p*-methoxy-substituted aldehyde might provide a range of options for the synthesis of the required enone. Several synthetic strategies exist for the synthesis of the required *p*-methoxylated aldehyde,[26] but we were interested in a simple strategy which would allow access to the desired methoxy-protected aldehyde (**Scheme 4.16**). With this in mind, a Corey-Chaikovky epoxidation would allow the formation of the corresponding epoxide,[27] which, upon rearrangement in acidic media, would allow the synthesis of the required aldehyde **207** from a simple ketone such as **205**.[28]

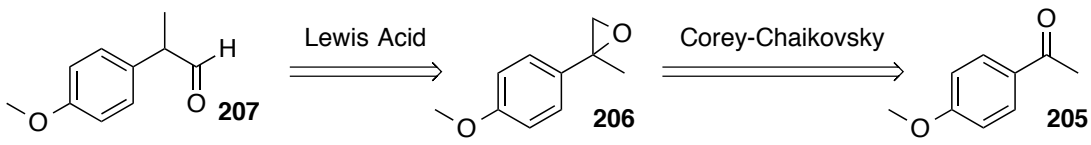

Scheme 4. 17

With the aldehyde in hand, new synthetic strategies could also be explored for the Robinson annulation reaction. The low yield obtained can be improved by exploring various bases, and the acid-catalysed Robinson annulation can be investigated.[29] If

such a strategy can be repeated efficiently for our synthesis, a much simpler synthesis of the enone could be established. Alkene reduction, followed by the asymmetric deprotonation reaction with the novel protected phenol could then be carried out, using our existing methodologies, to generate **188** and **(*S*)-189**.

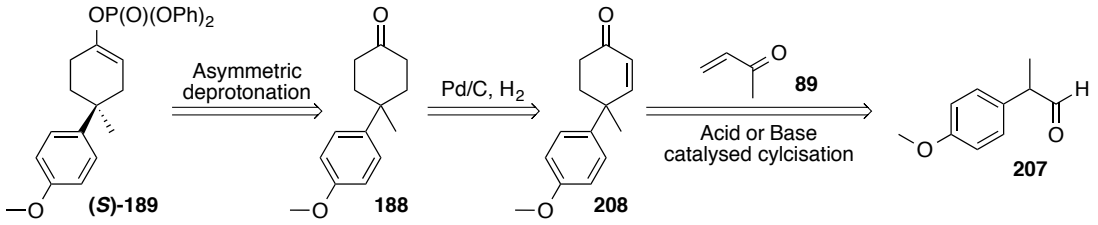

Scheme 4. 18

With the ketone in hand, the asymmetric deprotonation reaction could be attempted with the more efficient alkylmagnesium amide methodology presented in Chapter 3. We have previously described the asymmetric deprotonation reaction of ketone **204**, with the use of magnesium bisamide base **(*R*,*R*)-125**, which afforded the desired enol phosphate **(*S*)-73** in an excellent 95% yield and a good enantioselectivity of 87:13, which is comparable to the selectivity observed in the *p*-methoxy-containing substrate (*c.f.* **Scheme 4.11**).

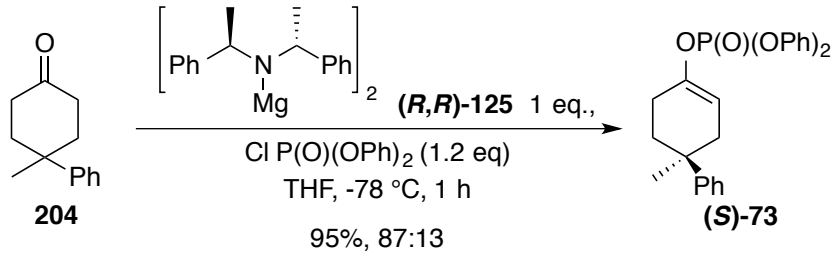

Scheme 4. 19

Having already optimised the synthesis and separation of a more simple enol phosphate ((**(*S*)-73**), and with previous work within the group carried out on the synthesis of enol phosphate **(*S*)-189**, more emphasis could be put out on the forward synthesis towards (*S*)-sporochnol A. As shown below in **Scheme 4.19**, following the

previous strategy, the desired (*S*)-sporochnol could be generated by the deprotection of the methoxy unit from the diene precursor **(*S*)-200**, derived from the dehydration of the diol **199**. This strategy relied on the ozonolysis of the cross coupled product **(*S*)-198**. We also envisaged one other route, based on the *p*-hydroxylation of the more simple **(*S*)-209** obtained form the cross coupling of the already synthesised **(*S*)-73**.[30] At this point, two pathways could be envisaged, either through the ozonolysis of the olefin **(*S*)-209** followed by the *p*-hydroxylation of **210** to generate **211**, with the final step being a dehydration. It was also proposed that the *p*-hydroxylation could be carried out on the diol **210**, derived from ozonolysis of the **(*S*)-209**. The strategy of dehydration prior to the *p*-hydroxylation was abandoned as it was considered that the presence of olefins might be problematic, since most *p*-hydroxylation methodologies require the use of strong oxidants such as hydrogen peroxide.

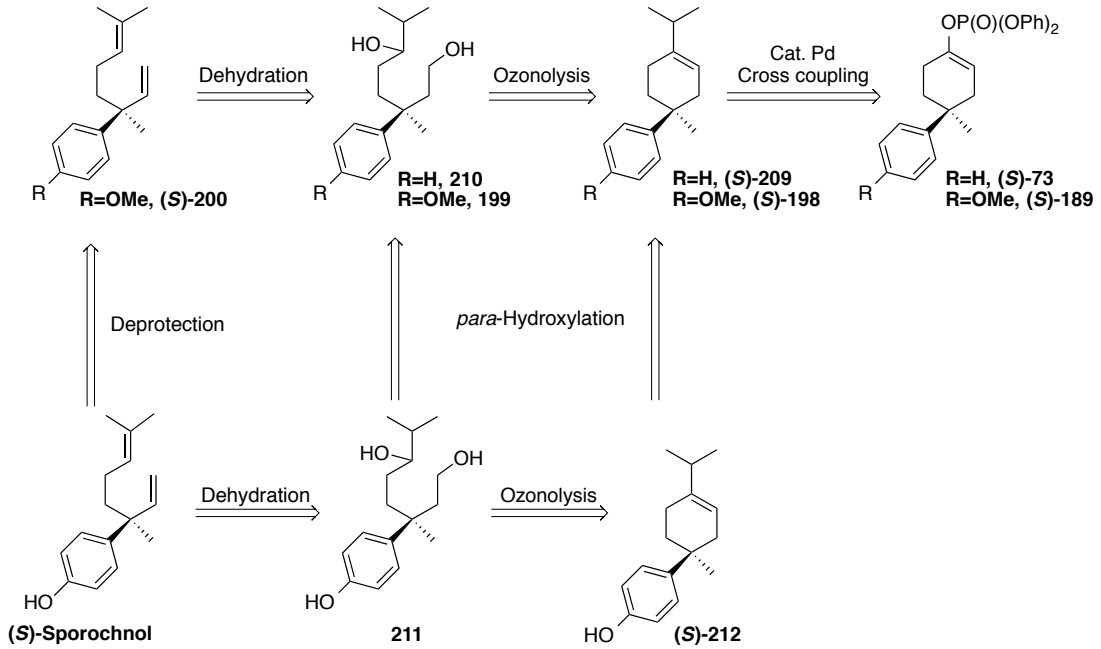

Scheme 4. 20

With a range of strategies towards the desired natural product, we proceeded in exploring the various methodologies described.

3. Results and Discussion

3.1. Synthesis of the Prochiral Ketone

3.1.1. Towards 4-methyl-4-phenylcyclohexanone 204

In the previous section was presented a range of possibilities to improve the group's synthesis of (*S*)-sporochnol. One of the first strategies described the use of a more simple and easily accessible ketone. The advantage of this strategy was the use of a readily explored and synthesised substrate (*vide supra*) and therefore only a few practical modifications were necessary in order to increase the overall yield of the transformation. Upon application of the methodology described by Zimmerman for the efficient synthesis of the enone under basic conditions, the reaction only afforded low yields.[24] These conditions, after several attempts, regardless of the purity of the reagents, allowed a maximum of 33% isolated yield of **203** (**Entry 1, Table 4.1**). Having encountered low levels of success for this transformation we turned our attention to the slightly modified acid-catalysed Robinson annulation conditions.[29] Across a range of substrates, good levels of product were obtained when H_2SO_4 was employed to mediate the reaction. Several conditions within the literature described the use of a dehydrating agent, allowing the formation of the required enone. Having explored a range of acids (TfOH, TFA) and dehydrating techniques, the best result was observed when the reaction was carried out under Dean-Stark conditions using H_2SO_4 as catalyst. However, this transformation, to our disappointment, still only afforded a poor 28% isolated (**Entry 2, Table 4.1**). Although primary studies of both base-catalysed and acid-catalysed transformations allowed a poor isolated yield of the desired enone, the scale at which these transformations were carried out and the low cost of the starting materials, allowed us to obtain sufficient product to advance the synthesis.

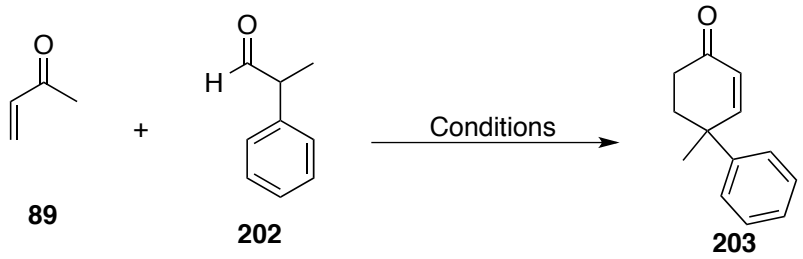

Scheme 4. 21

Entry	Conditions	Yield %
1	KOH in EtOH	33
2	H_2SO_4	28

Table 4. 1

3.1.2. Towards 4-Me-4-p-(OMe)phenyl-cyclohexanone

At this point, having obtained a poor yield for the Robinson annulation reaction, the strategy of having the *p*-methoxy group already in place was also explored. In should be noted that using the conditions described by Zimmerman (**Entry 1**, **Table 4.1**), TLC analysis of the crude reaction mixture presented least 7-8 different compounds. The specific workup described by Zimmerman had a fractional distillation step of the enone, with the boiling point of the enone given, allowing the isolation of the desired product. Unfortunately, physical data for the *p*-methoxy-substituted enone was not available. Additionally the starting aldehyde was not commerically available, thus requiring the synthesis of another intermediate. Our initial approach was to employ the Corey-Chaykovsky methodology to generate the corresponding epoxide from 4-methoxyacetophenone,[27b] which upon treatment with acid could isomerise to the desired aldehyde.[28] Preliminary studies on the Corey-Chaykovsky reaction resulted in only trace amounts of the desired product. It was discovered after further studies that the stability of the epoxide was extremely low, and it would readily rearrange (over time or simply in $CDCl_3$) to the aldehyde along with a range of by-products (**Scheme 4.21**). Therefore, studies were aimed at obtaining the final aldehyde directly, without isolation of the epoxide intermediate.

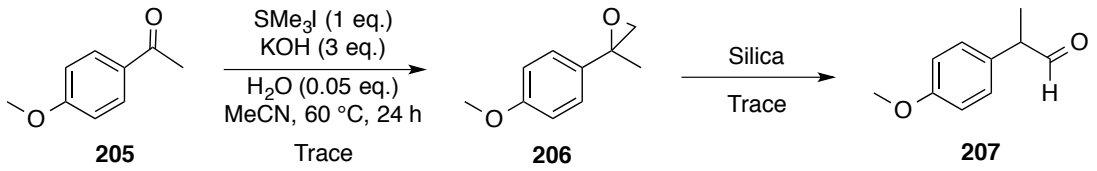

Scheme 4. 22

Although, only a low 5% yield was obtained over two steps, which was attributed to the lack of stability of the epoxide intermediate, we were keen to further explore the Robinson annulation reaction, as it remained a major challenge in our strategy. While exploring the Corey-Chaykovsky reaction, a publication by Nicolaou described an acid-catalysed methodology which described a related Robinson annulation.[31] As shown below (**Scheme 4.22**), epoxide **213**, which was obtained through a Corey-Chaykovsky reaction, was transformed to the intermediate aldehyde **214** using $InCl_3$ as a Lewis acid, followed by cyclisation using various Brønsted or Lewis acids to afford the desired enone **215** in high yield. The authors also noticed that submitting the epoxide **213** directly to PTSA catalysed the cyclisation, affording directly the desired enone product **215**.

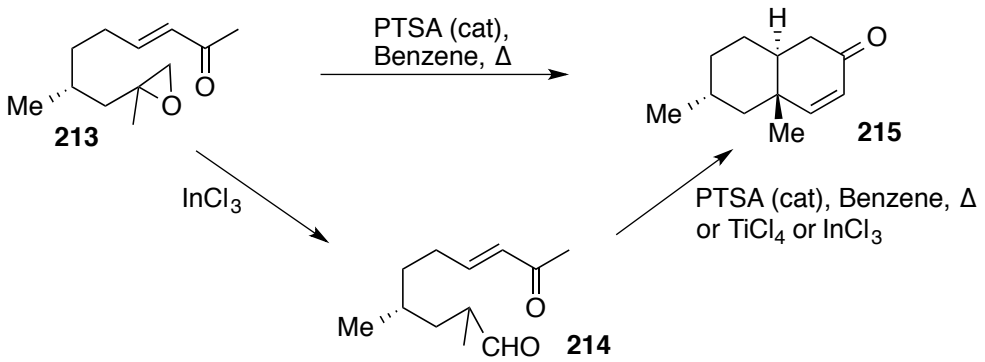

Scheme 4. 23

Although similar to our substrate, the system described by Nicolaou featured an intramolecular cyclisation using a more stable epoxide. Having a much more reactive species, we first explored the reactivity of the PTSA-catalysed cyclisation conditions using our key aldehyde obtained earlier (**Scheme 4.23**). Pleasingly, initial attempts at

the acid-catalysed reaction afforded an excellent 75% isolated yield of the required enone product (**Entry 1**, **Table 4.2**). Using toluene as solvent afforded a similar yield over a longer time period (**Entry 2**, **Table 4.2**). Surprisingly, the use of distilled methyl vinyl ketone dropped the yield dramatically to 53% yield (**Entry 3**, **Table 4.2**). This was attributed to the propensity of MVK to polymerise without the presence of a stabilizer.

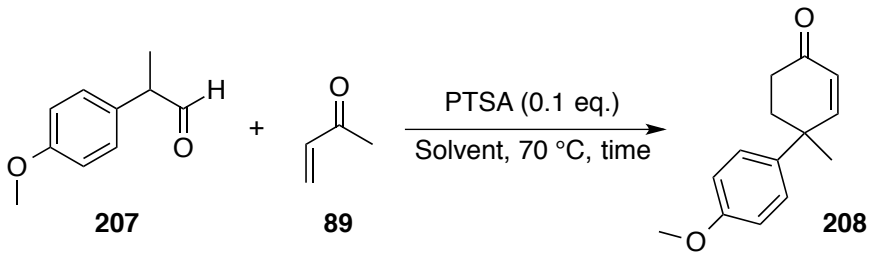

Scheme 4. 24

Entry	Solvent/time	Yield %
1	Benzene/3h	75
2	Toluene/16 h	75
3*	Toluene/16 h	53

* distilled MVK

Table 4. 2

Having accessed the enone in a high yield, we returned to the Corey-Chaykovsky reaction on *p*-methoxyaceotphenone. With further exploration of the reaction conditions it was discovered that the key aspects of the reaction were the high reactivity of the sulfur ylide (30 min half-life at room temperature) and the slow reactivity of the parent ketone.[32] It was therefore decided to carry out the reaction over a longer time period of 16 h, using double the equivalents of the ylide and starting the reaction at a lower 0 °C (**Scheme 4.24**). Under these optimised conditions, the reaction delivered full conversion to the required epoxide **206**, but unfortunately the high reactivity of the epoxide persisted, as only rapid ^{1}H NMR spectroscopic analysis allowed observation of the epoxide.

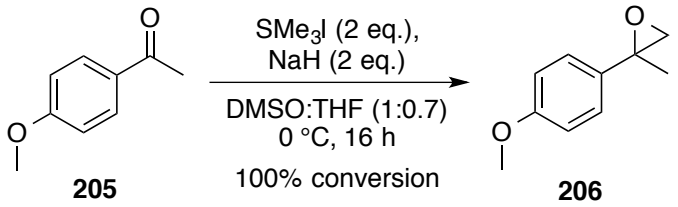

Scheme 4. 25

Nevertheless, the mixture of epoxide/aldehyde was directly subjected to the cyclisation conditions utilised previously in a sequential manner, as described by Nicoloau, affording an isolated yield of 70%, even on a 10 gram scale (**Scheme 4.25**).

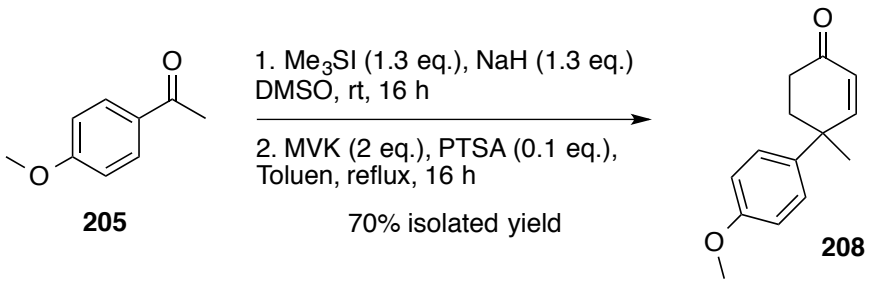

Scheme 4. 26

3.1.3. Synthesis of the Target Prochiral Ketone

Having completed the synthesis of the enone, our attention turned towards the reduction of the enone to form the prochiral ketone. This reaction was readily carried out using 2.5 mol% of palladium on charcoal catalyst, under Cook hydrogenation conditions, to afford nearly quantitative yield in the case of both enones (**Scheme 4.26**). As shown in **Entry 1**, **Table 4.3**, when the simple enone **203** was employed, the reaction afforded a quantitative yield of the desired ketone **204**, where the use of the *p*-methoxylated eneone **208** allowed a 99% isolated yield of **188**.

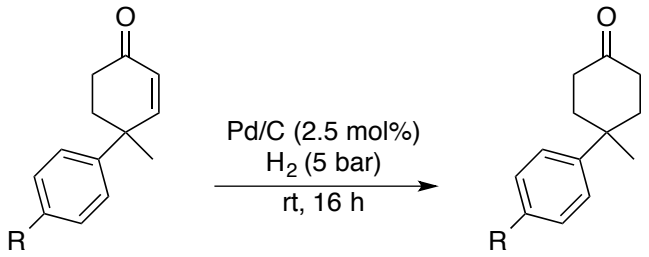

R= OMe, **208**
R= H, **203**

R= OMe, **188**
R= H, **204**

Scheme 4. 27

Entry	R	Yield %
1	H	100
2	OMe	99

Table 4. 3

3.2. Asymmetric Deprotonation Reaction

Thus far, the synthetic route contained a good level of flexibility, with two different ketone substrates available for study. Previous studies have shown that the asymmetric deprotonation reaction affords near quantitative yields, and good levels of selectivity. In our case, having defined a more efficient synthesis of the chiral base, (*i.e.* alkylmagnesium amide, Chapter 3) we envisaged the application of this base for the asymmetric deprotonation reaction to generate the enantioenriched enol phosphate. Using the optimised conditions defined in Chapter 3, the reaction was carried out on both substrates (**Scheme 4.27**). As shown below in **Table 4.4**, when the reaction was carried out using the simple ketone (**204**), the reaction afforded an excellent 89% isolated yield, with a selectivity of 87:13 (**Entry 1**), whereas when the substrate containing the *p*-methoxy unit (**188**), a near-quantitative transformation was observed (98%), and with a selectivity of 88:12 (**Entry 2**). It is important to note that the presence of the *p*-substituent did not affect the selectivity observed for the asymmetric deprotonation process.

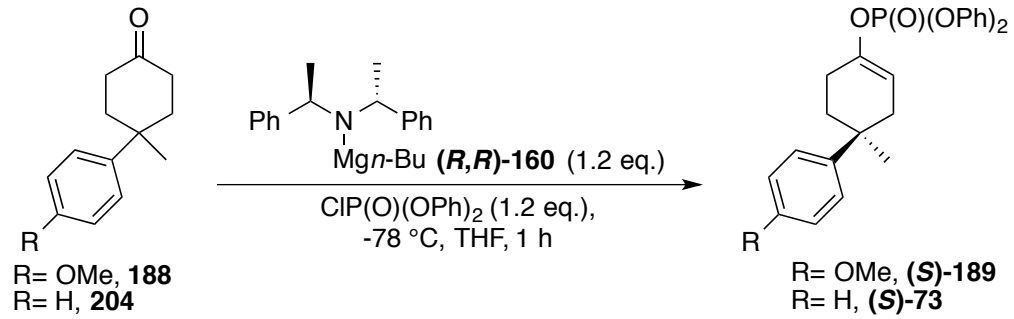

Scheme 4. 28

Entry	R	Yield %	e.r. (*S*:*R*)
1	H	89	87:13
2	OMe	98	88:12

Table 4. 4

We envisaged attempting the asymmetric deprotonation reaction using one of the *pseudo*-C_2-symmetric amides in order to achieve higher levels of selectivity for the desired transformation. Having established that the selectivity was not influenced by the *p*-substituent, studies were thus carried out using bases **(*R*,*R*)-145** and **(*R*,*R*)-147** on the simple ketone **204** (**Scheme 4.28**). Under the optimised conditions, the application of alkylmagnesium amide **(*R*,*R*)-145** afforded the enantioenriched enol phosphate **(*S*)-73** in an excellent 97% yield, and a selectivity of 88:12 (**Entry 1**, **Table 4.5**). The selectivity observed was only marginally imporved, when compared to the C_2-symmetric amide (*c.f.* **Scheme 4.27**). Finally, the application of amide **(*R*,*R*)-147** afforded a near quantitative yield, with a reduced selectivity of 86:14 **(Entry 2**, **Table 4.5)**. The scope of amides showed the narrow range of selectivity that could be obtained for this substrate. With high levels of selectivity observed when the benchmark C_2-symmetric amide **(*R*,*R*)-160** was used, this base was used for all further studies on the natural product.

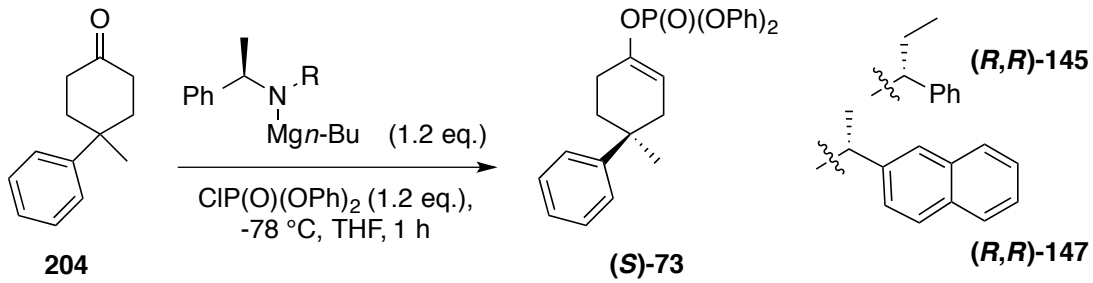

Scheme 4. 29

Entry	Amide	Yield %	er (*S*:*R*)
1	**(*R*,*R*)-145**	97	88:12
2	**(*R*,*R*)-147**	98	86:14

Table 4. 5

3.3. Synthesis of (*S*)-Sporochnol

3.3.1. Cross-Coupling Reaction of Enol Phosphates

So far, the synthesis of the *p*-methoxylated enol phosphate **(*S*)-189** has been improved, and a more simple and alternative route to novel enol phosphate **(*S*)-73**, containing the core structure of the natural product, established. Our next challenge consisted in the efficient cross-coupling of the enantioenriched enol phosphates. Previously, the direct cross-coupling of the alkylmetal species did not provide the selective synthesis of the required olefin.[14] We envisaged to further explore this reaction through an extensive study of the cross coupling reaction by exploring a range of palladium-catalysed conditions. As a result of this demand, we have developed a novel methodology for the Kumada coupling reaction of enol phosphates, and these studies will be further described in Chapter 5. Herein we present the optimised reaction conditions for the Kumada coupling reaction. As shown in **Scheme 4.29** below, the use of the Peppsi catalyst at 1 mol% allowed efficient cross-coupling using *i*-propylmagnesium bromide at room temperature. When **(*S*)-73** was used, an excellent 92% yield of the olefin **(*S*)-209** was obtained, whereas the use of enol phosphate **(*S*)-189** resulted in an excellent 80% isolated yield of the desired compound **(*S*)-198**.

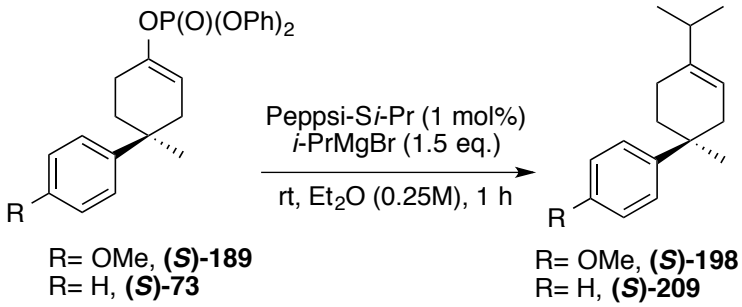

Scheme 4. 30

Entry	R	Yield %
1	**(*S*)-73**	92
2	**(*S*)-189**	80

Table 4. 6

Having efficiently synthesised the desired olefin using our developed cross-coupling methodology, we then turned our attention to the *p*-hydroxylation reaction.

3.3.2. Parahydroxylation Reaction

We envisaged attempting this transformation at the olefin step, as it was the first intermediate to have only one aryl moiety (N.B. the enol phosphate product contained two aryl units on the phosphorus). Although most *p*-hydroxylation methodologies involve the use of a strong oxidizing agent, and the presence of the substituted olefin could prove problematic, the separation and isolation of the phenol should be simplified due to the high difference in polarity with the starting material. Before attempting the reaction with the desired substrate, we first studied the reaction using a simple model substrate **216**. One of the main reasons for this choice was due to the availability of quantities of this olefin, produced during exploration of the cross coupling reaction. As shown below, when **216** was subjected to literature conditions[30] for *p*-hydroxylation, no reaction was observed and only starting material was recovered (**Scheme 4.30**). Although a range of conditions were screened in order to understand the scope and reactivity, no product was ever formed, and the starting material was returned unmodified.

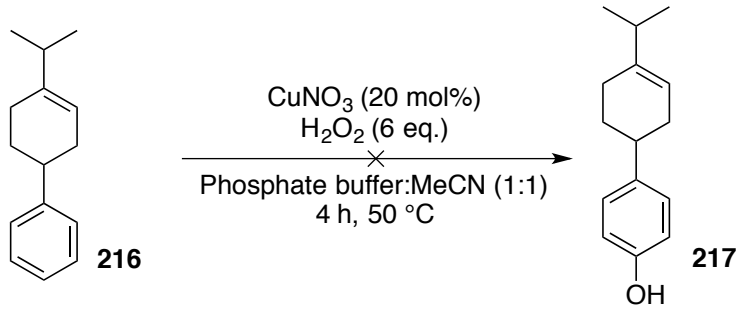

Scheme 4. 31

We therefore, re-examined the literature conditions and repeated the reaction using an alternative model substrate, anisole. In this case, the reaction proceeded with full conversion of the starting material (**Scheme 4.31**), but unfortunately the reaction furnished two inseparable and unquantifiable isomers, the *p*-hydroxylated product **219** and the *m*-hydroxylated compound **220**. This regioselectivity issue was troublesome when considered in the context of the total synthesis.

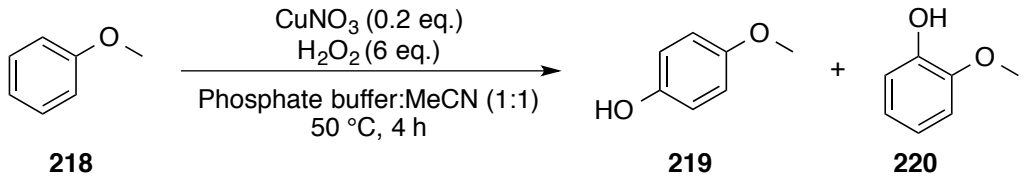

Scheme 4. 32

Disappointed by the lack of reactivity for the model substrate, and the lack of regioselectivity in the anisole system, we envisaged a slightly different approach, which consisted of *p*-borylation of the aryl group followed by oxidation of the borane using hydrogen peroxide.[33] The requisite *p*-borylation was described by Hartwig using $[Ir(COD)Cl]_2$, with a specific ligand, dtbpy, allowing the successful borylation of toluene. Compound **216** was thus submitted to the literature conditions (**Scheme 4.32**), but unfortunately no conversion to the desired compound was observed.

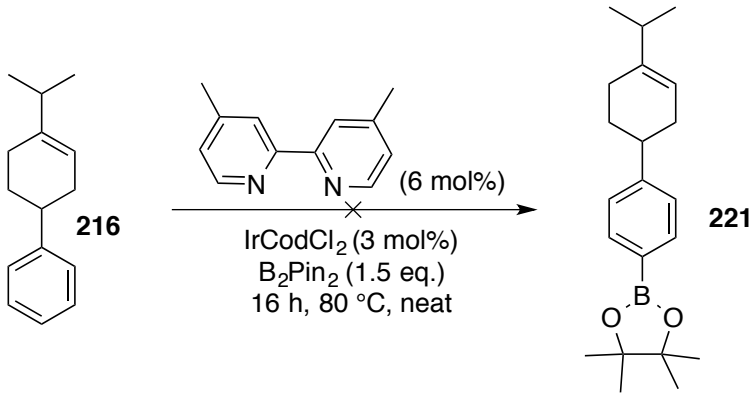

Scheme 4. 33

Having encountered a set of drawbacks along this route, it was decided to abandon this approach to concentrate on the synthetic route where the methoxy unit was already incorporated.

3.3.3. Ozonolysis of ***(S)-198***

The ozonolysis reaction was part of the route utilised by previous studies within the group, but it had not been fully explored. Therefore, it was decided to optimise the conditions using a model substrate; the simple olefin **(*S*)-209** (**Scheme 4.33**). Having abandoned the *p*-hydroxylation approach, the substrate for this route was used as a model to study further transformations. As show in **Entry 1**, **Table 4.7**, first attempts at this reaction only afforded a poor yield of 20%. Further investigation into the reaction conditions and the literature showed that the addition of a discrete quantity of MeOH allowed for higher yields.[34] In fact, it was noticed that when a mixture of DCM:MeOH (80:20) was used as the solvent, the reaction produced an isolated yield of 73% of **210** (**Entry 2**, **Table 4.7**).

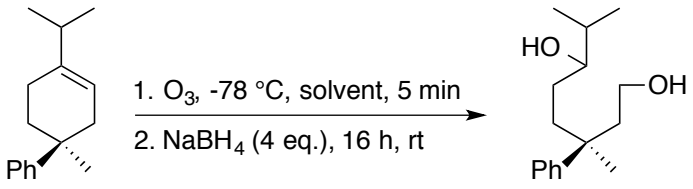

(*S*)-209 **210**

Scheme 4. 34

Entry	Solvent	Yield %
1	DCM	20
2	DCM:MeOH (8:2)	73

Table 4. 7

Although a range of other conditions were screened, such as altering the ratio of DCM:MeOH, and employing various $NaBH_4$ quenching methods, none of these provided a higher yield than that observed in **Entry 2**.

Having defined suitable conditions for the ozonolysis reaction, we turned our attention towards applying this methodology to the key olefin **(*S*)-198**. Although initial attempts gave similar yields to those observed with the model substrate, the yield of the desired product was increased through modifying the flow rate of the ozoniser. Using a smaller inlet, and a slower induction of ozone within the reaction mixture, a higher reactivity was observed. As shown in **Scheme 4.34** below, this resulted in an excellent yield of 91% of diol **199**, following work-up of the ozonolysis with $NaBH_4$.

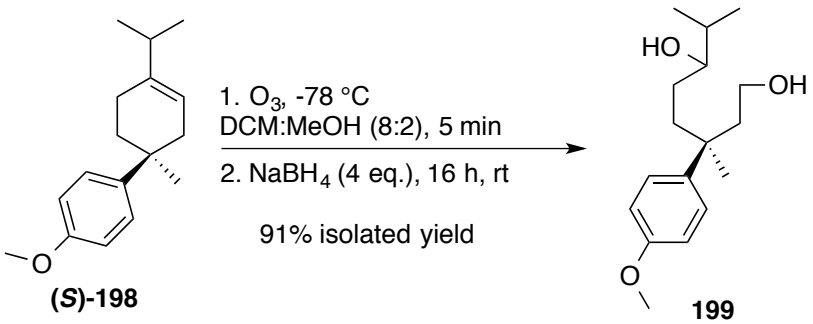

(*S*)-198 **199**

Scheme 4. 35

3.3.4. Dehydration

With the diol product in hand in excellent yield, only a double dehydration and deprotection remained in order to complete the total synthesis of (*S*)-sporochnol. With regard to the dehydration, there were two major challenges to consider while attempting this reaction, related to the two different alcohols. The secondary alcohol dehydration is required to deliver the thermodynamic olefin, and the primary alcohol, only able to form one isomer following dehydration, is more difficult to eliminate. With both aspects in mind we first envisaged an acid-mediated dehydration reaction, generally carried out under thermodynamic conditions. Unfortunately, applying various acidic conditions (H_2SO_4, TFA, Silica supported H_2SO_4, and HCl) to the diol did not afford any of the expected double dehydration. In all cases, the secondary alcohol was readily dehydrated, generating a mixture of thermodynamic and kinetic isomers, but, more importantly, the primary alcohol remained intact. In some cases, a range of by-products was also observed, and so overall, this approach was not pursued further. Next, a commerically available dehydrating agent, Martin's sulfurane,[35] was applied, and readily effected the dehydration of the secondary alcohol with high reactivity and selectivity towards the thermodynamic olefin. Unfortunately, the primary alcohol was not eliminated but was readily substituted by a nucleophilic component of the sulfurane reagent to generate compound **222** (**Scheme 4.35**).

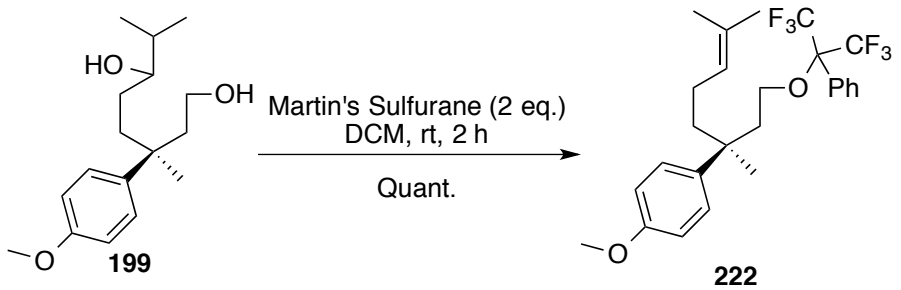

Scheme 4. 36

With the present result in hand, and the difficulties encountered with the double dehydration reaction, it was proposed to carry out each alcohol elimination sequentially. Moreover, the difficulty presented by the elimination of the primary alcohol led us to propose its elimination *via* a selenide. Nevertheless the high reactivity of Martin's sulfurane, coupled with its extraordinary selectivity for generating the desired thermodynamic olefin, made this process ideal for the secondary alcohol elimination.

As shown below, the new retrosynthetic pathway from the diol to (*S*)-sporochnol was defined through the selenide intermediate (**Figure 4.2**). Two different selenide intermediates were envisaged to carry out the reaction, a more traditional *o*-nitrophenylselenide, generating **224**, or a milder pyridylselenide intermediate, giving **223**. Both species required different oxidants to carry out the elimination reaction. Therefore, the sequence of elimination had to be carefully carried out as the presence of an alcohol or an olefin could be detrimental to the reaction sequence. Therefore, Pathway 2 would explore the direct elimination of the selenide **223** or **224** followed by dehydration using Martin's sulfurane, whereas in Pathway 1 the dehydration would be preferred first, followed by selenide elimination of **226** or **227**, giving access to the desired, methoxy-protected sporochnol **(*S*)-200**. The final deprotection reaction would then complete the total synthesis of the natural product.

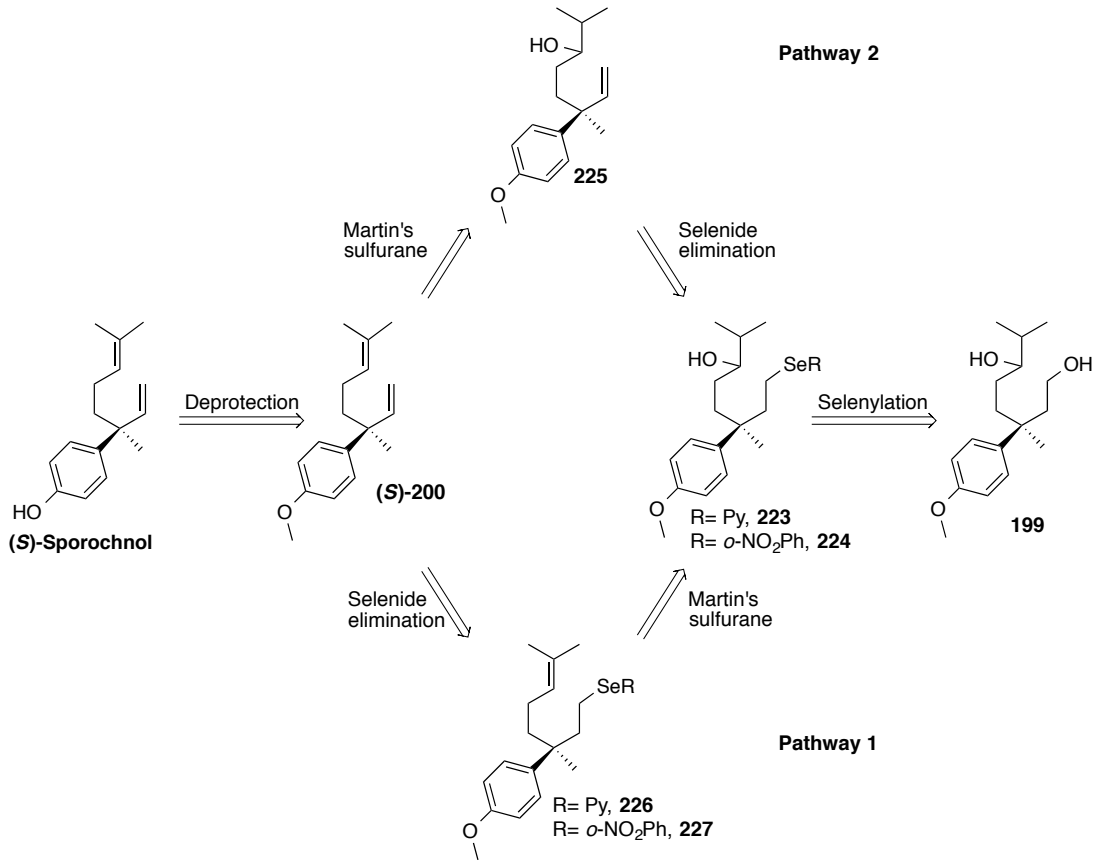

Figure 4. 2

3.3.5. Selenylation

As mentioned above, different selenides were explored for the elimination reaction. At first it was proposed to synthesise the pyridylselenide from the diol using trimethylphosphine and the corresponding diselenide.[36] This particular selenide was described as being highly reactive and extremely mild to remove, with the simple application of the Dess-Martin periodinane (DMP).[37] After extensive study, in varying the different parameters of the reaction, but having also examined the use of different phosphines, it was realised that the best levels reactivity were observed under the conditions described below in **Scheme 4.36**. Under these conditions, the reaction afforded the desired product **223** in a low 43% isolated yield.

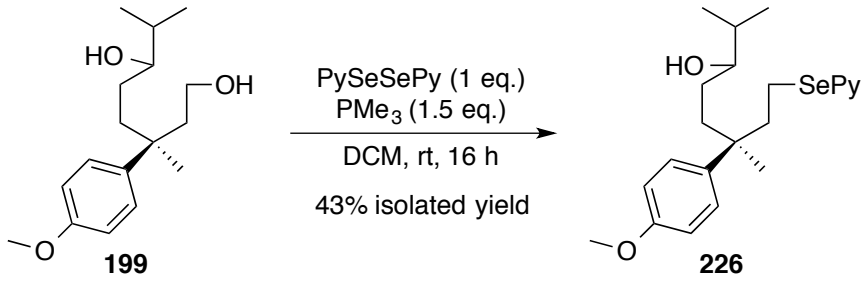

Scheme 4. 37

On the other hand, the more commonly used *o*-nitrophenylselenide was synthesised, using tri-*n*-butylphosphine and *o*-nitrophenylselenyl cyanide under room temperature conditions.[38] A brief study of the reagent loading allowed us to obtain high levels of reactivity, with an 85% isolated yield of the desired product **224** (**Scheme 4.37**). The optimisation required a subtle balance between full conversion of the starting diol compound and suppressing the generation of the di-selenated by-product produced from over-reaction of the product.

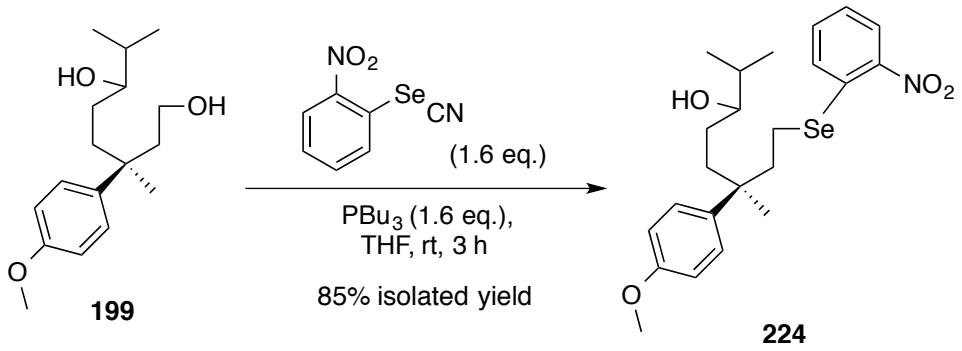

Scheme 4. 38

With both the selenides in hand, we turned our attention to exploring the different elimination pathways described in **Figure 4.2**.

3.3.6. Pathway 1

As described above in **Figure 4.2**, in Pathway 1, the well-explored dehydration of the secondary alcohol was initially carried out. Subjecting both selenides to two equivalents of Martin's sulfurane afforded the thermodynamic olefin in quantitative yield, under extremely mild reaction conditions (**Scheme 4.38**, **Table 4.8**).

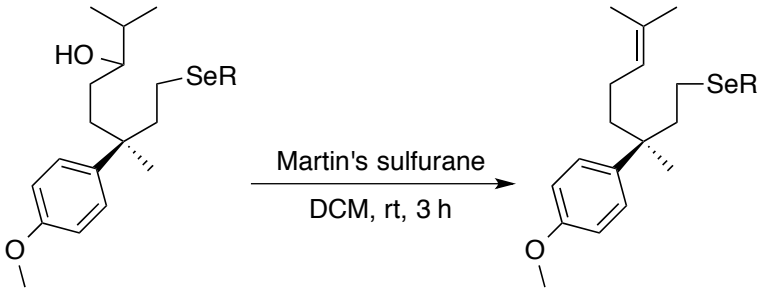

Scheme 4. 39

Entry	R	Yield %
1	*o*-NO_2-Ph	99
2	Py	98

Table 4. 8

Having readily accessed the thermodynamic olefin, the final elimination step was explored. Firstly, pyridylselenide **226** was explored, as its requirement for DMP under mild conditions was attractive. Unfortunately, only low yields were observed under literature conditions and varying the different reaction parameters did not result in any increasing reactivity towards the desired product. It was proposed that any acetic acid contained in the DMP might be detrimental, and therefore a buffered solution was employed to carry out the elimination reaction. To date, these buffered conditions correspond to the highest level of transformation for this process to furnish methoxy-protected sporochnol **(*S*)-200**. As shown below in **Scheme 4.39**, the use of potassium carbonate as buffer afforded a reasonable 55% yield of **(*S*)-200**.

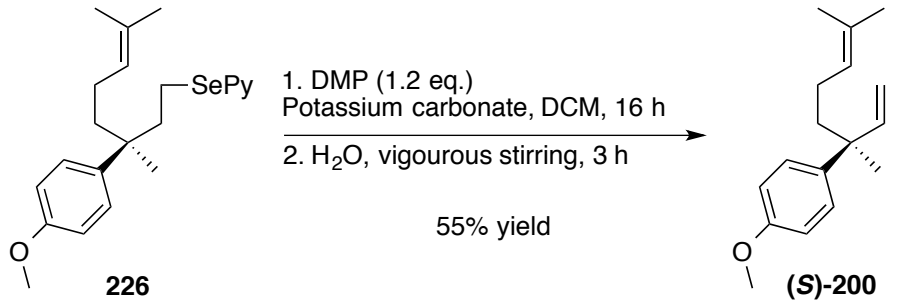

Scheme 4. 40

On the other hand, the *o*-nitrophenylselenide elimination required the use of H_2O_2 as oxidant. Although the oxidation of olefins using hydrogen peroxide is well precedented, we expected the mild conditions employed to allow a successful transformation. Unfortunately, upon application of **227** to the literature conditions, only a low 20% yield was obtained (**Scheme 4.40**). It was noted that the starting material was entirely consumed and a more polar and highly oxidized product was detected. It was assumed that the olefin might have been oxidised by selenide generated from the excess of H_2O_2 in solution, giving rise to a compound such as **228**.

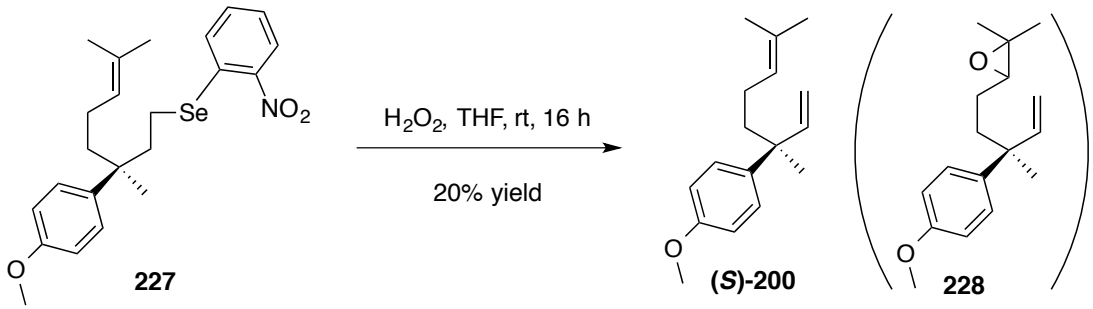

Scheme 4. 41

Although the reactions following Pathway 1 led to the desired methoxy-protected natural product, the yield observed for the selenide elimination was mediocre. We therefore turned our attention towards Pathway 2.

3.3.7. Pathway 2

This pathway consisted of eliminating the selenide in the presence of a potentially reactive secondary alcohol. The elimination of the pyridylselenide required the use of DMP, which is commonly used for the oxidation of secondary alcohols to ketones.[39] Therefore this pathway was considered unsuitable for compound **223**. Thus, the elimination of the pyridylselenide was attempted using hydrogen peroxide, but unfortunately only degradation and unidentifiable by-products were detected, effectively closing off this route for substrate **223**.

On the other hand, the elimination reaction of the *o*-nitrophenylselenide required the use of hydrogen peroxide. Although there is some literature describing the oxidation of alcohols using H_2O_2, this process is uncommon and often requires the presence of a catalyst; therefore the use of H_2O_2 was explored.[40] Pleasingly, as described below in **Scheme 4.41**, the reaction afforded a quantitative yield of the alcohol **225**.

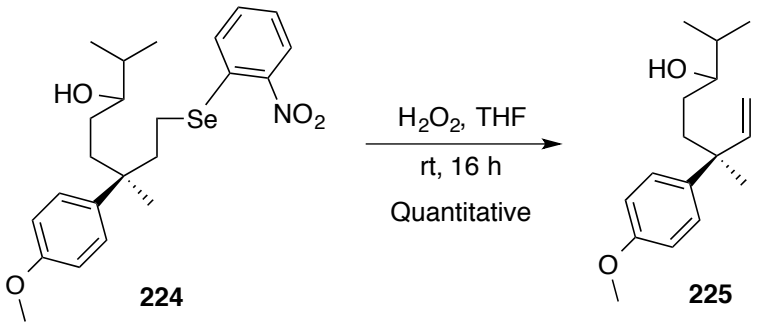

Scheme 4. 42

Having the alcohol in hand, the well-established elimination methodology using Martin's sulfurane was conducted, and, pleasingly, afforded a quantitative yield of the methoxy-protected sporochnol **(*S*)-200** (**Scheme 4.42**).

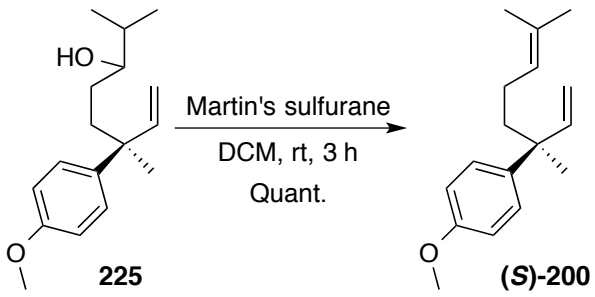

Scheme 4. 43

3.3.8. Methoxy Deprotection

Having completed the formal synthesis of Sporochnol, it was decided to carry out the literature precedented, final deprotection reaction.[3] Using literature conditions, the use of MeMgI at high temperature afforded the desired natural product (*S*)-sporochnol, in a good 85% isolated yield (**Scheme 4.43**). Optical rotation data on this sample of the natural product confirmed an enantioselectivity of 88:12 when compared to the literature,[3] and defined the absolute stereochemistry of the major enantiomer as (*S)*. We were pleased to observe that the final selectivity observed correspond to previous observations on the asymmetric deprotonation reaction (**Entry 2**, **Table 4.4**).

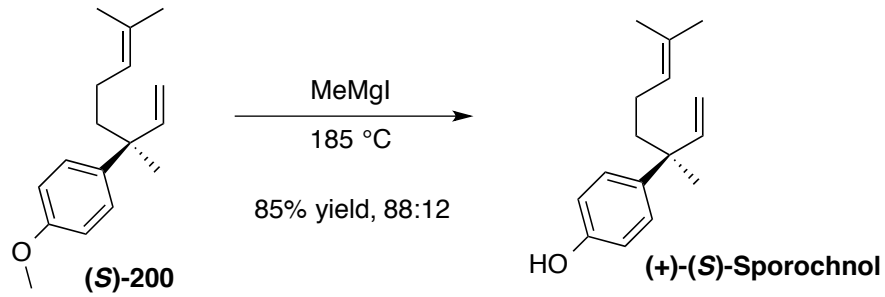

Scheme 4. 44

4. Summary

In this chapter we have presented a simple and efficient synthesis of (+)-(*S*)-sporochnol, a natural product found in marine algae. Through this synthesis our aim was to showcase the potential application of the asymmetric deprotonation reaction using our developed chiral magnesium amide bases. The final synthetic route is summarised in **Scheme 4.44**. Thus, the key prochiral ketone was obtained through a three-step process from *p*-methoxyacetophenone. The epoxidation of this ketone through the Corey-Chaykovsky method, followed by the Robinson annulation, allowed the formation of the enone **208** in 70% isolated yield over two steps, and was followed by a palladium-catalysed hydrogenation to generate **204**. The key asymmetric deprotonation reaction afforded the near quantitative formation of enantioenriched enol phosphate **(*S*)-189** in a enantiomeric ratio of 88:12. Kumada coupling of this enol phosphate resulted in the formation of the trisubstituted olefin **(*S*)-198** in a high 93% isolated yield. This cyclic olefin was then opened *via* a reductive ozonolysis, affording an excellent 91% yield of the diol **199**. Further transformation of the primary alcohol to selenide **224** was carried out in a high 85% yield, followed by elimination of the selenide unit in an excellent 89% yield to form alcohol **225**. The final dehydration of the secondary alcohol, using Martin's sulfurane, afforded the methoxy-protected natural product **(*S*)-200** in quantitative yield. Finally, the synthesis of the natural product (+)-(*S*)-sporochnol was completed in 85% after demethylation. Overall, the total synthesis was completed in 10 chemical steps with an overall yield of 36%.

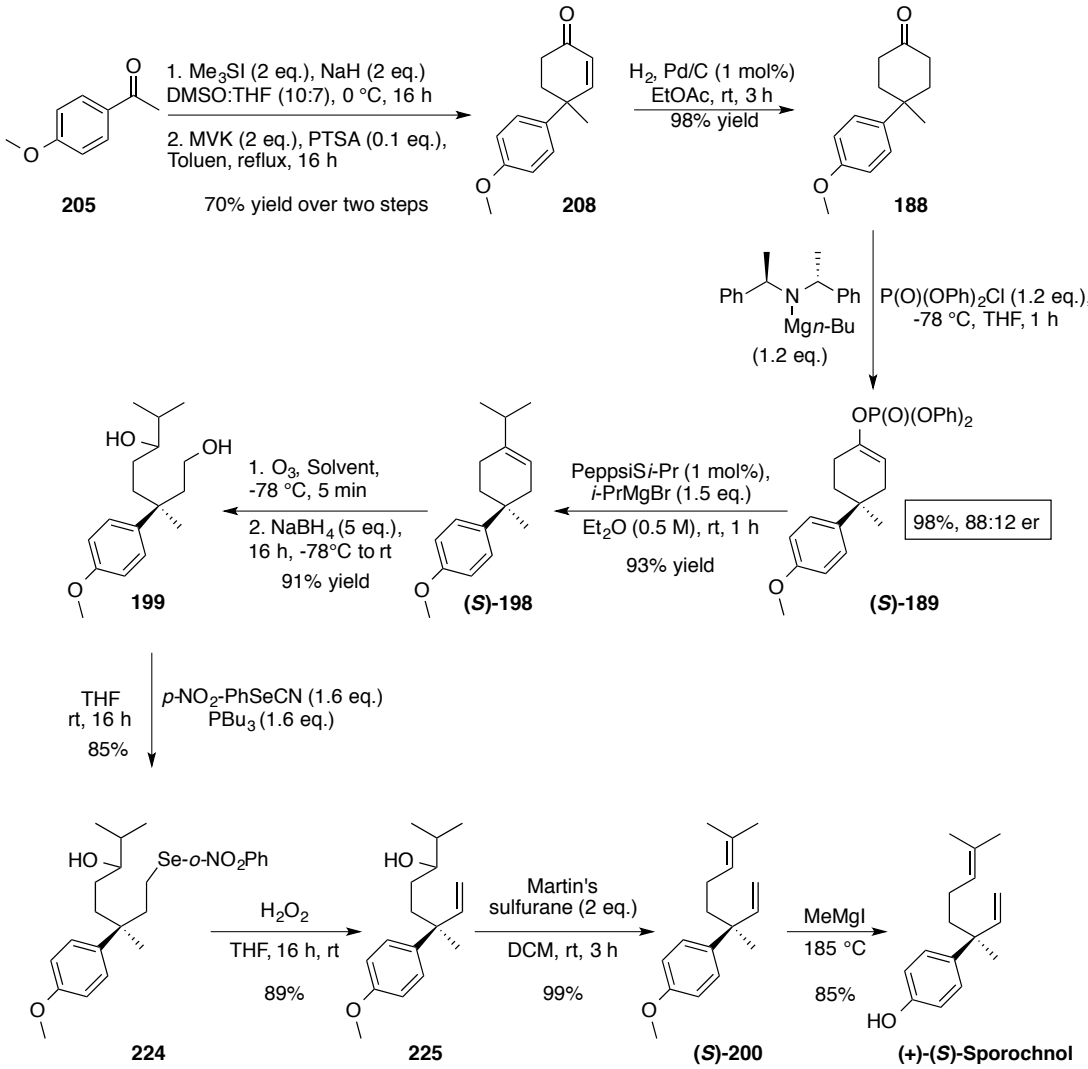
1. Me3SI (2 eq.), NaH (2 eq.)
DMSO:THF (10:7), 0 °C, 16 h
2. MVK (2 eq.), PTSA (0.1 eq.),
Toluen, reflux, 16 h
70% yield over two steps
205
208
H2, Pd/C (1 mol%)
EtOAc, rt, 3 h
98% yield
188
Ph
N
Ph
Mgn-Bu
(1.2 eq.)
P(O)(OPh)2Cl (1.2 eq.),
-78 °C, THF, 1 h
OP(O)(OPh)2
98%, 88:12 er
(S)-189
PeppsiSi-Pr (1 mol%),
i-PrMgBr (1.5 eq.)
Et2O (0.5 M), rt, 1 h
93% yield
(S)-198
1. O3, Solvent,
-78 °C, 5 min
2. NaBH4 (5 eq.),
16 h, -78°C to rt
91% yield
199
HO
OH
THF
rt, 16 h
85%
p-NO2-PhSeCN (1.6 eq.)
PBu3 (1.6 eq.)
Se-o-NO2Ph
224
H2O2
THF, 16 h, rt
89%
225
Martin's
sulfurane (2 eq.)
DCM, rt, 3 h
99%
(S)-200
MeMgI
185 °C
85%
(+)-(S)-Sporochnol

Scheme 4. 45

5. Experimental

5.1. General

All reagents were obtained from commercial suppliers (Aldrich, Lancaster, Alfa-aesar or Acros) and used without further purification, unless otherwise stated. Purification was carried out according to standard laboratory methods.[41]

- Dichloromethane, diethyl ether, hexane and toluene were obtained from an Innovative Technology, Pure Solv, SPS-400-5 solvent purification system.
- Tetrahydrofuran was dried by heating to reflux over sodium wire, using benzophenone ketyl as an indicator, then distilled under nitrogen.
- Diphenylphosphoryl chloride was distilled from CaH_2 under high vacuum and were stored over 4 Å molecular sieves under argon.
- Organometallic reagents were standardised using salicylaldehyde phenylhydrazone.[42]
- 4-methyl-4-phenylcyclohexanone,[24] was purified by recrystallization from hexane and were dried by storing *in vacuo* (0.005 mbar) for 16 h.
- Methyl vinyl ketone was distilled under argon by applying a slight vacuum and the distillate was collected in a cooled flask (-78 °C) filled and stored over 4 Å molecular sieves under argon

Thin layer chromatography was carried out using Camlab silica plates, coated with fluorescent indicator UV_{254}, and analysed using a Mineralight UVGL-25 lamp.

Flash column chromatography was carried out using Prolabo silica gel (230-400 mesh).

IR spectra were recorded on a SHIMADZU IRAFFINITY-1 spectrophotometer.

^{1}H, ^{13}C and ^{31}P NMR spectra were recorded on a Bruker DPX 400 spectrometer at 400 MHz, 100 MHz, and 162 MHz, respectively. Chemical shifts are reported in ppm. Coupling constants are reported in Hz and refer to $^{3}J_{H\text{-}H}$ interactions unless otherwise specified.

Optical rotation were obtained on Perkin Elmer 341 polarimeter using a cell with a path length of 1 dm. Concentration is expressed in g/100 cm^3.

Ozone was formed using a Fisher OZ 500 ozone generator.

High resolution mass-spectra were obtained on a Finnigan MAT900XLT, Water *xevo*, or *GCT* premier spectrometers at the EPSRC National Mass Spectrometry Services Centre, Swansea University, Swansea.

5.2. Synthesis of (*S*)-Sporochnol

5.2.1. Ketone Synthesis

Scheme 4.20

Table 4.1, **Entry 1**

A 250 mL round-bottom flask, which had been flame-dried under vacuum and purged with argon three times, was charged with methyl vinyl ketone **89** (9.0 g, 0.12 mol) and 2-phenylpropionaldehyde **202** (17 g, 0.12 mol) followed by the addition of anhydrous Et_2O (200 mL). The mixture was cooled to 0 °C, and stirred for 30 min, before slow addition (over 1 h, *via* syringe pump) of an ethanol solution (15 mL) of potassium hydroxide (2.8 g, 0.05 mol). The mixture became cloudy, then clear again, and finally developed a light yellow color. Stirring was continued for 2 h at 0 °C and then for 2 h at room temperature. The mixture was washed with 1 M HCl and water, dried ($MgSO_4$), and concentrated *in vacuo*, giving a yellow oil. Distillation of the crude product gave a colorless liquid (bp 93-94 °C, 0.25 mmHg), which crystallized (mp 30-35 °C) on standing. Recrystallization from methanol gave colorless crystals in 33% yield (8.5 g).

4-methyl-4-phenyl-4-methylcyclohexenone[24,43] **203**:

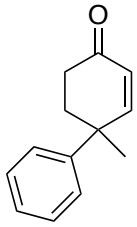

White solid, mp 41-42 °C

ν_{max}: 3085, 3058, 3024, 2964, 2869, 1683, 1600, 1222, 1110 cm^{-1}.

^{1}H NMR (500 MHz, $CDCl_3$): δ 7.38-7.34 (4H, m), 7.28-7.25 (1H, m), 6.94 (1H, d, *J* = 10.0Hz), 6.13 (1H, d, *J* = 10.0Hz), 2.44-2.38 (1H, m), 2.32-2.24 (2H, m), 2.18-2.12 (1H, m), 1.57 (3H, s).

^{13}C NMR (125 MHz, CDCl3): δ 199.53, 157.19, 145.28, 128.66, 128.58, 126.81, 126.20, 40.62, 38.13, 34.66, 27.64.

Table 4.1, **Entry 2**

A 250 mL round-bottom flask, which had been flame-dried under vacuum and purged with argon three times, was charged with methyl vinyl ketone **89** (9.0 g, 0.12 mol) and 2-phenylpropionaldehyde **202** (17 g, 0.12 mol), followed by the addition of anhydrous toluene (200 mL). Two drops of H_2SO_4 were added to the mixture and the solution was stirred under reflux using a Dean-Stark apparatus. After 2 h, no water was extracted from the mixture. The reaction was left to cool down to room temperature. The mixture was washed with twice with water, dried, and concentrated *in vacuo*, giving a yellow oil. Distillation of the crude product gave a colorless liquid (bp 93-94 °C, 0.25 mmHg), which crystallized (mp 30-35 °C) on standing. Recrystallization from methanol gave colorless crystals in 28% yield (7,2 g).

Scheme 4.21

Generation of epoxide **206** step 1:

To a 250 mL round-bottom flask, which had been flame-dried under vacuum and purged with argon three times, was added 4-methoxyacetophenone **205** (0.3 g, 2 mmol) followed by trimethylsulfonium iodide (0.4 g, 2 mmol), powdered potassium hydroxide (0.2 g, 4 mmol) and one drop of distilled H_2O (0.5 mmol) in acetonitrile (10 mL). The mixture was vigorously stirred for 3 h at 60 °C, then the reaction mixture was allowed to cool to room temperature. The mixture was filtered and the remaining solution was reduced *in vacuo*. Diethyl ether was added to the solution and solid potassium hydroxide was formed, which was removed by filtration. The organic phase was dried over Na_2SO_4, and reduced *in vacuo* to form a yellow oil. The crude mixture was directly used for the following step.

Generation of the aldehyde **207**[28] step 2:

To a 250 mL round-bottom flask, which had been flame-dried under vacuum and purged with argon three times, was added the crude mixture obtained above, and dissolved in of acetone (20 mL). Silica gel (0.5 g) was added to the reaction mixture, which was then stirred vigorously at room temperature for 2 h, before quenching the reaction by filtering the silica gel and reducing the solvent. The resulting crude pale yellow oil was purified by column chromatography on silica gel using 0-30 % Et_2O in petroleum ether (40-60 °C) to give the desired product in 5% yield (16 mg).

2-(4-methoxyphenyl)propanal,[27b] **207**:

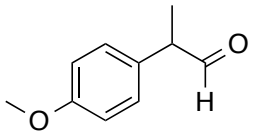

ν_{max}: 2933, 1717, 1610, 1585, 1510, 1457, 1303, 1244, 1178 cm^{-1}.

^{1}H NMR (400 MHz, $CDCl_3$) δ 9.65 (d, *J* = 1.2 Hz, 1H, CHO), 7.13 (d, *J* = 8.8 Hz, 2H, ArH), 6.92 (d, *J* = 8.4 Hz, 2H, ArH), 3.81 (s, 3H, CH_3), 3.61-3.56 (m, 1H, CH), 1.42 (d, *J* = 7.2 Hz, 3H, CH_3).
^{13}C NMR (100 MHz, $CDCl_3$) δ 201.2, 159.0, 129.6, 129.3, 114.5, 55.3, 52.1, 14.6.

Scheme 4.23
Entry 1, **Table 4.2**

A 250 mL round-bottom flask, which had been flame-dried under vacuum and purged with argon three times, was charged with commercial methyl vinyl ketone **89** (140 mg, 2 mmol) and 2-(4-methoxyphenyl)propanal, **207** (328 mg, 2 mmol), followed by anhydrous benzene (20 mL). Anhydrous *p*-toluenesulfonic acid (38 mg), was added to the mixture and the solution was stirred at 70 °C for 3 h. The solution was allowed to cool to room temperature and the dark mixture was filtered through a plug of silica gel and the filtrate reduced *in vacuo*. The yellow oil obtained was purified by column chromatography on silica gel using 0-40 % Et_2O in petroleum ether (40-60 °C) to give a colourless oil which was recrystallised from methanol, affording the desired product in 75% yield (324 mg).

Entry 2, **Table 4.2**

A 250 mL round-bottom flask, which had been flame-dried under vacuum and purged with argon three times, was charged with commercial methyl vinyl ketone **89** (140 mg, 2 mmol) and 2-(4-methoxyphenyl)propanal, **207** (328 mg, 2 mmol), followed by anhydrous toluene (20 mL). Anhydrous *p*-toluenesulfonic acid (38 mg) was added to the reaction mixture and the solution was stirred at 70 °C for 16 h. The solution was allowed to cool to room temperature and the dark mixture was filtered through a plug of silica gel and the filtrate reduced *in vacuo*. The yellow oil obtained was purified by column chromatography on silica gel using 0-40 % Et_2O in petroleum ether (40-60 °C) to give a colourless oil, which was recrystallised from methanol, affording the desired product in 75% yield (324 mg).

Entry 3, **Table 4.2**

A 250 mL round-bottom flask, which had been flame-dried under vacuum and purged with argon three times, was charged with distilled methyl vinyl ketone **89** (140 mg, 2 mmol) and 2-(4-methoxyphenyl)propanal, **207** (328 mg, 2 mmol), followed by anhydrous toluene (20 mL). Anhydrous *p*-toluenesulfonic acid (38 mg), was added to the mixture and the solution was stirred at 70 °C for 16 h. The solution was allowed to cool to room temperature and the dark mixture was filtered through a plug of silica gel and the filtrate reduced *in vacuo*. The yellow oil obtained was purified column chromatography on silica gel using 0-40 % Et_2O in petroleum ether (40-60 °C) to give a colourless oil, which was recrystallised from methanol, affording the desired product in 53% yield (229 mg).

Scheme 4.24

To a Schlenk flask, which had been flame-dried under vacuum and purged with argon three times, was added trimethylsulfonium iodide (812 mg, 4 mmol), which was dissolved in a solution of anhydrous DMSO:THF (1:0.7) and stirred at room temperature for 15 min. Sodium hydride (96 mg, 4 mmol) was added portion-wise and the mixture was stirred for 5 min at room temperature before cooling to 0 °C in an ice bath. The ylide was formed by continuous stirring for a further 30 min, before addition of 4-methoxyacetophenone **205** (0.3 g, 2 mmol) and the reaction left to warm up to room temperature overnight. The reaction was quenched by addition of water, the mixture extracted with Et_2O (3 × 20 mL) and the organic phases were combined before washing with brine (5 × 50 mL) and water, then drying over Na_2SO_4. The solvent was removed *in vacuo* to afford a pale yellow oil (328 mg), which was used without further purification.

2-(4-methoxyphenyl)-2-methyloxirane[27b] **206**:

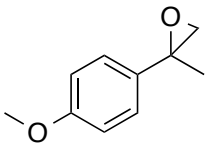

ν_{max}: 2977, 1613, 1514, 1463, 1304, 1243 cm^{-1}.
^{1}H NMR (400 MHz, $CDCl_3$): δ 7.29 (d, *J* = 8.8 Hz, 2H, ArH), 6.87 (d, *J* = 8.8 Hz, 2H, ArH), 3.79 (s, 3H, CH_3), 2.95 (d, *J* = 5.4 Hz, 1H, CH_2), 2.80 (d, *J* = 5.4 Hz, 1H, CH_2), 1.70 (s, 3H, CH_3).
^{13}C NMR (100 MHz, $CDCl_3$): δ 159.0, 133.3, 126.6, 113.8, 57.1, 56.6, 55.3, 22.

Scheme 4.25

Step 1 synthesis of the oxirane **206**:

To a Schelnk flask, which had been flame-dried under vacuum and purged with argon three times, was added trimethylsulfonium iodide (812 mg, 4 mmol), which was dissolved in a solution of anhydrous DMSO:THF (1:0.7) and stirred at room temperature for 15 min. Sodium hydride (96 mg, 4 mmol) was added portion-wise and the mixture was stirred for 5 min at room temperature before cooling to 0 °C in an ice bath. The ylide was formed by continuous stirring for a further 30 min before addition of 4-methoxyacetophenone **205** (0.3 g, 2 mmol) and the reaction left to warm up to room temperature overnight. The reaction was quenched by addition of water, the mixture extracted with Et_2O (3 × 20 mL) and the organic phases were combined before washing with brine (5 × 50 mL) and water, and dried over Na_2SO_4. The solvent was removed *in vacuo* to afford a pale yellow oil (328 mg), which was used without further purification.

Step 2 synthesis of the enone **208**:

A 250 mL round-bottom flask, which was flame-dried under vacuum and purged with argon three times, was charged with commercial methyl vinyl ketone **89** (140 mg, 2 mmol) and 2-(4-methoxyphenyl)-2-methyloxirane **206** (328 mg, 2 mmol),

followed by toluene (20 mL). Hydrous *p*-toluenesulfonic acid (38 mg), was added to the mixture and the solution was stirred at 70 °C for 16 h. The solution was allowed to cool to room temperature and the dark mixture was filtered through a plug of silica gel and the filtrate reduced *in vacuo*. The yellow oil obtained was purified by column chromatography on silica gel using 0-40 % Et_2O in petroleum ether (40-60 °C), to give a colourless oil, which was recrystallised from methanol, affording the desired product in 70% yield (302 mg).

4-(4-methoxyphenyl)-4-methylcyclohexenone[44] **208**:

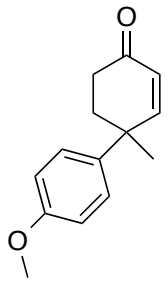

White solid

ν_{max}: 3085, 3058, 3024, 2964, 2869, 1683, 1600, 1222, 1110 cm^{-1}.

^1H NMR (400 MHz, $CDCl_3$): δ 7.13 (d, *J* = 8.8 Hz, 2H, ArH), 6.92 (d, *J* = 8.4 Hz, 2H, ArH), 6.94 (1H, d, *J*=10.0Hz, C=CH), 6.13 (1H, d, *J*=10.0Hz, C=CH), 2.44-2.38 (1H, m, CH_2), 2.32-2.24 (2H, m, CH_2), 2.18-2.12 (1H, m, CH_2), 1.57 (3H, s, CH_3).

^{13}C NMR (125 MHz, $CDCl_3$): δ 199.53, 157.19, 145.28, 128.66, 128.58, 126.81, 126.20, 40.62, 38.13, 34.66, 27.64.

Scheme 4.26

Entry 1, Table 4.3

A mixture of 4-methyl-4-phenylcyclohex-2-en-1-one **203** (2 mmol, 372 mg), and palladium on charcoal (52 mg, 2.5 mol%) were diluted in 15 mL of EtOAc. The mixture was subjected to a pressurised atmosphere of H_2 (5 bar) at room temperature for 16 h in a Cook hydrogenation apparatus. The reaction mixture was then filtered through Celite and the solution reduced *in vacuo*. The solid obtained was

recrystallised from boiling hexane to afford the desired ketone in 100% yield (375 mg).

4-Methyl-4-phenylcyclohexaone[24] **204**:

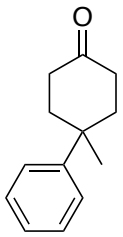

ν_{max}: 2953, 1710, 763.8 cm^{-1}

^{1}H NMR (400 MHz, $CDCl_3$): δ 7.50 – 7.35 (m, 4H, ArH), 7.28 – 7.23 (1H, ArH), 2.57 – 2.45 (m, 2H, CH_2), 2.43 – 2.27 (m, 4H, CH_2), 2.02 – 1.91 (m, 2H, CH_2), 1.33 (s, 3H, CH_3);

^{13}C NMR (100 MHz, $CDCl_3$): δ 211.0, 145.5, 128.3, 125.7, 125.1, 37.9, 37.2, 36.4, 30.6.

Entry 2, Table 4.3

A mixture of 4-(4-methoxyphenyl)-4-methylcyclohex-2-en-1-one **208** (2 mmol, 436 mg), and palladium on charcoal (52 mg, 2.5 mol%) were added to EtOAc (15 mL). The mixture was subjected to a pressurised atmosphere of H_2 (5 bar) at room temperature for 16 h in a Cook hydrogenation apparatus. The reaction mixture was then filtered through Celite and the solution reduced *in vacuo*. The solid obtained was recrystallised from boiling Hexane to afford the desired ketone in 99% yield (431 mg).

4-(4-methoxyphenyl)-4-methylcyclohexanone[14] **188**:

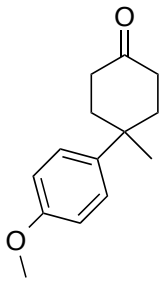

ν_{max}: 799, 891, 1184, 1246, 1707, 2868, 2899, 2959 cm^{-1}.

^1H NMR (400 MHz, $CDCl_3$): δ 7.35 (d, *J* = 8.9 Hz, 2H, ArH), 6.92 (d, *J* = 8.9 Hz, 2H, ArH), 3.81 (s, 3H, OCH_3), 2.42 - 2.48 (m, 2H, CH_2), 2.31 - 2.35 (m, 4H, CH_2), 1.89 - 1.96 (m, 2H, CH_2), 1.30 (s, 3H, CH_3).

^{13}C NMR (100 MHz, $CDCl_3$): δ 157.3, 137.5, 126.2, 113.6, 54.8, 37.9, 36.9, 36.8, 30.7, 0.52.

5.2.2. Asymmetric Deprotonation Reaction

Scheme 4.27

Entry 1, **Table 4.4**

A solution of *n*-Bu_2Mg in heptane was transferred to a Schlenk flask, which had been flame-dried under vacuum (0.005 mbar) and allowed to cool under an atmosphere of argon, and the heptane was removed *in vacuo* (0.005 mbar) until a white solid was obtained. THF (10 mL) was then added, followed by amine **(*R*,*R*)-142** (0.22 mL 1 mmol), and the solution was stirred for 0.5 h at room temperature then heated to reflux for 1.5 h and allowed to cool to room temperature. The solution of magnesium base in THF was then cooled to -78 °C under argon. The Schlenk flask was then charged with $P(O)(OPh)_2Cl$ (0.25 mL, 1.2 eq.), and the reaction mixture was stirred for a further 10 min. 4-Methyl-4-phenylcyclohexanone **204** (150 mg, 0.8 mmol) was then added as a solution in THF (2 mL) over 1 h using a syringe pump. The reaction mixture was stirred at -78 °C for 1 h before being quenched with a saturated solution of $NaHCO_3$ (10 mL) and allowed to warm to room temperature. The aqueous phase was extracted with Et_2O (50, 25, 25 mL) and the organic phases were combined and washed with 1M HCl (2 × 10 mL) to recover the amine. Removal of the solvent *in vacuo* gave an oil, which was purified by column chromatography on silica gel using 0-30% Et_2O in petroleum ether (40-60 °C) to give the desired product as a white solid in 89% yield (299 mg) and an e.r. of 87:13.

Entry 2, **Table 4.4**

A solution of *n*-Bu_2Mg in heptane was transferred to a Schlenk flask, which had been flame-dried under vacuum (0.005 mbar) and allowed to cool under an atmosphere of argon, and the heptane was removed *in vacuo* (0.005 mbar) until a white solid was obtained. THF (10 mL) was then added, followed by amine **(*R*,*R*)-142** (0.22 mL 1 mmol), and the solution was stirred for 0.5 h at room temperature then heated to reflux for 1.5 h and allowed to cool to room temperature. The solution of magnesium base in THF was cooled to -78 °C under argon. The Schlenk flask was then charged with $P(O)(OPh)_2Cl$ (0.25 mL, 1.2 eq.), and the reaction mixture was stirred for a further 10 min. 4-(4-methoxyphenyl)-4-methylcyclohexanone, **188** (174 mg, 0.8 mmol) was then added as a solution in THF (2 mL) over 1 h using a syringe pump. The reaction mixture was then stirred at -78 °C for 1 h before being quenched with a saturated solution of $NaHCO_3$ (10 mL) and allowed to warm to room temperature. The aqueous phase was extracted with Et_2O (50, 25, 25 mL) and the organic phases were combined and washed with 1M HCl (2 × 10 mL) to recover the amine. The removal of the solvent *in vacuo* gave an oil, which was purified by column chromatography on silica gel using 0-30% Et_2O in petroleum ether (40-60 °C) to give the desired product as a white solid in 98% yield (352 mg) and an e.r. of 88:12.

(*S*)-4'-methoxy-1-methyl-1,2,3,6-tetrahydro-[1,1'-biphenyl]-4-yl diphenyl phosphate[14] **(*S*)-189**:

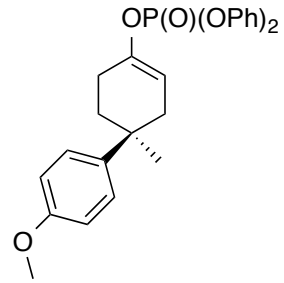

ν_{max}: 943, 1072, 1186, 1250, 1294, 1487, 1589, 1687, 2868, 2910, 2953, 3061 cm^{-1}.
^1H NMR (400 MHz, $CDCl_3$): δ 7.43 - 7.48 (m, 4H, ArH) 7.2. – 7.33 (m, 2H, Ar*H*), 7.19 -7.22 (m, 6H, ArH), 6.86 (d, 2H, *J* = 8.9 Hz, ArH), 5.66 – 5.68 (m, 1H, C=CH),

3.80 (s, 3H, OCH_3), 2.56 - 2.60 (m, 1H, CH), 2.21 – 2.26 (m, 2H, CH_2), 2.01 - 2.07 (m, 2H, CH_2), 1.81 - 1.88 (m, 1H, CH), 1.29 (s, 3H, CH3).

^{13}C NMR (100 MHz, $CDCl_3$): δ 157.7, 150.7 (d, 1C, $2J_{C-P}$ = 7.9 Hz), 147.3 (d, 1C, $2J_{C-P}$ = 9.5 Hz), 139.9, 129.9, 126.8, 125.5, 120.2 (d, 2C, $3J_{C-P}$ = 5.0 Hz), 113.7, 110.6 (d, 1C, $3J_{C-P}$ = 6.0 Hz), 55.3, 36.0, 35.6, 35.2, 28.8, 25.7 (d, 1C, $3J_{C-P}$ = 3.9 Hz).

^{31}P NMR (400 MHz, $CDCl_3$): δ -17.7.

HRMS (ESI) Calculated for $C_{26}H_{31}O_5PN$ $[M+NH_4]^+$: 468.1934; found: 468.1921.

Chiral HPLC analysis: Chiralcel OJ column, 50% IPA in *n*-hexane, 1.20 mL/min flow rate, t_R (major) = 18.1 min, t_R (minor) = 20.3 min.

$[\alpha]D^{20}$ = +17.6 º (87:13, c = 1, CHCl3). No literature data are available for comparison.

Scheme 4.28

Entry 1, **Table 4.5**

A solution of *n*-Bu_2Mg in heptane was transferred to a Schlenk flask, which had been flame-dried under vacuum (0.005 mbar) and allowed to cool under an atmosphere of argon, and the heptane was removed *in vacuo* (0.005 mbar) until a white solid was obtained. THF (10 mL) was then added, followed by amine **(*R*,*R*)-128** (0.24 mL 1 mmol), and the solution was stirred for 0.5 h at room temperature then heated to reflux for 1.5 h and allowed to cool to room temperature. The solution of magnesium base in THF was cooled to -78 °C under argon. The Schlenk flask was then charged with $P(O)(OPh)_2Cl$ (0.25 mL, 1.2 eq.), and the reaction mixture was stirred for a further 10 min. 4-Methyl-4-phenylcyclohexaone **204** (150 mg, 0.8 mmol) was then added as a solution in THF (2 mL) over 1 h using a syringe pump. The reaction mixture was stirred at -78 °C for 1 h before being quenched with a saturated solution of $NaHCO_3$ (10 mL) and allowed to warm to room temperature. The aqueous phase was extracted with Et_2O (50, 25, 25 mL) and the organic phases were combined and washed with 1M HCl (2 × 10 mL) to recover the amine. Removal of the solvent *in vacuo* gave an oil, which was purified by column chromatography on silica gel using

0-30% Et_2O in petroleum ether (40-60 °C) to give the desired product as a white solid in 97% yield (326 mg) and an e.r. of 88:12.

Entry 1, **Table 4.5**

A solution of *n*-Bu_2Mg in heptane was transferred to a Schlenk flask, which had been flame-dried under vacuum(0.005 mbar) and allowed to cool under an atmosphere of argon, and the heptane was removed *in vacuo* (0.005 mbar) until a white solid was obtained. THF (10 mL) was then added, followed by amine **(*R*,*R*)-136** (0.28 mL 1 mmol), and the solution was stirred for 0.5 h at room temperature then heated to reflux for 1.5 h and allowed to cool to room temperature. The solution of magnesium base in THF was cooled to -78 °C under argon. The Schlenk flask was then charged with $P(O)(OPh)_2Cl$ (0.25 mL, 1.2 eq.), and the reaction mixture was stirred for a further 10 min. 4-Methyl-4-phenylcyclohexaone, **204** (150 mg, 0.8 mmol) was then added as a solution in THF (2 mL) over 1 h using a syringe pump. The reaction mixture was stirred at -78 °C for 1 h before being quenched with a saturated solution of $NaHCO_3$ (10 mL) and allowed to warm to room temperature. The aqueous phase was extracted with Et_2O (50, 25, 25 mL) and the organic phases were combined and washed with 1M HCl (2 × 10 mL) to recover the amine. Removal of the solvent *in vacuo* gave an oil, which was purified by column chromatography on silica gel using 0-30% Et_2O in petroleum ether (40-60 °C) to give the desired product as a white solid in 98% yield (328 mg) and an e.r. of 86:14.

5.2.3. Kumada Coupling Reaction

Scheme 4.29

Entry 1, **Table 4.6**

To an oven-dried flask was added (*S*)-1-methyl-1,2,3,6-tetrahydro-[1,1'-biphenyl]-4-yl diphenyl phosphate **(*S*)-73** (420 mg, 1 mmol), followed by dry Et_2O (4 mL) and Peppsi S-*i*-Pr (6.8 mg, 1 mol%). The mixture was stirred under argon and *i*-PrMgBr (0.5 mL, 2.9 M in 2-MeTHF, 1.5 mmol) was rapidly added and the reaction mixture stirred at room temperature for 1 h before being quenched by addition of water. The

organic phase was extracted with Et_2O and the dried over Na_2SO_4, before being reduced *in vacuo*. The resulting dark oil was purified by column chromatography on silica gel using 0-1% Et_2O in petroleum ether (40-60 °C) to give the desired product as a colourless oil in 92% yield (197 mg).

(*S*)-4-isopropyl-1-methyl-1,2,3,6-tetrahydro-1,1'-biphenyl, **(*S*)-209**:

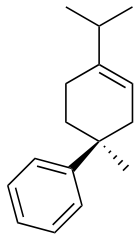

ν_{max}: 2996, 2922, 1444, 759 cm^{-1}.

^1H NMR (400 MHz, $CDCl_3$): δ 7.40 – 7.35 (m, 2H, ArH), 7.32 – 7.28 (m, 2H, ArH), 7.20 – 7.16 (m, 1H, ArH), 5.50 – 5.46 (m, 1H, C=CH), 2.52 – 2.43 (m, 1H, CH), 2.21 – 2.09 (m, 2H, CH_2), 2.05 – 1.95 (m, 1H, CH_2), 1.95 – 1.87 (m, 1H, CH_2), 1.80 – 1.71 (m, 2H, CH_2), 1.27 (s, 3H, CH_3), 0.96 (d, J = 6.8 Hz, 6H, CH_3).

^{13}C NMR (100 MHz, $CDCl_3$): δ 149.2, 142.2, 127.3, 125.2, 124.9, 116.6, 37.2, 35.8, 34.9, 34.4, 27.7, 23.3, 20.9.

HRMS (ESI) Calculated for $C_{16}H_{21}$ $[M-H]^+$: 213.1638; found: 213.1639.

Entry 2, **Table 4.6**

To an oven-dried flask was added (*S*)-4'-methoxy-1-methyl-1,2,3,6-tetrahydro-[1,1'-biphenyl]-4-yl diphenyl phosphate **(*S*)-189** (450 mg, 1 mmol), followed by dry Et_2O (4 mL) and Peppsi S-*i*-Pr (6.8 mg, 1 mol%). The reaction mixture was stirred under argon and *i*-PrMgBr (0.5 mL, 2.9 M in 2-MeTHF, 1.5 mmol) was rapidly added and the reaction was stirred at room temperature for 1 h before being quenched by

addition of water. The organic phase was extracted with Et_2O and the dried over Na_2SO_4, before being reduced *in vacuo*. The dark oil was purified by column chromatography on silica gel using 0-1% Et_2O in petroleum ether (40-60 °C) to give the desired product as a colourless oil in 80% yield (195 mg).

(*S*)-4-isopropyl-4'-methoxy-1-methyl-1,2,3,6-tetrahydro-1,1'-biphenyl (*S*)-198:

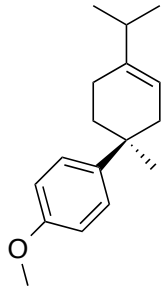

ν_{max}: 2919, 1610, 1513, 1250, 1184, 1037, 812 cm^{-1}.

^1H NMR (400 MHz, $CDCl_3$): δ 7.30 – 7.26 (m, 2H, ArH), 6.87 – 6.82 (m, 2H, ArH), 5.49 – 5.44 (m, 1H, C=CH), 3.80 (s, 3H, CH_3), 2.48 – 2.39 (m, 1H, CH), 2.20 – 2.06 (m, 2H, CH_2), 2.02 – 1.93 (m, 1H, CH_2), 1.89 – 1.81 (m, 1H, CH_2), 1.77 – 1.68 (m, 2H, CH_2), 1.23 (s, 3H, CH_3), 0.96 (d, J = 6.8 Hz, 6H, CH_3).

^{13}C NMR (100 MHz, $CDCl_3$): δ 154, 142, 141.4, 126, 116, 112, 59.9, 54, 37, 34.3, 35, 27.9, 20.9, 23.31.

HRMS (ESI) Calculated for $C_{17}H_{23}O$ $[M-H]^+$: 243.1743; found: 243.1745.

Scheme 4.30

To a solution of 4-*iso*-propyl-1,2,3,6-tetrahydro-1,1'-biphenyl **216** (200 g, 1 mmol) in acetonitrile (5 mL), was added neutral phosphate buffer (99,7 mg, 0.36 mmol) in water (5 rnL) in a round-bottom flask. To this solution was added cupric nitrate (50 mg, 0.21 mmol) in water (1 mL) followed by the addition of 30% H_2O_2 (0.7 mL, 0.00618 mol) in a single portion. The mixture was heated at 50 °C for 4 h. Upon analysis by TLC or ^1H NMR spectroscopy, only starting material was observed.

Scheme 4.31

To a round-bottom flask was added anisole **218** (1.08 g, 0.01 mole), which was dissolved in acetonitrile (10 mL), and neutral phosphate buffer (997 mg, 3.6 mmol) in water (10 mL) was added. To this mixture was added cupric nitrate (0.5 g, 2.1 mmol) in water (2 mL) followed by the addition of 30% H_2O_2 (7 mL, 0.0618 mol) in three portions. The reaction mixture was then heated to 50 °C for 4 h. After completion of the reaction, as indicated by TLC analysis, the reaction mixture was diluted with water (10 mL) and extracted with ethyl acetate (20 mL). The organic layer was washed with water and dried over Na_2SO_4 then the solvent was removed *in vacuo*. A qualitative analysis was carried out by ^{1}H NMR spectroscopy, which revealed the presence of two sets of signals corresponding to the products **219** and **220** with a combined 40% yield and a selectivity of 2:1.

4-methoxyphenol[45] **4.58**:

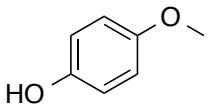

ν_{max}: 3380 cm^{-1}.

^{1}H NMR (400 MHz, $CDCl_3$) δ 6.76 - 6.82 (4H, m), 4.77 (1H, br s), 3.78 (3H, s);

^{13}C NMR (100 MHz, $CDCl_3$) δ 153.7, 149.4, 116.0, 114.9, 55.8.

2-methoxyphenol[46] **4.59**:

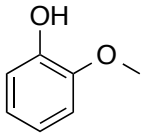

ν_{max}: 3330, 1509 cm^{-1}.

^{1}H NMR (400 MHz, $CDCl_3$) δ 6.97 - 6.94 (m, 1H), 6.91 - 6.85 (m, 3H), 5.62 (s, 1H), 3.79 (s, 3H).

^{13}C NMR (100 MHz, $CDCl_3$): δ 146.5, 145.8, 121.6, 120.3, 114.6, 110.8, 56.0.

Scheme 4.32

In a microwave vial which had been flame-dried under vacuum and purged under argon, were added 4-*iso*-propyl-1,2,3,6-tetrahydro-1,1'-biphenyl **216** (200 g, 1 mmol), B_2Pin_2 (378 mg, 1.5 mmol), $[Ir(COD)Cl]_2$ (20 mg, 0.03 mmol), 4,4'-dimethyl-2,2'-bipyridine (11 mg, 0.06 mmol) and THF (5 mL). The reaction mixture was heated in the sealed vessel at 80 °C for 16 h. The reaction mixture was then allowed to cool to room temperature and H_2O was added. The aqueous phase was extracted with Et_2O (2 × 10 mL), the organic phase was dried over Na_2SO_4, and the solvent removed *in vacuo*. The crude NMR spectrum and TLC analysis indicated only the presence of starting material.

5.2.4. Ozonolysis

Scheme 4.33

Entry 1, **Table 4.7**

To a three-necked flask was added (*S*)-4-*iso*-propyl-1-methyl-1,2,3,6-tetrahydro-1,1'-biphenyl **(*S*)-209** (428 mg, 2 mmol), followed by DCM (10 mL), and solution was cooled to -78 °C. The reaction solution was then subjected to O_3 *via* an ozoniser, until the solution turned blue (5-8 min), at which point the ozoniser was turned off and a continuous flow of O_2 was used to remove the unreacted O_3. To this solution was added $NaBH_4$ (302 mg, 8 mmol) and the mixture was left to warm slowly to room temperature overnight. The reaction mixture was quenched with a saturated solution of NH_4Cl, the aqueous phase was extracted with DCM (3 × 15 mL), the organic phase was dried over Na_2SO_4, and the solvent removed *in vacuo*. The crude mixture was purified by column chromatography on silica gel using 0-15% MeOH in DCM to give the desired product as a sticky colourless oil in 20% yield (100 mg).

(3*S*)-3,7-dimethyl-3-phenyloctane-1,6-diol 210:

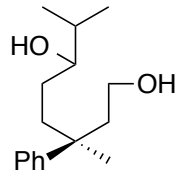

^{1}H NMR (400 MHz, $CDCl_3$): δ 7.35 – 7.30 (m, 4H, ArH), 7.22 – 7.17 (m, 1H, ArH), 3.62 – 3.53 (m, 1H, CH_2), 3.50 – 3.42 (m, 1H, CH_2), 3.26 – 3.22 (m, 1H, CH), 2.12 – 1.70 (br m, 4H, CH, CH_2), 1.36 (s, 3H, CH_3) 1.32 – 0.99 (br m, 3H, CH_2), 0.88 – 0.79 (m, 6H, CH_3).
^{13}C NMR (100 MHz, $CDCl_3$): δ 146.6, 127.7, 125.7, 125.2, 76.7, 58.9, 45.1, 44.9, 39.1, 38.9, 32.7, 28.0, 23.9, 23.7, 18.5, 16.7, 16.5.

Entry 2, **Table 4.7**

To a three-necked flask was added (*S*)-4-*iso*-propyl-1-methyl-1,2,3,6-tetrahydro-1,1'-biphenyl **(*S*)-209** (428 mg, 2 mmol), followed by DCM (8 mL) and MeOH (2 mL), and solution was cooled to -78 °C. The reaction mixture was then subjected to O_3 *via* an ozoniser until the solution turned blue (5-8 min), at which point the ozoniser was turned off and a continuous flow of O_2 was used to remove the unreacted O_3. To this solution was added $NaBH_4$ (302 mg, 8 mmol) and the mixture was left to warm slowly to room temperature overnight. The reaction mixture was quenched with a saturated solution of NH_4Cl, the aqueous phase was extracted with DCM (3 × 15 mL), the organic phase was dried over Na_2SO_4, and the solvent removed *in vacuo*. The crude mixture was purified by column chromatography on silica gel using 0-15% MeOH in DCM to give the desired product as a sticky colourless oil in 73% yield (365 mg).

Scheme 4.34

To a three-necked flask was added (*S*)-4-*iso*-propyl-4'-methoxy-1-methyl-1,2,3,6-tetrahydro-1,1'-biphenyl **(*S*)-198** (488 mg, 2 mmol), followed by DCM (8 mL) and

MeOH (2 mL), and solution was cooled to -78 °C. The reaction mixture was then subjected to O_3 *via* an ozoniser until the solution turned blue (5-8 min), at which point the ozoniser was turned off and a continuous flow of O_2 was used to remove the unreacted O_3. To this solution was added $NaBH_4$ (302 mg, 8 mmol) and the reaction mixture was left to warm slowly to room temperature overnight. The rection mixture was then quenched with a saturated solution of NH_4Cl, the aqueous phase was extracted with DCM (3 × 15 mL), the organic phase was dried over Na_2SO_4, and the solvent removed *in vacuo*. The crude mixture was purified by column chromatography on silica gel using 0-15% MeOH in DCM to give the desired product as a sticky colourless oil in 91% yield (509 mg).

(3*S*)-3-(4-methoxyphenyl)-3,7-dimethyloctane-1,6-diol 199:

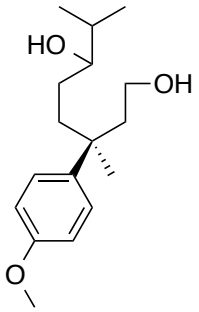

ν_{max}: 3354 (br), 2957, 1512, 1466, 1248, 1033, 829 cm^{-1}.

^1H NMR (400 MHz, $CDCl_3$): δ 7.26 – 7.21 (m, 2H, ArH), 6.88 – 6.83 (m, 2H, ArH), 3.81 (s, 3H, OCH_3), 3.62 – 3.52 (m, 1H, CH_2), 3.51 – 3.42 (m, 1H, CH_2), 3.28 – 3.21 (m, 1H, CH), 2.08 – 1.99 (m, 1H, CH), 1.90 – 1.81 (m, 1H, CH_2), 1.80 – 1.71 (m, 1H, CH_2), 1.60 – 1.56 (m, 1H, CH_2), 1.32 (s, 3H, CH_3) 1.30 – 1.22 (m, 1H, CH_2), 1.19 – 0.99 (m, 2H, CH_2), 0.87 – 0.86 (m, 6H, CH_3).

^{13}C NMR (100 MHz, $CDCl_3$): δ 156.9, 138.4, 126.7, 113.1, 59.3, 54.7, 45.4, 39.17, 38.5, 32.7, 28.1, 23.7, 18.4, 16.5.

HRMS (ESI) Calculated for $C_{17}H_{28}O_3Na$ $[M+Na]^+$: 303.1931; found: 303.1931.

Scheme 4.35

In an oven-dried flask, (3*S*)-3-(4-methoxyphenyl)-3,7-dimethyloctane-1,6-diol **199** (140 mg, 0.5 mmol) was dissolved in dry DCM (5 mL). The mixture was stirred at room temperature and Martin's sulfurane (672 mg, 1 mmol) was added to the solution and the reaction left at room temperature until complete consumption of the starting material (2 h). The solvent was removed *in vacuo* and the resulting crude oil was purified by column chromatography on silica gel using 0-5% Et_2O in petroleum ether (40-60 °C) to give the product as a pale yellow oil in quantitative yield (244 mg).

(*S*)-1-(1-((1,1,1,3,3,3-hexafluoro-2-phenylpropan-2-yl)oxy)-3,7-dimethyloct-6-en-3-yl)-4-methoxybenzene 222:

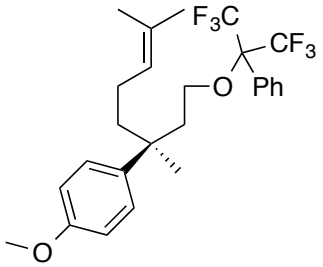

^{1}H NMR (400 MHz, $CDCl_3$): δ (ppm) 7.47 – 7.37 (m, 5H, ArH), 7.21 – 7.16 (m, 2H, ArH), 6.85 – 6.80 (m, 2H, ArH), 5.05 – 4.99 (m, 1H, C=CH), 3.80 (s, 3H, CH_3), 3.51 – 3.42 (m, 1H, CH_2), 3.39 – 3.31 (m, 1H, CH_2), 2.21 – 2.12 (m, 1H, CH_2), 2.08 – 2.00 (m, 1H, CH_2), 1.88 – 1.76 (m, 1H, CH_2), 1.72 – 1.61 (m, 2H, CH_2), 1.64 (s, 3H, CH_3), 1.59 – 1.55 (m, 1H, CH_2), 1.48 (s, 3H, CH_3), 1.29 (s, 3H, CH_3).

5.2.5. Selenylation

Scheme 4.36

A round-bottom flask was flame dried under vacuum and purged with argon. The flask was then charged with (3*S*)-3-(4-methoxyphenyl)-3,7-dimethyloctane-1,6-diol

199 (280 mg, 1 mmol), anhydrous DCM (5 mL) and 2-(phenyldiselanyl)pyridine[48] (316 mg, 1 mmol), and the mixture stirred at room temperature for 5 min before addition of a solution of trimethylphosphine (0.1 mL, 1.5 mmol). Following the last addition, the reaction was left to react overnight and the mixture was quenched with water. The aqueous phase was extracted with DCM (2 × 10 mL) and the combined organic phases were dried over Na_2SO_4 and concentrated *in vacuo*. The resulting crude oil was purified by column chromatography on silica gel using 0-60% Et_2O in petroleum ether (40-60 °C) to give the desired product as a bright yellow oil in 43% yield (180 mg).

(6*S*)-6-(4-methoxyphenyl)-2,6-dimethyl-8-(pyridin-2-ylselanyl)octan-3-ol 223:

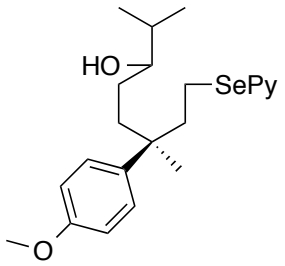

ν_{max}: 3500 (br), 2953, 1573, 1512, 1411, 1249, 1184, 1109, 1035, 829, 754 cm^{-1}.

^1H NMR (400 MHz, $CDCl_3$): δ (ppm) 8.32 - 8.40 (m, 1H, PyH), 7.43 - 7.37 (m, 1H, PyH), 7.26 - 7.22 (m, 2H, ArH), 7.21 - 7.18 (m, 1H, PyH), 7.02 – 6.98 (m, 1H, PyH), 6.89 – 6.85 (m, 2H, ArH), 3.82 (s, 3H, OCH_3), 3.25 (m, 1H, CH), 3.03 – 2.91 (m, 1H, CH_2), 2.86 – 2.78 (m, 1H CH_2), 2.24 – 2.15 (m, 1H, CH_2), 2.08 – 1.90 (m, 2H, CH, CH_2), 1.84- 1.58 (m, 2H, CH_2), 1.37 (s, 3H, CH_3), 1.31 – 1.19 (m, 2H, CH_2), 0.91 – 0.81 (m, 6H, CH_3).

^{13}C NMR (100 MHz, $CDCl_3$): δ (ppm) 156.9, 149.5, 138.0, 135.3, 126.9, 124.7, 119.6, 113.0, 54.7, 43.5, 40.7, 38.9, 38.3, 32.7, 28.3, 23.5, 23.4, 20.4, 18.5, 16.5, 16.4.

HRMS (ESI) Calculated for $C_{22}H_{32}NO_2Se$ $[M+H]^+$: 422.1593; found: 422.1592.

Scheme 4.37

A round-bottom flask was flame-dried under vacuum and purged with argon. The flask was then charged with (3*S*)-3-(4-methoxyphenyl)-3,7-dimethyloctane-1,6-diol **199** (280 mg, 1 mmol), anhydrous THF (5 mL) and 2-nitrophenyl selenocyanate (363 mg, 1.6 mmol), and the mixture stirred at room temperature for 5 min before the addition of a solution of tri-*n*-butylphosphine (0.4 mL, 1.6 mmol). Upon this addition, an intense color change was observed (dark red), and the rmixture was left to react for 3 h then quenched with water. The aqueous phase was extracted with DCM (2 × 10 mL) and the combined organic phases were dried over Na_2SO_4 and concentrated *in vacuo*. The resulting crude oil was purified by column chromatography on silica gel using 0-60% Et_2O in petroleum ether (40-60 °C) to give the desired product as a bright yellow oil in 85% yield (394 mg).

(6*S*)-6-(4-methoxyphenyl)-2,6-dimethyl-8-((2-nitrophenyl)selanyl)octan-3-ol 224:

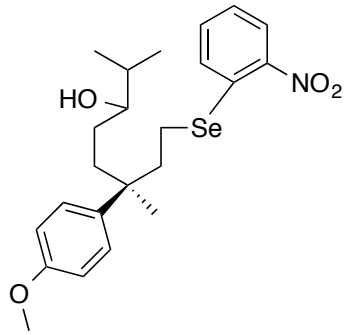

ν_{max}: 2953, 1609, 1510, 1330, 1248, 1185, 1036, 830, 729 cm^{-1}.

^1H NMR (400 MHz, $CDCl_3$): δ 8.29 – 8.25 (m, 1H, ArH), 7.42 – 7.36 (m, 1H, ArH), 7.30 – 7.23 (m, 3H, ArH), 7.16 – 7.12 (m, 1H, ArH), 6.95 – 6.89 (m, 2H, ArH), 3.83 (s, 3H, CH_3), 3.31 – 3.22 (m, 1H, CH), 2.76 – 2.67 (m, 1H, CH_2), 2.58 – 2.50 (m, 1H, CH_2), 2.15 – 1.89 (br m, 3H, CH, CH_2), 1.82 – 1.74 (m, 1H, CH_2), 1.39 (s, 3H, CH_3), 1.35 – 1.08 (br m, 3H, CH_2), 0.87 – 0.80 (m, 6H, CH_3).

^{13}C NMR (100 MHz, $CDCl_3$): δ 157.2, 146.2, 137.4, 137.3, 133.0, 128.4, 126.9, 125.9, 124.7, 113.2, 76.7, 54.7, 42.0, 40.7, 38.7, 38.6, 32.7, 28.3, 23.0, 22.8, 20.7, 18.5, 16.5, 16.4.

HRMS (ESI) Calculated for $C_{23}H_{34}N_2O_4Se$ $[M+NH_4]^+$: 482.1678; found: 482.1432.

5.2.6. Dehydration

Scheme 4.38

Entry 1, **Table 4.8**

In an oven-dried flask, (6*S*)-6-(4-methoxyphenyl)-2,6-dimethyl-8-((2-nitrophenyl)selanyl)octan-3-ol **224** (232 mg, 0.5 mmol) was dissolved in dry DCM (5 mL). The mixture was stirred while Martin's sulfurane (672 mg, 1 mmol) was added to the solution and the reaction left at room temperature until complete consumption of the starting material (3 h). The solvent was removed *in vacuo* and the crude residue was purified by column chromatography on silica gel using 0-5% Et_2O in petroleum ether (40-60 °C) to give the observed product as a pale yellow oil in 99% yield (220 mg).

(*S*)-(3-(4-methoxyphenyl)-3,7-dimethyloct-6-en-1-yl)(2-nitrophenyl)selane 227:

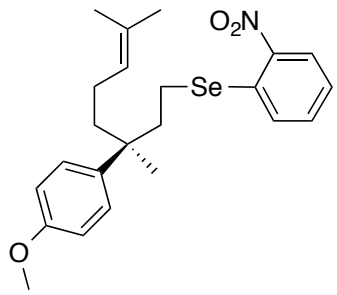

ν_{max}: 2358, 2330, 1512, 1330, 1301, 1251, 1196, 1035, 831, 731 cm^{-1}.

^{1}H NMR (400 MHz, $CDCl_3$): δ (ppm) 8.29 – 8.24 (m, 1H, ArH), 7.42 – 7.36 (m, 1H, ArH), 7.30 – 7.27 (m, 1H, ArH), 7.27 – 7.23 (m, 2H, ArH), 7.16 – 7.13 (m, 1H, ArH),

6.94 – 6.89 (m, 1H, ArH), 5.10 – 5.00 (m, 1H, C=CH), 3.84 (s, 3H, CH_3), 2.76 – 2.66 (m, 1H, CH_2), 2.59 – 2.50 (m, 1H, CH_2), 2.14 – 2.04 (m, 1H, CH_2), 1.99 – 1.89 (m, 1H, CH_2), 1.89 – 1.81 (m, 1H, CH_2), 1.80 – 1.66 (m, 2H, CH_2), 1.65 (s, 3H, CH_3), 1.61 – 1.56 (m, 1H, CH_2), 1.50 (s, 3H, CH_3), 1.40 (s, 3H, CH_3).

^{13}C NMR (100 MHz, $CDCl_3$): δ (ppm) 157.1, 137.4, 133.1, 132.9, 130.9, 128.4, 126.9, 125.9, 124.7, 123.9, 113.1, 54.7, 42.7, 41.9, 40.9, 25.2, 22.8, 22.4, 20.7, 17.0.

Entry 2, **Table 4.8**

In an oven-dried flask, (6*S*)-6-(4-methoxyphenyl)-2,6-dimethyl-8-(pyridin-2-ylselanyl)octan-3-ol **223** (210 mg, 0.5 mmol) was dissolved in dry DCM (5 mL). The mixture was stirred while Martin's sulfurane (672 mg, 1 mmol) was added to the solution and the reaction left at room temperature until complete consumption of the starting material (3 h). The solvent was removed *in vacuo* and the crude residue was purified by column chromatography on silica gel using 0-5% Et_2O in petroleum ether (40-60 °C) to give the observed product as a pale yellow oil in 98% yield (198 mg).

(*S*)-2-((3-(4-methoxyphenyl)-3,7-dimethyloct-6-en-1-yl)selanyl)pyridine 226:

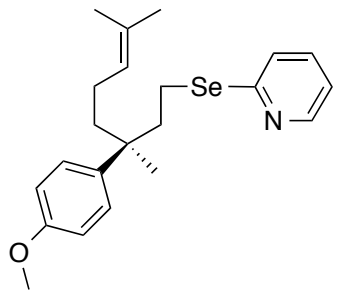

ν_{max}: 2692, 2926, 1610, 1573, 1512, 1450, 1411, 1377, 1247, 1184, 1109, 1037, 829, 752, 700 cm^{-1}.

^{1}H NMR (400 MHz, $CDCl_3$): δ (ppm) 8.43 - 8.40 (m, 1H, PyH), 7.42 - 7.37 (m, 1H, PyH), 7.27 - 7.23 (m, 2H, ArH), 7.19 - 7.16 (m, 1H, PyH), 7.02 – 6.97 (m, 1H, PyH), 6.90 – 6.85 (m, 2H, ArH), 5.08 – 5.01 (m, 1H, C=CH), 3.82 (s, 3H, OCH_3), 3.01 – 2.93 (m, 1H, CH_2), 2.84 – 2.76 (m, 1H CH_2), 2.22 – 2.13 (m, 1H, CH_2), 2.06 – 1.96

(m, 1H, CH_2), 1.90- 1.76 (m, 1H, CH_2), 1.75- 1.66 (m, 2H, CH_2), 1.64 (s, 3H, CH_3), 1.60 – 1.56 (m, 1H, CH_2), 1.49 (s, 3H, CH_3), 1.38 (s, 3H, CH_3).

^{13}C NMR (100 MHz, $CDCl_3$): δ (ppm) 157.5, 150, 149, 149.4, 135.5 135.3, 126.9, 124.6, 124.2, 119.9, 119.5, 112.9, 54.7, 43.5, 42.6, 25.1, 23.2, 27.4, 22.1, 20.6.

HRMS (ESI) Calculated for $C_{22}H_{30}NOSe$ $[M+H]^+$: 404.1487; found: 404.1479.

Scheme 4.39

In an oven-dried flask, (*S*)-2-((3-(4-methoxyphenyl)-3,7-dimethyloct-6-en-1-yl)selanyl)pyridine **226** (402 mg, 1 mmol) was dissolved in dry DCM (5 mL), and Dess-Martin periodinane (509 mg, 1.2 mmol) and potassium carbonate (690 mmol, 5 mmol) were added. The reaction mixture was stirred at room temperature overnight, followed by addition of H_2O (3 mL) then the mixture was vigorously stirred for a further 3 h before separating the phases. The aqueous phase was extracted with DCM (2 mL) and the organic phases were combined and dried over Na_2SO_4. The solvent was removed *in vacuo* and the crude residue was purified by column chromatography on silica gel using 0-3% Et_2O in petroleum ether (40-60 °C) to give the observed product as a colourless oil in 55% yield (67 mg).

(*S*)-1-(3,7-dimethylocta-1,6-dien-3-yl)-4-methoxybenzene (*S*)-200:

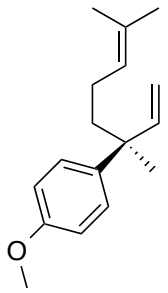

ν_{max}: 2960, 1630 1610, 1580, 1510, 1250, 1180, 1040 cm^{-1}.

^1H NMR (400 MHz, $CDCl_3$): δ 7.25 (br d, *J*=9 Hz, 2H), 6.85 (br d, J=9 Hz, 2H), 6.03 (dd, J_{trans}=17.4 Hz, J_{cis}=10.8 Hz, 1H), 5.10 (dd, J_{cis}=10.8 Hz, *J*=1.2 Hz, 1H), 5.05 (dd,

J_{trans}=17.4 Hz, J=1.2 Hz, 1H), 5.18 - 5.04 (m, 1H), 3.80 (s, 3H), 2.00 - 1.60 (m, 4H), 1.68 (br s, 3H), 1.04 (br s, 3H), 1.37 (s, 3H).
^{13}C NMR (100 MHz, $CDCl_3$): δ 157.5, 139.5, 127.6, 113.3, 147.2, 131.2, 124.7, 111.4, 55.1, 43.6 41.2 25.7 25.0, 23.3, 17.5.
HRMS (ESI) Calculated for $C_{17}H_{23}O$ $[M-H]^+$: 243.1743; found: 243.1744.

Scheme 4.40

In a round-bottom flask, (*S*)-(3-(4-methoxyphenyl)-3,7-dimethyloct-6-en-1-yl)(2-nitrophenyl)selane **227** (446 mg, 1 mmol), was dissolved in THF (5 mL), and an aqueous solution of H_2O_2 (0.5 mL, 5 mmol) was. The reaction mixture was stirred at room temperature overnight followed by the addition of H_2O (3 mL). The aqueous phase was extracted with DCM (2 mL) and the organic phases were combined and dried over Na_2SO_4. The solvent was removed *in vacuo* and the crude resiude was purified by column chromatography on silica gel using 0-3% Et_2O in petroleum ether (40-60 °C) to give the observed product as a colourless oil in 20% yield (49 mg).

Scheme 4.41

In a round-bottom flask, (6*S*)-6-(4-methoxyphenyl)-2,6-dimethyl-8-((2-nitrophenyl)selanyl)octan-3-ol **224** (464 mg, 1 mmol) was dissolved in THF (5 mL), and an aqueous solution of H_2O_2 (0.5 mL, 5 mmol) was added. The reaction mixture was stirred at room temperature overnight followed by the addition of H_2O (3 mL). The aqueous phase was extracted with DCM (2 × 2 mL) and the organic phases were combined and dried over Na_2SO_4. The solvent was removed *in vacuo* and the crude residue was purified by column chromatography on silica gel using 0-15% Et_2O in petroleum ether (40-60 °C) to give the observed product as a colourless oil in quantitative yield (262 mg).

(6*S*)-6-(4-methoxyphenyl)-2,6-dimethyloct-7-en-3-ol 225:

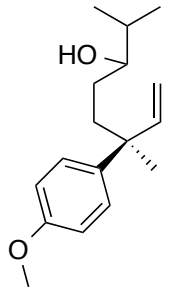

ν_{max}: 3411 (br), 2957, 2631, 2342, 1511, 1464, 1248, 1181, 1035, 912, 826 cm^{-1}.

^1H NMR (400 MHz, $CDCl_3$): δ 7.26 – 7.22 (m, 2H, ArH), 6.87 – 6.83 (m, 2H, ArH), 6.02 (dd, J_{trans}=17.4 Hz, J_{cis}=10.8 Hz, 1H), 5.9 (dd, J_{cis}=10.8 Hz, J=1.6 Hz, 1H), 5.04 (dd, J_{trans}=17.4 Hz, J=1.5 Hz, 1H), 3.80 (s, 3H, CH_3), 3.34 – 3.26 (m, 1H, CH), 2.06 - 1.89 (m, 1H), 1.80 – 1.58 (br m, 2H, CH_2), 1.36 (s, 3H), 1.34 – 1.15 (br s, 2H, CH_2), 0.9 – 0.84 (m, 6H, CH_3).

^{13}C NMR (100 MHz, $CDCl_3$): δ 157, 146.6, 141,8, 127, 112, 111, 54.7, 42.9, 36.8, 32.7, 28.7, 24.6, 18.5, 16.4, 16.3.

HRMS (ESI) Calculated for $C_{17}H_{30}NO_2$ $[M+NH_4]^+$: 280.2271; found: 280.2271.

Scheme 4.42

In an oven-dried flask, (6*S*)-6-(4-methoxyphenyl)-2,6-dimethyloct-7-en-3-ol **225** (131 mg, 0.5 mmol) was dissolved in dry DCM (5 mL). The mixture was stirred while Martin's sulfurane (672 mg, 1 mmol) was added to the solution and the reaction left at room temperature until complete consumption of the starting material (3 h). The solvent was removed *in vacuo* and the crude oil was purified by column chromatography on silica gel using 0-1% Et_2O in petroleum ether (40-60 °C) to give the observed product as a pale yellow oil in quantitative yield (122 mg).

5.2.7. Synthesis of the Natural Product

Scheme 4.43

To an oven-dried, flame-dried and argon purged microwave vial was added (*S*)-1-(3,7-dimethylocta-1,6-dien-3-yl)-4-methoxybenzene **(*S*)-200** (122 mg, 0.5 mmol). To this sealed tube was added methylmagnesium iodide (0.5 mL, 3 M in THF, 3 mmol). The solvent was removed *in vacuo*, with a slight heating at 40 °C (1 h). The vacuum was then replaced by argon, and the mixture was heated to 185 °C, resulting in the formation of a foam in the reaction mixture. Care was taken not to leave the mixture for more than 15 min when the oil bath had reached the desired temperature of 185 °C (in total 45 min), upon which the flask was allowed to cool down to room temperature and the mixture slowly diluted in Et_2O and added to a 1M HCl solution. The aqueous phase was extracted with Et_2O (2 × 5 mL) and the organic phases were combined and dried over Na_2SO_4. The solvent was removed *in vacuo* and the crude residue was purified by column chromatography on silica gel using 0-2% Et_2O in petroleum ether (40-60 °C) to give (*S*)-sporochnol as a colourless oil in 85% yield (98 mg).

(+)-(*S*)-Sporochnol

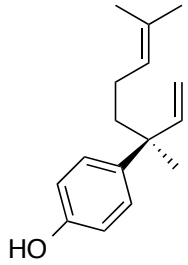

ν_{max}: 3365, 2980, 1630, 1608, 1590, 1510, 1240, 1176, 930 cm^{-1}.

^1H NMR (400 MHz, $CDCl_3$): δ (ppm) 7.19 (br d, J = 9 Hz, 2H), 6.77 (br d, J = 9 Hz, 2H), 6.01 (dd, J_{trans} = 17.2 Hz, J_{cis} = 10.8 Hz, 1H), 5.09 (dd, J_{cis} = 10.8 Hz, J = 1.4 Hz, 1H), 5.03 (dd, J_{trans} = 17.2 Hz, J =1.4 Hz, 1H), 5.18–5.00 (m, 1H), 4.78 (br, s, OH), 2.00 - 1.58 (m, 4H), 1.66 (br, s, 3H), 1.53 (br, s, 3H), 1.35 (s, 3H).

^{13}C NMR (100 MHz, $CDCl_3$): δ (ppm) 153.3, 139.7, 127.8, 114.8, 147.1, 131.3, 124.7, 111.4, 43.6, 41.1, 25.6, 25.0, 23.2, 17.5.

HRMS (ESI) Calculated for $C_{16}H_{26}NO$ $[M+NH_4]^+$: 248.2009; found: 248.2005.

6. References

1. Shen, Y.-C.; Tsai, P. I.; Fenical, W.; Hay, M. E., *Phytochemistry*, **1992**, *32* (1), 71.
2. (a) Li, Y.; Yuan, H.; Lu, B.; Li, Y.; Teng, D., *J. Chem. Res.*, **2000**, *2000* (11), 530. (b) Shan, S.; Ha, C., *Synth. Commun.*, **2004**, *34* (21), 4005. (c) Martín, R.; Buchwald, S. L., *Org. Lett.*, **2008**, *10* (20), 4561. (d) Chukicheva, I. Y.; Fedorova, I. V.; Koroleva, A. A.; Kuchin, A. V., *Chem. Nat. Compd.*, **2012**, 1.
3. Takahashi, M.; Shioura, Y.; Murakami, T.; Ogasawara, K., *Tetrahedron Asymmetry*, **1997**, *8* (8), 1235.
4. Fadel, A.; Vandromme, L., *Tetrahedron Asymmetry*, **1999**, *10* (6), 1153.
5. Ohira, S.; Kuboki, A.; Hasegawa, T.; Kikuchi, T.; Kutsukake, T.; Nomura, M. *Tetrahedron Lett* **2002**, *43* (26), 4641.
6. Kita, Y.; Furukawa, A.; Futamura, J.; Ueda, K.; Sawama, Y.; Hamamoto, H.; Fujioka, H., *J. Org. Chem.*, **2001**, *66* (26), 8779.
7. Luchaco-Cullis, C. A.; Mizutani, H.; Murphy, K. E.; Hoveyda, A. H.; *Angew. Chem. Int. Ed.*, **2001**, *40* (8), 1456.
8. Sonawane, R. P.; Jheengut, V.; Rabalakos, C.; Larouche-Gauthier, R.; Scott, H. K.; Aggarwal, V. K., *Angew. Chem. Int. Ed.*, **2011**, *50* (16), 3760.
9. Fujii, A.; Hashiguchi, S.; Uematsu, N.; Ikariya, T.; Noyori, R., *J. Am. Chem. Soc.*, **1996**, *118* (10), 2521.
10. Alibés, R.; Busqué, F.; Bardají, G. G.; de March, P.; Figueredo, M.; Font, J., *Tetrahedron Asymmetry*, **2006**, *17* (18), 2632.
11. Bassindale, M. J.; Hamley, P.; Harrity, J. P., *Tetrahedron Lett.*, **2001**, *42* (51), 9055.
12. Carswell, E. L. *PhD Thesis*; University of Strathclyde; 2005.
13. (a) Watson, A. J. B. *PhD Thesis*; University of Strathclyde; 2007. (b) Bennie, L. S. *PhD Thesis*; University of Strathclyde; 2012.
14. Monks, N. R. *PhD Thesis*; University of Strathclyde; 2013.
15. DeGraffenreid, M. R.; Bennett, S.; Caille, S.; Gonzalez-Lopez de Turiso, F.; Hungate, R. W.; Julian, L. D.; Kaizerman, J. A.; McMinn, D. L.; Rew, Y.; Sun, D.; Yan, X.; Powers, J. P., *J. Org. Chem.*, **2007**, *72* (19), 7455.

16. (a) Pearson, A. J.; Fang, X., *J. Org. Chem.*, **1997**, *62* (16), 5284. (b) Kitbunnadaj, R.; Hoffmann, M.; Fratantoni, S. A.; Bongers, G.; Bakker, R. A.; Wieland, K.; Jilali, A. el; De Esch, I. J. P.; Menge, W. M. P. B.; Timmerman, H.; Leurs, R., *Bioorg. Med. Chem.*, **2005**, *13* (23), 6309.
17. Tang, Y.; Dong, Y.; Vennerstrom, J. L., *Synthesis*, **2004**, *2004* (15), 2540.
18. Evans, D. A.; Dow, R. L.; Shih, T. L.; Takacs, J. M.; Zahler, R., *J. Am. Chem. Soc.*, **1990**, *112* (13), 5290.
19. Ling, T.; Chowdhury, C.; Kramer, B. A.; Vong, B. G.; Palladino, M. A.; Theodorakis, E. A., *J. Org. Chem.*, **2001**, *66* (26), 8843.
20. (a) Larsen, U. S.; Martiny, L.; Begtrup, M., *Tetrahedron Lett.*, **2005**, *46* (24), 4261. (b) William, A. D.; Kobayashi, Y., *J. Org. Chem.*, **2002**, *67* (25), 8771. (c) Hansen, A. L.; Ebran, J.-P.; Gøgsig, T. M.; Skrydstrup, T., *J. Org. Chem.,* **2007**, *72* (17), 6464. (d) Krasovskiy, A.; Knochel, P., *Angew. Chem. Int. Ed.*, **2004**, *43* (25), 3333. (e) Miller, J. A., *Tetrahedron Lett.*, **2002**, *43* (39), 7111.
21. Gauthier, D.; Beckendorf, S.; Gøgsig, T. M.; Lindhardt, A. T.; Skrydstrup, T., *J. Org. Chem.*, **2009**, *74* (9), 3536.
22. Blay, G.; Schrijvers, R.; Wijnberg, J. B. P. A.; de Groot, A., *J. Org. Chem.*, **1995**, *60* (7), 2188.
23. Oishi, T.; Ando, K.; Inomiya, K.; Sato, H.; Iida, M.; Chida, N., *Bull. Chem. Soc. Jpn.*, **2002**, *75* (9), 1927.
24. Zimmerman, H. E.; Jones, G., *J. Am. Chem. Soc.*, **1970**, *92* (9), 2753.
25. Hardie, W. R.; Hidalgo, J.; Halverstadt, I. F.; Allen, R. E., *J. Med. Chem.*, **1966**, *9* (1), 127.
26. (a) Sharma, A.; Sharma, N.; Kumar, R.; Sharma, U. K.; Sinha, A. K., *Chem. Commun.*, **2009**, No. 35, 5299. (b) Witten, M. R.; Jacobsen, E. N., *Org. Lett.*, **2015**, *17* (11), 2772. (c) Uhlemann, M.; Doerfelt, S.; Börner, A., *Tetrahedron Lett.*, **2013**, *54* (18), 2209.
27. (a) Tan, C. K.; Er, J. C.; Yeung, Y.-Y., *Tetrahedron Lett.*, **2014**, *55* (6), 1243. (b) Vyas, D. J.; Larionov, E.; Besnard, C.; Guénée, L.; Mazet, C., *J. Am. Chem. Soc.*, **2013**, *135* (16), 6177.
28. Lemini, C.; Ordoez, M.; Pérez-Flores, J.; Cruz-Almanza, R., *Synth. Commun.*, **1995**, *25* (18), 2695.

29. Heathcock, C. H.; Ellis, J. E.; McMurry, J. E.; Coppolino, A., *Tetrahedron Lett.*, **1971**, *12* (52), 4995.
30. Nasreen, A.; Adapa, S. R., *Org. Prep. Proced. Int.*, **2000**, *32* (4), 373.
31. Nicolaou, K. C.; Shi, L.; Lu, M.; Pattanayak, M. R.; Shah, A. A.; Ioannidou, H. A.; Lamani, M., *Angew. Chem. Int. Ed.*, **2014**, *126* (41), 11150.
32. Corey, E. J.; Chaykovsky, M., *J. Am. Chem. Soc.*, **1965**, *87* (6), 1353.
33. Murphy, J. M.; Tzschucke, C. C.; Hartwig, J. F., *Org. Lett.*, **2007**, *9* (5), 757.
34. Chevalley, A.; Prunet, J.; Mauduit, M.; Férézou, J.-P., *Eur. J. Org. Chem.*, **2013**, *2013* (36), 8265.
35. Martin, J. C.; Arhart, R. J., *J. Am. Chem. Soc.*, **1971**, *93* (17), 4327.
36. Toshimitsu, A.; Owada, H.; Uemura, S.; Okano, M., *Tetrahedron Lett.*, **1980**, *21* (52), 5037.
37. Andreou, T.; Burés, J.; Vilarrasa, J., *Tetrahedron Lett.,* **2010**, *51* (14), 1863.
38. Sharpless, K. B.; Young, M. W., *J. Org. Chem.*, **1975**, *40* (7), 947.
39. Tohma, H.; Kita, Y., *Adv. Synth. Catal.*, **2004**, *346* (23), 111.
40. Noyori, R.; Aoki, M.; Sato, K., *Chem. Commun.*, **2003**, No. 16, 1977.
41. Perrin, D., D.; Armarego, W. L. F., *Purification of Laboratory Chemicals*; Pergaman: Oxford; 1988.
42. Love, B. E.; Jones, E. G., *J. Org. Chem.*, **1999**, *64* (10), 3755–3756.
43. Hyde, A. M.; Buchwald, S. L., *Angew. Chem. Int. Ed.*, **2008**, *47* (1), 177.
44. Rieke, R. D.; Schulte, L. D.; Dawson, B. T.; Yang, Sheng S., *J. Am. Chem. Soc.*, **1990** , *112* (23), 8388.
45. Rayment, E. J.; Summerhill, N.; Anderson, E. A., *J. Org. Chem.*, **2012**, *77* (16), 7052.
46. Xiao, Y.; Xu, Y.; Cheon, H.-S.; Chae, J., *J. Org. Chem.*, **2013**, *78* (11), 5804.

Chapter 5
Kumada Coupling Reaction

Content

1. Introduction

The use of magnesium-based chemistry, under kinetic or asymmetric deprotonation conditions, has allowed us to access enol phosphates in a highly efficient and facile fashion. We have shown in Chapter 1 that the use of carbon-centred bases allowed a highly efficient transformation of ketones into kinetic enol phosphate products, whereas the use of chiral magnesium amide bases, discussed in Chapters 2 and 3, allowed us to develop methodology providing high levels of both enantioselectivity and reactivity towards enantioenriched enol phosphates. This strategy has been successfully applied to the efficient total synthesis of the natural product (*S*)-sporochnol.

1.1. Towards the Target Compound

While exploring the synthesis of this natural product, we were pleased to observe that the desired enantioenriched enol phosphate was successfully synthesised using our chiral magnesium amide bases (**Scheme 4.27**). On the other hand, one other key step required the successful transformation of this enol phosphate product into a substituted olefin, using a cross-coupling reaction with a secondary alkyl partner. Unfortunately, previous studies within the group had shown that such a transformation was low yielding and, moreover, did not allow selective formation of the olefin **(*S*)-198** (**Scheme 5.1**).[1] It was noted that with the use of the Negishi coupling, even with a variety of ligands generally reported for this transformation in the literature,[2] an isomerised olefin, **(*S*)-229**, was detected alongside the desired product. The other drawback from that reaction was also the fact the desired compound **(*S*)-198**, was not separable from the isomerised by-product **(*S*)-229**. Therefore, it was envisaged to carry out a cross-coupling of an alkenyl Grignard reagent,[3] followed by the selective reduction of the terminal olefin.[4] Having developed an efficient route towards these valuable enol phosphates, we were interested in further exploring their reactivity by studying the range of conditions

described within the literature for the cross-coupling of enol phosphates with alkylmetal partners.

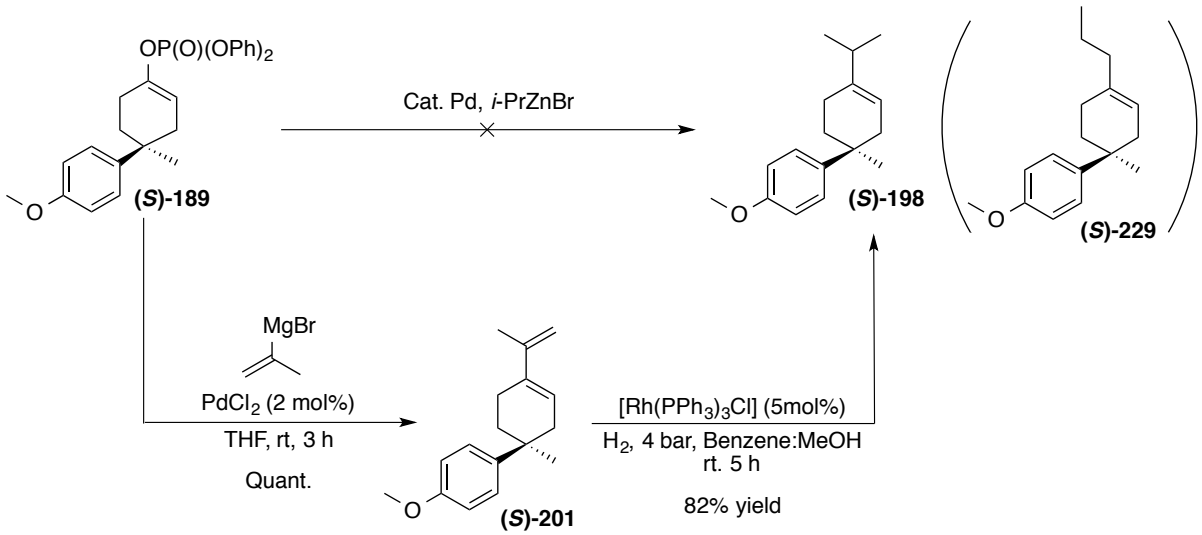

Scheme 5. 1

In fact, this isomerisation reaction has been extremely well studied within the cross-coupling of secondary alkyl organometallic reagents such as organozinc and organomagnesium species.[5] For example, Organ has studied the selectivity between branched product and rearrangement towards a linear product through experimental observations and DFT calculations of the potential energy surface of the various transition states.[6] While using simple model substrates such as bromobenzene **230** and *i*-PrZnBr, along with Peppsi catalysts, the resulting organopalladium intermediate **231** afforded the desired branched product **232**, and the linear product **233**. This suggest that the branched product was obtained through ß-hydride elimination of the *i*-propyl unit, and the rearrangement of the olefin to **235** occurred before the oxidative addition step to generate **236**, which upon reductive elimination allowed the formation of the linear compound.

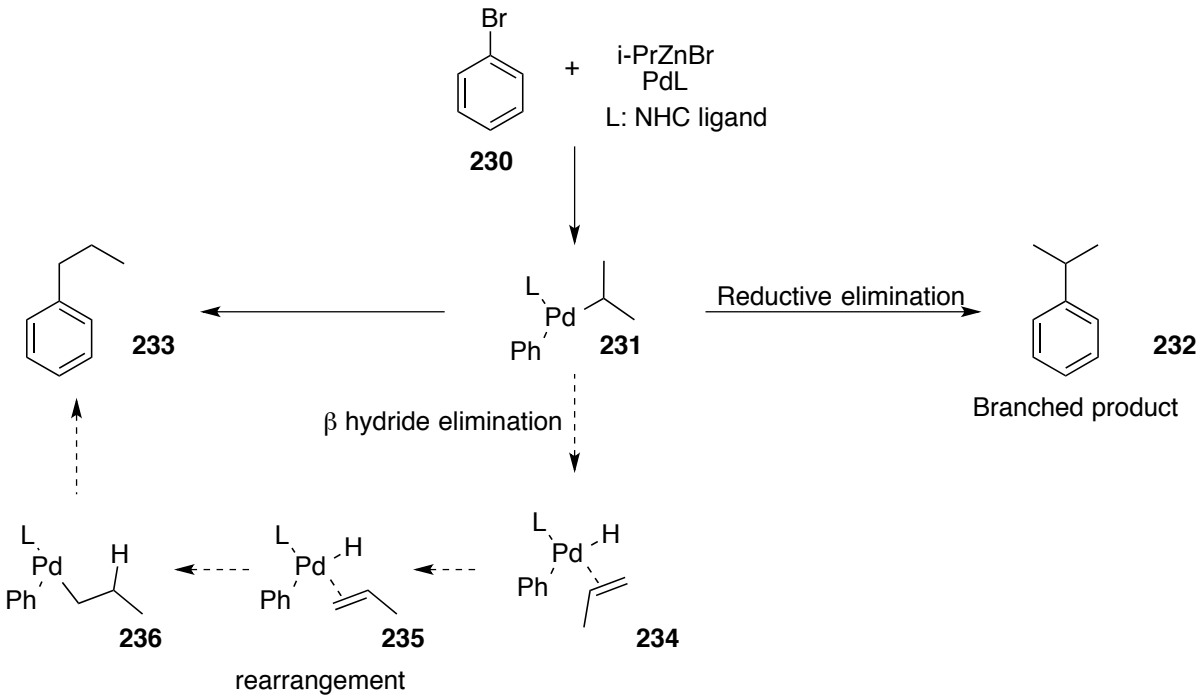

Scheme 5. 2

In their studies, the authors revealed that although the energy for the transition state leading to the branched product is lower, the reductive elimination step of the linear compound **236** was lower in energy and was also a faster reaction. The authors also cited research on cationic Pd^{II} species for the olefin polymerisation process;[7] where the ß-hydride elimination of primary and secondary alkyl units was generally faster than insertion into the olefin (i.e. **235** to **236**). Furthermore, within their examples, they have shown that subtle changes on the ligand could greatly influence the selectivity obtained.

1.2. Cross Coupling of Enol Phosphates

1.2.1. Transition Metal Catalysis

On the other hand, very few examples describe the use of enol phosphates in cross-coupling reactions with alkyl units. The very first example of cross-coupling with enol phosphates was described by Blaszack in 1976, where the use of the enol phosphate **16**, with the cuprate *n*-Bu_2CuLi, allowed access to olefin **237** in a

moderate 59% yield (**Scheme 5.3**). It was also described that modification of the cuprate species to a simpler Me_2CuLi allowed only a low 11% yield of the corresponding product.

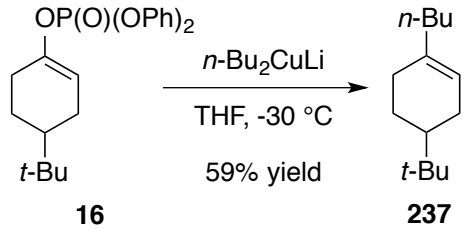

Scheme 5. 3

The use of transition metal-catalysed cross-coupling of enol phosphates with Grignard reagents was reported by Miller in 2002.[8] For example, cross-coupling of the enol phosphate **69** with *n*-BuMgCl resulted in the formation of olefin **238** in high yield (**Scheme 5.4**).

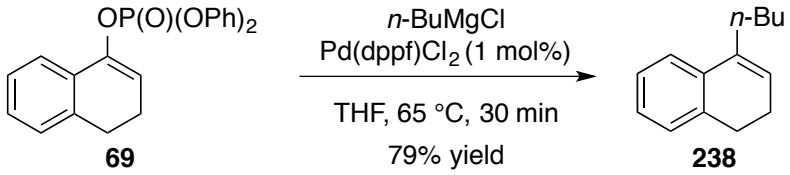

Scheme 5. 4

Within their earlier studies in 2007, Skrydstrup described an efficient process for the cross-coupling of commercially-available organozinc reagents such as **239**, **242** and **245** with simple enol phosphates (**75**, **241**, and **244** respectively) under palladium catalysed conditions.[9] As shown below in **Scheme 5.5**, 75% and 80% yields were obtained of compounds **5.12** and **5.18**, respectively, whereas only a 50% yield was observed in the formation of **5.15**. Skrydstrup studied this cross-coupling on a range of aryl- and alkyl-substituted enol phosphates, affording moderate to good levels product in most cases.

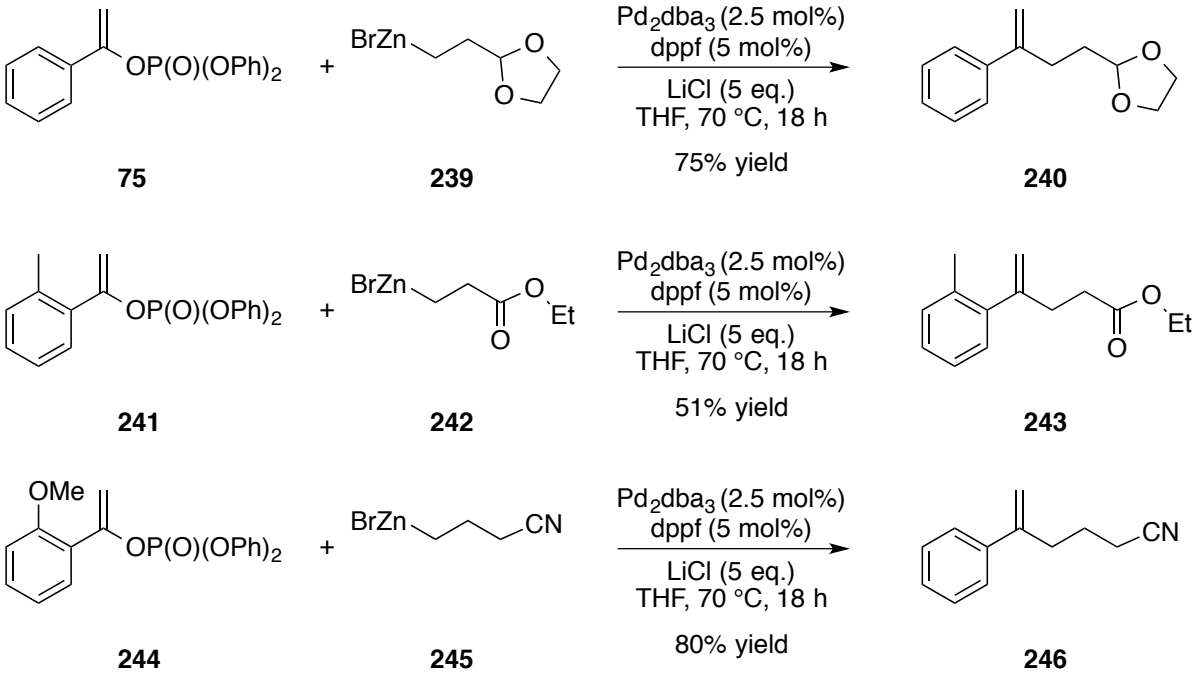

Scheme 5. 5

A year later, in 2008, a cross-coupling catalysed by $Fe(acac)_2$ was used by Cahiez, to couple an enol phosphate with a Grignard reagent.[10] As shown below in **Scheme 5.6** (a), the use of a dienol phosphate, such as **247**, afforded the olefin **248** using 1 mol% of $Fe(acac)_3$ and octylmagnesium chloride. These conditions have been applied to a range of different dienol phosphate systems, and in all cases afforded good to excellent levels of reactivity and selectivity, with only a minor loss in selectivity observed. In 2009, Skrydstrup, applied a similar iron-catalysed cross-coupling of aryl phosphate species using an alkyl Grignard reagent, **Scheme 5.6** (b), generating up to 88% yield of the alkylated pyrimidine compound **250**.[11]

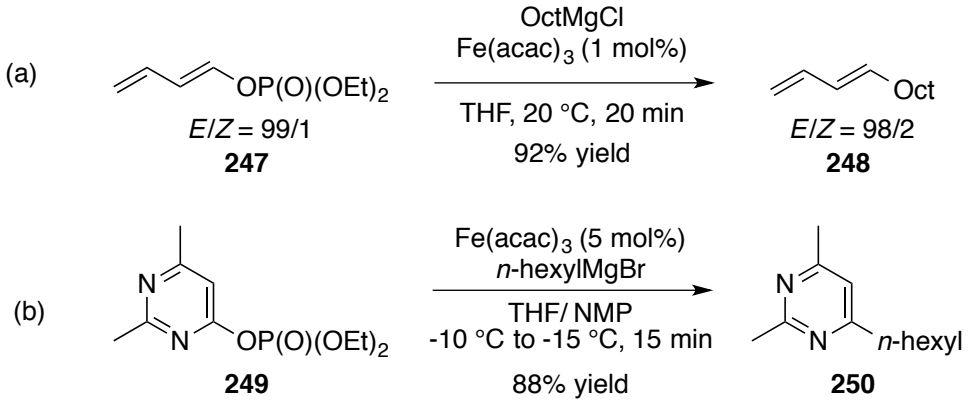

Scheme 5. 6

1.2.2. Un-activated Enol Phosphates

As shown above, most examples used in cross-coupling with the phosphate moiety to an alkyl partner require the use of either an organozinc or organomagnesium species. Moreover, very few cross-coupling reactions have been reported on unactivated enol phosphates. It can be readily seen that most of the substrates bearing the enol phosphate unit either have a heteroatom such as a nitrogen or oxygen at the α-position (**A**, **Figure 1**); or more generally have either an aromatic unit or olefin allowing conjugation with the enol phosphate (**B**, **Figure 5.1**).

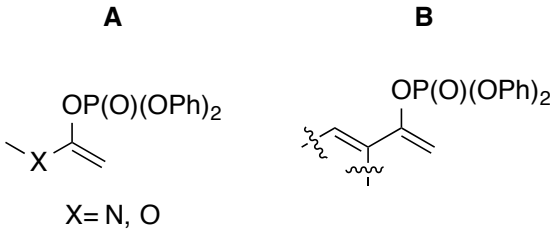

Figure 5. 1

Nevertheless, some sparse examples of non-activated enol phosphates have been described in the literature, such as the one presented above with the use of cuprate reagents (**Scheme 5.3**). Presented below in **Scheme 5.7** are the few examples where non-activated substrates have been employed. Aggarwal used the 8-membered-cyclic enol phosphate to carry out a highly efficient Stille coupling to generate **(*S*)-23** (a).[12] Skrydstrup used the simple $PdCl_2$ as catalyst with tolylmagnesium bromide to

generate **29** in high yields (b),[3] whereas a more complex dppf ligand was required (c) to carry out the Negishi coupling reaction on the non activate and sterically encumbered **26** to generate the desired olefin **27**.[9] In entry (d) is shown an example from Larsen, where the enol phosphate **251** was coupled to a simple boronic acid to generate the cross-coupled compound **252**.[13] Finally, Ackerman has demonstrated that direct arylations with enol phosphates could be carried out using dppe as ligand with palladium diacetate, to form compound **255** (e).

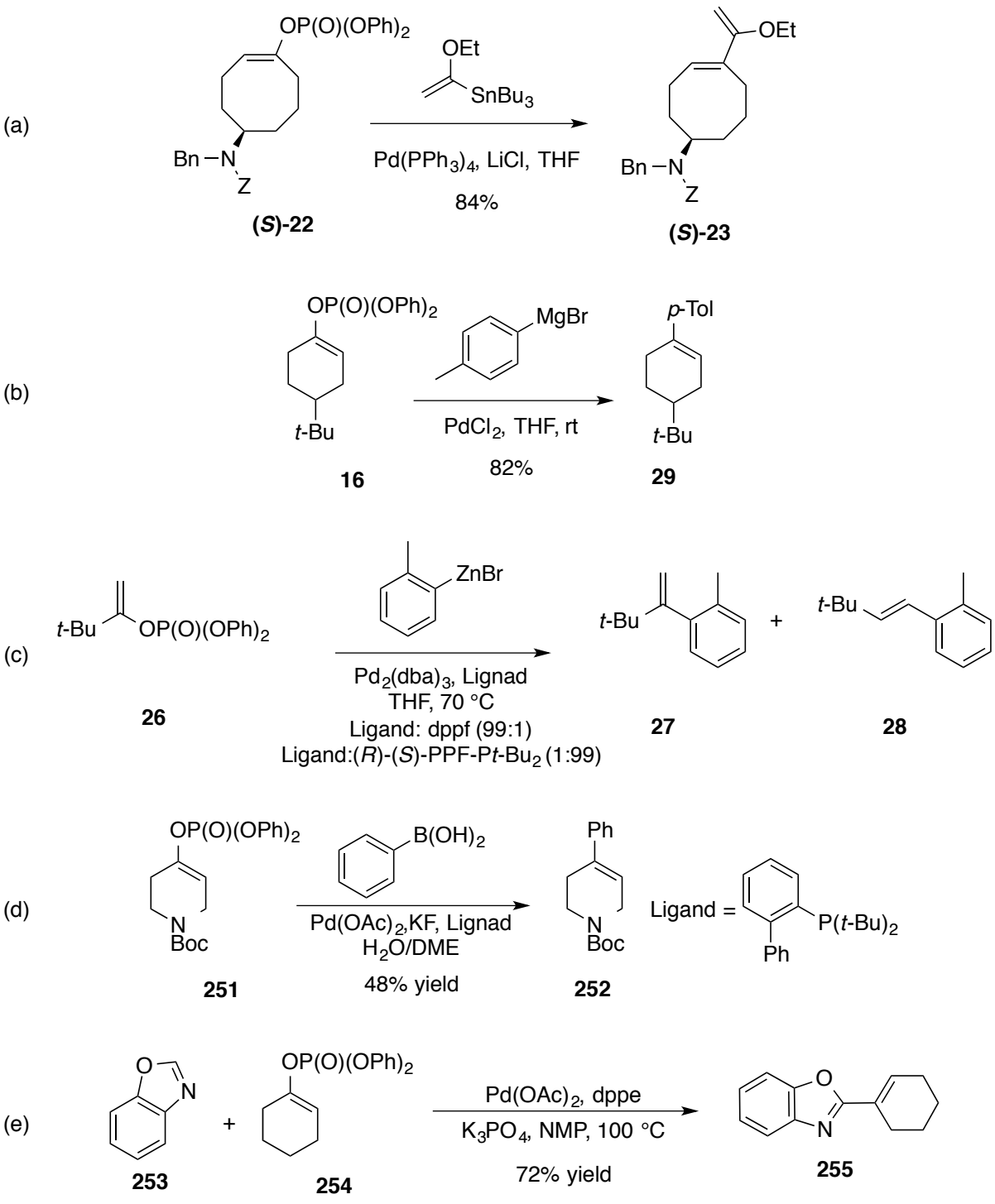
(a)
OP(O)(OPh)2
OEt
SnBu3
Bn–N
Z
Pd(PPh3)4, LiCl, THF
84%
OEt
Bn–N
Z
(S)-22
(S)-23
(b)
OP(O)(OPh)2
MgBr
p-Tol
t-Bu
PdCl2, THF, rt
82%
t-Bu
16
29
(c)
t-Bu
OP(O)(OPh)2
ZnBr
Pd2(dba)3, Lignad
THF, 70 °C
Ligand: dppf (99:1)
Ligand:(R)-(S)-PPF-Pt-Bu2 (1:99)
t-Bu
+
t-Bu
26
27
28
(d)
OP(O)(OPh)2
B(OH)2
N
Boc
Pd(OAc)2,KF, Lignad
H2O/DME
48% yield
Ph
N
Boc
Ligand =
P(t-Bu)2
Ph
251
252
(e)
O
N
+
OP(O)(OPh)2
Pd(OAc)2, dppe
K3PO4, NMP, 100 °C
72% yield
O
N
253
254
255

Scheme 5. 7

Although a range of examples exist involving various organometallic coupling partners, none of them feature the use of an alkyl unit which would allow efficient access to our desired coupled product for the synthesis of sporochnol. In fact, several attempts at the cross coupling of an *i*-propyl unit with enol phosphates have carried our in our laboratories. As shown below, neither the use of $Fe(acac)_3$ nor $Ni(acac)_3$ resulted in the desired compound (**Scheme 5.8**), and in fact several conditions were screened with the use of such coupling species but in all cases no reactivity was observed.

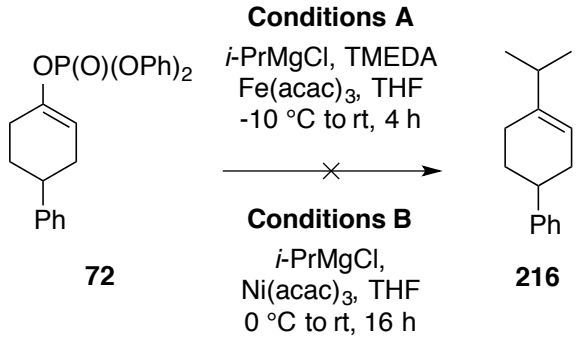

Scheme 5. 8

The only set of conditions which allowed conversion of the starting material was when palladium catalysis was used. The use of dppf as ligand with a Pd^0 species allowed the Negishi cross coupling reaction to take place, affording up to 66% isolated yield of cross-coupled product which turned out to be the isomerised product **256** (**Conditions A**, **Scheme 5.9**). On the other hand, using a Grignard reagent with $PdCl_2$, with or without phosphine, resulted in the conversion of the starting material, but in all cases, again, only the isomerised compound **256** was observed, with the highest yield observed when PPh_3 was used as ligand (**Conditions B**, **Scheme 5.9**).

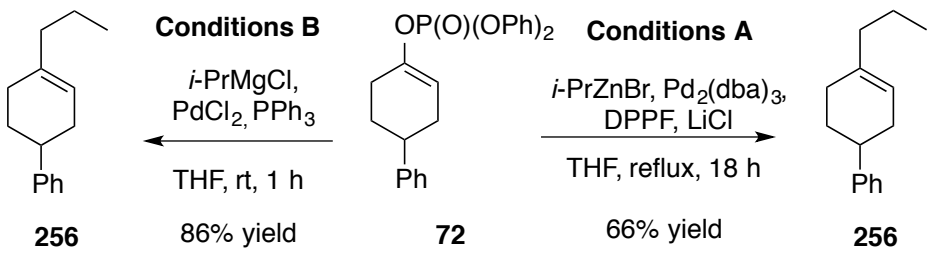

Scheme 5. 9

2. Proposed Work

We have presented above a range of methodologies that have been developed for the efficient cross-coupling of enol phosphates with various organometallic species. Furthermore, some general trends can be noted from the existing literature. Firstly, in most cases the organometallic reagent used to generate the alkyl species was either an organozinc or an organomagnesium reagent (**Schemes 5.3-5.6**). Furthermore, we have also shown with the use of non-activated enol phosphates, that Negishi and Kumada couplings afforded the highest yields for in the desired transformation (**Scheme 5.7**). Finally, the generation of various by-products, such as homo-coupled and isomerised compounds, were studied and described by a range of experimental and theoretical studies (**Scheme 5.2**). With the range of conditions previously attempted in our laboratory, we have gained a wide range of knowledge of the behaviour of our enol phosphate substrates. With this in mind, we first decided to explore a range of complex palladium catalysts, such as bulky phosphine and Peppsi catalysts, to study the overall reactivity. We postulated that one of the key aspects of the selectivity was the temperature at which the reaction took place. As shown in **Scheme 5.9**, Grignard reagents with simple catalyst systems have shown high reactivity at room temperature, although only the undesired branched product was observed. More recently, a range of novel catalysts were used in the cross coupling of enol phosphates,[14] and various selective Kumada coupling reactions were carried out at room temperature.[15] Finally the need for a highly active palladium species was required to overcome the sterically encumbered substrate and the low reactivity of the enol phosphate bond. We aimed to identify a highly reactive catalyst capable of performing the cross-coupling reaction at room temperature with high levels of selectivity, and such catalyst would require to be optimised for application to our natural product synthesis. Finally, we also aimed to develop a process-friendly transformation. Since we have established an efficient synthesis of enol phosphates, the development powerful transformations of these substrates would further promote our existing methodologies.

3. Results and Discussion

As mentioned earlier, our main interest within the area of palladium-catalysed cross-coupling reactions essentially consisted in developing an efficient cross-coupling of the enantioenriched enol phosphate **(*S*)-189**, or **(*S*)-73**, to access the desired intermediate, **(*S*)-198** or **(*S*)-209**, which would allow an efficient synthesis of the natural product, (*S*)-sporochnol (**Figure 2**).

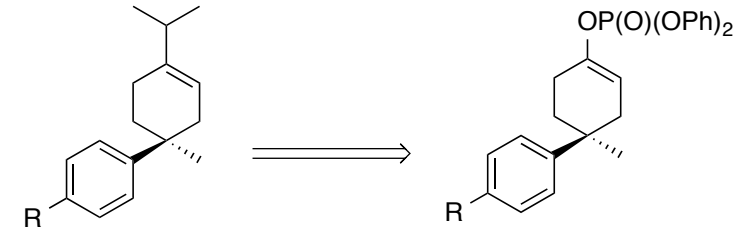

Figure 5. 2

3.1. Fishing the Right Catalyst

3.1.1. Primary Screen

As described in the Proposed Work section, we were interested in studying a range of palladium catalyst to perform either the Negishi or Kumada coupling. We first considered the reaction temperature as the cut-off point for the selection of the appropriate palladium catalyst. DFT studies carried out by Organ,[6] on the Negishi coupling indicate that the difference in energy between the transition states for the branched and linear products was slightly lower for system studied by Organ,[6] but generally the ß-hydride elimination was accessible. Under milder temperature conditions, and with the appropriate catalyst, higher selectivity could be achieved. It should be noted that this first reaction simply consisted in observing the transformation of the substrate, therefore analytic levels of the reagents were added in an LCMS vial and directly analysed. Furthermore, we choose to use model

substrate **(*S*)-73**, as this starting material represents a good approximation of the natural product system

The first catalyst explored was Pd(dtbf)Cl_2 (**257**), which has recently been described in the highly efficient Kumada cross-coupling reaction of alkenyl halides with high levels of selectivity.[15] Unfortunately, as depicted in **Table 5.1**, **Entries 1-2**, no transformation was observed. We then explored the use of the XPhos ligand described by Brown for the cross coupling reaction of enol phosphates,[14] and in order to facilitate the reaction, used the Pd(XPhos) precatalysts G1 (**258**) and G2 (**259**).[16] Upon application of these catalysts, no conversion of the starting enol phosphate observed (**Entries 3-6**). The last phosphine catalyst selected was Pd$(Cy_3)_2Cl_2$ (**260**),[17] but unfortunately no conversion of the substrate was again observed. In fact, if reacted at a higher 40 °C, all the catalysts allowed transformation of the enol phosphate substrate when the Grignard species was used. Although further exploration of the reaction could be carried out, our first objective was to find a suitable catalyst which could perform at room temperature. With this in mind, we explored the use of Peppsi catalysts Peppsi *i*-Pr (**261**) and S*i*-Pr (**262**) for the same transformation.[18] Interestingly, both catalysts fully converted the starting enol phosphate at room temperature when using Grignard reagents (**Entries 9** and **11**). Surprisingly, the use of commercial organozinc compounds resulted in no reaction.

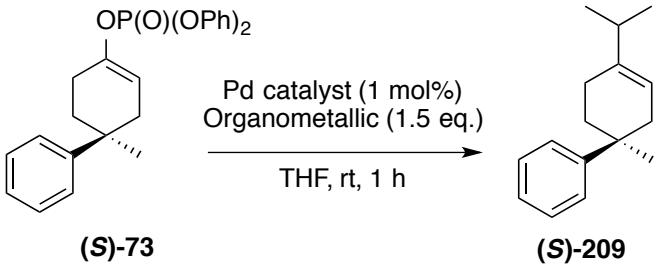

Scheme 5. 10

Entry	Pd Catalyst	Metal	Reaction
1	$Pd(dtbf)Cl_2$ **257**	Mg	-
2	$Pd(dtbf)Cl_2$ **257**	Zn	-
3	Pd(XPhos) G1 **258**	Mg	-
4	Pd(XPhos) G1 **258**	Zn	-
5	Pd(XPhos) G2 **259**	Mg	-
6	Pd(XPhos) G2 **259**	Zn	-
7	$Pd(Pcy_3)_2Cl_2$ **260**	Mg	-
8	$Pd(Pcy_3)_2Cl_2$ **260**	Zn	-
9	Peppsi *i*-pr **261**	Mg	Reaction
10	Peppsi *i*-pr **261**	Zn	-
11	Peppsi S*i*-pr **262**	Mg	Reaction
12	Peppsi S*i*-pr **262**	Zn	-

Table 5. 1

Our first aim, to find a catalyst capable of performing the cross-coupling reaction at room temperature, was achieved, as both Peppsi catalysts performed the Kumada coupling reaction. In order to further optimise the reactivity and selectivity of the catalyst, a range of Peppsi catalysts were subjected to the transformation conditions described in **Scheme 5.12.** It should be stated at this point that 2-MeTHF was used as solvent as the commercial Grignard solution was provided in 2-MeTHF. Furthermore, having based our primary catalyst screen on the desired substrate, we then used more common benchmark substrate **72** to optimise the reaction conditions. Moreover, we

were now interested in the selectivity observed with the use of various Peppsi catalysts, as previous work on Negishi cross-coupling reactions developed by Organ had shown that a small change in the catalyst could dramatically vary the reaction outcome.[6] Upon analysis of the quenched reaction, we observed full conversion of all substrates when the reaction was carried out using the conditions described in **Scheme 5.11**. Unexpectedly, within these reaction conditions, we observed the presence of three different products: a, b and c (**Scheme 5.11**). The product (a) was identified as the desired cross-coupled compound **216**; (b) was the reduced by-product **263**; and, finally, (c) was the homo-coupled product **264**. In fact, under our present conditions, the isomerised product was not detected. As shown in **Table 5.2**, the use of Peppsi S*i*-Pr **262**, allowed an excellent 91% selectivity towards the desired product **216**. The other by-products were obtained in 5% and 4% yields for **263** and **264** respectively (**Entry 1**). The use of the SiMes NHC ligand on palladium (**265**) resulted in an erosion in selectivity, giving a 19:38:42 ratio of a:b:c (**Entry 2**). The use of a larger catalyst, Peppsi *i*-pent **266**, resulted in good levels of selectivity, affording a 71:11:18 ratio of a:b:c in favour of the desired product (**Entry 3**). Finally, the present reaction conditions were compared with the use of $PdCl_2$,[19] a more simple catalyst which has been used previously for the same transformation. Interestingly, although full conversion of the substrate was observed, neither the desired product nor any by-products were detected (**Entry 4**). It was interesting to note that our primary screening for the choice of a catalyst was useful as the Peppsi catalysts not only allowed the desired transformation to take place at room temperature, but moreover, high levels of selectivity were already observed.

3.1.2. Towards Peppsi Catalysts

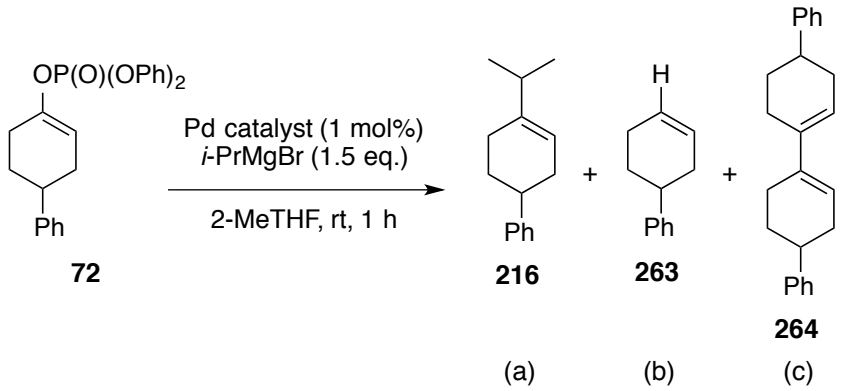

Scheme 5. 11

Entry	Pd Catalyst	Conversion %	Result (a:b:c)
1	Peppsi S*i*-pr **262**	99	91:5:4
2	S-imes/$pd_2(dba)_3$ **265**	99	19:38:42
3	Peppsi S*i*-pent **266**	99	71:11:18
4	$PdCl_2$	99	Unidentified mixture

Table 5. 2

3.2 Cross Coupling of Enol Phosphates

Pleased by the encouraging results observed under these mild conditions, we were interested in exploring further the reactivity, mainly due to isolation issues with the products. In fact, although high levels of conversion were observed, the desired product **216** co-eluted with the reduced product **263** on purification by flash column chromatography. Among the range of parameters studied, we were surprised to realise that the concentration had a slight impact on the overall selectivity observed. As shown below in **Scheme 5.12**, concentrations lower or at 0.5 mol/l consistently provided full conversion and selectivities of 94:3:3 a:b:c.

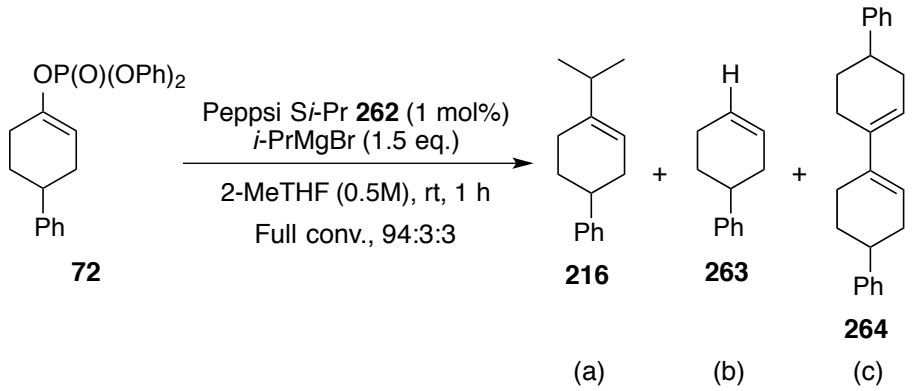

Scheme 5. 12

3.2.1. Solvent Scope

With in mind the necessity for more environmentally friendly processes, especially for industrial settings, we were interested in further exploring the reactivity of the present system. Furthermore, we intended to develop an easily applicable methodology, where any commercially provided Grignard reagent, in a given solvent, could be used directly. Therefore, using the optimised conditions obtained so far, we examined the reactivity and selectivity obtained using a range of solvents. It should be noted that for some solvents, there were solubility issues with the substrate, which required the addition of more solvent and therefore the concentrations are below 0.5 mol/l. In most cases, all the reactions proceeded efficiently, providing conversions between 95-99% (**Scheme 5.13**, **Entries 1-7**, **Table 5.3).** The first surprising result was observed when the reaction was carried out in THF instead of the usual 2-MeTHF, where the ratio dropped to 79:14:7 (**Entry 1**). Although structurally similar, these two solvents provided completely different results when it came to the selectivity of the cross coupling reaction. On the other hand, when the reaction was carried out in hexanes, an improved ratio of 95:3:2 was observed (**Entry 2**), and furthermore the use of Et_2O and DCM both allowed extremely high selectivities of 96:2:2 (**Entries 3** and **4**). The use of toluene provided a selectivity of 93:4:3 (**Entry 5**), and CPME gave a ratio of 94:3:3 (**Entry 6**); whereas the ratio in TBME was 84:5:11 (**Entry 7**). The main conclusion from this table of results is that the selectivity for the desired transformation is highly solvent dependant. High levels of selectivities were not directly correlated to the polarity of the solvent (*e.g.* hexane and Et_2O both afforded high selectivities), and at the same time, ether-based solvents

such as CPME and TBME showed a broader selectivity. One may also postulate that the concentration, and therefore the solubility of the substrate, may impact the reaction, but no clear evidence was provided in this case, as the selectivity of 93:4:3 with toluene and 79:14:7 with THF were observed at the same concentration of 0.5 mol/l. One of the key elements we questioned was the use of the Grignard reagent itself. In fact generally the reactivity and selectivity obtained for Kumada cross-coupling reactions are associated with the ligand present on palladium (*i.e.* its size, its ability to electron donate or withdraw).[6] Furthermore, some evidence was recently provided in the area of lithium chemistry, where the key cross-coupling transformation was controlled by the precise aggregate of the organometallic species in solution.[20] We postulated that the Grignard reagent aggregate in solution had similar effects on the reactivity in our system.

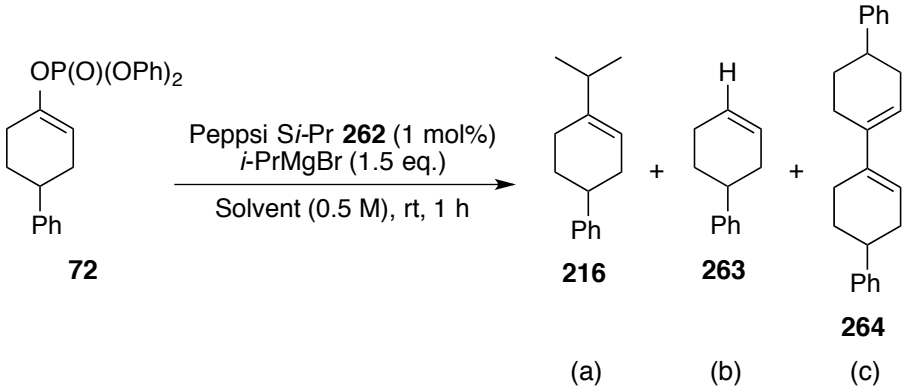

Scheme 5. 13

Entry	Solvent (concentration)	Conversion	Selectivity (a:b:c)
1	THF (0.5)	96%	79:14:7
2	Hexane (0.2 M)	97%	95:3:2
3	Diethylether (0.25m)	99%	96:2:2
4	DCM (0.5M)	95%	96:2:2
5	Toluene (0.5 M)	96%	93:4:3
6	CPME (0.5 M)	95%	94:3:3
7	TBME (0.1 M)	92%	84:5:11

Table 5. 3

So far we had been able to develop unprecedented levels of selectivity in the Kumada cross-coupling reaction of enol phosphates. The reaction is been carried using a commercial Grignard reagent and a very low 1 mol% loading of a commercially available Peppsi catalyst (**262**), at room temperature within one hour. This extremely simple process provides up to 96:2:2 selectivity towards the desired product. Having identified a range of capable solvents, it was decided, for purely technical purposes, to use Et_2O as the solvent for the further development of the Kumada coupling reaction. Having established our optimised conditions, we next explored the potential and scope of the cross-coupling reaction.

3.2.2. The Grignard Scope

Having successfully cross-coupled *i*-PrMgBr with our enol phosphate **72**, we were interested in exploring a range of different alkyl Grignard reagents to establish the generality of this process. Upon application of a range of commercial Grignard reagents available in various solvents and concentrations to the reaction, high yields have been obtained with only a small amount of by-products. As shown below, using the conditions presented in **Scheme 5.14**, the use of cylopropyl, cyclohexyl and cylcoheptyl Grignard reagents afforded 94% of **267**, 84% of **268** and 87% yield of **269**, respectively, and the use of the *i*-butyl Grignard reagent allowed a 91% isolated yield of **270**. When moving to a linear Grignard reagent, *n*-BuMgCl, the reactivity lost its selectivity, affording a low 73:22:2 ratio of **271**, whereas the use of phenylmagnesium bromide afforded the desired cross-coupled product **272** in a good 75% yield. Surprised by the low selectivity obtained when using *n*-BuMgCl, we decided to investigate this substrate further.

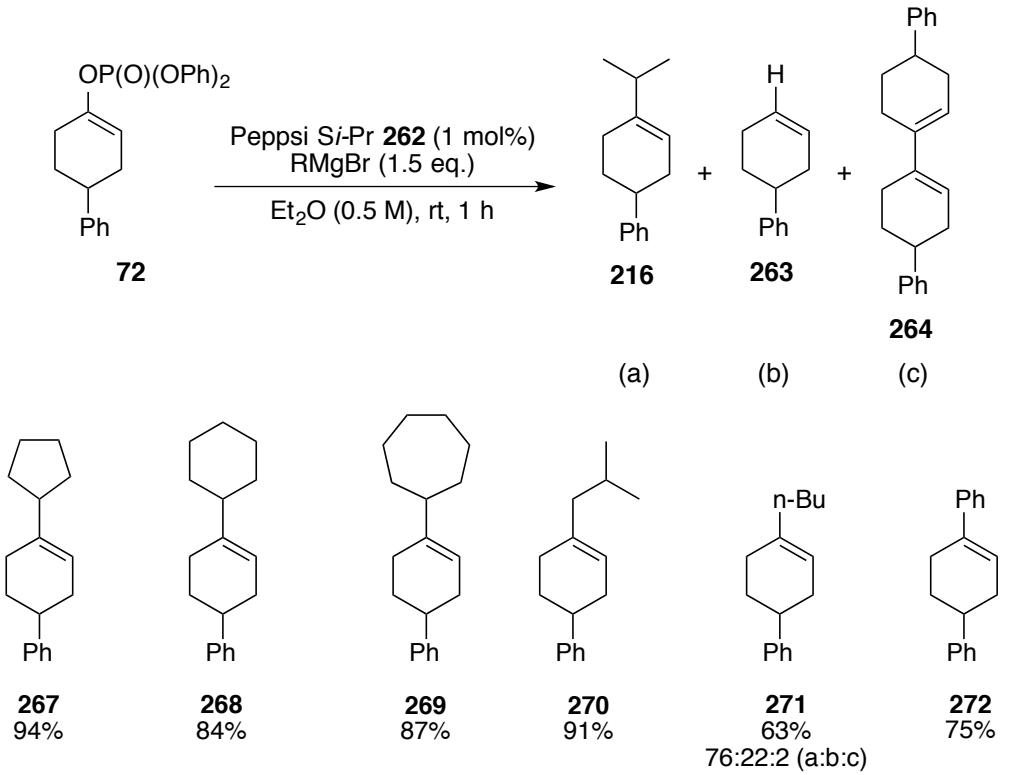

Scheme 5. 14

3.3. Optimising the use of *n*-BuMgBr

3.3.1. Temperature Study

We started our investigation by varying the temperature. In fact, one of our first hypotheses consisted in the belief that a high temperature would lead to more side reactions. Having observed two main side products (the reduced compound **263** and the homo coupled compound **264**), we wanted to know if each of the processes leading to their formation had similar kinetics at various temperatures. Therefore, we carried out a cross-coupling reaction at 40 °C, which resulted in full conversion, with a ratio of 70:26:4 (**Entry 1**, **Table 5.4**), and a reaction at 0 °C, which gave 90% conversion with a selectivity of 90:10:0 (**Entry 2**, **Table 5.4**) using the conditions described in **Scheme 5.15**. This experiment clearly provided evidence that the temperature played a significant a role in the formation of the by-products; and furthermore, the homocoupling side reaction was inexistent at 0 °C.

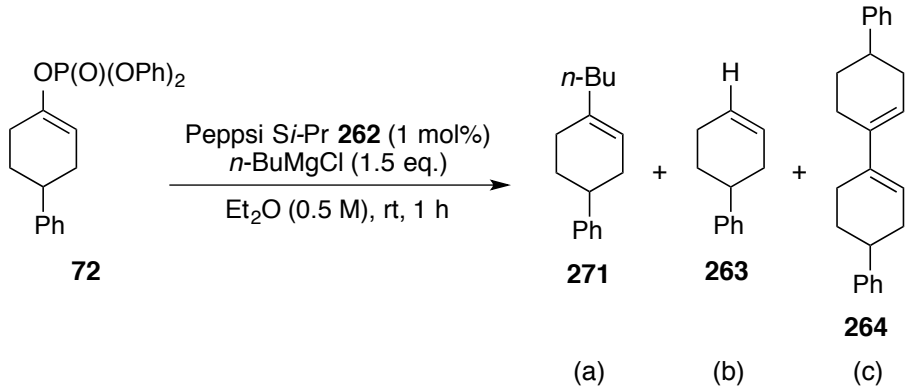

Scheme 5. 15

Entry	Temp.	Conv.	Selectivity (a:b:c)
1	40 °C	100%	70:26:4
2	0 °C	90%	90:10:0

Table 5. 4

In the meantime, we were confronted with a major solubility problem when carrying out reactions at 0 °C. The starting material was insoluble in Et_2O below 0 °C, and only the addition of the Grignard solution in THF aided the dissolution of the enol phosphate. We were also concerned about the high volatility of our product, making the isolation difficult; this was initially one of the reasons for choosing Et_2O over a solvent like CPME or toluene. Another polar solvent, which provided high reactivity and which has a low boiling point, is DCM, although this solvent raised some concern due to its potential incompatibility with Grignard reagents. Nevertheless, a reaction in DCM was attempted, however, disappointingly, this resulted in a lower reactivity and a disastrous selectivity. At room temperature, only 76% conversion was observed with a selectivity of 17:68:15 (**Scheme 5.16**, **Entry 1**, **Table 5.5**), and, when carried out at 0 °C, only a 45% conversion was observed with a selectivity of 20:62:18 (**Scheme 5.16**, **Entry 2**, **Table 5.5**). Further decrease of the reaction temperature only resulted in a further drop in reactivity, until no transformation was observed at all, and with only a low increase in selectivity. The use of additives, such as LiCl, changed neither the reactivity nor the selectivity of the process.

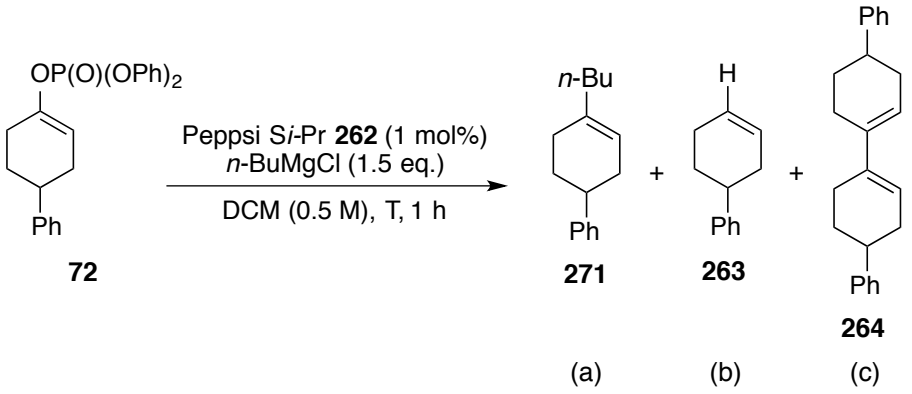

Scheme 5. 16

Entry	Temp.	Conv.	Selectivity (a:b:c)
1	rt	76%	17:68:15
2	0 °C	45%	20:62:18

Table 5. 5

At this point, we developed the theory of the Grignard reagent aggregate having an impact on the overall reactivity of the process. To validate this hypothesis, we first carried out a reaction that involved the corresponding dialkylmagnesium species. Use of the commercial *n*-Bu_2Mg for the present reaction in DCM, although providing low levels of reactivity, significantly improved the ratio to 36:49:15 (**Scheme 5.17**). We have shown previously that the homocoupling product was more sensitive to the reaction temperature than the cross-coupling and the reduction products, and this was evident when the levels of homocoupling were compared to **Entry 1**, **Table 5.5**, where similar levels of homocoupling were observed (15%). On the other hand, the ratio of cross-coupling increased from 17% (*cf*. **Entry 1**, **Table 5.5**) to 36% (**Scheme 5.17**) by simply changing the active Grignard species in solution.

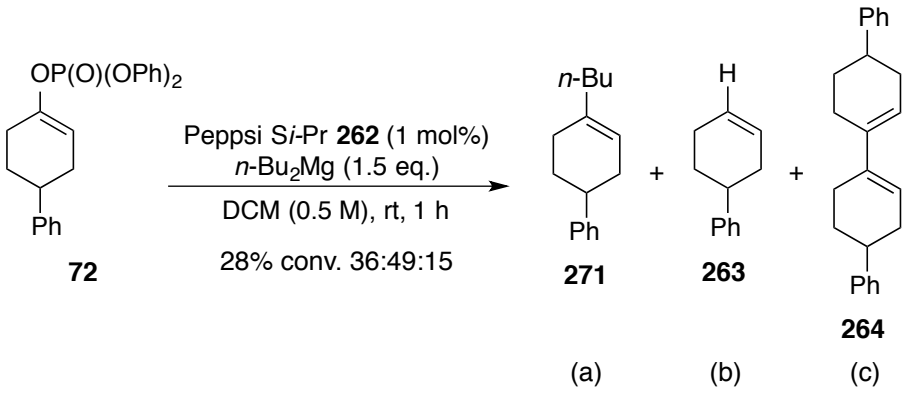

Scheme 5. 17

3.3.2. Varying the Catalyst

These results clearly showed that there was a direct correlation between the Grignard aggregate or species present in solution and the outcome of the reaction. To further verify the effect of the catalyst in this system, we employed the Peppsi *i*-Pr^{*OMe} catalyst, whose ligand has been recently reported as being one of the bulkiest and most efficient for a range of catalysed transformations.[21] Upon application of this catalyst (**Scheme 5.18**) to the present reaction in DCM, a conversion of 78% with a selectivity of 16:67:16 was observed (**Entry 1**, **Table 5.6**), which was identical to the results obtained by using Peppsi S*i*-Pr. On the other hand, the use of Et_2O as solvent resulted in a 93% conversion, but surprisingly dropped the selectivity to 37:61:2 (**Entry 2**, **Table 5.6**). The observation of these results shows that the aggregation state of the Grignard reagent alone, in a given solvent, cannot be fully responsible for the overall reactivity.

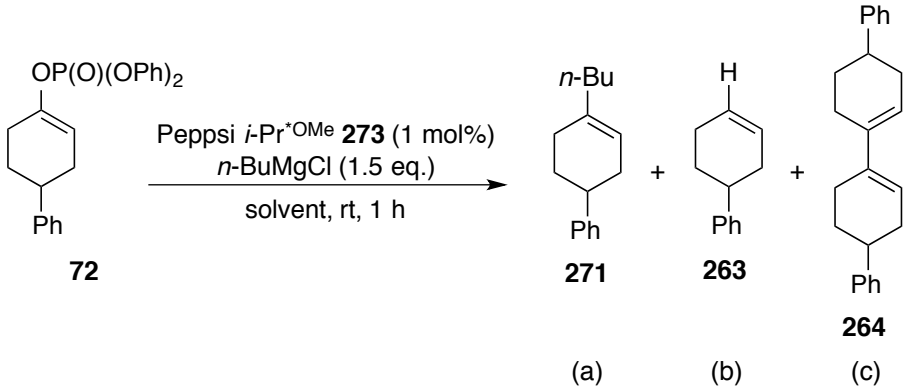

Scheme 5. 18

Entry	Solvent	Conv.	Selectivity (a:b:c)
1	DCM (0.5 M)	78%	16:67:16
2	Et_2O (0.25 M)	93%	37:61:2

Table 5. 6

We propose that a difference in solvent cage obtained influences both the catalyst and the Grignard reagent during the transmetalation process.

3.3.3. Final Optimisations

So far, the most promising results have arisen from lowering the reaction temperature, but further investigation was halted due to the lack of solubility of the enol phosphate **72** in Et_2O. We therefore changed the solvent to toluene, despite having isolation difficulties, and investigated the effect of the temperature and the solvent on the overall system (**Scheme 5.19**, **Table 5.7**). As shown below, the optimised conditions in toluene at room temperature resulted in a 94% yield and a selectivity of 32:48:20 (**Entry 1**). Although higher than that observed using DCM, the process afforded poor selectivity for the cross-coupling product. Decreasing the reaction temperature to 0 °C lowered the conversion to 74% but improved the selectivity to 50:43:7 (**Entry 2**). By reaching a temperature of -20 °C, albeit affording a low 41% conversion, a satisfying 91:9:0 selectivity was observed (**Entry 3**). Furthermore, by performing the reaction at -40 °C, a low 12% conversion was obtained, but with only the desired product (ratio 100:0:0) obtained (**Entry 4),** making these conditions the most selective to date.

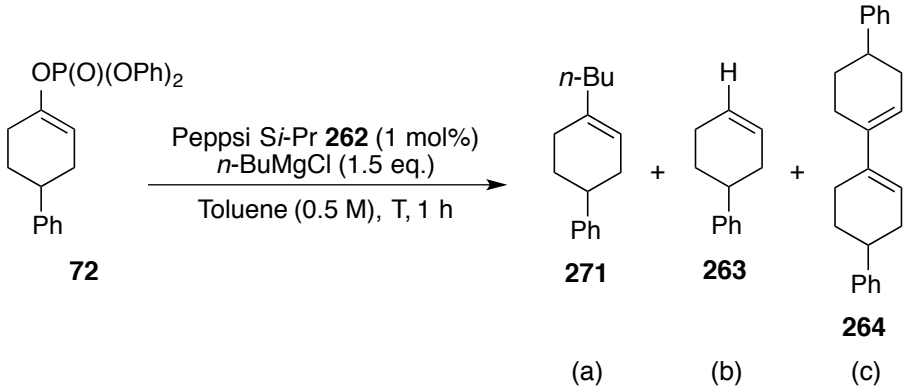

Scheme 5. 19

Entry	Temp	Conv.	Selectivity (a:b:c)
1	rt	94%	32:48:20
2	0 °C	74%	50:43:7
3	-20 °C	41%	91:9 :0
4	-40 °C	12%	100 :0 :0

Table 5. 7

3.3.4. Optimised conditions for the use of n-BuMgBr

Pleased with this last set of results, we were keen on improving the reactivity by extending the reaction time to 16 h. As presented below, under such conditions, although the reaction lost some of its selectivity, a 97:3:0 ratio and an isolated 88% yield of **271** was obtained (**Scheme 5.20**).

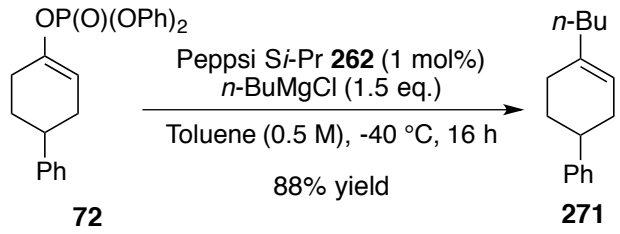

Scheme 5. 20

We investigated below in **Scheme 5.21** two other linear Grignard reagents, EtMgBr and *n*-PrMgBr; both displayed unique reactivity and selectivities. EtMgBr only required a temperature of 0 °C in toluene to afford a high selectivity of 98:2:0 a:b:c and a good yield of 78% of **274** in two hours, whereas *n*-PrMgBr, afforded a ratio of 87:12:1 a:b:c and a 71% yield of **275** at room temperature in Et_2O.

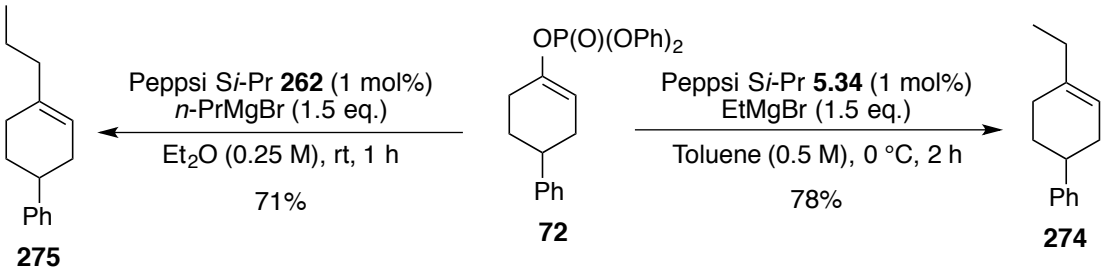

Scheme 5. 21

So far, we have shown that the outcome of the reaction is generally Grignard reagent dependant, and that in most cases the use of bulky Grignard species allows high reactivity with excellent selectivity at room temperature in Et_2O. On the other hand, when the cross-coupling reaction involved flexible groups, altering the results, we have developed a simple alternative, thus extending the scope of the present process. Having completed a range of cross-coupling reactions with various Grignard reagents, we next evaluated the enol phosphate scope for the novel sp^2-sp^3 coupling.

3.4. Enol Phosphate Substrate Scope

With the range of enol phosphates synthesised in Chapter 1, we had access to a library of substrates that could be tested in the cross-coupling reaction. Among the substrates tested, a range of them delivered excellent results under the optimised conditions. As shown in **Scheme 5.22** below, 4-substituted cyclohexanone-derived enol phosphates, such as the *t*-Bu-, -OTBS, *n*-Pr-, 4-Me-4-Ph-, and acetal derivatives, resulted in 98% of **5.46**, 87% of **5.47**, 73% of **5.48**, 98% of **4.46**, and 85% **5.49** respectively. Increasing the steric bulk around the olefinic coupling partner, the product from the kinetic enol phosphate provided an 88% yield of the desired product **5.50**, whereas the corresponding thermodynamic substrate, containing a trisubstituted olefin, required heating at 40 °C over 8 h to result in 64% yield of **5.51**. Finally, when an even more bulky, trisubstituted, menthone-derived enol phosphate was used, the same 64% yield of **5.52** was obtained after heating at 40 °C for 8 h.

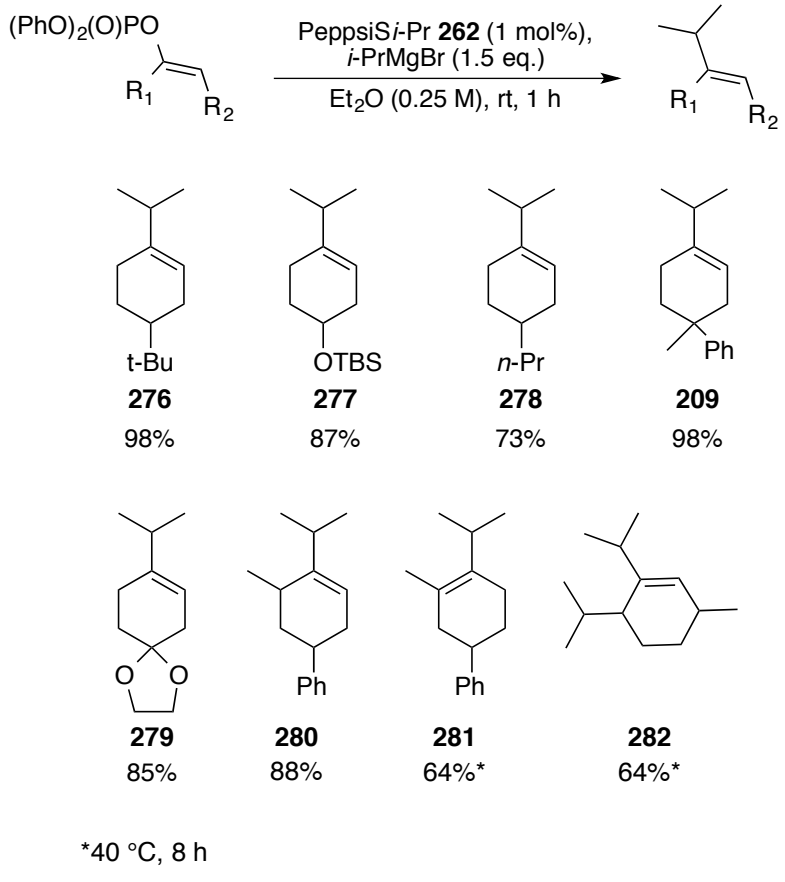

Scheme 5. 22

3.5. Future work

We have successfully developed a method for the facile cross-coupling of enol phosphates, using Peppsi catalysts. Despite establishing a broad substrate scope, nevertheless, a number of Grignard reagents and enol phosphates did not afford the desired cross-coupled compound. In some cases, some substrates resulted in no reaction and only the return of starting material (**Figure 5.3**).

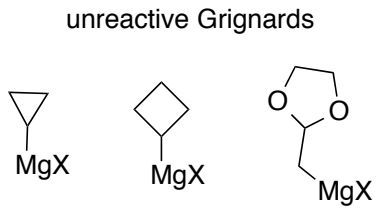

Figure 5. 3

On the other hand, some of the cross-coupled products were revealed to be extremely sensitive and degraded very quickly, while highly reactive partners gave a range of by-products.

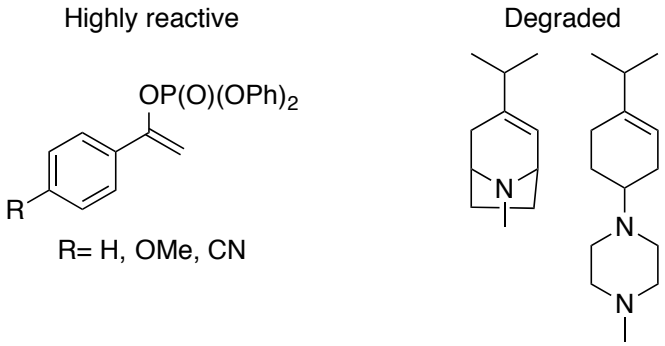

Figure 5. 4

Having revealed that the subtle change of the Grignard species in solution greatly modified the reactivity (see **Scheme 5.17**), further investigation of the nature of the

above Grignard reagents or substrates might allow improved isolation of the cross-coupled products.

Furthermore, the specific interaction between Peppsi S*i*-Pr and the benchmark enol phosphate has resulted in a high reactivity for the Kumada cross-coupling, and therefore applying these catalyst parameters to other transmetallating species, such as boronic ester/acids, might be useful (**Figure 5.5**).

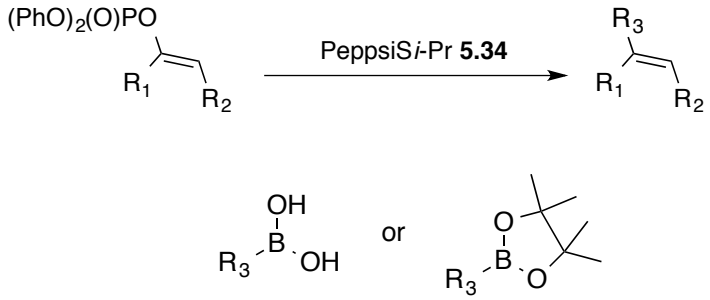

Figure 5. 5

4. Summary

Herein we have developed a novel methodology for the cross-coupling reaction of enol phosphates with alkyl Grignard reagents. Our initial interest in this methodology was to afford an efficient route to the synthesis of (*S*)-sporochnol (*c.f.* Chapter 4). Through exploration of the current reaction conditions and the novel process provided by this facile transformation, we have further developed the scope of the Kumada cross-coupling reaction. Specifically, we have established an efficient, rapid and flexible transformation, requiring a commercially available Peppsi catalyst and applicable with a range of solvents. Furthermore, the reactions take place mainly at room temperature and are robust enough to tolerate a mild increase or decrease in temperature to accommodate a variety of Grignard reagents or substrates. We have explored a range of alkyl Grignard reagents, providing high levels of isolated yields of the desired olefins, and have established a range of enol phosphate substrates which also provided the cross-coupled products in good yields.

5. Experimental

5.1. General

All reagents were obtained from commercial suppliers (Aldrich, Lancaster, Alfa-aesar or Acros) and used without further purification, unless otherwise stated. Purification was carried out according to standard laboratory methods.[22]

- Dichloromethane, diethyl ether, hexane, THF and toluene were obtained from an Innovative Technology, Pure Solv, SPS-400-5 solvent purification system.
- 2-Methyltetrahydrofuran was dried by heating to reflux over sodium wire, using benzophenone ketyl as an indicator, then distilled under nitrogen. N.B. commercially available anhydrous 2MeTHF can also be used.
- Organometallic reagents were standardised using salicylaldehyde phenylhydrazone.[23]

Thin layer chromatography was carried out using CamLab silica plates, coated with fluorescent indicator UV_{254}, and analysed using a Mineralight UVGL-25 lamp.

Flash column chromatography was carried out using Prolabo silica gel (230-400 mesh).

IR spectra were recorded on a SHIMADZU IRAFFINITY-1 spectrophotometer.

^{1}H, ^{13}C and ^{31}P NMR spectra were recorded on a Bruker DPX 400 spectrometer at 400 MHz, 100 MHz, and 162 MHz, respectively. Chemical shifts are reported in ppm. Coupling constants are reported in Hz and refer to $^{3}J_{H\text{-}H}$ interactions unless otherwise specified.

5.2. General Procedures

General Procedure A: Kumada cross-coupling reaction

To an oven-dried 25 mL microwave vial was added the requisite enol phosphate and the palladium catalyst, and the vial was sealed with a suba-seal and purged with argon. The stated solvent was added and the mixture stirred for 5 min before rapid addition of the Grignard reagent. The reaction was left to stir under the temperature and time stated and then quenched with water 2 mL. The mixture was partitioned with Et_2O, the aqueous phase was extracted with Et_2O (2 × 5 mL) and the organic phases were combined and washed with 1M HCl and brine. The organic phase was dried over Na_2SO_4 and concentrated *in vacuo* to afford a dark oil. The selectivity and conversion was obtained through analysis of this crude sample *via* integration of the olefinic protons in the ^{1}H NMR spectrum. The crude mixture was purified by column chromatography on silica gel using 0-5% Et_2O in petroleum ether (40-60 °C) to give the desired product.

5.3. Kumada coupling reaction

Scheme 5.10

The screening reaction was carried out under the following conditions. In a 1 mL LCMS vial equipped with an appropriate stirrer bar was added 5 mg of **(*S*)-73**, followed by commercial anhydrous THF (0.5 mL) and the stated palladium catalyst (0.5 mg). To this mixture was added a solution of the organometallic reagent (0.1 mL). The mixture was quenched with water and extracted with DCM (5 mL), the organic phase dried through a phase separator then reduced *in vacuo*. The crude mixture was analysed ^{1}H NMR spectroscopy and the conversion was based on the signals obtained and quantified via the modification of the olefinic signal at δ 5.50 – 5.46 ppm.

Following this procedure, data are presented as (a) Palladium catalyst, (b) Organometallic reagent and (c) conversion.

Table 5.1

Entry 1: Following the procedure described above: (a) $Pd(dtbf)Cl_2$ **257**, (b) *i*-PrMgBr and (c) -.

Entry 2: Following the procedure described above: (a) $Pd(dtbf)Cl_2$ **257**, (b) *i*-PrZnBr and (c) -.

Entry 3: Following the procedure described above: (a) Pd(XPhos) G1 **258**, (b) *i*-PrMgBr and (c) -.

Entry 4: Following the procedure described above: (a) Pd(XPhos) G2 **259**, (b) *i*-PrZnBr and (c) -.

Entry 5: Following the procedure described above: (a) Pd(XPhos) G2 **259**, (b) *i*-PrMgBr and (c) -.

Entry 6: Following the procedure described above: (a) Pd(XPhos) G1 **258**, (b) *i*-PrZnBr and (c) -.

Entry 7: Following the procedure described above: (a) $Pd(Pcy_3)_2Cl_2$ **260**, (b) *i*-PrMgBr and (c) -.

Entry 8: Following the procedure described above: (a) $Pd(Pcy_3)_2Cl_2$ **260**, (b) *i*-PrZnBr and (c) -.

Entry 9: Following the procedure described above: (a) Peppsi *i*-Pr **261**, (b) *i*-PrMgBr and (c) conversion towards new products.

Entry 10: Following the procedure described above: (a) Peppsi *i*-Pr **261**, (b) *i*-PrZnBr and (c) -.

Entry 11: Following the procedure described above: (a) Peppsi S*i*-Pr **262**, (b) *i*-PrMgBr and (c) conversion towards new products.

Entry 12: Following the procedure described above: (a) Peppsi S*i*-Pr **262**, (b) *i*-PrZnBr and (c) -.

Scheme 5.11

Following General Procedure A for the Kumada coupling reaction, data are presented as (a) enol phosphate, (b) palladium catalyst, (c) solvent, (d) Grignard, (e) Temperature, (f) time, (g) conversion, and (h) selectivity (a:b:c)

Table 5.2

Entry 1: Following General Procedure A: (a) diphenyl (1,2,3,6-tetrahydro-[1,1'-biphenyl]-4-yl) phosphate **72**, 203 mg, 0.5 mmol, (b) Peppsi S*i*-Pr **262**, 3.4 mg, 1 mol%, (c) 2-methyltetrahydrofuran, 5 mL, (d) *i*-PrMgBr, 2.9 M, 0.26 mL, 0.75 mmol, (e) rt, (f) 1 h, (g) 99% and (h) 91:5:4

4-isopropyl-1,2,3,6-tetrahydro-1,1'-biphenyl[24] **216**:

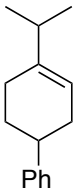

ν_{max}: 2996, 2922, 1492, 1452, 1190, 1016, 958, 756 cm^{-1}.

^{1}H NMR (400 MHz, $CDCl_3$): δ 7.34 – 7.28 (m, 2H, ArH), 7.26 – 7.18 (m, 3H, ArH), 5.53 – 5.49 (m, 1H, C=CH), 2.81 – 2.71 (m, 1H, CH), 2.36 – 2.26 (m, 1H, CH_2), 2.25 – 2.05 (m, 4H, CH_2), 2.02 – 1.94 (m, 1H, CH_2), 1.81 – 1.76 (m, 1H, CH), 1.04 (d, *J*, = 6.9 Hz, 6H, CH_3).

^{13}C NMR (100 MHz, $CDCl_3$): δ 143.0, 127.8, 126.4, 125.4, 117.5, 39.9, 34.5, 33.1, 29.7, 26.1, 21.2, 20.8.

1,2,3,6-tetrahydro-1,1'-biphenyl[25] **263**:

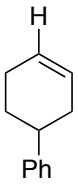

ν_{max}: 3061, 3024, 2917, 2837, 1942, 1876, 1799, 1492, 1452 cm^{-1}.

^{1}H NMR (400 MHz, $CDCl_3$): δ 7.37-7.10 (m, 5H, ArH); 5.81-5.69 (m, 2H, C=CH); 2.84-2.73 (m, 1H, CH); 2.35-2.05 (m, 4H, CH_2), 1.97-1.86 (m, 1H, CH_2); 1.80-1.67 (m, 4H, CH_2).
^{13}C NMR (100 MHz, $CDCl_3$): δ 147.27, 128.31, 126.85, 126.84, 126.73, 125.91, 40.12, 33.39, 29.68, 25.87 (*t*).

1',2',2'',3',3'',4'',5'',6'-octahydro-1,1':4',1'':4'',1'''-quaterphenyl[26] **264**:

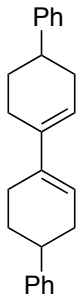

^{1}H NMR (400 MHz, $CDCl_3$): δ 7.37 – 7.30 (m, 4H, ArH), 7.27 – 7.19 (m, 6H, ArH), 5.94 – 5.87 (m, 2H, C=CH), 2.86 – 2.76 (m, 2H, CH), 2.53 – 2.24 (m, 8H, CH_2), 2.12 – 2.03 (m, 2H, CH_2), 1.89 – 1.76 (m, 2H, CH_2).

Entry 2: Following General Procedure A: (a) diphenyl (1,2,3,6-tetrahydro-[1,1'-biphenyl]-4-yl) phosphate, **72**, 203 mg, 0.5 mmol, (b) Simes, 1.53 mg, Pd_2dba_3, 2.5 mg, **265**, 1 mol%, (c) 2-methyltetrahydrofuran, 5 mL, (d) *i*-PrMgBr, 2.9 M, 0.26 mL, 0.75 mmol, (e) rt, (f) 1 h, (g) 99% and (h) 19:38:42

Entry 3: Following General Procedure A: (a) diphenyl (1,2,3,6-tetrahydro-[1,1'-biphenyl]-4-yl) phosphate, **72**, 203 mg, 0.5 mmol, (b) Peppsi S*i*-pent, **266**, 4 mg, 1 mol%, (c) 2-methyltetrahydrofuran, 5 mL, (d) *i*-PrMgBr, 2.9 M, 0.26 mL, 0.75 mmol, (e) rt, (f) 1 h, (g) 99% and (h) 71:11:18

Entry 4: Following General Procedure A: (a) diphenyl (1,2,3,6-tetrahydro-[1,1'-biphenyl]-4-yl) phosphate, **72**, 203 mg, 0.5 mmol, (b) $PdCl_2$, 0.9 mg, 1 mol%, (c) 2-

methyltetrahydrofuran, 5 mL, (d) *i*-PrMgBr, 2.9 M, 0.26 mL, 0.75 mmol, (e) rt, (f) 1 h, (g) 99% and (h) -

Scheme 5.12

Following General Procedure for the Kumada coupling reaction, data are presented as (a) enol phosphate, (b) palladium catalyst, (c) solvent, (d) Grignard, (e) Temperature, (f) time, (g) conversion, and (h) selectivity (a:b:c)
Following General Procedure A: (a) diphenyl (1,2,3,6-tetrahydro-[1,1'-biphenyl]-4-yl) phosphate **72**, 203 mg, 0.5 mmol, (b) Peppsi S*i*-Pr **262**, 3.4 mg, 1 mol%, (c) 2-methyltetrahydrofurane, 1 mL, 0.5 M, (d) *i*-PrMgBr, 2.9 M, 0.26 mL, 0.75 mmol, (e) rt, (f) 1 h, (g) 99% and (h) 94:3:3

5.3.1. Solvent Scope

Scheme 5.13

Table 5.3

Following General Procedure for the Kumada coupling reaction, data are presented as (a) enol phosphate, (b) palladium catalyst, (c) solvent, (d) Grignard, (e) Temperature, (f) time, (g) conversion, and (h) selectivity (a:b:c)
Entry 1: Following General Procedure A: (a) diphenyl (1,2,3,6-tetrahydro-[1,1'-biphenyl]-4-yl) phosphate **72**, 203 mg, 0.5 mmol, (b) Peppsi S*i*-Pr **262**, 3.4 mg, 1 mol%, (c) tetrahydrofurane, 1 mL, 0.5 M, (d) *i*-PrMgBr, 2.9 M, 0.26 mL, 0.75 mmol, (e) rt, (f) 1 h, (g) 96% and (h) 79:14:7

Entry 2: Following General Procedure A: (a) diphenyl (1,2,3,6-tetrahydro-[1,1'-biphenyl]-4-yl) phosphate **72**, 203 mg, 0.5 mmol, (b) Peppsi S*i*-Pr **262**, 3.4 mg, 1 mol%, (c) hexanes, 2.5 mL, 0.5 M, (d) *i*-PrMgBr, 2.9 M, 0.26 mL, 0.75 mmol, (e) rt, (f) 1 h, (g) 97% and (h) 95:3:2

Entry 3: Following General Procedure A: (a) diphenyl (1,2,3,6-tetrahydro-[1,1'-biphenyl]-4-yl) phosphate **72**, 203 mg, 0.5 mmol, (b) Peppsi S*i*-Pr **262**, 3.4 mg, 1

mol%, (c) diethyl ether, 2 mL, 0.25 M, (d) *i*-PrMgBr, 2.9 M, 0.26 mL, 0.75 mmol, (e) rt, (f) 1 h, (g) 99% and (h) 96:2:2

Entry 4: Following General Procedure A: (a) diphenyl (1,2,3,6-tetrahydro-[1,1'-biphenyl]-4-yl) phosphate **72**, 203 mg, 0.5 mmol, (b) Peppsi S*i*-Pr **262**, 3.4 mg, 1 mol%, (c) dichloromethane, 1 mL, 0.5 M, (d) *i*-PrMgBr, 2.9 M, 0.26 mL, 0.75 mmol, (e) rt, (f) 1 h, (g) 95% and (h) 96:2:2

Entry 5: Following General Procedure A: (a) diphenyl (1,2,3,6-tetrahydro-[1,1'-biphenyl]-4-yl) phosphate **72**, 203 mg, 0.5 mmol, (b) Peppsi S*i*-Pr **262**, 3.4 mg, 1 mol%, (c) toluene, 1 mL, 0.5 M, (d) *i*-PrMgBr, 2.9 M, 0.26 mL, 0.75 mmol, (e) rt, (f) 1 h, (g) 96% and (h) 93:4:3

Entry 6: Following General Procedure A: (a) diphenyl (1,2,3,6-tetrahydro-[1,1'-biphenyl]-4-yl) phosphate **72**, 203 mg, 0.5 mmol, (b) Peppsi S*i*-Pr **262**, 3.4 mg, 1 mol%, (c) cyclopentylmethyl ether, 1 mL, 0.5 M, (d) *i*-PrMgBr, 2.9 M, 0.26 mL, 0.75 mmol, (e) rt, (f) 1 h, (g) 95% and (h) 94:3:3

Entry 7: Following General Procedure A: (a) diphenyl (1,2,3,6-tetrahydro-[1,1'-biphenyl]-4-yl) phosphate **72**, 203 mg, 0.5 mmol, (b) Peppsi S*i*-Pr **262**, 3.4 mg, 1 mol%, (c) *tert*-butyl methyl ether, 5 mL, 0.1 M, (d) *i*-PrMgBr, 2.9 M, 0.26 mL, 0.75 mmol, (e) rt, (f) 1 h, (g) 92% and (h) 84:5:11

5.3.2. Grignard Scope

Scheme 5.14

Following General Procedure for the Kumada coupling reaction, data are presented as (a) enol phosphate, (b) palladium catalyst, (c) solvent, (d) Grignard, (e) Temperature, (f) time, (g) isolated yield run 1, and (h) isolated yield run 2

Synthesis of **267**: Following General Procedure A: (a) diphenyl (1,2,3,6-tetrahydro-[1,1'-biphenyl]-4-yl) phosphate **72**, 203 mg, 0.5 mmol, (b) Peppsi S*i*-Pr **262**, 3.4 mg,

1 mol%, (c) diethyl ether, 2 mL, 0.25 M, (d) cyclopentylmagnesium bromide, 2 M, 0.37 mL, 0.75 mmol, (e) rt, (f) 1 h, (g) 94%, 106 mg and (h) 93%, 105 mg

4-cyclopentyl-1,2,3,6-tetrahydro-1,1'-biphenyl[27] **267**:

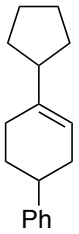

ν_{max}: 2949, 2910, 2966, 2360, 2331, 1490, 1450, 754 cm^{-1}.

^{1}H NMR (400 MHz, $CDCl_3$): δ 7.27 – 7.21 (m, 2H, ArH), 7.19 – 7.11 (m, 3H, ArH), 5.49 – 5.45 (m, 1H, C=CH), 2.75 – 2.64 (m, 1H, CH), 2.36 – 2.19 (m, 2H, CH, CH_2), 2.14 – 1.98 (m, 1H, CH_2), 1.95 – 1.87 (m, 1H, CH_2), 1.76 – 1.65 (m, 3H, CH_2), 1.64 – 1.56 (m, 2H, CH_2), 1.56 – 1.48 (m, 2H, CH_2), 1.37 – 1.28 (m, 1H, CH_2).

^{13}C NMR (100 MHz, $CDCl_3$): δ 140.3, 127.8, 126.3, 125.4, 117.9, 46.7, 39.9, 33.1, 30.7, 30.2, 29.7, 27.1, 24.7.

HRMS (ESI) Calculated for $C_{17}H_{21}$ $[M-H]^+$: 225.1638; found: 225.1637.

Synthesis of **268**: Following General Procedure A: (a) diphenyl (1,2,3,6-tetrahydro-[1,1'-biphenyl]-4-yl) phosphate **72**, 203 mg, 0.5 mmol, (b) Peppsi S*i*-Pr **262**, 3.4 mg, 1 mol%, (c) diethyl ether, 2 mL, 0.25 M, (d) cyclohexylmagnesium chloride, 1 M, 0.75 mL, 0.75 mmol, (e) rt, (f) 1 h, (g) 84%, 100 mg and (h) 82%, 98 mg

4-phenyl-[1,1'-bi(cyclohexan)]-1-ene 268:

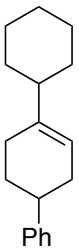

ν_{max}: 2920, 2848, 1490, 1446, 810, 752 cm^{-1}.

^1H NMR (400 MHz, $CDCl_3$): δ 7.33 – 7.28 (m, 2H, ArH), 7.26 – 7.17 (m, 3H, ArH), 5.50 - 5.46 (m, 1H, C=CH), 2.80 – 2.71 (m, 1H, CH), 2.34 – 2.25 (m, 1H, CH_2), 2.21 – 2.04 (m, 3H, CH_2), 1.99 – 1.92 (m, 1H, CH), 1.85 – 1.68 (m, 6H, CH_2), 1.34 – 1.13 (m, 6H, CH_2).

^{13}C NMR (100 MHz, $CDCl_3$): δ (ppm) 139.6, 127.8, 126.4, 125.4, 117.9, 45.0, 39.9, 33.3, 31.3, 29.7, 26.8, 26.34, 26.31, 25.9.

HRMS (ESI) Calculated for $C_{18}H_{23}$ $[M-H]^+$: 239.1794; found: 239.1794.

Synthesis of **269**: Following General Procedure A: (a) diphenyl (1,2,3,6-tetrahydro-[1,1'-biphenyl]-4-yl) phosphate **72**, 203 mg, 0.5 mmol, (b) Peppsi S*i*-Pr **262**, 3.4 mg, 1 mol%, (c) diethyl ether, 2 mL, 0.25 M, (d) cycloheptylmagnesium bromide, 2 M, 0.37 mL, 0.75 mmol, (e) rt, (f) 1 h, (g) 87%, 110 mg and (h) 87%, 109 mg

4-cycloheptyl-1,2,3,6-tetrahydro-1,1'-biphenyl 269:

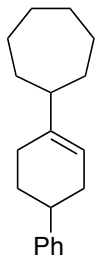

ν_{max}: 2918, 2880, 1489, 1450, 954, 808, 756 cm^{-1}.

^1H NMR (400 MHz, $CDCl_3$): δ 7.33 – 7.27 (m, 2H, ArH), 7.26 – 7.17 (m, 3H, ArH), 5.51 - 5.45 (m, 1H, C=CH), 2.80 – 2.69 (m, 1H, CH), 2.35 – 2.24 (m, 1H, CH_2), 2.24 – 2.00 (m, 4H, CH_2), 1.99 – 1.92 (m, 1H, CH), 1.79 – 1.67 (m, 5H, CH_2), 1.66 – 1.57 (m, 2H, CH_2), 1.54 – 1.41 (m, 6H, CH_2).

^{13}C NMR (100 MHz, $CDCl_3$): δ 143.8, 127.8, 126.4, 125.3, 117.5, 47.2, 39.9, 33.6, 33.2, 33.0, 29.8, 27.6, 26.7, 26.2.

HRMS (ESI) Calculated for $C_{19}H_{25}$ $[M-H]^+$: 253.1951; found: 253.1949.

Synthesis of **270**: Following General Procedure A: (a) diphenyl (1,2,3,6-tetrahydro-[1,1'-biphenyl]-4-yl) phosphate **72**, 203 mg, 0.5 mmol, (b) Peppsi S*i*-Pr **262**, 3.4 mg, 1 mol%, (c) diethyl ether, 2 mL, 0.25 M, (d) *iso*-butylmagnesium bromide, 2 M, 0.37 mL, 0.75 mmol, (e) rt, (f) 1 h, (g) 91%, 97 mg and (h) 90%, 96 mg

4-isobutyl-1,2,3,6-tetrahydro-1,1'-biphenyl 270:

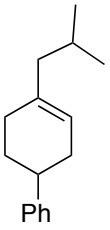

ν_{max}: 2951, 2904, 1452, 754 cm^{-1}.

^{1}H NMR (400 MHz, $CDCl_3$): δ 7.34 – 7.28 (m, 2H, ArH), 7.26 – 7.17 (m, 3H, ArH), 5.50 - 5.46 (m, 1H, C=CH), 2.81 – 2.72 (m, 1H, CH), 2.36 – 2.25 (m, 1H, CH_2), 2.22 – 2.07 (m, 2H, CH_2), 2.05 – 2.01 (m, 1H, CH_2), 2.00 – 1.92 (m, 1H, CH_2), 1.90 – 1.84 (m, 2H, CH_2), 1.82 – 1.72 (m, 2H, CH, CH_2), 0.89 (d, J = 6.5 Hz 6H, CH_3).

^{13}C NMR (100 MHz, $CDCl_3$): δ 146.8, 136.4, 127.8, 126.4, 125.4, 121.2, 47.0, 39.7, 33.0, 29.7, 28.3, 25.5, 22.2.

HRMS (ESI) Calculated for $C_{16}H_{21}$ $[M-H]^+$: 213.1638; found: 213.1638.

Synthesis of **271**: Following General Procedure A: (a) diphenyl (1,2,3,6-tetrahydro-[1,1'-biphenyl]-4-yl) phosphate **72**, 203 mg, 0.5 mmol, (b) Peppsi S*i*-Pr **262**, 3.4 mg, 1 mol%, (c) diethyl ether, 2 mL, 0.25 M, (d) *n*-butylmagnesium chloride, 2 M, 0.37 mL, 0.75 mmol, (e) rt, (f) 1 h, (g) 63%, 67 mg and (h) 60%, 64 mg

In this case the compound was not isolated, however the crude product was analysed and a selectivity of 76:22:2 (a:b:c) was determined.

4-butyl-1,2,3,6-tetrahydro-1,1'-biphenyl 271:

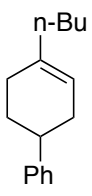

ν_{max}: 2922, 1602, 1452, 754 cm^{-1}.

^1H NMR (400 MHz, $CDCl_3$): δ 7.34 – 7.26 (m, 2H, ArH), 7.26 – 7.18 (m, 3H, ArH), 5.54 – 5.46 (m, 1H, C=CH), 2.81 – 2.72 (m, 1H, CH), 2.35 – 2.25 (m, 1H, CH_2), 2.23 – 2.10 (m, 2H, CH_2), 2.09 – 1.93 (m, 4H, CH_2), 1.84 – 1.71 (m, 1H, CH_2), 1.48 – 1.26 (m, 4H, CH_2), 0.93 (t, J = 7.2 Hz, 3H, CH_3).

^{13}C NMR (100 MHz, $CDCl_3$): δ 146.9, 137.3, 127.8, 126.4, 125.4, 119.9, 39.7, 39.3, 33.0, 29.6, 28.3, 20.3, 23.1, 13.3.

HRMS (ESI) Calculated for $C_{16}H_{21}$ $[M-H]^+$: 213.1638; found: 213.1638.

Synthesis of **272**: Following General Procedure A: (a) diphenyl (1,2,3,6-tetrahydro-[1,1'-biphenyl]-4-yl) phosphate **72**, 203 mg, 0.5 mmol, (b) Peppsi S*i*-Pr **262**, 3.4 mg, 1 mol%, (c) diethyl ether, 2 mL, 0.25 M, (d) phenylmagnesium chloride, 1 M, 0.75 mL, 0.75 mmol, (e) rt, (f) 1 h, (g) 73%, 85 mg and (h) 75%, 88 mg

1',2',3',6'-tetrahydro-1,1':4',1''-terphenyl[28] **272**:

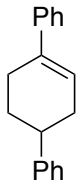

ν_{max}: 1479, 1429, 729 cm^{-1}.

^1H NMR (400 MHz, $CDCl_3$): δ 7.46 – 7.41 (m, 2H, ArH), 7.37 – 7.26 (m, 6H, ArH), 7.27 – 7.21 (m, 2H, ArH), 6.25 – 6.20 (m, 1H, C=CH), 2.96-2.86 (m, 1H, CH), 2.65 – 2.50 (m, 3H, CH_2), 2.42 – 2.31 (m, 1H, CH_2), 2.19 – 2.11 (m, 1H, CH_2), 2.00 – 1.88 (m, 1H, CH_2).

^{13}C NMR (100 MHz, $CDCl_3$): δ 152.2, 146.2, 142.2, 127.9, 127.7, 126.4, 126.2, 125.6, 124.5, 123.7, 39.2, 33.5, 29.6, 27.4.

HRMS (ESI) Calculated for $C_{18}H_{19}$ $[M+H]^+$: 235.1481; found: 235.1693.

5.3.3. Temperature Study

Scheme 5.15

Table 5.4

Following General Procedure for the Kumada coupling reaction, data are presented as (a) enol phosphate, (b) palladium catalyst, (c) solvent, (d) Grignard, (e) Temperature, (f) time, (g) conversion, and (h) selectivity (a:b:c)

Entry 1: Following General Procedure A: (a) diphenyl (1,2,3,6-tetrahydro-[1,1'-biphenyl]-4-yl) phosphate **72**, 203 mg, 0.5 mmol, (b) Peppsi S*i*-Pr **262**, 3.4 mg, 1 mol%, (c) Diethyl ether, 2 mL, 0.25 M, (d) *n*-BuMgCl, 2 M, 0.37 mL, 0.75 mmol, (e) 40 °C, (f) 1 h, (g) 100% and (h) 70:26:4

Entry 2: Following General Procedure A: (a) diphenyl (1,2,3,6-tetrahydro-[1,1'-biphenyl]-4-yl) phosphate **72**, 203 mg, 0.5 mmol, (b) Peppsi S*i*-Pr **262**, 3.4 mg, 1 mol%, (c) Diethyl ether, 2 mL, 0.25 M, (d) *n*-BuMgCl, 2 M, 0.37 mL, 0.75 mmol, (e) 0 °C, (f) 1 h, (g) 100% and (h) 90:10:0

Scheme 5.16

Table 5.5

Following General Procedure for the Kumada coupling reaction, data are presented as (a) enol phosphate, (b) palladium catalyst, (c) solvent, (d) Grignard, (e) Temperature, (f) time, (g) conversion, and (h) selectivity (a:b:c)

Entry 1: Following General Procedure A: (a) diphenyl (1,2,3,6-tetrahydro-[1,1'-biphenyl]-4-yl) phosphate **72**, 203 mg, 0.5 mmol, (b) Peppsi S*i*-Pr **262**, 3.4 mg, 1 mol%, (c) DCM, 1 mL, 0.5 M, (d) *n*-BuMgCl, 2 M, 0.37 mL, 0.75 mmol, (e) rt, (f) 1 h, (g) 76% and (h) 17:68:15

Entry 2: Following General Procedure A: (a) diphenyl (1,2,3,6-tetrahydro-[1,1'-biphenyl]-4-yl) phosphate **72**, 203 mg, 0.5 mmol, (b) Peppsi S*i*-Pr **262**, 3.4 mg, 1

mol%, (c) DCM, 1 mL, 0.5 M, (d) *n*-BuMgCl, 2 M, 0.37 mL, 0.75 mmol, (e) 0 °C, (f) 1 h, (g) 45% and (h) 20:62:18

Scheme 5.17

Following General Procedure for the Kumada coupling reaction, data are presented as (a) enol phosphate, (b) palladium catalyst, (c) solvent, (d) Grignard, (e) Temperature, (f) time, (g) conversion, and (h) selectivity (a:b:c)

Following General Procedure A: (a) diphenyl (1,2,3,6-tetrahydro-[1,1'-biphenyl]-4-yl) phosphate **72**, 203 mg, 0.5 mmol, (b) Peppsi S*i*-Pr **262**, 3.4 mg, 1 mol%, (c) DCM, 1 mL, 0.5 M, (d) *n*-Bu_2Mg, 1 M, 0.75 mL, 0.75 mmol, (e) rt, (f) 1 h, (g) 28% and (h) 36:49:15

Scheme 5.18

Table 5.5

Following General Procedure for the Kumada coupling reaction, data are presented as (a) enol phosphate, (b) palladium catalyst, (c) solvent, (d) Grignard, (e) Temperature, (f) time, (g) conversion, and (h) selectivity (a:b:c)

Entry 1: Following General Procedure A: (a) diphenyl (1,2,3,6-tetrahydro-[1,1'-biphenyl]-4-yl) phosphate **72**, 203 mg, 0.5 mmol, (b) Peppsi *i*-Pr*^{OMe} **273**, 6 mg, 1 mol%, (c) DCM, 1 mL, 0.5 M, (d) *n*-BuMgCl, 2 M, 0.37 mL, 0.75 mmol, (e) rt, (f) 1 h, (g) 78% and (h) 16:67:16

Entry 2: Following General Procedure A: (a) diphenyl (1,2,3,6-tetrahydro-[1,1'-biphenyl]-4-yl) phosphate **72**, 203 mg, 0.5 mmol, (b) Peppsi *i*-Pr*^{OMe} **273**, 6 mg, 1 mol%, (c) diethyl ether, 2 mL, 0.25 M, (d) *n*-BuMgCl, 2 M, 0.37 mL, 0.75 mmol, (e) 0 °C, (f) 1 h, (g) 93% and (h) 37:61:2

Scheme 5.19

Table 5.7

Following General Procedure for the Kumada coupling reaction, data are presented as (a) enol phosphate, (b) palladium catalyst, (c) solvent, (d) Grignard, (e) Temperature, (f) time, (g) conversion, and (h) selectivity (a:b:c)

Entry 1: Following General Procedure A: (a) diphenyl (1,2,3,6-tetrahydro-[1,1'-biphenyl]-4-yl) phosphate **72**, 203 mg, 0.5 mmol, (b) Peppsi S*i*-Pr **262**, 3.4 mg, 1 mol%, (c) toluene, 1 mL, 0.5 M, (d) *n*-BuMgCl, 2 M, 0.37 mL, 0.75 mmol, (e) rt, (f) 1 h, (g) 94% and (h) 32:48:20

Entry 2: Following General Procedure A: (a) diphenyl (1,2,3,6-tetrahydro-[1,1'-biphenyl]-4-yl) phosphate **72**, 203 mg, 0.5 mmol, (b) Peppsi S*i*-Pr **262**, 3.4 mg, 1 mol%, (c) toluene, 1 mL, 0.5 M, (d) *n*-BuMgCl, 2 M, 0.37 mL, 0.75 mmol, (e) 0 °C, (f) 1 h, (g) 74% and (h) 50:43:7

Entry 3: Following General Procedure A: (a) diphenyl (1,2,3,6-tetrahydro-[1,1'-biphenyl]-4-yl) phosphate **72**, 203 mg, 0.5 mmol, (b) Peppsi S*i*-Pr **262**, 3.4 mg, 1 mol%, (c) toluene, 1 mL, 0.5 M, (d) *n*-BuMgCl, 2 M, 0.37 mL, 0.75 mmol, (e) -20 °C, (f) 1 h, (g) 41% and (h) 91:9:0

Entry 4: Following General Procedure A: (a) diphenyl (1,2,3,6-tetrahydro-[1,1'-biphenyl]-4-yl) phosphate **72**, 203 mg, 0.5 mmol, (b) Peppsi S*i*-Pr **262**, 3.4 mg, 1 mol%, (c) toluene, 1 mL, 0.5 M, (d) *n*-BuMgCl, 2 M, 0.37 mL, 0.75 mmol, (e) -40 °C, (f) 1 h, (g) 12% and (h) 100:0:0

5.3.4. Optimised conditions for the use of n-BuMgBr

Scheme 5.20

Following General Procedure for the Kumada coupling reaction, data are presented as (a) enol phosphate, (b) palladium catalyst, (c) solvent, (d) Grignard, (e) Temperature, (f) time, (g) isolated yield run 1, and (h) isolated yield run 2

Following General Procedure A: (a) diphenyl (1,2,3,6-tetrahydro-[1,1'-biphenyl]-4-yl) phosphate **72**, 203 mg, 0.5 mmol, (b) Peppsi S*i*-Pr **262**, 3.4 mg, 1 mol%, (c)

toluene, 1 mL, 0.5 M, (d) *n*-BuMgCl, 1 M, 0.75 mL, 0.75 mmol, (e) -40 °C, (f) 16 h, (g) 88%, 94 mg and (h) 88%, 95 mg

5.3.5. Enol Phosphate Substrate Scope

Scheme 5.21

Following General Procedure for the Kumada coupling reaction, data are presented as (a) enol phosphate, (b) palladium catalyst, (c) solvent, (d) Grignard, (e) Temperature, (f) time, (g) isolated yield run 1, and (h) isolated yield run 2

Synthesis of **274**: Following General Procedure A: (a) diphenyl (1,2,3,6-tetrahydro-[1,1'-biphenyl]-4-yl) phosphate **72**, 203 mg, 0.5 mmol, (b) Peppsi S*i*-Pr **262**, 3.4 mg, 1 mol%, (c) toluene, 1 mL, 0.5 M, (d) methylmagnesium bromide, 3 M, 0.26 mL, 0.75 mmol, (e) 0 °C, (f) 2 h, (g) 78%, 106 mg and (h) 77%, 105 mg

4-ethyl-1,2,3,6-tetrahydro-1,1'-biphenyl[29] **274**:

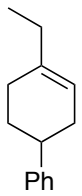

ν_{max}: 2960, 2914, 2954, 1452, 1435, 756 cm^{-1}.

^1H NMR (400 MHz, $CDCl_3$): δ 7.34 – 7.28 (m, 2H, ArH), 7.26 – 7.18 (m, 3H, ArH), 5.51 – 5.48 (m, 1H, C=CH), 2.81 – 2.72 (m, 1H, CH), 2.34 – 2.27 (m, 1H, CH_2), 2.21 – 2.16 (m, 1H, CH_2), 2.09 – 1.94 (m, 4H, CH_2), 1.82 – 1.74 (m, 2H, CH_2), 0.97 (t, J = 7.5 Hz.).

^{13}C NMR (100 MHz, $CDCl_3$): δ 127.9, 127.8, 126.5, 126.4, 125.4, 118.5, 39.8, 33.0, 29.7, 29.6, 18.5, 11.9.

HRMS (ESI) Calculated for $C_{14}H_{17}$ $[M-H]^+$: 185.1325; found: 185.1322.

Synthesis of **275**: Following General Procedure A: (a) diphenyl (1,2,3,6-tetrahydro-[1,1'-biphenyl]-4-yl) phosphate **72**, 203 mg, 0.5 mmol, (b) Peppsi S*i*-Pr **262**, 3.4 mg,

1 mol%, (c) diethyl ether, 2 mL, 0.25 M, (d) *n*-propylmagnesium chloride, 1 M, 0.75 mL, 0.75 mmol, (e) rt °C, (f) 1 h, (g) 71%, 71 mg and (h) 70%, 70 mg

4-propyl-1,2,3,6-tetrahydro-1,1'-biphenyl, **275**:

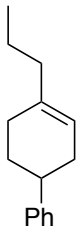

ν_{max}: 2954, 2918, 2358, 1492, 1452, 754 cm^{-1}.

^{1}H NMR (400 MHz, $CDCl_3$): δ 7.35 – 7.28 (m, 2H, ArH), 7.26 – 7.18 (m, 3H, ArH), 5.53 – 5.47 (m, 1H, C=CH), 2.81 – 2.71 (m, 1H, CH), 2.36 – 2.25 (m, 1H, CH_2), 2.22 – 2.11 (m, 2H, CH_2), 2.68 – 1.92 (m, 4H, CH_2), 1.84 – 1.71 (m, 1H, CH_2), 1.46 (q, J = 7.4 Hz, 2H, CH_2), 0.92 (t, J = 7.4 Hz, 3H, CH_3).

^{13}C NMR (100 MHz, $CDCl_3$): δ 146.9, 137.3, 127.8, 126.4, 125.4, 119.9, 39.7, 39.3, 33.0, 29.6, 28.3, 20.3, 13.3.

HRMS (ESI) Calculated for $C_{15}H_{19}$ $[M-H]^+$: 199.1481; found: 199.1482.

Scheme 5.22

Following General Procedure for the Kumada coupling reaction, data are presented as (a) enol phosphate, (b) palladium catalyst, (c) solvent, (d) Grignard, (e) Temperature, (f) time, (g) isolated yield run 1, and (h) isolated yield run 2

Synthesis of **276**: Following General Procedure A: (a) 4-(*tert*-butyl)cyclohex-1-en-1-yl diphenyl phosphate **16**, 193 mg, 0.5 mmol, (b) Peppsi S*i*-Pr **262**, 3.4 mg, 1 mol%, (c) diethyl ether, 2 mL, 0.25 M, (d) *i*-PrMgBr, 2.9 M, 0.26 mL, 0.75 mmol, (e) rt, (f) 1 h, (g) 98%, 88 mg and (h) 86%, 105 mg

4-(*tert*-butyl)-1-isopropylcyclohex-1-ene[30] **276**:

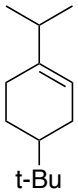

ν_{max}: 2918, 1452, 1363, 808, 756 cm^{-1}.

^1H NMR (400 MHz, $CDCl_3$): δ 5.45 – 5.39 (m, 1H, C=CH), 2.24 – 2.12 (m, 1H, CH), 2.09 – 1.97 (m, 3H, CH, CH_2), 1.89 – 1.73 (m, 2H, CH_2), 1.97 – 1.10 (m, 2H, CH_2), 1.01 (d, J = 6.8 Hz, 6H, CH_3), 0.88 (s, 9H, $(CH_3)_3$).

^{13}C NMR (100 MHz, $CDCl_3$): δ 142.9, 117.09, 43.9, 34.3, 26.9, 26.7, 26.2, 23.9, 21.2, 20.7.

HRMS (ESI) Calculated for $C_{13}H_{23}$ $[M-H]^+$: 179.1794; found: 179.1792.

Synthesis of **277**: Following General Procedure A: (a) 4-((*tert*-butyldimethylsilyl)oxy)cyclohex-1-en-1-yl diphenyl phosphate **81**, 230 mg, 0.5 mmol, (b) Peppsi S*i*-Pr **262**, 3.4 mg, 1 mol%, (c) diethyl ether, 2 mL, 0.25 M, (d) *i*-PrMgBr, 2.9 M, 0.26 mL, 0.75 mmol, (e) rt, (f) 1 h, (g) 87%, 110 mg and (h) 87%, 109 mg

***tert*-butyl((4-isopropylcyclohex-3-en-1-yl)oxy)dimethylsilane 277**:

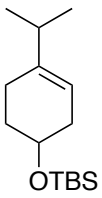

ν_{max}: 2996, 2927, 2895, 1492, 1259, 1091, 892, 833, 771 cm^{-1}.

^1H NMR (400 MHz, $CDCl_3$): δ 5.28 – 5.25 (m, 1H, C=CH), 3.90 – 3.80 (m, 1H, CH), 2.28 – 1.91 (m, 5H, CH_2, CH), 1.85 – 1.77 (m, 1H, CH_2), 1.64 – 1.51 (m, 1H, CH_2), 0.99 (d, J = 6.9 Hz, 6H, CH_3), 0.90 (s, 9H, $(CH_3)_3$), 0.07 (s, 6H, CH_3).

^{13}C NMR (100 MHz, $CDCl_3$): δ 142,6, 115.5, 68.0, 34.7, 34.2, 31.7, 25.4, 24.6, 21.0, 20.8, -5.1.

HRMS (ESI) Calculated for $C_{15}H_{29}OSi$ $[M-H]^+$: 253.1980; found: 253.1982.

Synthesis of **278**: Following General Procedure A: (a) Diphenyl (4-propylcyclohexenyl)phosphate, **74**, 186 mg, 0.5 mmol, (b) Peppsi S*i*-Pr **262**, 3.4 mg, 1 mol%, (c) diethyl ether, 2 mL, 0.25 M, (d) *i*-PrMgBr, 2.9 M, 0.26 mL, 0.75 mmol, (e) rt, (f) 1 h, (g) 73%, 60 mg and (h) 70%, 58 mg

1-isopropyl-4-propylcyclohex-1-ene 278:

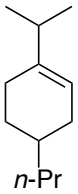

ν_{max}: 2980, 2358, 2341, 1597, 1453, 1149, 1095 cm^{-1}.
^{1}H NMR (400 MHz, $CDCl_3$): δ 5.41 – 5.37 (m, 1H, C=CH), 2.23- 2.07 (m, 2H, CH, CH_2), 2.03 – 1.97 (m, 2H, CH_2), 1.81 – 1.75 (m, 1H, CH_2), 1.65 – 1.58 (m, 1H, CH_2),1.54 – 1.45 (m, 1H, CH), 1.40 – 1.32 (m, 2H, CH_2), 1.29 – 1.15 (m, 3H, CH_2), 1.01 (d, J = 6.9 Hz, 6H, CH_3), 0.92 (t, J = 7.3 Hz, 3H, CH_3).
^{13}C NMR (100 MHz, $CDCl_3$): δ 142.9, 117.4, 38.4, 34.5, 33.0, 32.5, 29.0, 25.6, 21.3, 20.7, 19.5.
HRMS (ESI) Calculated for $C_{12}H_{21}$ $[M-H]^+$: 165.1638; found: 165.1634.

Synthesis of **209**: Following General Procedure A: (a) Diphenyl 1-methyl-1,2,3,6-tetrahydro-[1,1'-biphenyl]-4-yl phosphate, **73**, 186, 0.5 mmol, (b) Peppsi S*i*-Pr **262**, 3.4 mg, 1 mol%, (c) diethyl ether, 2 mL, 0.25 M, (d) *i*-PrMgBr, 2.9 M, 0.26 mL, 0.75 mmol, (e) rt, (f) 1 h, (g) 98%, 117 mg and (h) 97%, 116 mg

Synthesis of **279**: Following General Procedure A: (a) diphenyl (1,4-dioxaspiro[4.5]dec-7-en-8-yl) phosphate, **83**, 194 mg, 0.5 mmol, (b) Peppsi S*i*-Pr **262**, 3.4 mg, 1 mol%, (c) diethyl ether, 2 mL, 0.25 M, (d) *i*-PrMgBr, 2.9 M, 0.26 mL, 0.75 mmol, (e) rt, (f) 1 h, (g) 85%, 77 mg and (h) 84%, 76 mg

8-isopropyl-1,4-dioxaspiro[4.5]dec-7-ene[31] **279**:

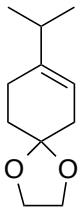

ν_{max}: 2958, 2930, 2875, 1733, 1717 , 1683, 1059,1036 cm^{-1}.

^{1}H NMR (400 MHz, $CDCl_3$): δ 5.35 – 5.31 (m, 1H, C=CH), 4.01 – 3.98 (m, 4H, CH_2), 2.32- 2.18 (m, 5H, CH, CH_2), 1.81 – 1.75 (m, 2H, CH_2), 1.03 (d, *J* = 6.9 Hz, CH_3).

^{13}C NMR (100 MHz, $CDCl_3$): δ 142.5, 115, 114.9, 107.8, 63.9, 35.2, 30.9, 24.7, 20.9.

HRMS (ESI) Calculated for $C_{11}H_{17}O_2P$ $[M-H]^+$: 181.1223; found: 181.1220.

Synthesis of **280**: Following General Procedure A: (a) 3-methyl-1,2,3,6-tetrahydro-[1,1'-biphenyl]-4-yl diphenyl phosphate, **92**, 210 mg, 0.5 mmol, (b) Peppsi S*i*-Pr **262**, 3.4 mg, 1 mol%, (c) diethyl ether, 2 mL, 0.25 M, (d) *i*-PrMgBr, 2.9 M, 0.26 mL, 0.75 mmol, (e) rt, (f) 1 h, (g) 88%, 94 mg and (h) 86%, 92 mg

4-isopropyl-3-methyl-1,2,3,6-tetrahydro-1,1'-biphenyl 280:

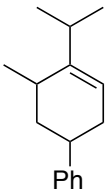

ν_{max}: 2958, 2908, 1602, 1492, 1452, 1377, 1029 cm^{-1}.

^{1}H NMR (400 MHz, $CDCl_3$): δ 7.35 – 7.29 (m, 4H, ArH), 7.27 – 7.16 (m, 6H, ArH), 5.52 – 5.45 (m, 2H, C=CH), 2.97 – 2.87 (m, 1H, CH), 2.82 - 2.72 (m, 1H, CH), 2.57 – 2.46 (m, 1H, CH_2), 2.43 – 2.33 (m, 2H, CH), 2.32 – 2.23 (m, 2H, CH_2), 2.21 – 2.07 (m, 2H, CH_2), 2.05 – 1.98 (m, 1H, CH), 1.97 – 1.88 (m, 1H, CH), 1.78 – 1.70 (m, 1H, CH_2), 1.56 – 1.44 (m, 2H, CH_2), 1.15 (d, *J* = 7.1 Hz, 3H, CH_3), 1.11 – 1.06 (m, 9H, CH_3), 1.04 (d, *J* = 4.8 Hz, 3H, CH_3), 1.02 (d, *J* = 4.7 Hz, 3H, CH_3).

^{13}C NMR (100 MHz, $CDCl_3$): δ 147.9, 147, 146.9, 127.8, 127.7, 126.5, 126.3, 125.4, 117.2, 116.8, 40.2, 40.0, 37.4, 34.7, 33.9, 33.5, 32.7, 31.2, 31.1, 28.9, 22.9, 22.1, 21.4, 20.6, 19.8, 19.4.
HRMS (ESI) Calculated for $C_{16}H_{21}$ $[M-H]^+$: 213.1638; found: 213.1638.

Synthesis of **281**: Following General Procedure A: (a) 5-methyl-1,2,3,6-tetrahydro-[1,1'-biphenyl]-4-yl diphenyl phosphate, **283**, 210 mg, 0.5 mmol, (b) Peppsi S*i*-Pr **262**, 3.4 mg, 1 mol%, (c) diethyl ether, 2 mL, 0.25 M, (d) *i*-PrMgBr, 2.9 M, 0.26 mL, 0.75 mmol, (e) 40 °C, (f) 8 h, (g) 64%, 68 mg and (h) 62%, 66 mg

4-isopropyl-5-methyl-1,2,3,6-tetrahydro-1,1'-biphenyl 281:

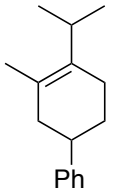

ν_{max}: 2958, 2922, 2602, 1494, 1452, 754 cm^{-1}.
^{1}H NMR (400 MHz, $CDCl_3$): δ 7.34 – 7.28 (m, 2H, ArH), 7.26 – 7.21 (m, 3H, ArH), 2.27 – 2.85 (m, 1H, CH), 2.81 - 2.71 (m, 1H, CH), 2.19 – 2.11 (m, 3H, CH_2), 2.11 – 2.03 (m, 2H, CH_2), 2.0 – 1.92 (m, 1H, CH_2), 1.67 (s, 3H, CH_3), 0.99 (d, 3H, J = 6.9 Hz, CH_3), 0.97 (d, 3H, J = 6.9 Hz, CH_3).
^{13}C NMR (100 MHz, $CDCl_3$): δ 147, 134.2, 127.8, 126.4, 125.4, 123.5, 40.3, 40.2, 29.8, 28.7, 23.2, 20.3, 19.8, 18.0.
HRMS (ESI) Calculated for $C_{16}H_{21}$ $[M-H]^+$: 213.1638; found: 213.1638.

Synthesis of 283

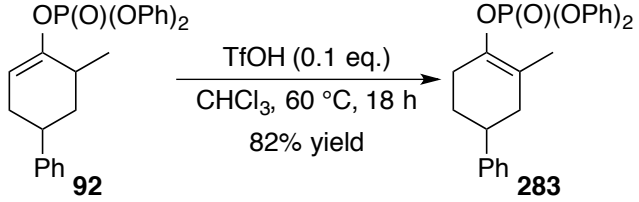

Scheme 5. 23

To a solution of the kinetic enol phosphate 1.47 (1.7 g, 4 mmol) in an oven-dried flask under argon was added dry $CHCl_3$, and distilled trifluoromethanesulfonic acid (46 mg, 0.4 mmol) and the mixture was heated to 60 °C. After 18 h the mixture was allowed to cool to room temperature and the solvents removed *in vacuo*. The crude oil was purified by column chromatography on silica gel using 0-20% Et_2O in petroleum ether (40-60 °C) to give the desired product as a colourless oil in 82% yield, 1.3 g.

5-methyl-1,2,3,6-tetrahydro-[1,1'-biphenyl]-4-yl diphenyl phosphate 283

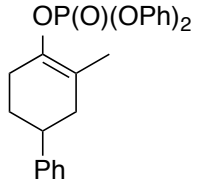

ν_{max}: 3026, 2941, 1589, 1487, 1292, 1186, 1091, 947, 754 cm^{-1}.

^1H NMR (400 MHz, $CDCl_3$): δ 7.41 – 7.28 (m, 10H, ArH), 7.25 – 7.18 (m, 5H, ArH), 2.90 – 2.81 (m, 1H, CH), 2.62 – 2.49 (m, 1H, CH_2), 2.47 – 2.37 (m, 1H, CH_2), 2.28 – 2.21 (m, 2H, CH_2), 2.03 – 1.96 (m, 1H, CH_2), 1.94 – 1.86 (m, 2H, CH_2), 1.64 (s, 3H, CH_3).

^{13}C NMR (100 MHz, $CDCl_3$): δ 157,8, 147, 129.2, 127.9, 126.3, 125.8, 124.8, 119.7, 39.2, 37.7, 29.6, 27.7, 15.6.

^{31}P NMR (400 MHz, $CDCl_3$): δ -16.9.

HRMS (ESI) Calculated for $C_{25}H_{26}O_4P$ $[M-H]^+$: 421.1563; found: 421.1562.

Synthesis of **282**: Following General Procedure A: (a) 6-isopropyl-3-methylcyclohexenyl diphenyl phosphate, **84**, 193 mg, 0.5 mmol, (b) Peppsi S*i*-Pr **262**, 3.4 mg, 1 mol%, (c) diethyl ether, 2 mL, 0.25 M, (d) *i*-PrMgBr, 2.9 M, 0.26 mL, 0.75 mmol, (e) 40 °C, (f) 8 h, (g) 64%, 57 mg and (h) 60%, 54 mg

1,6-diisopropyl-3-methylcyclohex-1-ene 282:

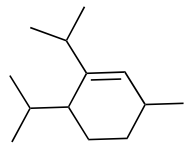

Presented as a mixture of diastereomers.

ν_{max}: 2954, 2926, 1456, 1382, 1365, 854 cm^{-1}.

^{1}H NMR (400 MHz, $CDCl_3$): δ 5.44 – 5.38 (m, 1H, C=CH), 5.33 – 5.29 (m, 1.2H, C=CH), 2.32 – 2.19 (m, 2H, CH), 2.18 – 2.10 (m, 3H, CH, CH_2), 2.09 – 2.01 (m, 3H, CH, CH_2), 1.80 – 1.73 (m, 2H, CH, CH_2), 1.71 – 1.64 (m, 2H, CH, CH_2), 1.63 – 1.56 (m, 2H, CH, CH_2), 1.50 – 1.45 (m, 2H, CH_2), 1.34 – 1.24 (m, 3H, CH_2), 1.04 (d, J = 6.8 Hz, 6H, CH_3), 1.00 – 0.99 (m, 21H, CH_3), 0.77 (d, J = 6.8 Hz, 3H, CH_3), 0.69 (d, J = 6.8 Hz, 6H, CH_3).

^{13}C NMR (100 MHz, $CDCl_3$): δ 126.2, 125.3, 41.0, 40.9, 30.7, 30.0, 28.7, 28.3, 28.2, 27.1, 22.9, 22.8, 22.0, 21.4, 21.3, 20.9, 20.7, 20.6, 20.4, 20.3, 17.6, 15.5.

HRMS (ESI) Calculated for $C_{13}H_{23}$ $[M-H]^+$: 179.1800; found: 179.1798.

6. References

1. Monks, N. R. *PhD Thesis*; University of Strathclyde; 2013.
2. Sellars, J. D.; Steel, P. G., *Chem. Soc. Rev.*, **2011**, *40* (10), 5170.
3. Gauthier, D.; Beckendorf, S.; Gøgsig, T. M.; Lindhardt, A. T.; Skrydstrup, T., *J. Org. Chem.*, **2009**, *74* (9), 3536.
4. Blay, G.; Schrijvers, R.; Wijnberg, J. B. P. A.; de Groot, A., *J. Org. Chem.*, **1995**, *60* (7), 2188.
5. Jana, R.; Pathak, T. P.; Sigman, M. S., *Chem. Rev.*, **2011**, *111* (3), 1417.
6. Pompeo, M.; Froese, R. D. J.; Hadei, N.; Organ, M. G., *Angew. Chem. Int. Ed.*, **2012**, *51* (45), 11354.
7. (a) Musaev, D. G.; Svensson, M.; Morokuma, K.; Strömberg, S.; Zetterberg, K.; Siegbahn, P. E. M., *Organometallics*, **1997**, *16* (9), 1933. (b) Shultz, L. H.; Tempel, D. J.; Brookhart, M., *J. Am. Chem. Soc.*, **2001**, *123* (47), 11539.
8. Miller, J. A., *Tetrahedron Lett.*, **2002**, *43* (39), 7111.
9. Hansen, A. L.; Ebran, J.-P.; Gøgsig, T. M.; Skrydstrup, T., *J. Org. Chem,.* **2007**, *72* (17), 6464.
10. Cahiez, G.; Habiak, V.; Gager, O., *Org. Lett.*, **2008**, *10* (12), 2389.
11. Gøgsig, T. M.; Lindhardt, A. T.; Skrydstrup, T., *Org. Lett.*, **2009**, *11* (21), 4886.
12. Aggarwal, V. K.; Humphries, P. S.; Fenwick, A., *Angew. Chem. Int. Ed.*, **1999**, *38* (13-14), 1985.
13. Larsen, U. S.; Martiny, L.; Begtrup, M., *Tetrahedron Lett.*, **2005**, *46* (24), 4261.
14. You, W.; Li, Y.; Brown, M. K., *Org. Lett.*, **2013**, *15* (7), 1610.
15. Krasovskiy, A. L.; Haley, S.; Voigtritter, K.; Lipshutz, B. H., *Org. Lett.*, **2014**, *16* (16), 4066.
16. (a) Strotman, N. A.; Chobanian, H. R.; Guo, Y.; He, J.; Wilson, J. E., *Org. Lett.*, **2010**, *12* (16), 3578. (b) Han, S.; Movassaghi, M., *J. Am. Chem. Soc.*, **2011**, *133* (28), 10768.
17. Yi, C.; Hua, R., *Tetrahedron Lett.*, **2006**, *47* (15), 2573.
18. Kantchev, E. A. B.; O'Brien, C. J.; Organ, M. G., *Angew. Chem. Int. Ed.*, **2007**, *46* (16), 2768.

19. Gauthier, D.; Beckendorf, S.; Gøgsig, T. M.; Lindhardt, A. T.; Skrydstrup, T., *J. Org. Chem.*, **2009**, *74* (9), 3536.

20. (a) Heijnen, D.; Hornillos, V.; Corbet, B. P.; Giannerini, M.; Feringa, B. L., *Org. Lett.*, **2015**, *17* (9), 2262. (b) Giannerini, M.; Fañanás-Mastral, M.; Feringa, B. L., *Nat. Chem.*, **2013**, *5* (8), 667.

21. Meiries, S.; Speck, K.; Cordes, D. B.; Slawin, A. M. Z.; Nolan, S. P., *Organometallics*, **2013**, *32* (1), 330.

22. Perrin, D., D.; Armarego, W. L. F., *Purification of Laboratory Chemicals*; Pergaman: Oxford; 1988.

23. Love, B. E.; Jones, E. G., *J. Org. Chem.*, **1999**, *64* (10), 3755.

24. Dorta, R. L.; Suárez, E.; Betancor, C., *Tetrahedron Lett.*, **1994**, *35* (28), 5035.

25. Imboden, C.; Villar, F.; Renaud, P., *Org. Lett.*, **1999**, *1* (6), 873.

26. Jutand, A.; Négri, S., *Eur. J. Org. Chem.*, **1998**, *1998* (9), 1811.

27. Azemi, T.; Kitamura, M.; Narasaka, K., *Tetrahedron*, **2004**, *60* (6), 1339.

28. Eliel, E. L.; Manoharan, M.; Levine, S. G.; Ng, A., *J. Org. Chem.*, **1985**, *50* (24), 4978.

29. Posner, G. H.; Shulman-Roskes, E. M.; Oh, C. H.; Carry, J.-C.; Green, J. V.; Clark, A. B.; Dai, H.; Anjeh, T. E. N., *Tetrahedron Lett.*, **1991**, *32* (45), 6489.

30. Harada, T.; Inoue, A.; Wada, I.; Uchimura, J.; Tanaka, S.; Oku, A., *J. Am. Chem. Soc.*, **1993**, *115* (17), 7665.

31. Hawley, R. C.; Schreiber, S. L., *Synth. Commun.*, **1990**, *20* (8), 1159–1165.